RPS

Seismic Source Array Modelling

d84F.R-EL

Seismic Source Array Modelling
d84F.R-EL

Prepared for:

Petroceltic

Prepared by:
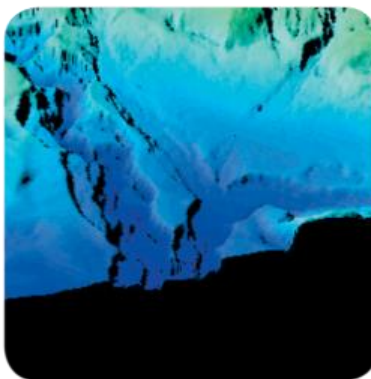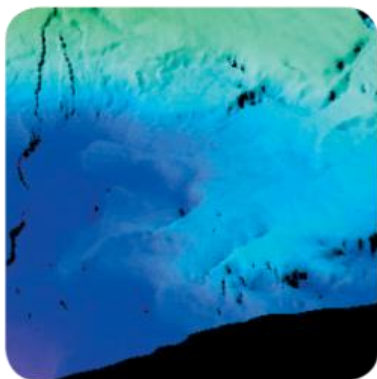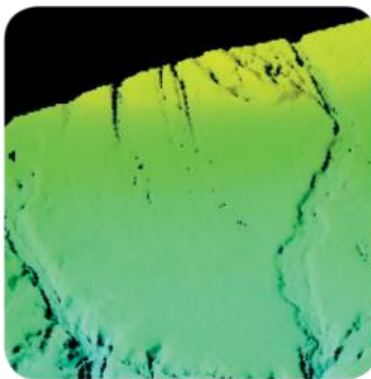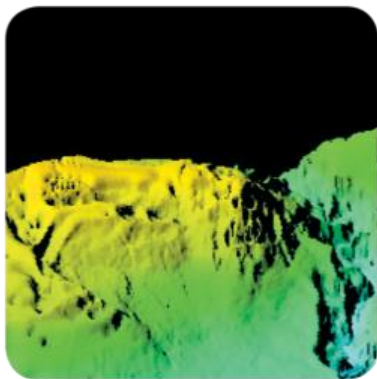
RPS Energy

07/07/2017

DISCLAIMER

COPYRIGHT
© RPS Energy

Project Title	Seismic Source Array Modelling - d84F.R-EL		
Project Number	ECD1589	Date of Issue:	07/07/2017
	Author:	Project Manager	Peer Review
Name		RudlingC	Chris Helly

Document Description	Date	Issued By	Checked By	Accepted by Client	Comments
Version Draft	23/05/2017	RudlingC	Chris Helly	No	
Version Final	07/07/2017	RudlingC	Chris Helly	Yes	
File Location:	RPS Goldvale House 27-41 Church Street West, Woking, Surrey, GU21 6DH, United Kingdom **T** +44 (0)1483 746500 **F** +44 (0)1483 746505 **E** rpswo@rpsgroup.com **W** www.rpsgroup.com				

Table of Contents

List of Illustrations and Figures

1.0   INTRODUCTION

1.1   Introduction

Petroceltic requested RPS to provide an assessment of the effects of underwater noise from seismic operations on marine life for their proposed 3D seismic survey in the Southern Ionian. In order to achieve the objectives the project has been split in 3 phases:

1. Phase 1: Define range of array geometries consistent with objectives and water depth
2. Phase 2: Source array modelling using industry standard software
3. Phase 3: Modelling of "noise" signature associated with these different arrays within frequency range likely to impact marine mammals. Definition of lowest impact array/ exclusion zone associated with that array

In addition to this Petroceltic would like feedback on the proposed survey polygon with focus on fully imaging current leads whilst considering constraints, environmental or otherwise. This work is detailed in Appendix B.

1.2   Legacy Seismic Data

Existing seismic datasets consist of loose grid publicly available Ministerial data acquired in 1975 on a 10x10km grid, and 553 km 2D seismic acquired in 2001 by Western Geco.

The Ministerial data was acquired with a 2400m long streamer with 48 channels separated by 50m and towed at 19m. An 8Hz low cut acquisition filter was applied significantly reducing the low frequencies. A Vaporchoc source was used and this was towed at 6m.

The 2001 2D data was acquired with a 5000m streamer with 400 channels at 8m tow depth and 12.5m spacing and a shot spacing of 25m with a 6m tow depth.

1.3   Environmentally Sensitive Areas

Figure 1-1 displays a map with environmentally sensitive areas around the survey area. The blue dots represents zones of white coral, these areas have high sensitivity. The other high sensitivity area is the orange square which represents the deep sea fisheries restricted area. The area containing orange lines in the North of the polygon represent medium to high sensitivity as it is a scarp area. The grey shaded area represents medium sensitivity due to possible presence of white corals. Finally the green shaded region represents the trawling area where there is likely no white corals, this represents the low sensitivity zones. The sensitivity zones are categorized into colours within the survey polygon on Figure 1-2.
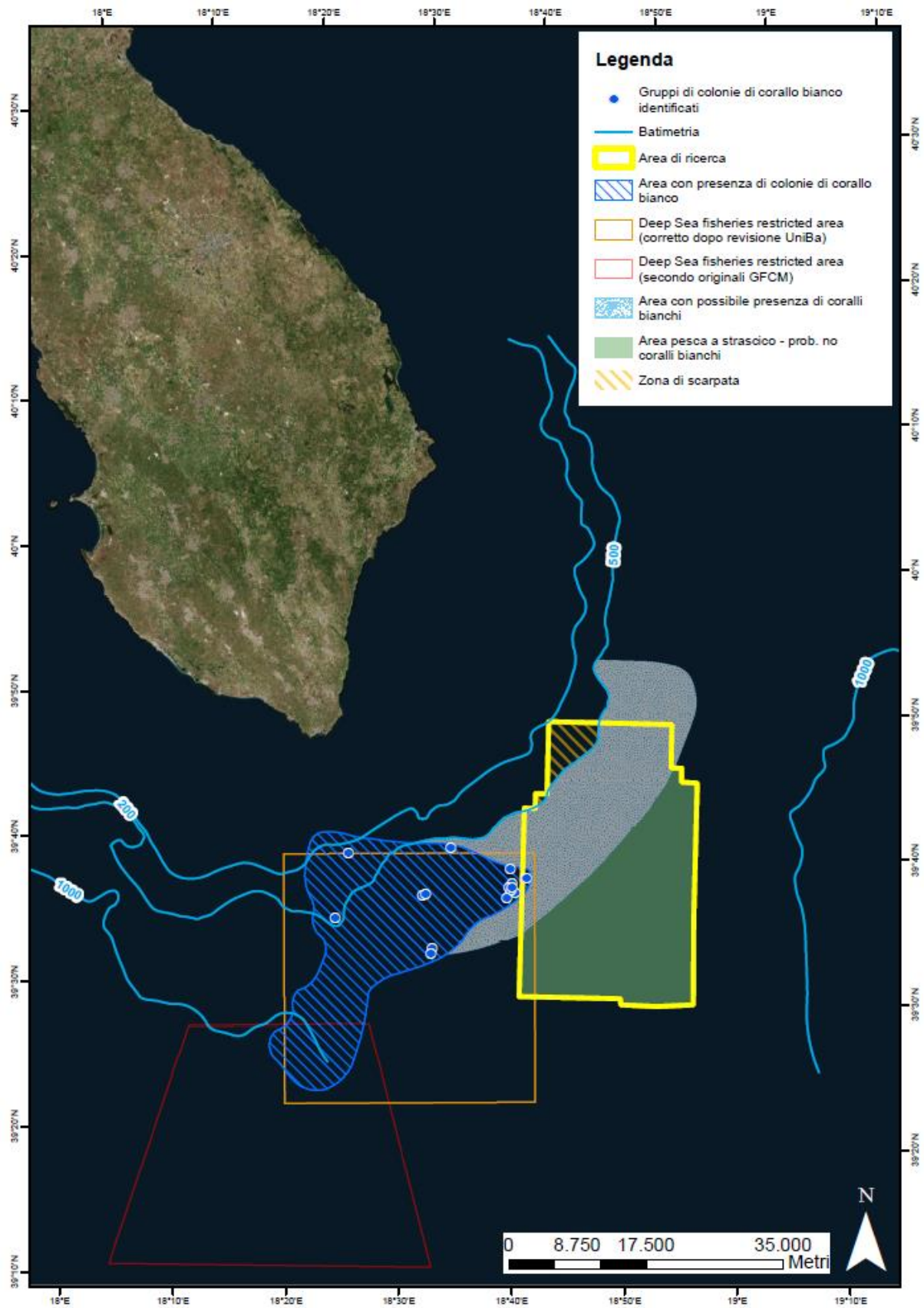
Figure 1-1 - Environmental sensitive areas
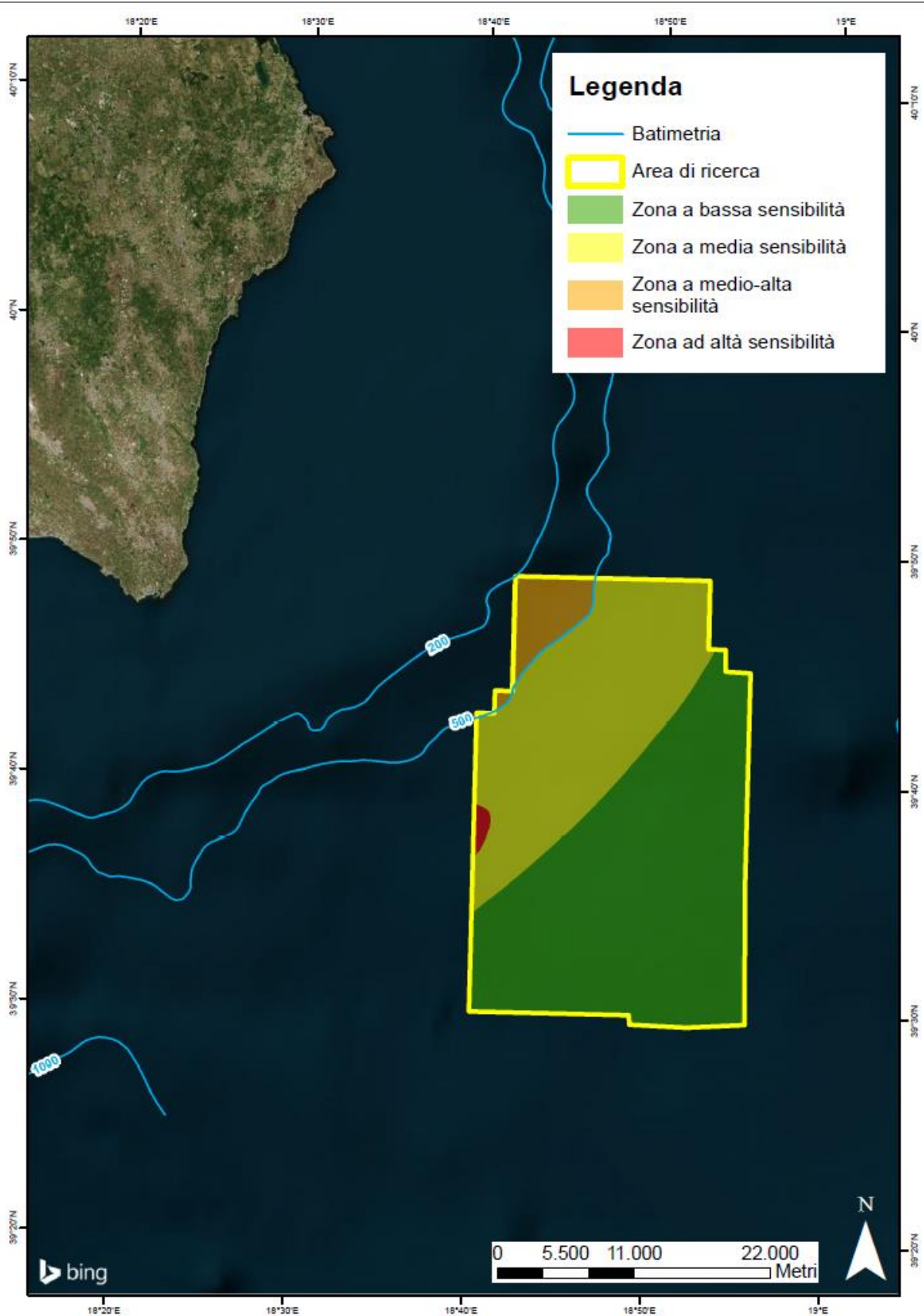
Figure 1-2 – Environmental sensitive regions within survey polygon

1.4   Geological Background

The current geological interpretation is shown on Figure 1-3. We have a classic Adriatic type geology into a deep water setting. Water depth is approximately ~1000m. The two main plays identified within the Carbonate sequence are the Cretaceous slope carbonates – Aquila/Esla analogue and the Liassic platform carbonates – Vega analogue. Figure 1-4 shows a TWT map of the primary objective. There are three structural culminations: F1 NW – large structural culmination ~70km^2 closure. F1 straddles international border into Greek Block 2. F1 S poorly defined lead in south of block.
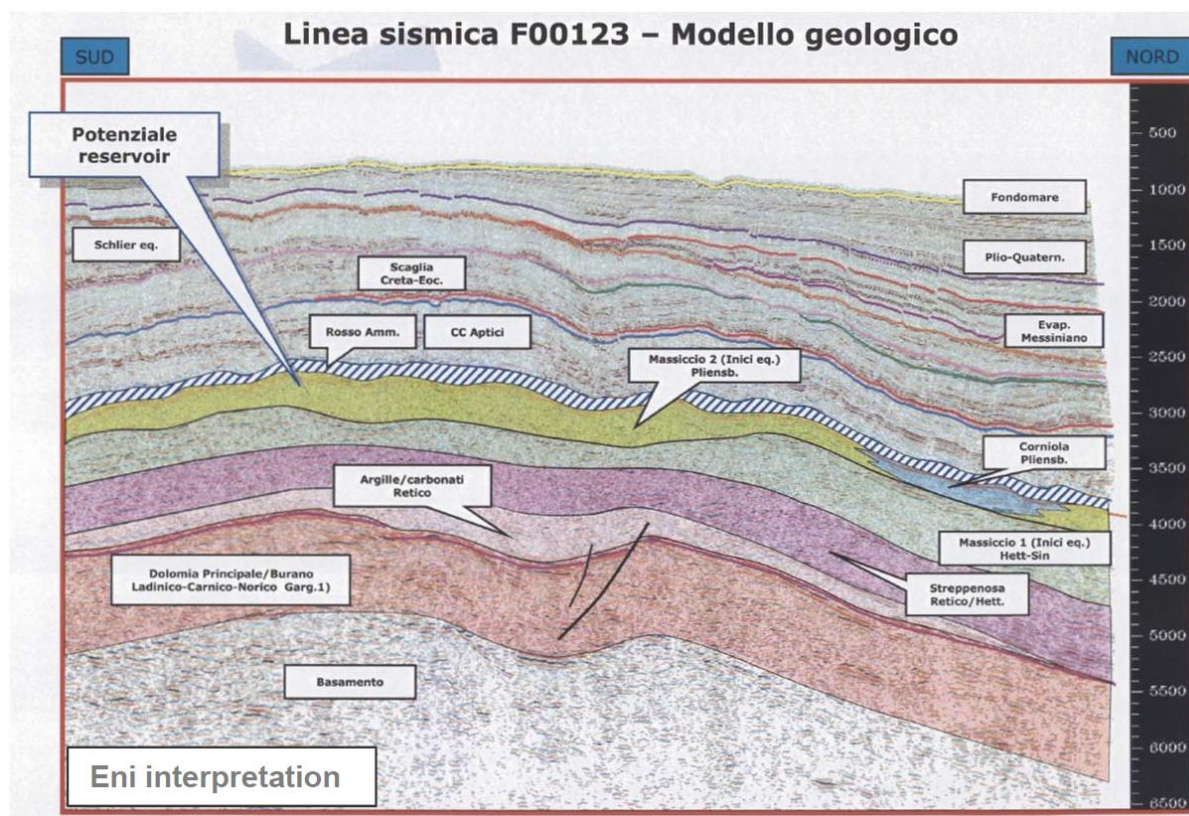
Figure 1-3 – Current interpretation
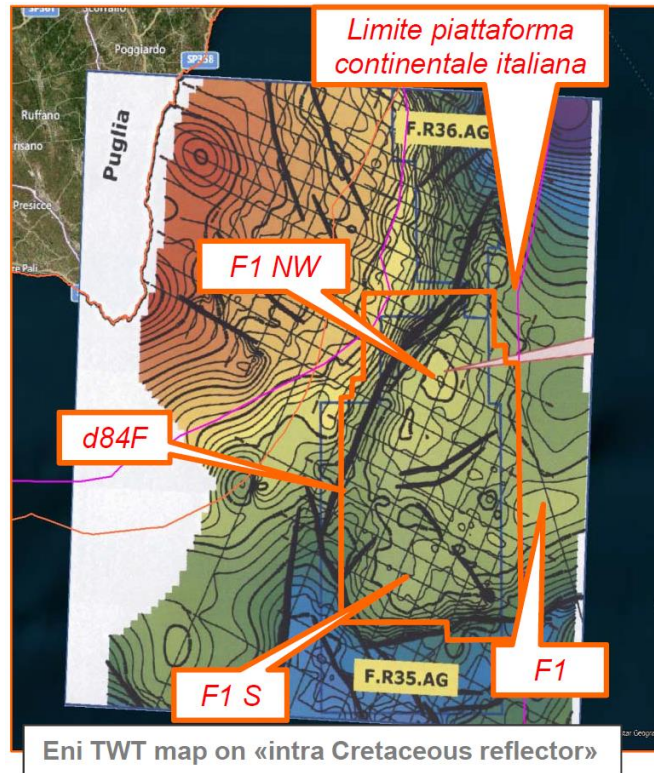
Figure 1-4 - TWT map of intra Cretaceous reflector

2.0   KEY CHARACTERISTICS FOR IMAGING WITH A SEISMIC SOURCE

When considering acoustic seismic sources two key factors need to be taken in to account when considering seismic data quality.   These are:

1. Ambient and undesired source generated energy

2. The temporal bandwidth of the source signature wavelet

2.1   The Marine Seismic Source

A seismic source can be considered as any device which releases energy into the earth in the form of seismic waves. The air-gun array has been the most popular source in the industry since the 1970's. The pulses from an air-gun array are predictable, repeatable and controllable.

Energy sent out from a modern air-gun array is dominantly directed vertically downwards. The broad-band range of frequencies form a pulse with peak-to-peak amplitude in the range 14-28 bar-m. The amplitude levels emitted horizontally tend to be 15-24dB lower. We can quantitatively measure an arrays performance by the vertically downward travelling far-field signature. Two important parameters of an air-gun array signature are its peak-to-peak (P-P) strength and primary to bubble ratio (PBR). The PBR should be as high as possible so that the overall signature is close to an ideal pulse. P-P is a measure of "strength", the useful part of the signal.

When an air gun is fired under water it forms an oscillating bubble due to the pressure differential between the compressed air released and hydrostatic pressure. The oscillating bubble eventually stops due to frictional forces which cause it to break to the sea surface. It is this cyclic motion immediately after the first expansion of the bubble that stops the air gun from being an ideal signal close to a single spike. By using an air gun array we minimize the bubble effects by tuning the array: guns with different volumes will have different bubble periods, leading to a constructive summation of the first primary peak and destructive summation of the bubble amplitudes as demonstrated in Figure 2-1.

This tuning effect is critical to understanding the impact of source volume. Acoustic efficiency is a measure of the total output of an array. Low acoustic efficiency means that more energy is "spent" increasing the PBR. In this way the total output of a large array can be less than that from a smaller more "efficient" array.

In summary then we need to define our ideal source not in terms of volume but in terms of peak to peak amplitude, Peak to bubble ratio and directivity i.e. directing the energy down in to the earth rather than out.
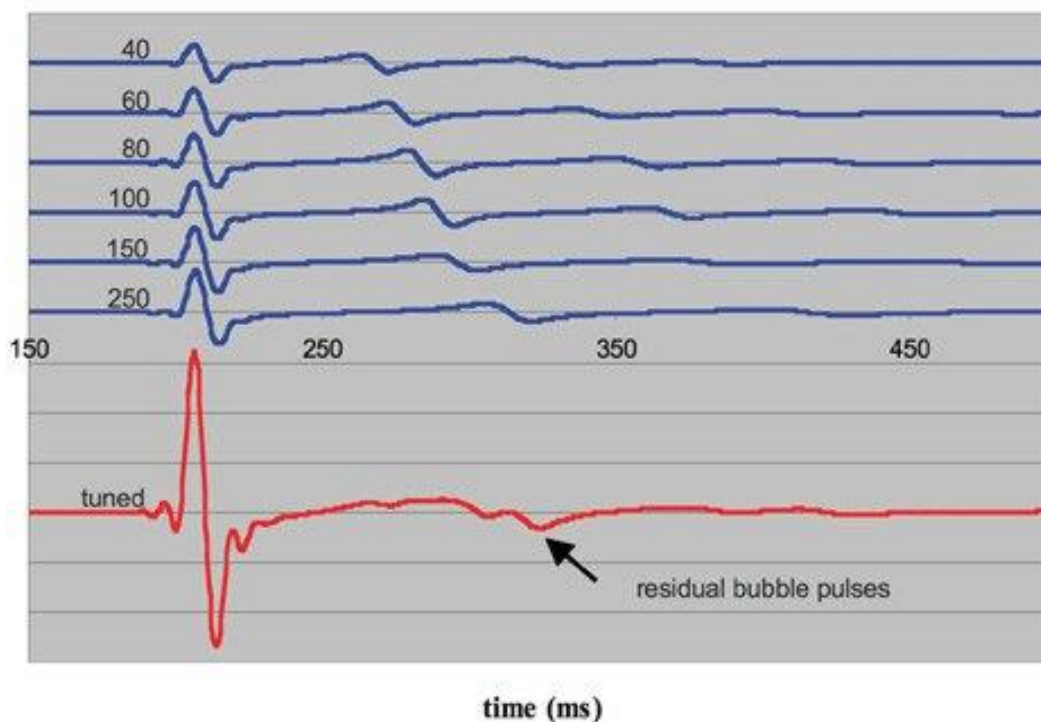
Figure 2-1 – Example far field signatures of individual guns with gun volume labelled. The tuned signature is obtained when the six guns are fired simultaneously ©WesternGeco (taken from Landrø et al. 2010)

2.2   Analysis of Existing Data

Several 2D stacked sections were supplied to RPS from the 1970's vintage. One example, F75-36.sgy is shown on Figure 2-2. The source used was a Vaporchoc source. The Vaporchoc source consists of superheated steam stored in a submerged tank. On the opening of a valve, the steam escapes forming a bubble. As the steam condenses the bubble collapses and finally disappears. The initial steam injection produces a forerunner pulse when the valve is opened, however the main seismic pulse is a result of the collapse of the bubble.

A wavelet was extracted from the data. This was done by first flattening the waterbottom reflection and removing erroneous traces. The preconditioned data is shown in Figure 2-3. The data were then stacked along the flattened water bottom and truncated to 500ms. By stacking along the flattened water bottom it is hoped that any geological affects will average out leaving only a first order estimate of the source wavelet used in the legacy aquistion.

This wavelet is shown in Figure 2-4.   The extracted wavelet is as expected from a Vaporchoc source with an initial pulse followed by a larger pulse as the bubble collapses. Some geology is still present in the source signature as can be sen by the double peak of the pulse folllowing the main pulse nevertheless we have a reasonable first order approximation to source signature used during the 1970's aquisition.
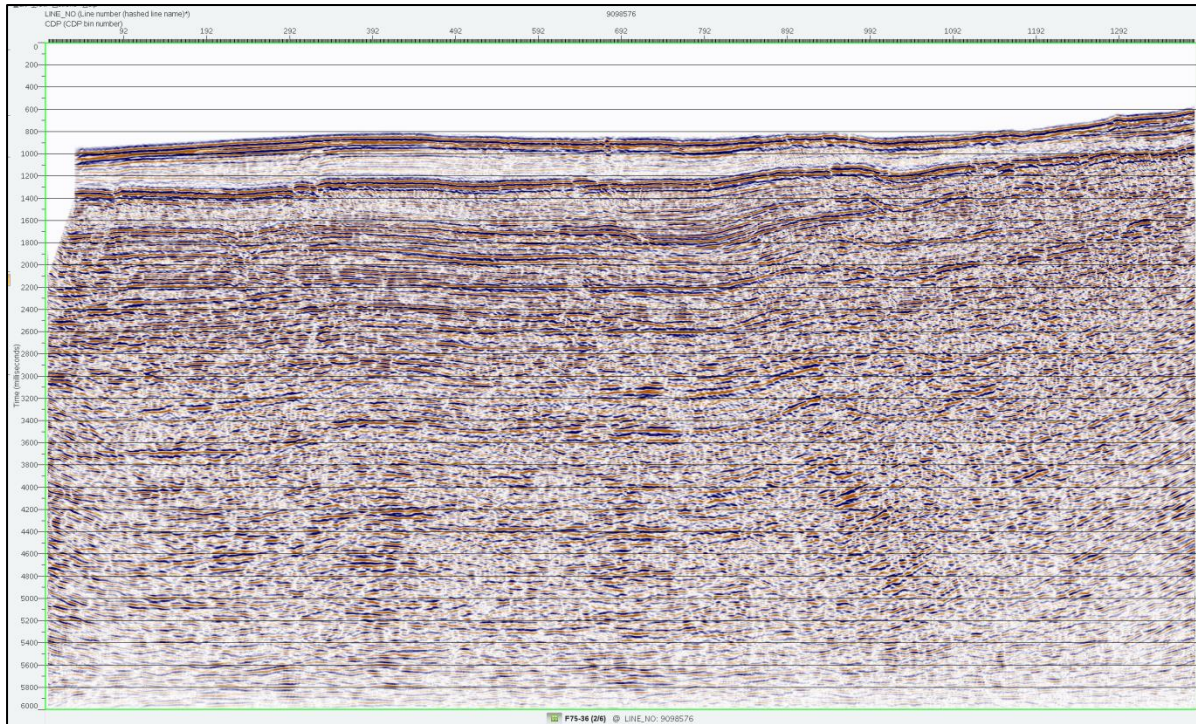
Figure 2-2 - Legacy seismic data F75-36.sgy
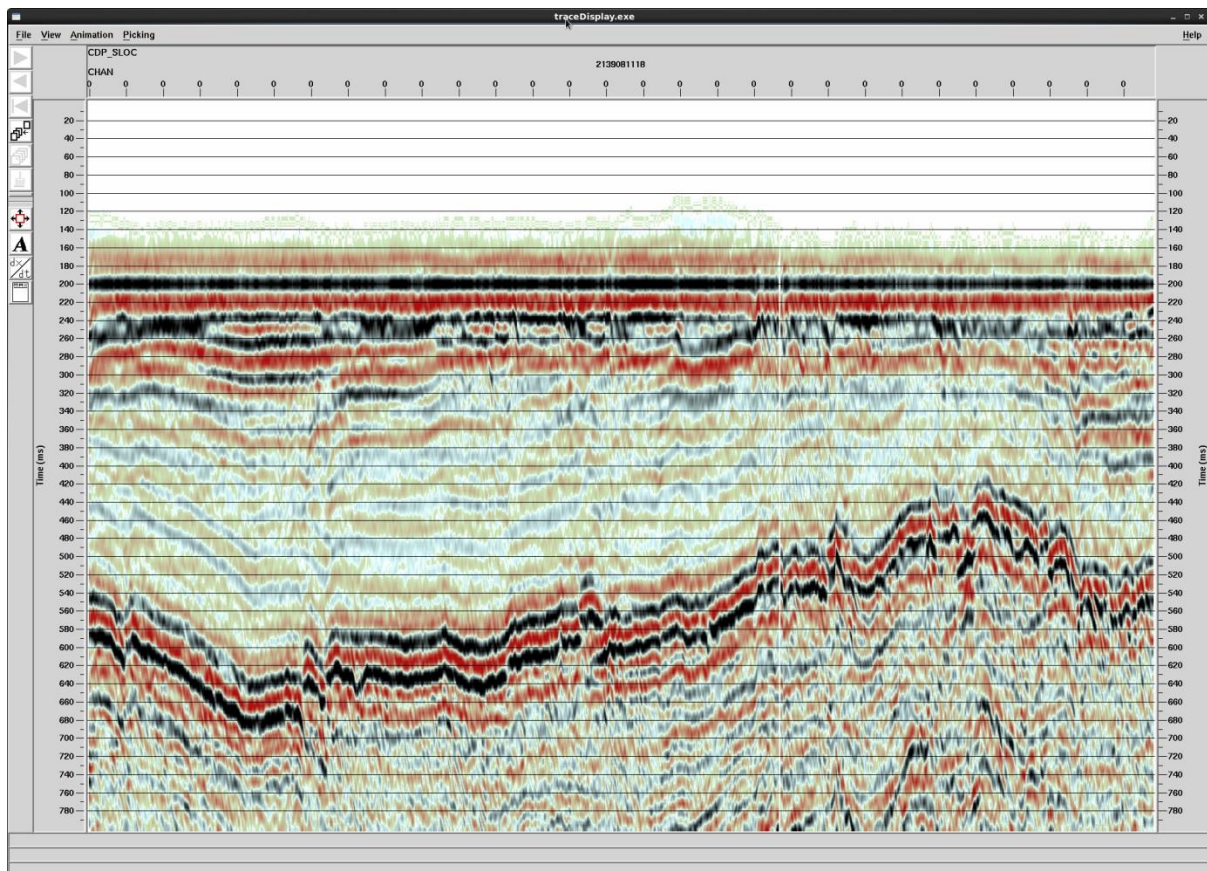
Figure 2-3 - Data pre-conditioning to extract wavelet
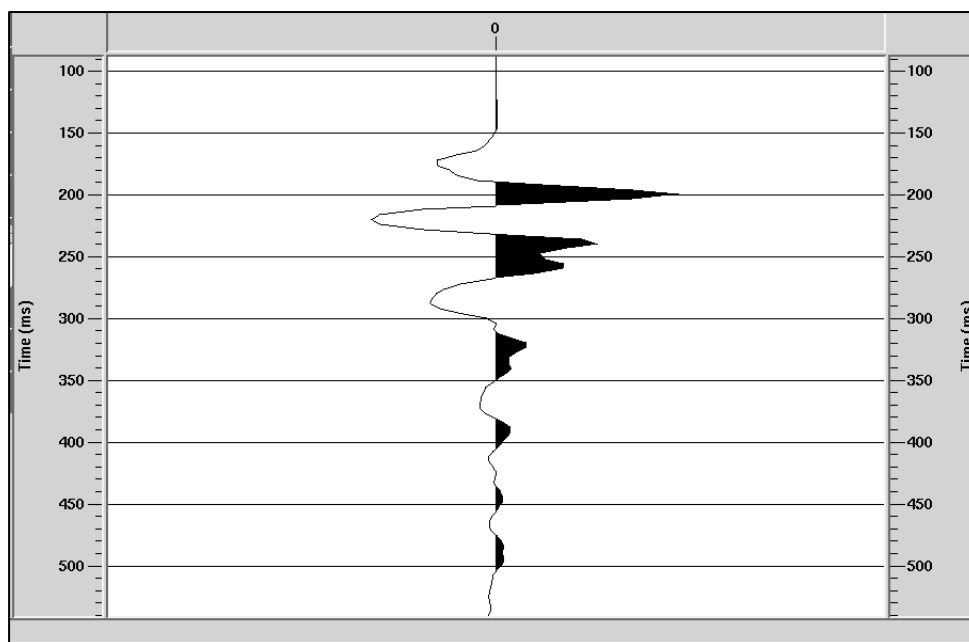
Figure 2-4 - Extracted wavelet

The corresponding amplitude spectrum is shown on Figure 2-5. The 6dB down points are commonly used to measure the useable bandwidth and this is the convention we will use in this report. The useable bandwidth in this case is 12-32Hz. The shape of the spectrum suggests:

- Minimal low frequencies due to the acquisition filters and processing.

- Multiple notches in the spectra due to the streamer ghost (19m tow depth results in a notch every ~40Hz).

The Vaporchoc source is not used any more due to it's unrealibility, the mixed phase of the source signature and its undesirable source charteristics; Low peak to peak and low PBR. In order to make a first order approximation at source signature properties we take the autocorrelation of the extracted wavelet shown in Figure 2-6. The primary to bubble ratio (PBR) is calculated by the ratio of P-P to B-B as shown on the figure. The peak to peak amplitude can not be calculated because we do not know the units used for the ampltude. The resulting value of PBR is ~4 which is extremely low by modern industry standards. Nevertheless the analysis does suggest a low PBR compared to modern standards.

When looking at the legacy data we can see that interpretion would be difficult due to the low peak to bubble ratio and the mixed phase nature of the source signature. In short the legacy data shows us why modern sources have developed as they have toward high PBR and high peak to peak amplitudes.
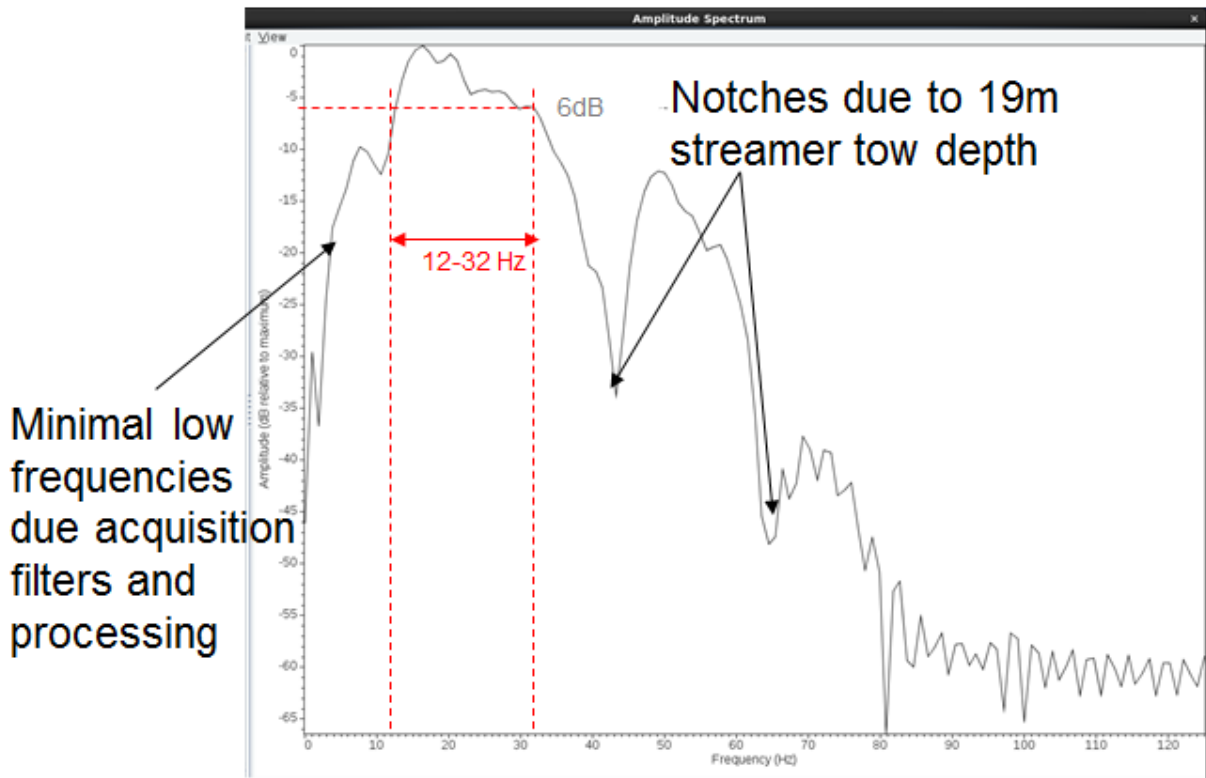
Figure 2-5 - Amplitude spectrum of extracted wavelet
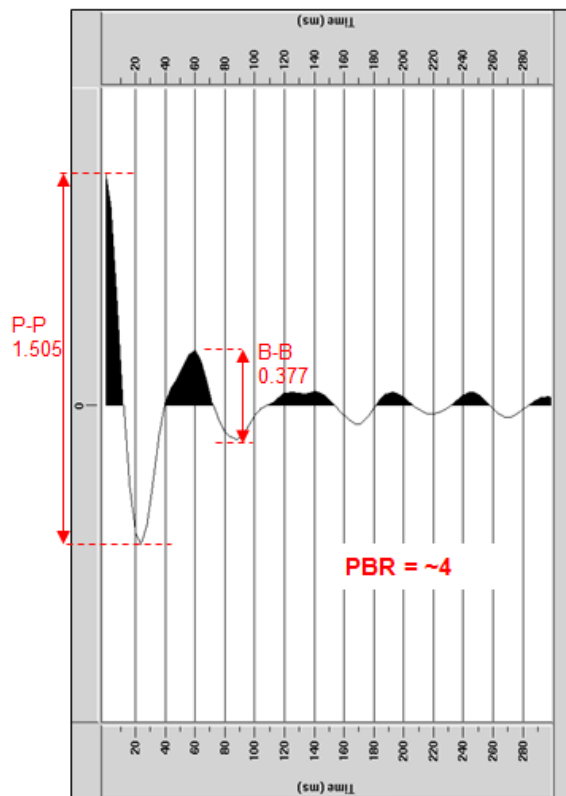
Figure 2-6 - Autocorrelation of extracted wavelet

2.3   Ambient and Source Generated Noise

The conventional understanding is that larger sources are required for improved signal-to-noise ratio and deep penetration. Results from a number of reduced source-strength tests (R.M. Laws et al, 2008) suggest that this is only partly true; at the lower end of the seismic bandwidth, we can benefit from more power (we are governed by non-shot-generated noise such as swell noise, SI, etc..), but for the majority of the seismic bandwidth, we can accept less power (we are governed by shot-generated noise). Note that the article refers to power not source volume.

If a seismic survey is performed twice in quick succession the two images will not be exactly the same. Part of the difference will result from ambient noise and part from shot-generated energy. The shot-generated noise originates both from the previous shot and from perturbations to the acquisition such as small differences in shot and receiver positions i.e. repeatability noise. Only if the ambient noise is higher than the shot-generated noise will increasing the source output improve the overall signal-to-noise ratio of the image.

As discussed above the key characteristic here is peak to peak amplitude. We will later show some examples of industry standard source arrays. This survey area contains some challenging geology with the strong impedance contrasts that will act to reduce source penetration and bandwidth.   The mid cretaceous target sits below the messinian evaporate sequence in places. The messinian evaporates are known regionally to be both a strong multiple generator and depending on thickness a barrier to source penetration. Improving penetration for this target comes at the risk of increasing the amount of multiple but nonetheless signal to noise i.e. high peak to peak amplitude is still important to successfully imaging the mid cretaceous target.   Key to reducing the risk associated with the deeper target; the top Jurassic platform, is imaging of its internal geometry. This is very challenging because internally the reflectivity is low and hence we require very high signal to overcome any noise.   From an acquisition perspective this points towards larger peak to peak amplitude.

2.4   The Temporal Bandwidth of the Source Signature Wavelet

When we consider what are the desirable characteristics of a seismic source from an interpreters perspective, Figure 2-7 taken from Hart et. al. 2013 is a great example of the importance of bandwidth. The top part of the image shows input geology, and the two corresponding images beneath show the area imaged with 1) a 75Hz Ricker wavelet and 2) a 25Hz Ricker wavelet. From these images we can point out that resolution depends on both high and low frequencies, high frequencies will reduce the width of the main lobe and improve resolution, low frequencies reduce the side lobes of a wavelet and reduce the potential interference between two neighboring events, i.e. tuning.
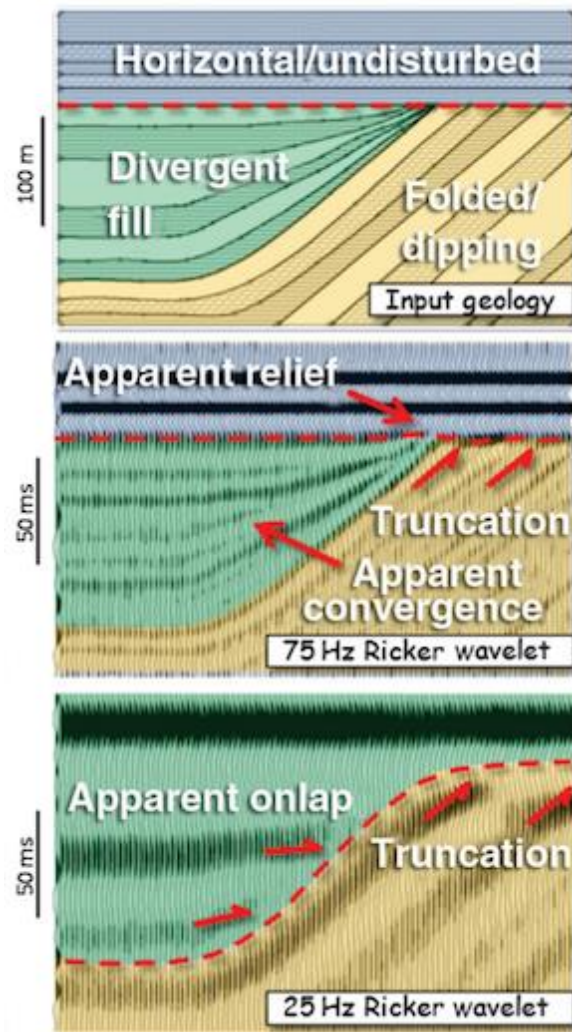
Figure 2-7 - Wavelet comparison

The output of a gun array depends on many factors such as gun size, air pressure, separation of guns, depth of tow, etc. Of the factors affecting spectral content the depth of tow from the sea surface has the greatest effect on the spectral content due to the effect of the ghost. This ghost effect is generated both at source and receiver side of the acquisition system.

The figure below illustrates the effect on available spectra caused by the interaction of source and receiver ghosts at various tow depths.
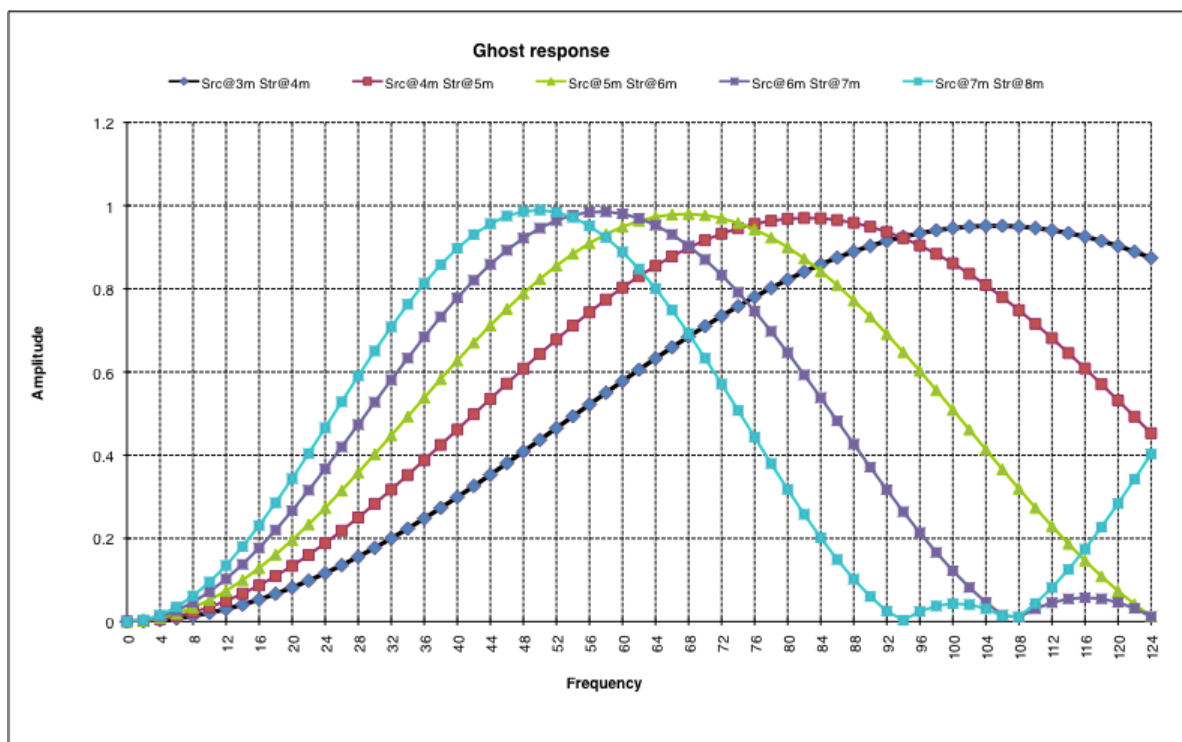
Figure 2-8 - Illustration of the interaction between source and streamer ghost

From this figures we can see that a shallow tow depth will preserve the higher frequencies but the lower frequencies will be attenuated. This can be desirable if the target is shallow and maximum resolution is required. A deep tow depth will preserve the lower frequencies but will suffer from notches in the mid-range frequencies. Such situations can be advantageous if the target is only detectable with low frequencies such as is the case for sub-basalt, sub-salt or difficult data areas. We can see from the legacy source wavelet the negative effect of the 19m tow depth at the high frequencies with multiple notches present in typical usable seismic bandwidth of 4-125Hz.

When we consider the ideal source wavelet we would like a spike. In reality we can only aim to approach this ideal scenario by increasing the bandwidth of our source signature. From an interpreters point of view we want the central peak to be as sharp as possible and we want minimum side lobe energy. Figure 2-9 describes how we can approach the ideal source wavelet by showing the effects of varying bandwidth on a synthetic wavelet. Only by increasing high frequencies can we sharpen the central peak as outlined on the top row of the figure. Only by increasing low frequency content can we reduce side lobes. This example demonstrates the importance of both high and low frequencies.
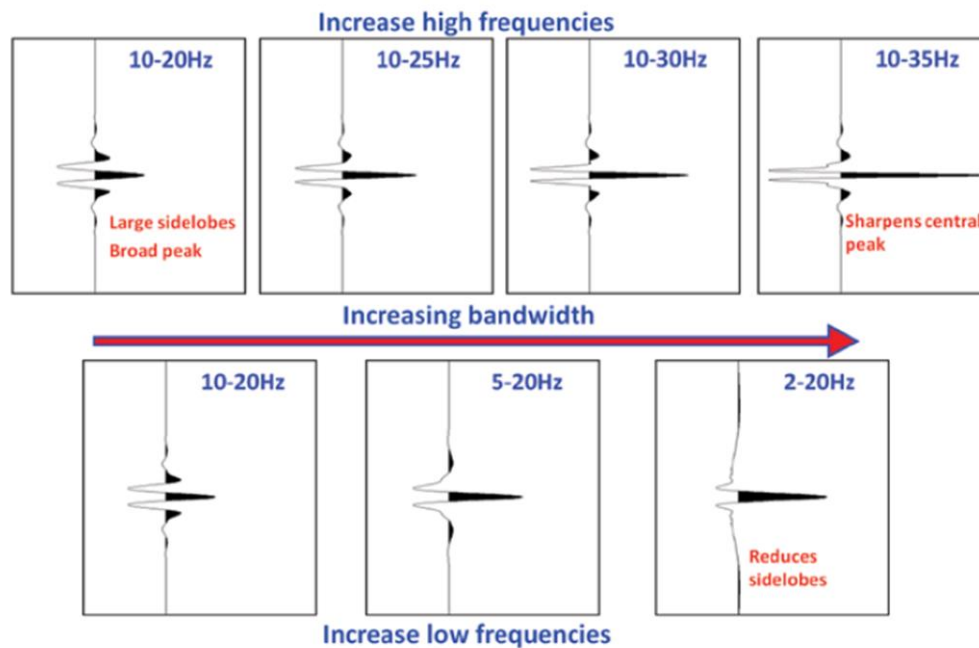
Figure 2-9 - Effect of increasing high and low frequencies on synthetic wavelet (Duval 2012)

We are limited somewhat in how much high frequency energy we can recover due to absorption effects in the Earth. If we wish to improve resolution with 3D seismic we should therefore pay close attention to recovering low frequencies. Increasingly the industry is recognizing the importance of low frequencies in seismic analysis. Low frequencies can be considered to be advantageous in three areas (Kroode et al, 2013):

- Improved resolution
- Increased penetration and reduced scattering of the incident wave field at low frequencies
- Improved outcome of inversion techniques – impedance and waveform inversion

Whilst there are physical limits in marine acquisition on the source side (Hegna et al 2011) and to a more limited extent on the receiver side for towed streamer acquisition to obtaining low frequencies modern broadband and/or deep tow techniques have been demonstrated to deliver an improved low frequency content when compared to standard marine acquisition techniques.

2.5 RPS recommended modern source arrays

One of the key project objectives is to define a range of array geometries consistent with geological objectives and water depth. Using the analysis of legacy data as well as general experience on the subject matter RPS suggests the following bolt-gun arrays:

1. 3640 in^3 @7m

2. 4100 in^3 @7m

3. 4390 in^3 @7m

Array 1 is the Polarcus 3640 in^3 source array and represents the minimum source volume to fulfill the survey objectives as recommended by RPS. Array 2 is the CGG 4100 in^3 source array and represents the medium volume recommended by RPS. The higher volume is the 4390 in^3 source array. All arrays have been modelled at 7m depth which was chosen to maximise bandwidth at target depth.

All three source arrays are industry standard arrays and are proven to work well in a wide range of geological environments. RPS considers the high peak to peak amplitude of ~100bar-m to be suitable for both the primary and secondary targets for the seismic survey. Array 3 is a higher volume source and as expected it has higher P-P strength and PBR. With the larger P-P and PBR on array 3 we anticipate a greater chance of success when we consider the deeper secondary top Jurassic platform target.

As a starting point we will consider the minimum volume Polarcus 3640 in^3 array. We will then consider the other two arrays and discuss their strengths and weaknesses.

2.5.1 Array 1 – 3640 in^3

The 3640 in^3 array is shown on Figure 2-10. The P-P strength is 94.9 bar-m and PBR is 15.2 (assuming DFS-V instrumentation). Proposed depth of tow is 7m. It is RPS opinion that a source volume of this magnitude represents a good solution. That is to say it will be widely available and meets or exceeds the required characteristics.

Specific details on the source array modelling are as follows:

- Modeled using SERES/Nucleus Software by Greg Glanville (RPS)
- All models sampled at 0.5ms.
- Filters used include:
  - Out-800/375 0.8 Nyquist Minimal Phase filter for 0-1000hz bandwidth displays.
  - Standard DFSV Out-128/72 for source comparisons
  - Sercel Seal Out-200/370 – typical production filter.
- **Note:** The Out-200/370 Seal filter includes the analog 3 Hz 6dB/octave streamer response.

Figure 2-11 - Figure 2-13 display the far field signature, relative and absolute spectra for the Filter Out-800/375 model. Figure 2-14 - Figure 2-16 display directivity plots for azimuths of 0, 45 and 90 degrees respectively. Figure 2-17 - Figure 2-19 display directivity plots for vertical angles of 0, 45 and 90 degrees respectively. Figure 2-20 - Figure 2-26 display directivity plots at various frequencies between 30-1000Hz.

Note that directivity can negatively impact data quality. In this regard it is recommended that any proposed source arrays have a minimum of two strings. Directional de-signature is offered by many processing contractors and can be used in processing to mitigate the effects of source array directionality on data quality and AVA.

Figure 2-27 - Figure 2-29 display the far field signature, relative and absolute spectra for the model filtered with standard DFSV Out-128/72. Finally Figure 2-30 - Figure 2-32 display the far field signature, relative and absolute spectra for the model filtered with Sercel Seal Out-200/370.

Array : Pol3640-7m

Total volume : 3640.0 cubic inch

◀ - Active guns
◁ - Inactive guns
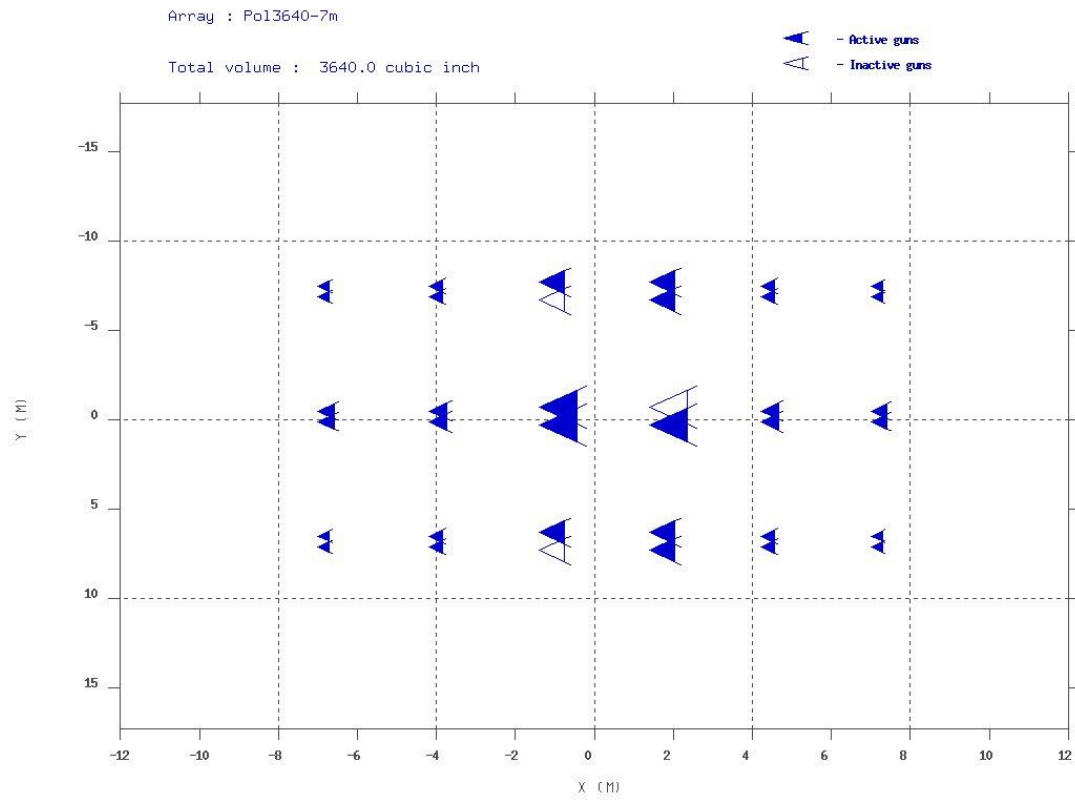
Figure 2-10 - POL3640@7m_Array_Layout

Far-field signature of array: Pol3640-7m
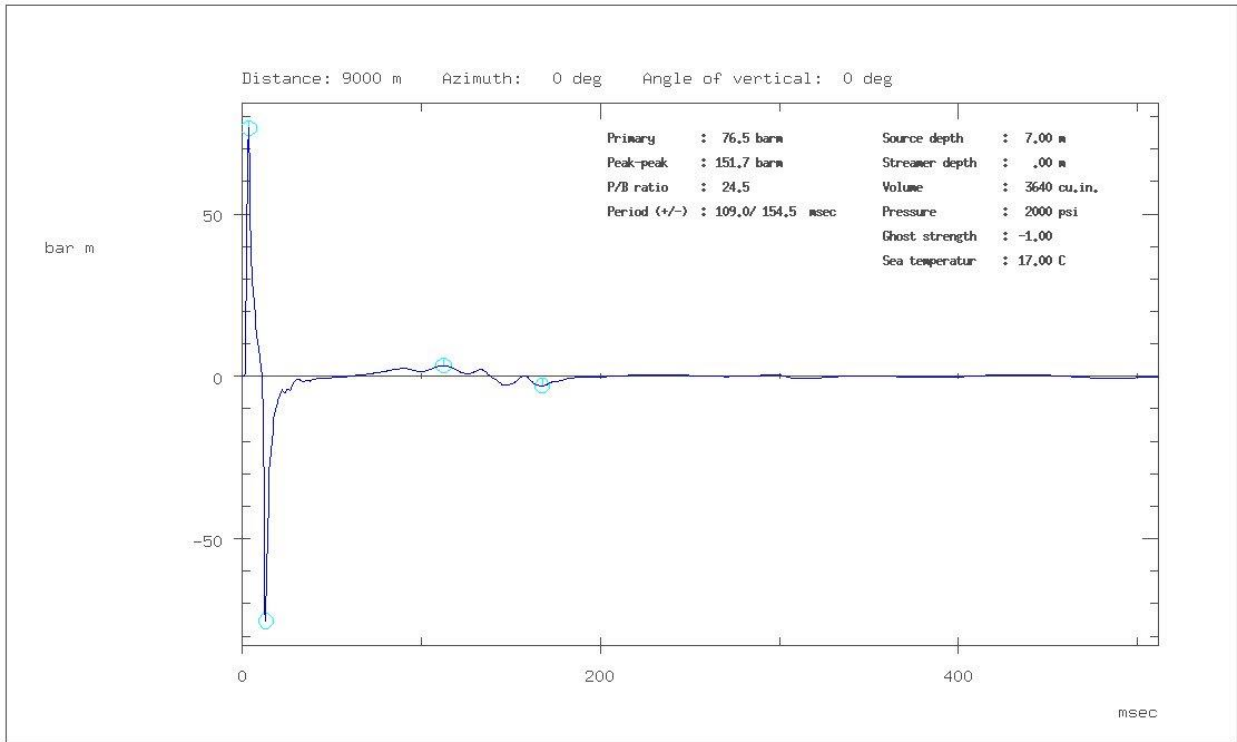
POL3640@7M Out-800/375 0.8 Nyquist Filter

Figure 2-11 - POL3640@7m_OUT-800-375_signature

Amplitude spectrum of far-field signature of array: Pol3640-7m

Distance: 9000 m   Azimuth: 0 deg   Angle of vertical: 0 deg
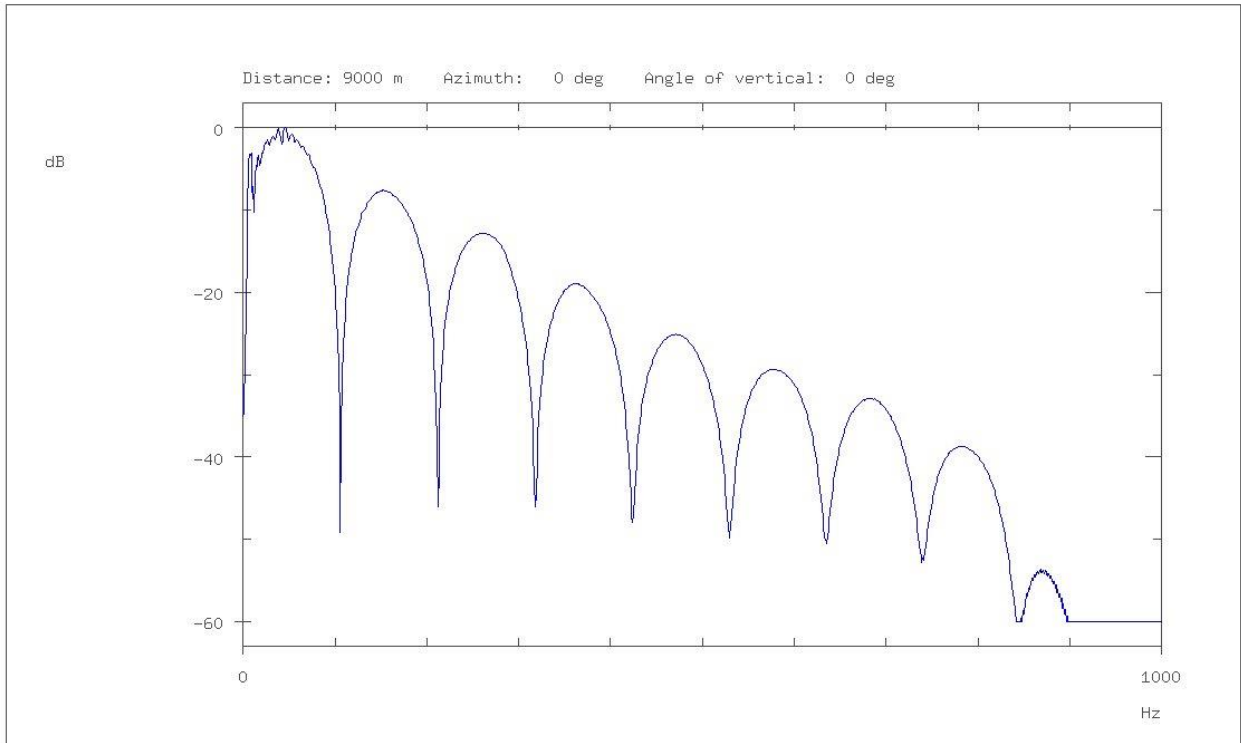
POL3640@7M Out-800/375 0.8 Nyquist Filter

Figure 2-12 - POL3640@7m_OUT-800-375_Relative_Spectrum

Amplitude spectrum of far-field signature of array: Pol3640-7m

Distance: 9000 m   Azimuth: 0 deg   Angle of vertical: 0 deg

POL3640@7M Out-800/375 0.8 Nyquist Filter

Figure 2-13 - POL3640@7m_OUT-800-375_Absolute_Spectrum
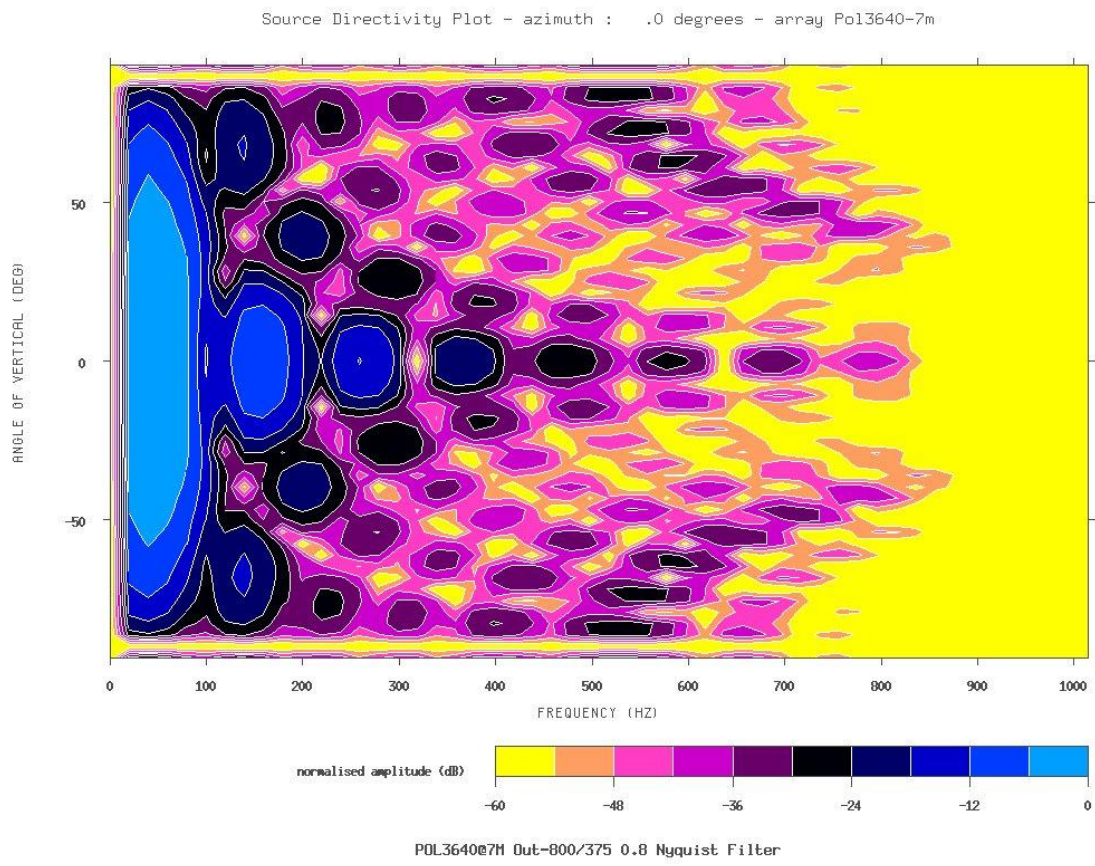
Figure 2-14 - POL3640@7m_OUT-800-375_Directivity_Azimuth_0deg_0-1000Hz

Source Directivity Plot – azimuth : 45.0 degrees – array Pol3640-7m

POL3640@7M Out-800/375 0.8 Nyquist Filter
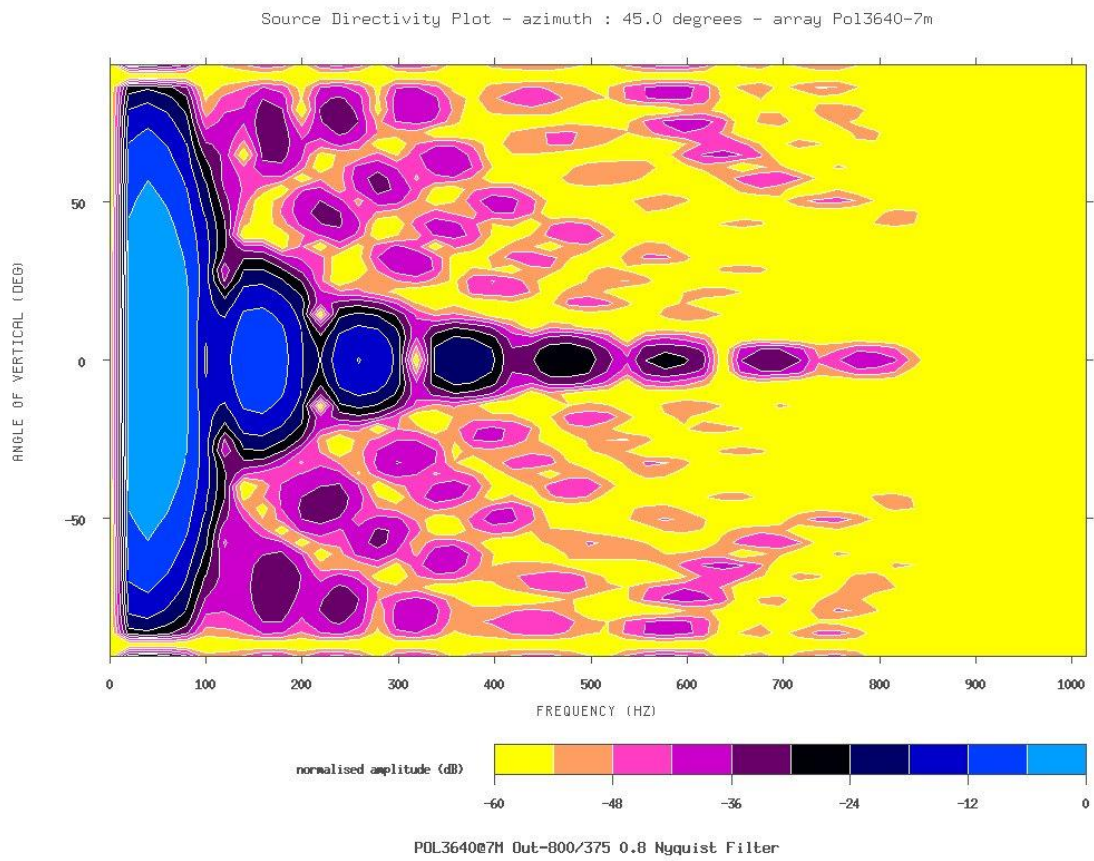
Figure 2-15 - POL3640@7m_OUT-800-375_Directivity_Azimuth_45deg_0-1000Hz

Source Directivity Plot – azimuth : 90.0 degrees – array Pol3640-7m

POL3640@7M Out-800/375 0.8 Nyquist Filter
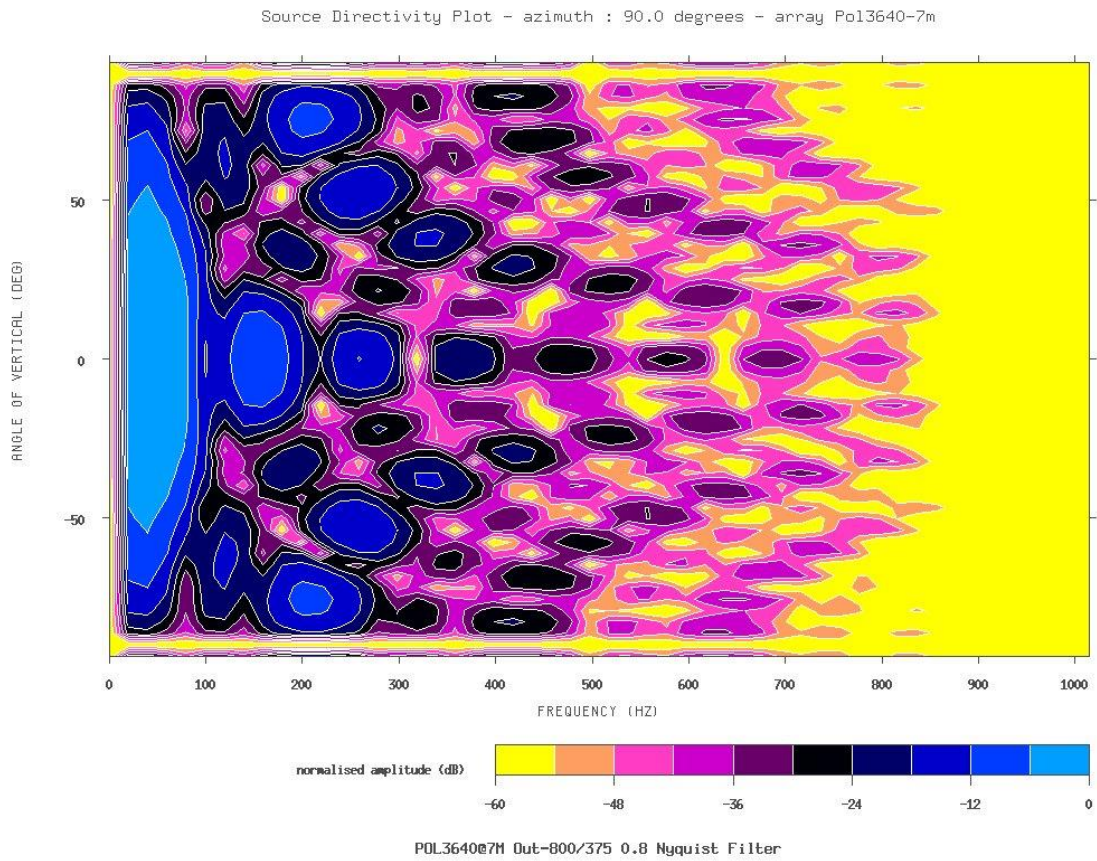
Figure 2-16 - POL3640@7m_OUT-800-375_Directivity_Azimuth_90deg_0-1000Hz
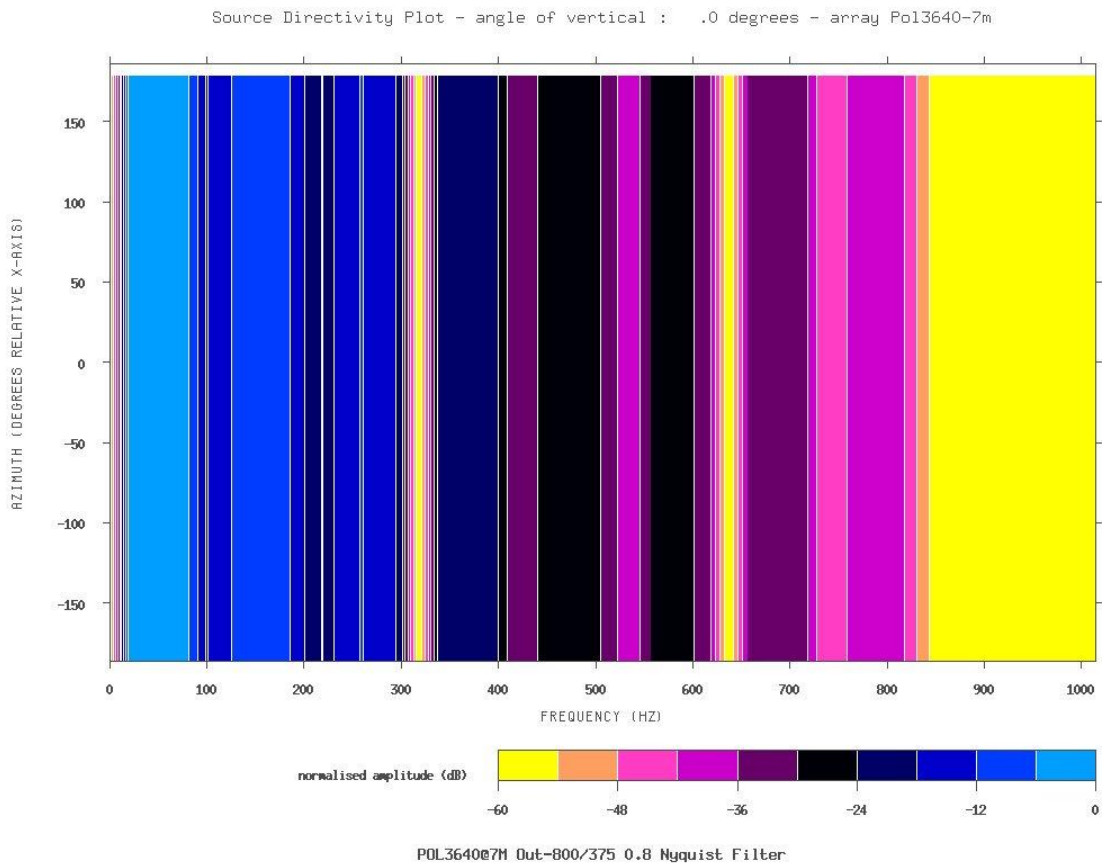
Figure 2-17 - POL3640@7m_OUT-800-375_Directivity_Angle_of_Vertical_0deg_0-1000Hz

Source Directivity Plot - angle of vertical : 45.0 degrees - array Pol3640-7m

POL3640@7M Out-800/375 0.8 Nyquist Filter
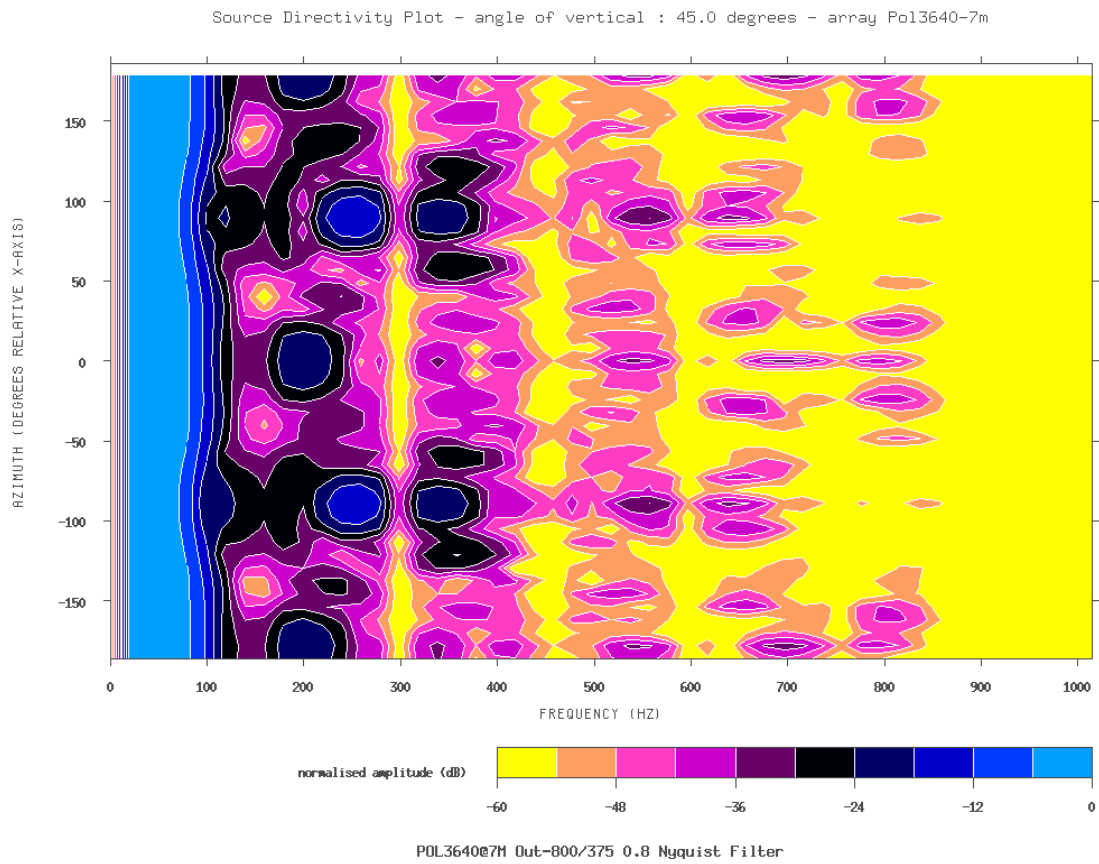
Figure 2-18 - POL3640@7m_OUT-800-375_Directivity_Angle_of_Vertical_45deg_0-1000Hz

Source Directivity Plot — angle of vertical : 90.0 degrees — array Pol3640-7m

POL3640@7M Out-800/375 0.8 Nyquist Filter
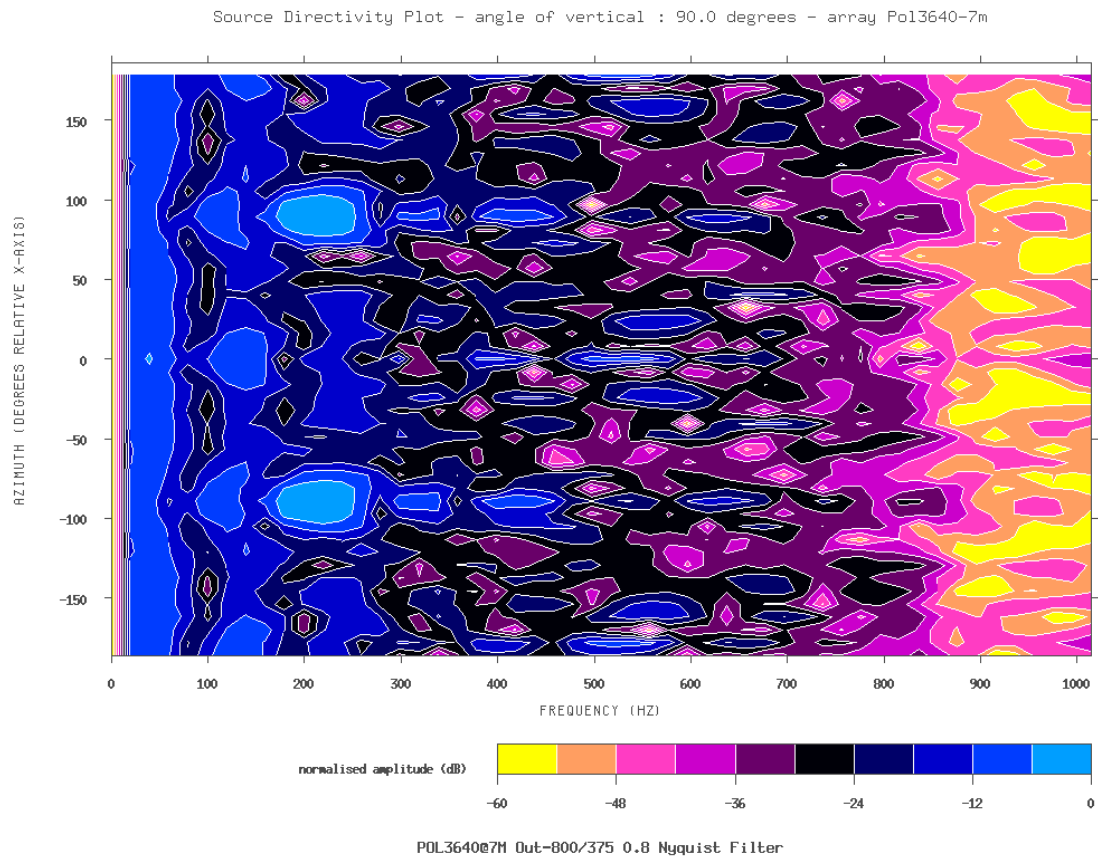
Figure 2-19 - POL3640@7m_OUT-800-375_Directivity_Angle_of_Vertical_90deg_0-1000Hz

Source Directivity Plot – frequency : 30.0 Hz. – array Pol3640-7m

POL3640@7M Out-800/375 0.8 Nyquist Filter
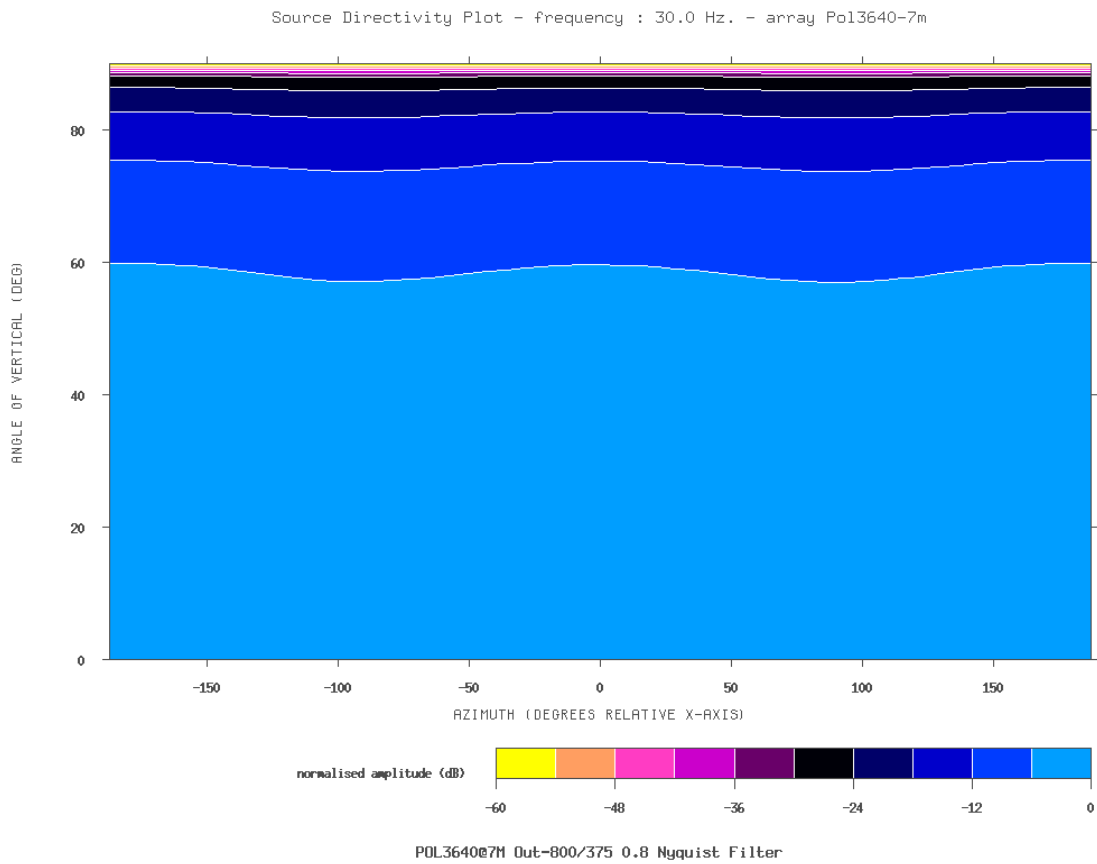
Figure 2-20 - POL3640@7m_OUT-800-375_Directivity_Frequency_30_Hz

Source Directivity Plot - frequency :100.0 Hz. - array Pol3640-7m

POL3640@7M Out-800/375 0.8 Nyquist Filter
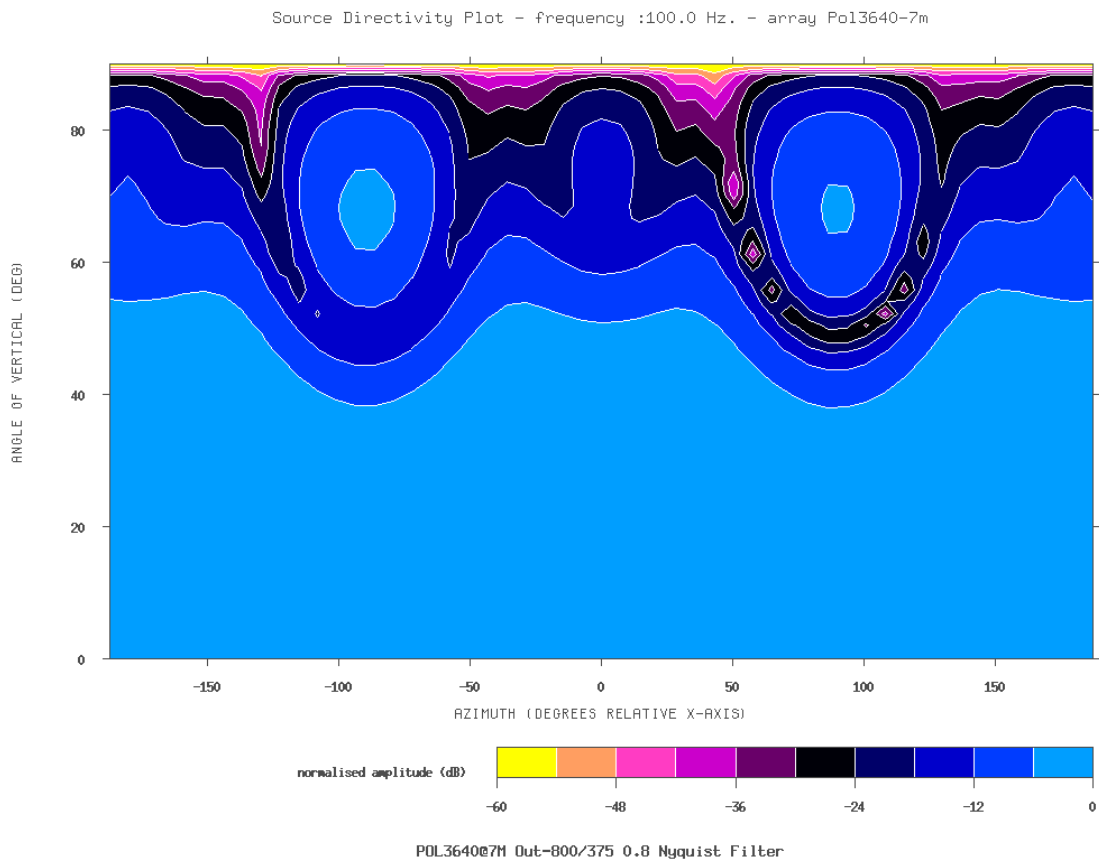
Figure 2-21 - POL3640@7m_OUT-800-375_Directivity_Frequency_100_Hz

Source Directivity Plot — frequency :200.0 Hz. — array Pol3640-7m

POL3640@7M Out-800/375 0.8 Nyquist Filter
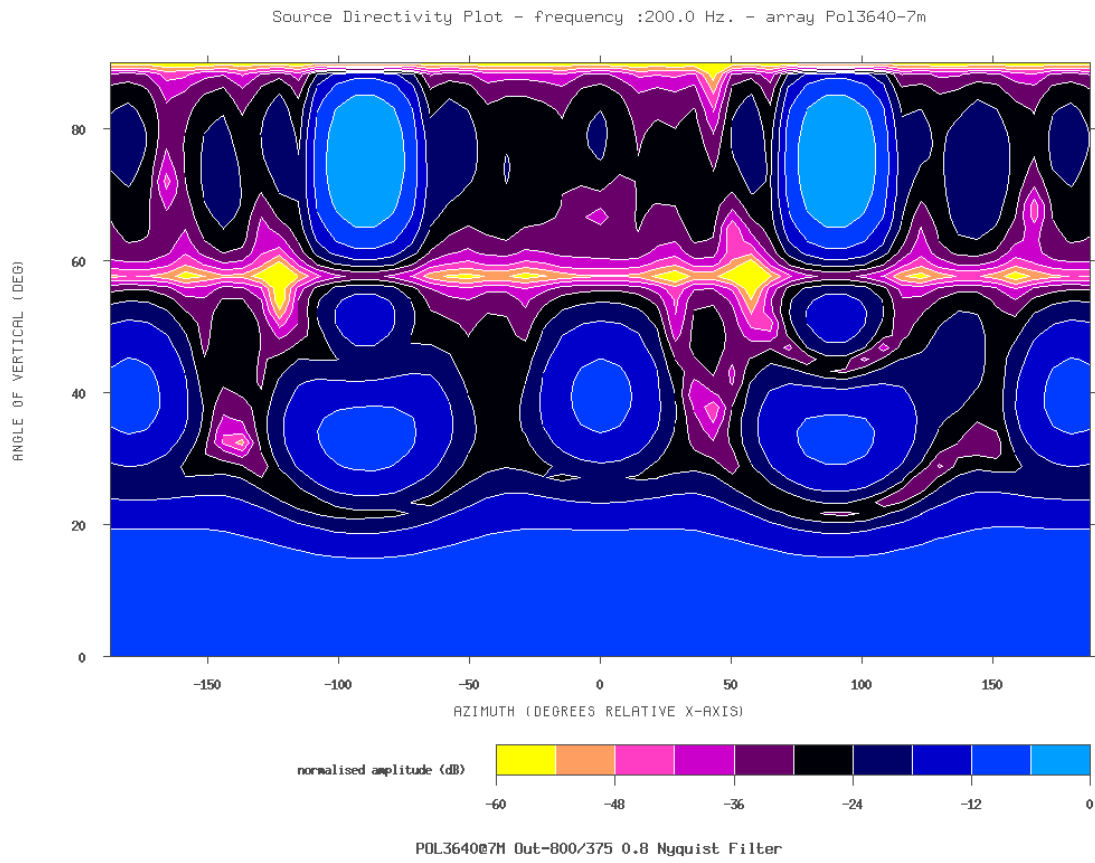
Figure 2-22 - POL3640@7m_OUT-800-375_Directivity_Frequency_200_Hz
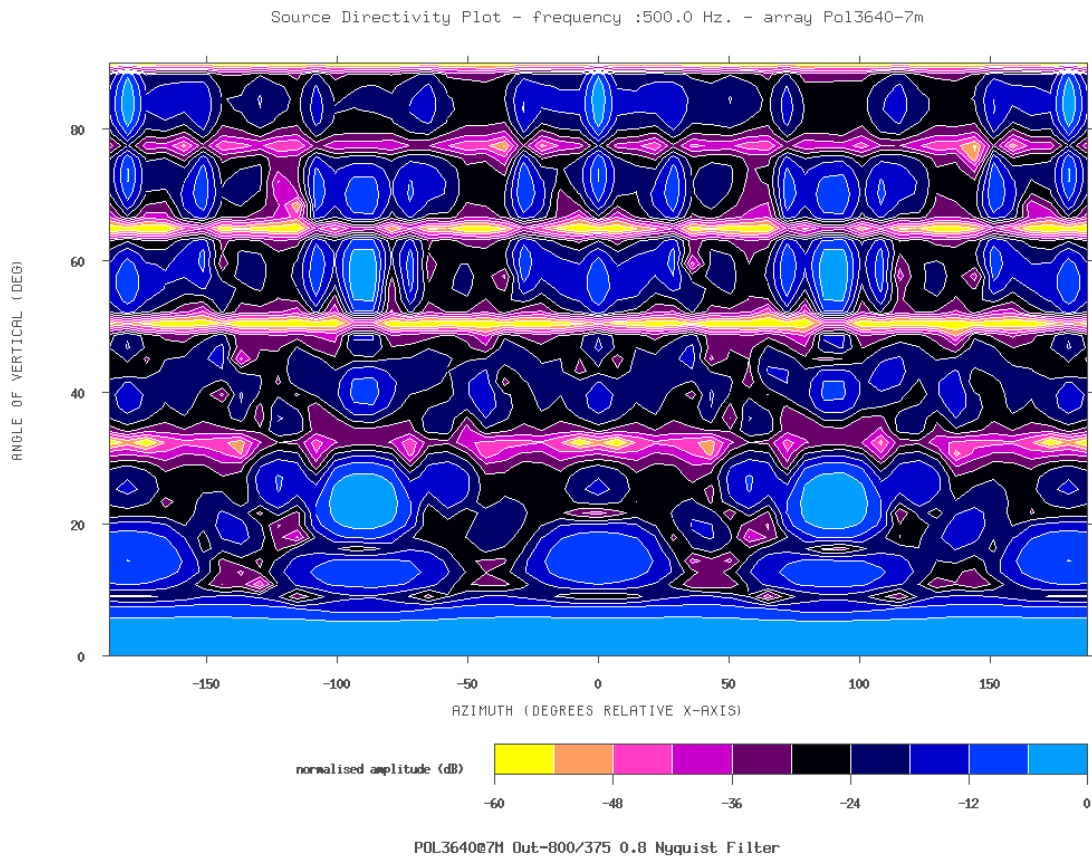
Figure 2-23 - POL3640@7m_OUT-800-375_Directivity_Frequency_500_Hz
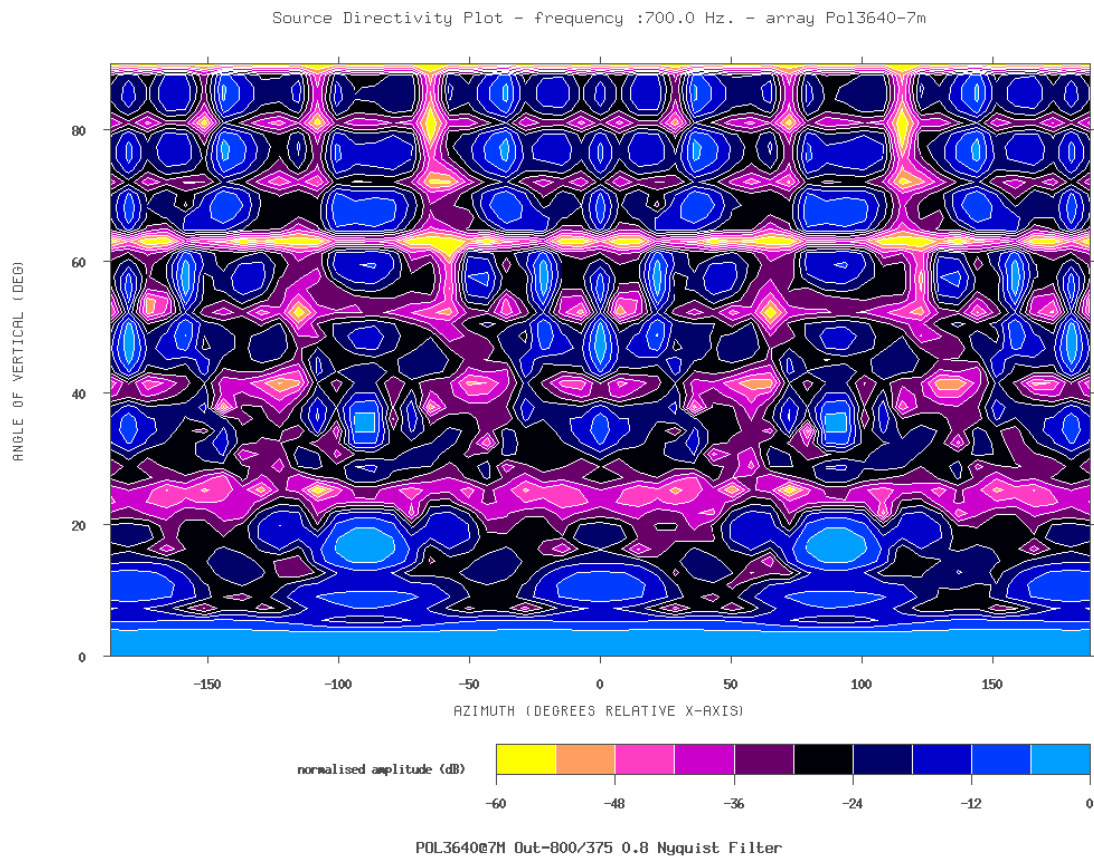
Figure 2-24 - POL3640@7m_OUT-800-375_Directivity_Frequency_700_Hz

Source Directivity Plot — frequency :900.0 Hz. — array Pol3640-7m

POL3640@7M Out-800/375 0.8 Nyquist Filter
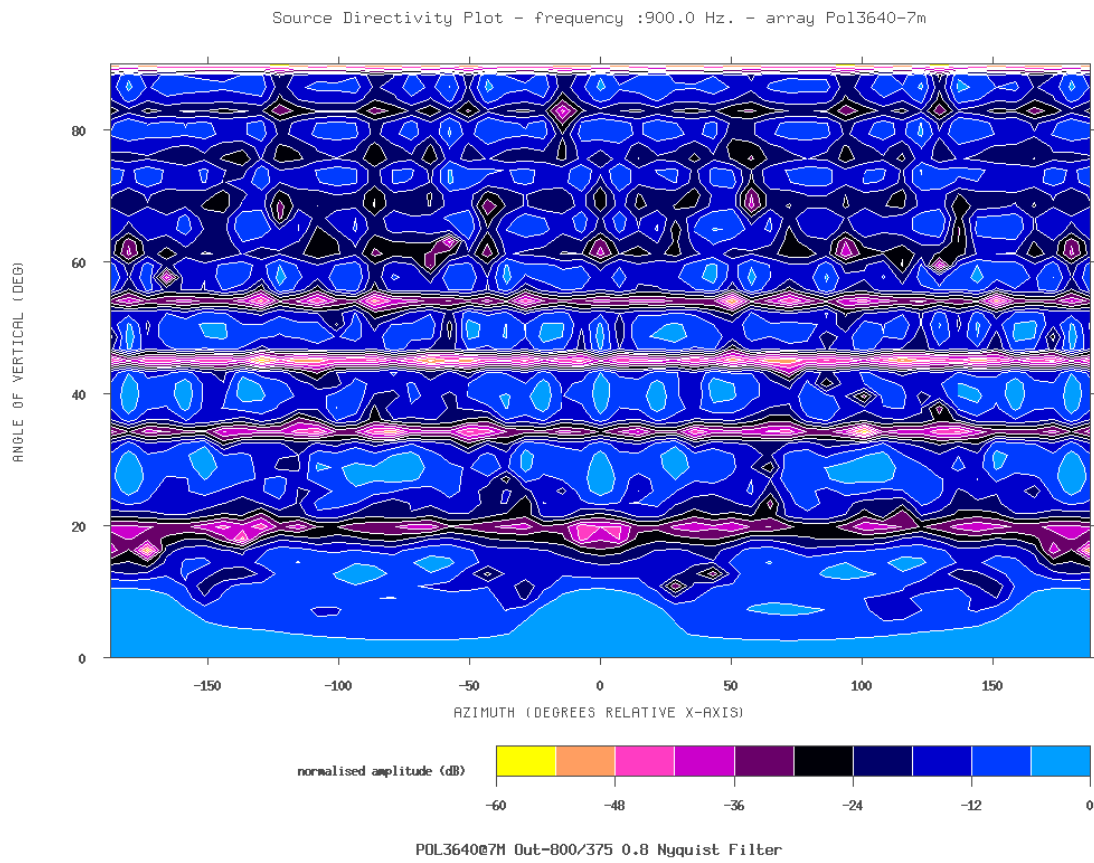
Figure 2-25 - POL3640@7m_OUT-800-375_Directivity_Frequency_900_Hz
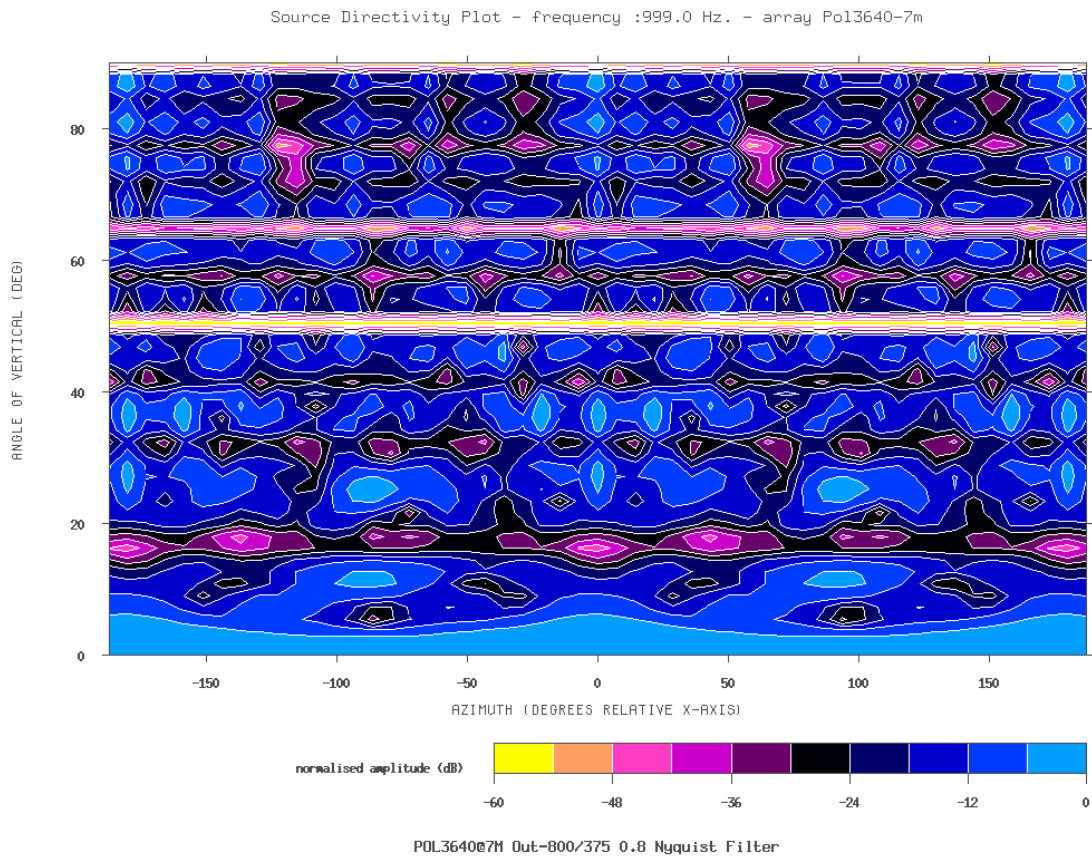
Figure 2-26 - POL3640@7m_OUT-800-375_Directivity_Frequency_999_Hz
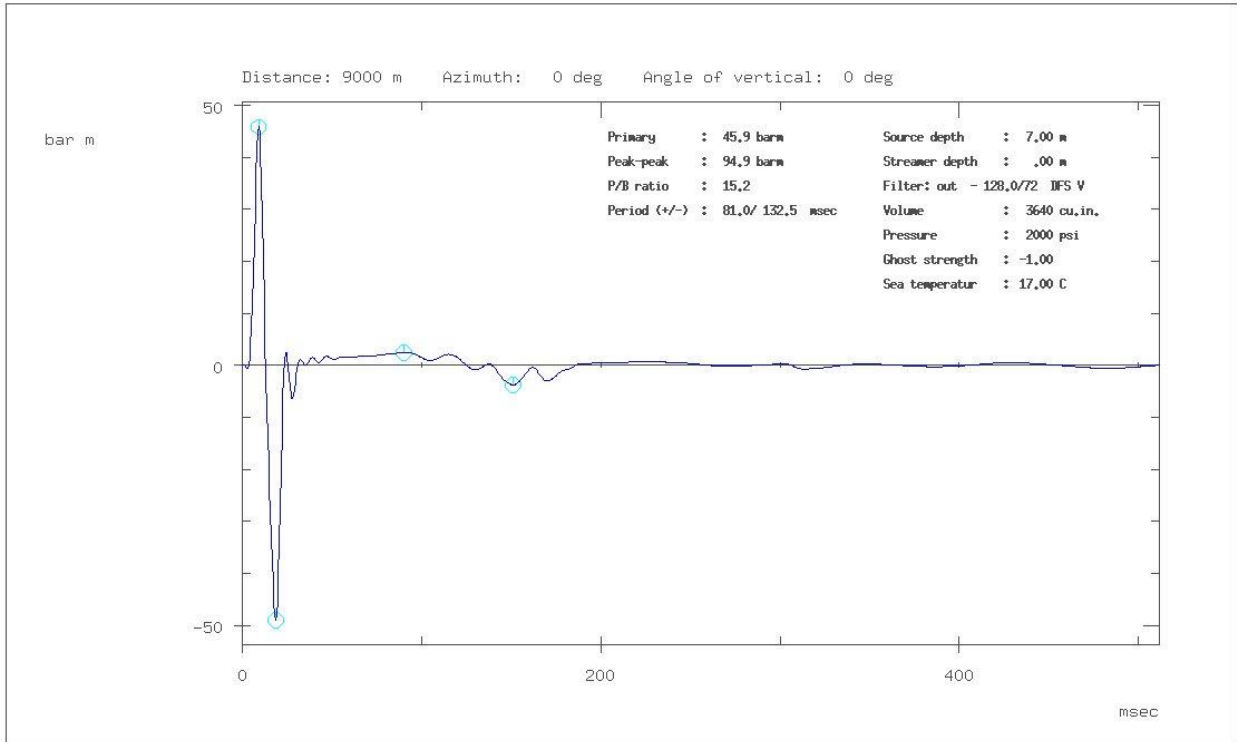
Figure 2-27 - POL3640@7m_DFSV_OUT-128-72_signature

Amplitude spectrum of far-field signature of array: Pol3640-7m

Distance: 9000 m   Azimuth: 0 deg   Angle of vertical: 0 deg
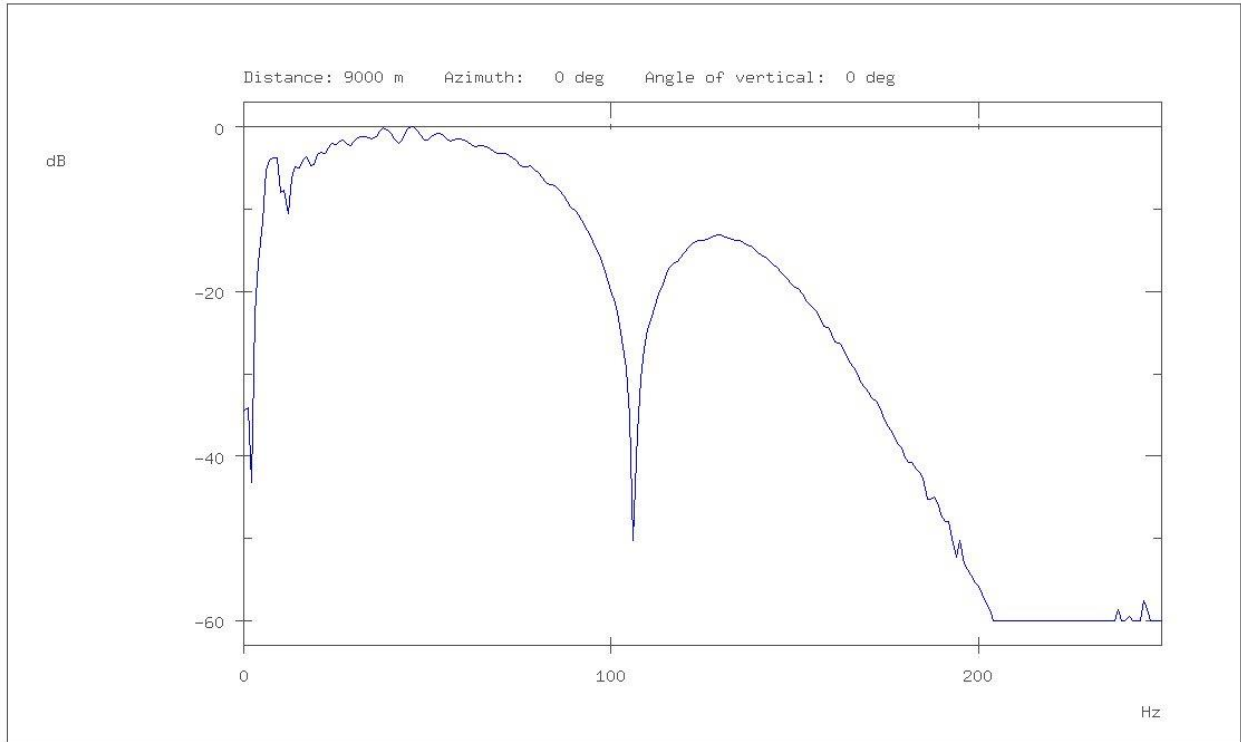
POL 3640@7M DFSV Out-128/72 Filter

Figure 2-28 - POL3640@7m_DFSV_OUT-128-72_Relative_Spectrum

Amplitude spectrum of far-field signature of array: Pol3640-7m

Distance: 9000 m   Azimuth: 0 deg   Angle of vertical: 0 deg
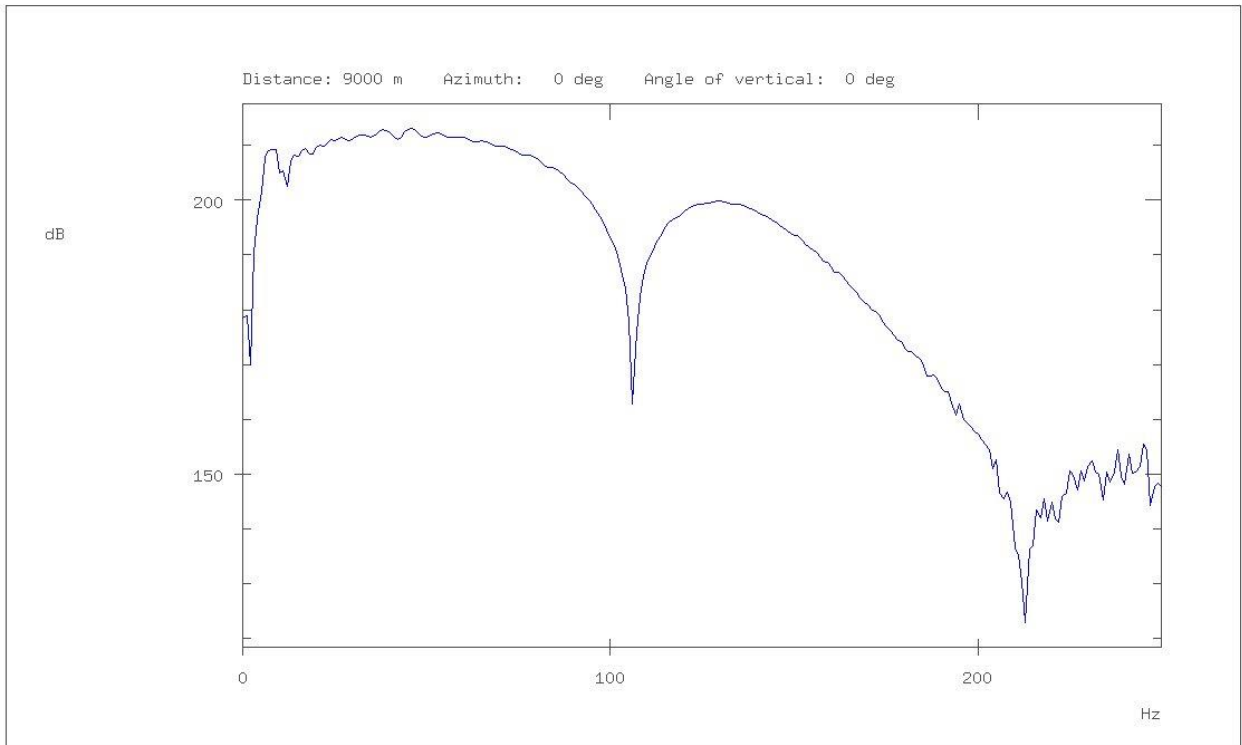
POL 3640@7M DFSV Out-128/72 Filter

Figure 2-29 - POL3640@7m_DFSV_OUT-128-72_Absolute_Spectrum
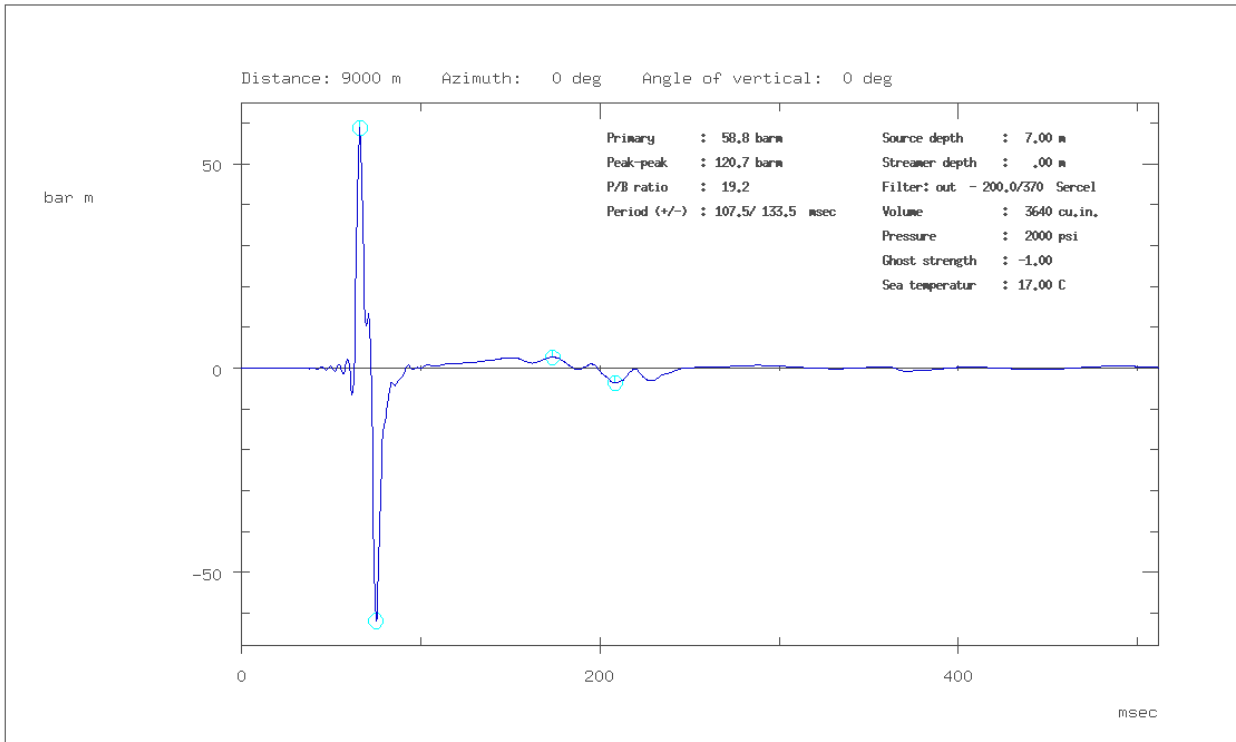
Far-field signature of array: Pol3640-7m

Figure 2-30 - POL3640@7m_Seal_OUT-200-370_signature

Amplitude spectrum of far-field signature of array: Pol3640-7m

Distance: 9000 m   Azimuth: 0 deg   Angle of vertical: 0 deg
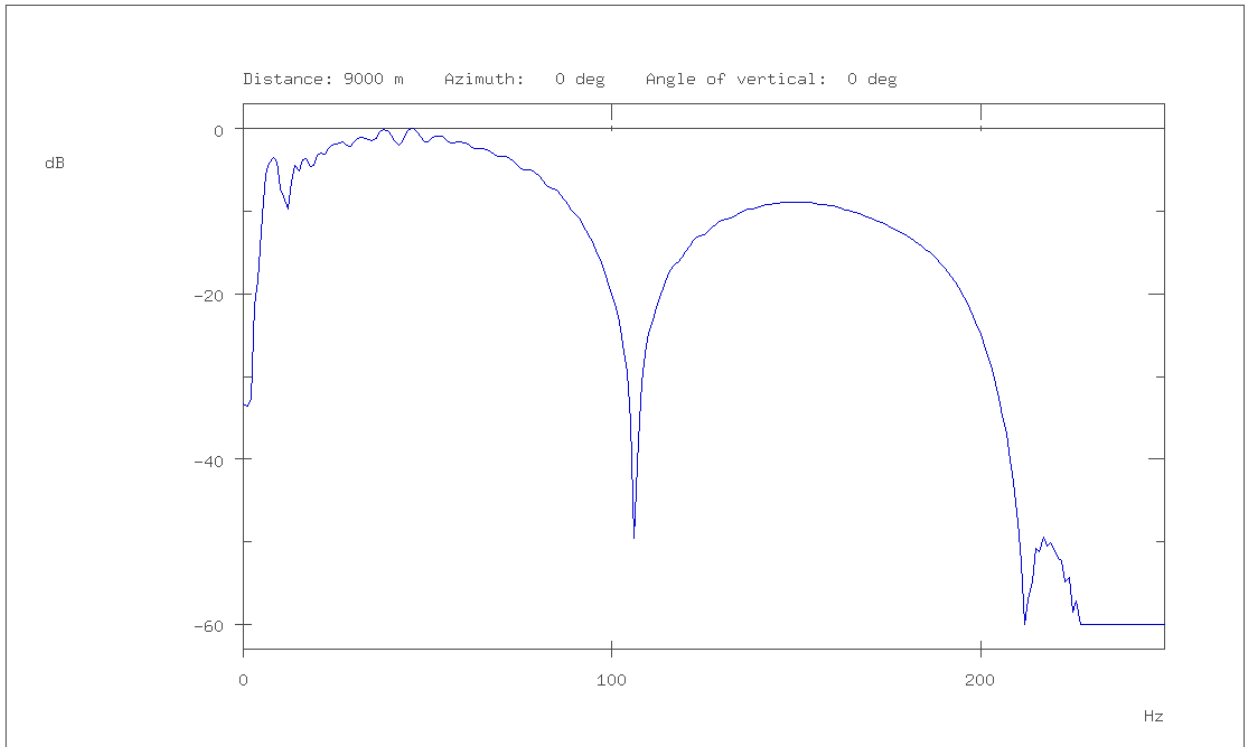
POL3640@7M Seal Out-200/370 Filter

Figure 2-31 - POL3640@7m_Seal_OUT-200-370_Relative_Spectrum

Amplitude spectrum of far-field signature of array: Pol3640-7m

POL3640@7M Seal Out-200/370 Filter
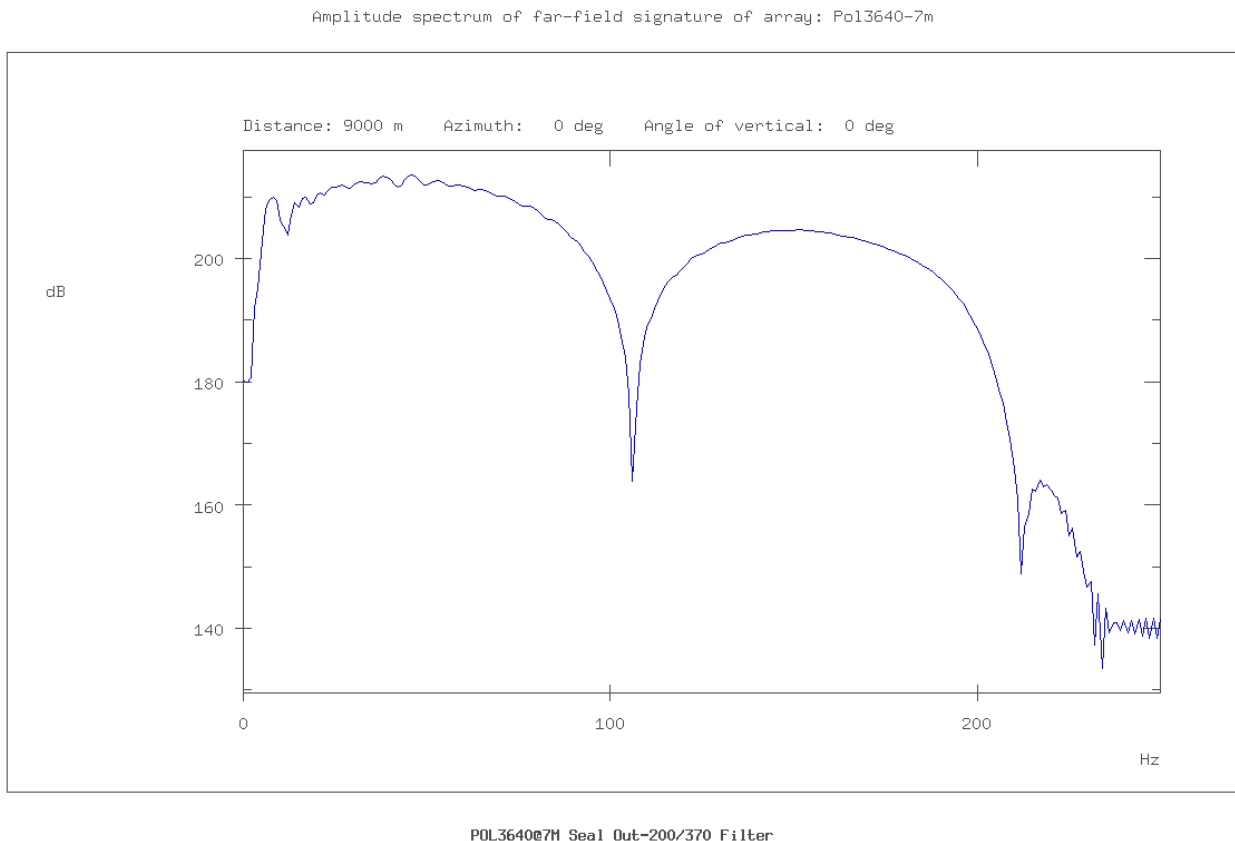
Figure 2-32 - POL3640@7m_Seal_OUT-200-370_Absolute_Spectrum

2.5.2   Array 2 – 4100 in^3

The second array we consider is the 4100in^3 array as illustrated in Figure 2-33. The P-P strength is 98.8 bar-m and PBR is 13.7 (assuming DFS-V instrumentation). Proposed depth of tow is 7m. This is a slightly stronger source compared to the first array in terms of P-P strength although PBR is slightly lower. Again it is RPS' opinion that a source volume of this magnitude represents a good solution. That is to say it will be widely available and meets or exceeds the required characteristics.

Specific details on the source array modelling are as follows:

- Modeled using SERES/Nucleus Software by Greg Glanville (RPS)
- All models sampled at 0.5ms.
- Filters used include:
    - Out-800/375 0.8 Nyquist Minimal Phase filter for 0-1000hz bandwidth displays.
    - Standard DFSV Out-128/72 for source comparisons
    - Sercel Seal Out-200/370 – typical production filter.
- **Note:** The Out-200/370 Seal filter includes the analog 3 Hz 6dB/octave streamer response.

Figure 2-34 - Figure 2-36 display the far field signature, relative and absolute spectra for the Filter Out-800/375 model. Figure 2-37 - Figure 2-39 display directivity plots for azimuths of 0, 45 and 90 degrees respectively. Figure 2-40 - Figure 2-42 display directivity plots for vertical angles of 0, 45 and 90 degrees respectively. Figure 2-43 - Figure 2-49 display directivity plots at various frequencies between 30-1000Hz.

Studying the array directivity plots we can see that although similar, array 2 is very slightly inferior to the first array such that more energy is directed vertically on array 1 (for example compare Figure 2-38 to Figure 2-15 top).

Figure 2-50 - Figure 2-52 display the far field signature, relative and absolute spectra for the model filtered with standard DFSV Out-128/72. Finally Figure 2-53 - Figure 2-55 display the far field signature, relative and absolute spectra for the model filtered with Sercel Seal Out-200/370.
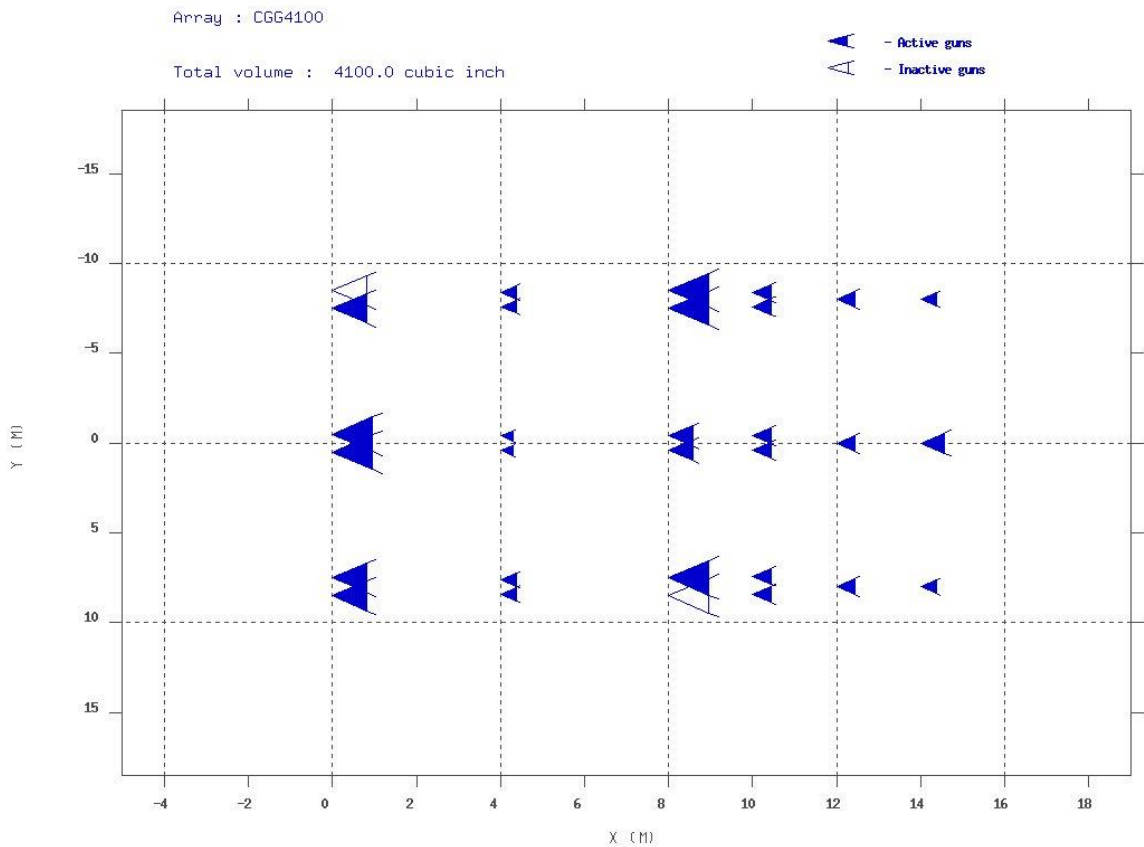

Figure 2-33 - CGG4100@7m_Array_Layout

Far-field signature of array: CGG4100

Distance: 9000 m   Azimuth: 0 deg   Angle of vertical: 0 deg

Primary : 77.8 barm	Source depth : 7.00 m
Peak-peak : 153.5 barm	Streamer depth : .00 m
P/B ratio : 21.2	Volume : 4100 cu.in.
Period (+/-) : 127.0/ 149.0 msec	Pressure : 2000 psi
	Ghost strength : -1.00
	Sea temperatur : 17.00 C
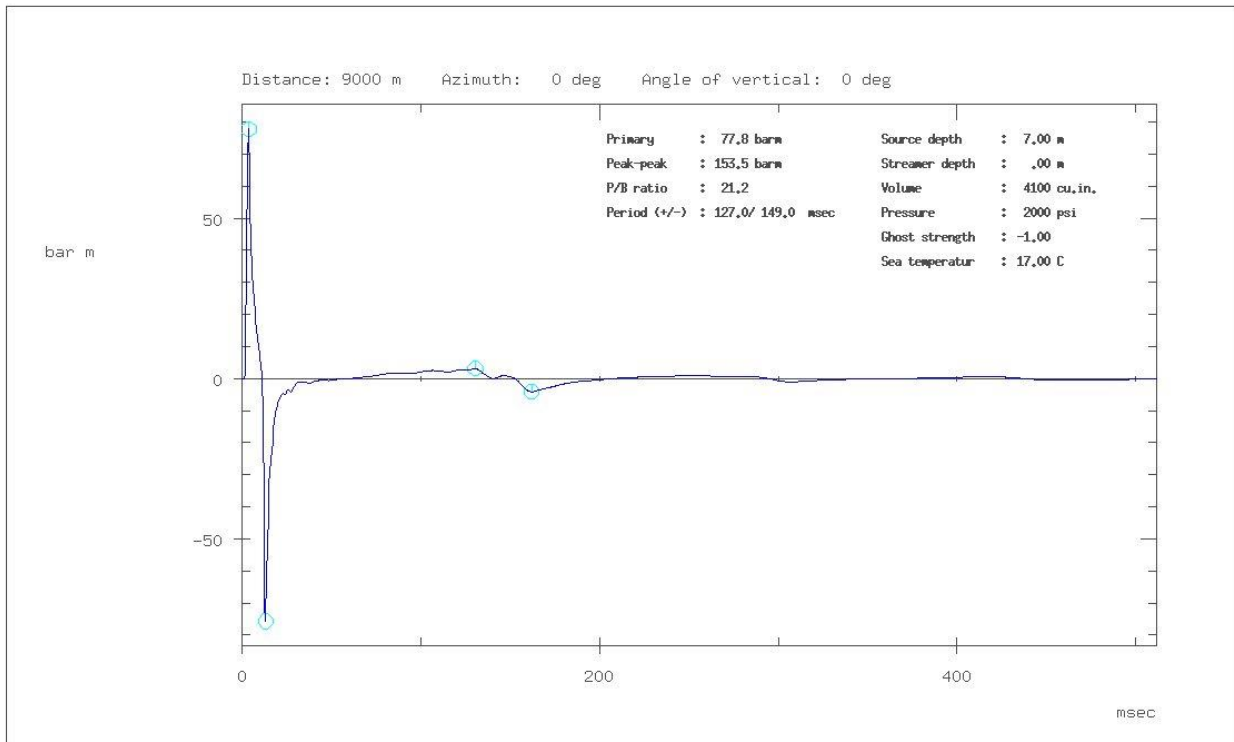
4100 array @7m 800 hz-375db 0.8 Nyquist filter

Figure 2-34 - CGG4100@7m_Out-800Hz-375_Signature_

Amplitude spectrum of far-field signature of array: CGG4100
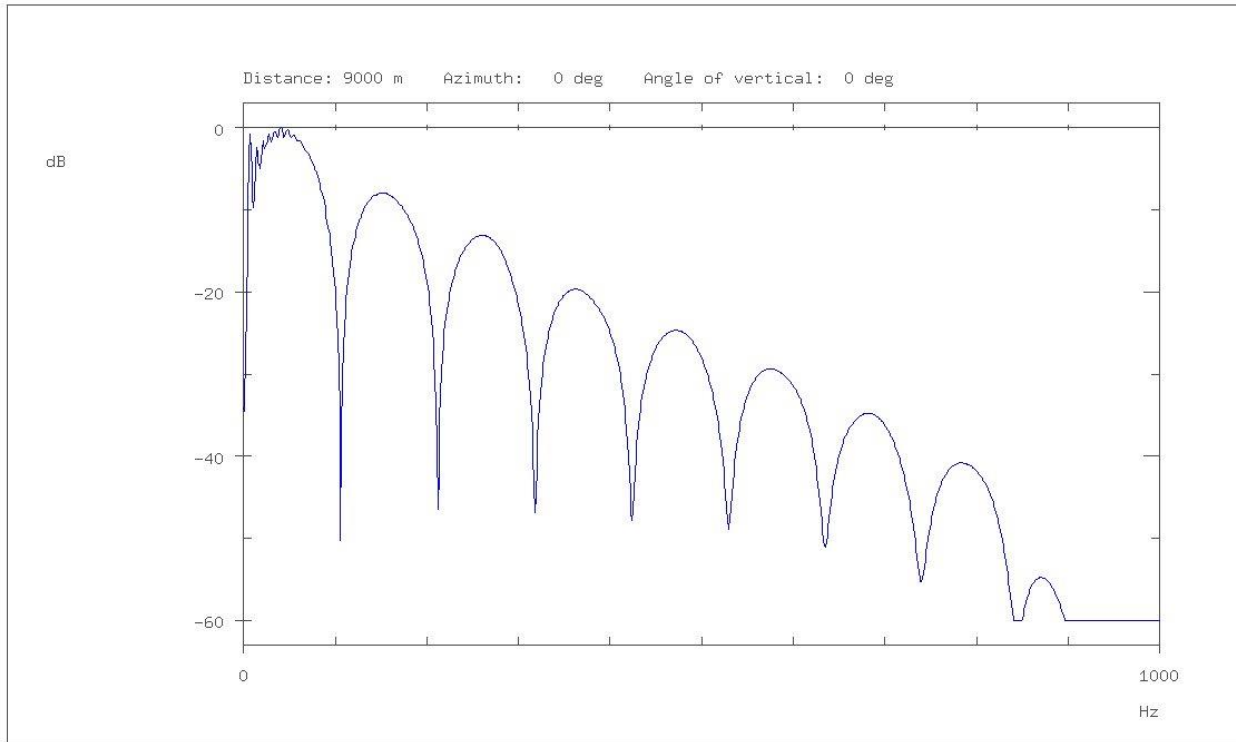
4100 array @7m 800 hz-375db 0.8 Nyquist filter

Figure 2-35 - CGG4100@7m_Out-800Hz-375_Relative_Spectrum_

Amplitude spectrum of far-field signature of array: CGG4100

Distance: 9000 m   Azimuth: 0 deg   Angle of vertical: 0 deg

4100 array @7m 800 hz-375db 0.8 Nyquist filter
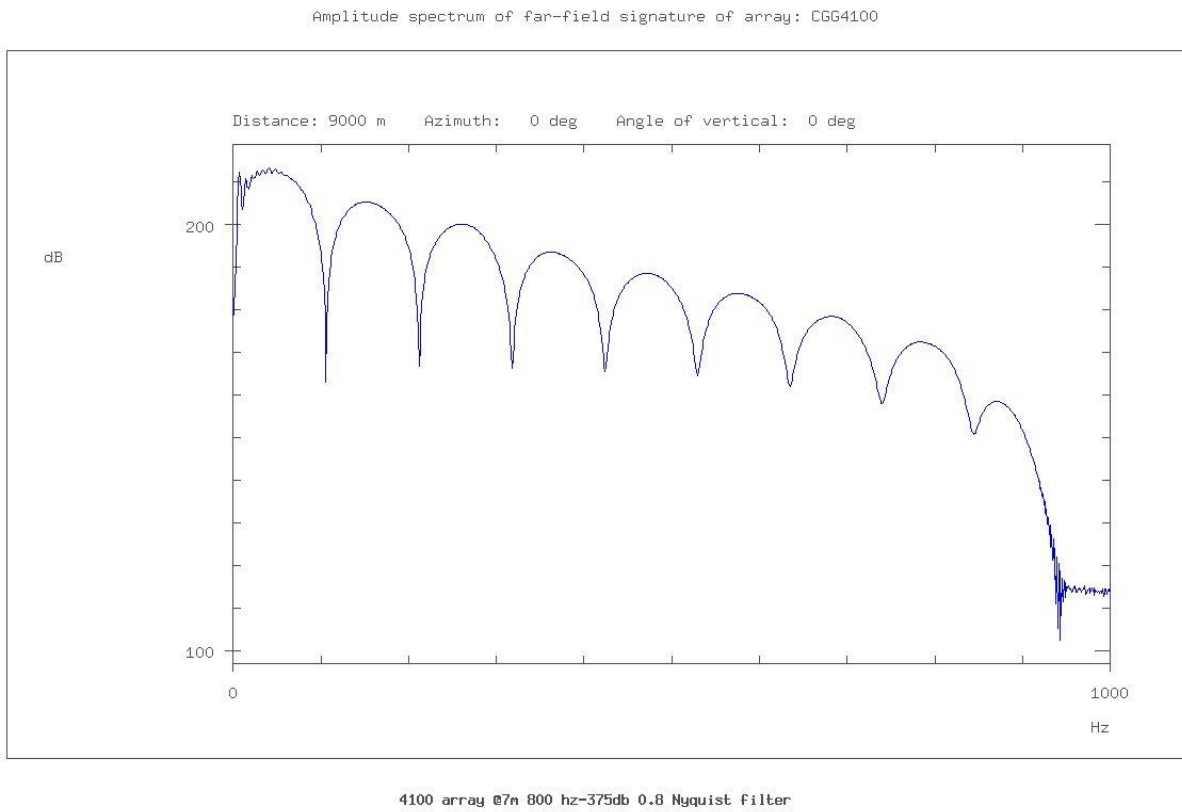
Figure 2-36 - CGG4100@7m_Out-800Hz-375_Absolute_Spectrum

Source Directivity Plot - azimuth :   .0 degrees - array CGG4100
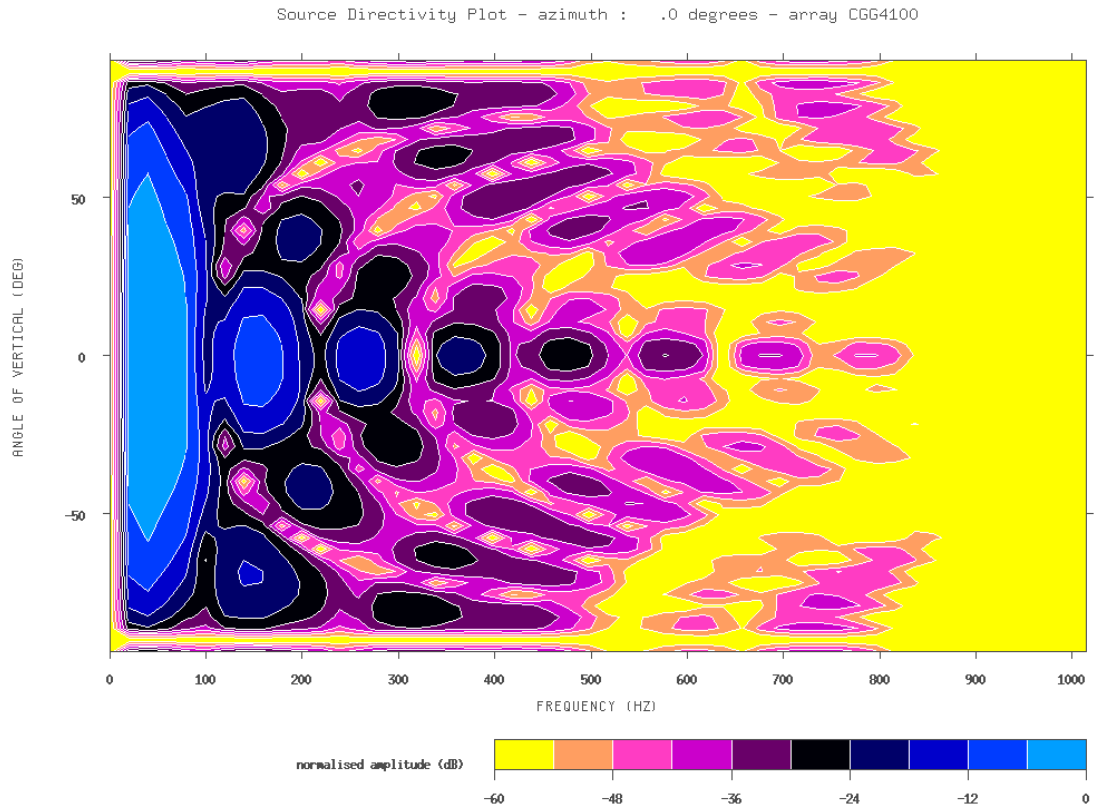
Figure 2-37 - Directivity-azimuth-0_deg_0-1000Hz

Source Directivity Plot - azimuth : 45.0 degrees - array CGG4100

4100 Array @7m Out-800/370 0.8 Nyquist Filter
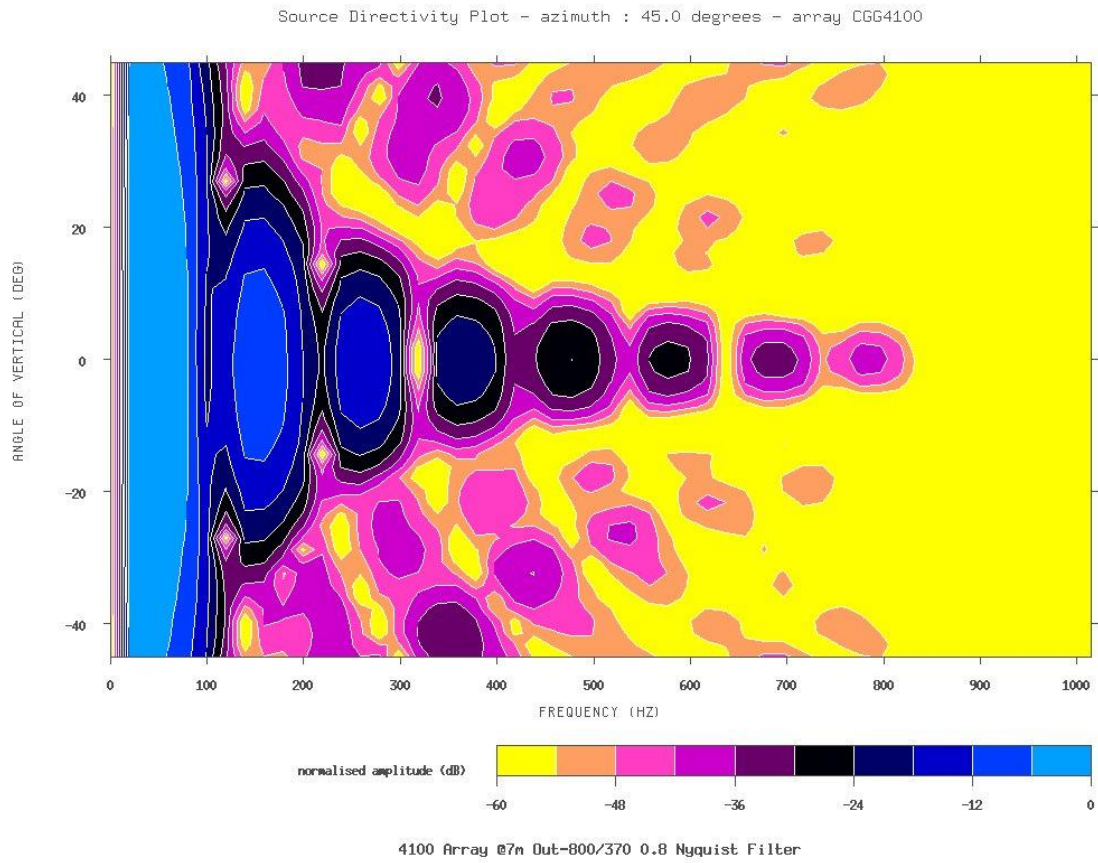
Figure 2-38 - Directivity-azimuth45_deg_0-1000Hz

Source Directivity Plot - azimuth : 90.0 degrees - array CGG4100

4100 Array @7m Out-800/370 0.8 Nyquist Filter
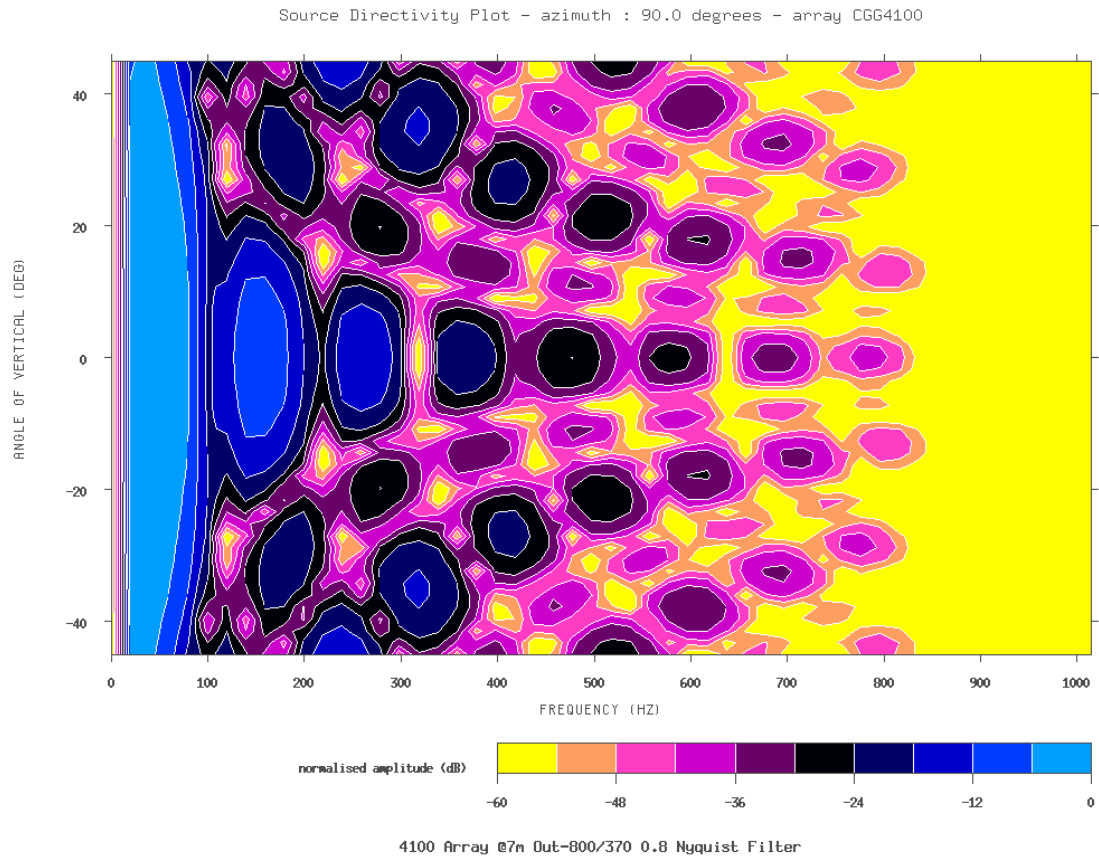
Figure 2-39 - Directivity-azimuth90_deg_0-1000Hz
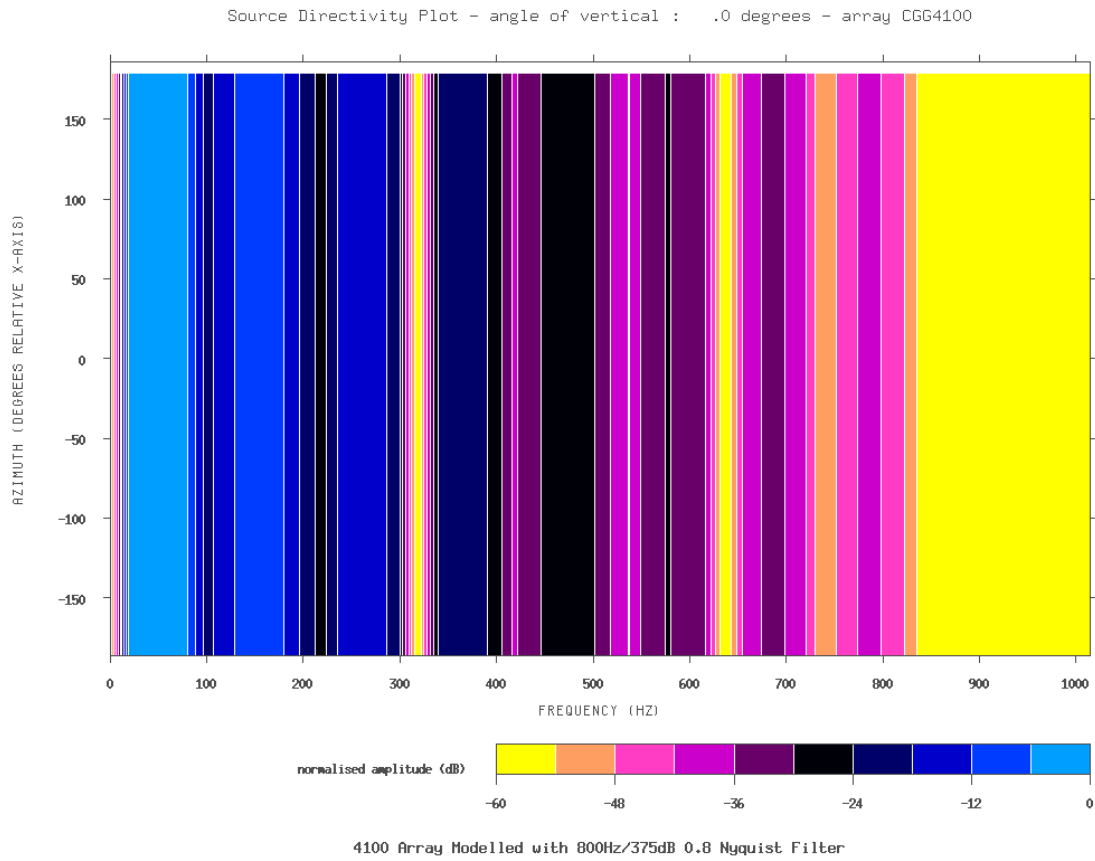
Figure 2-40 - Directivity-angle_of_vertical_-0_deg_0-1000Hz

Source Directivity Plot – angle of vertical : 45.0 degrees – array CGG4100

4100 Array @7m Out-800/370 0.8 Nyquist Filter
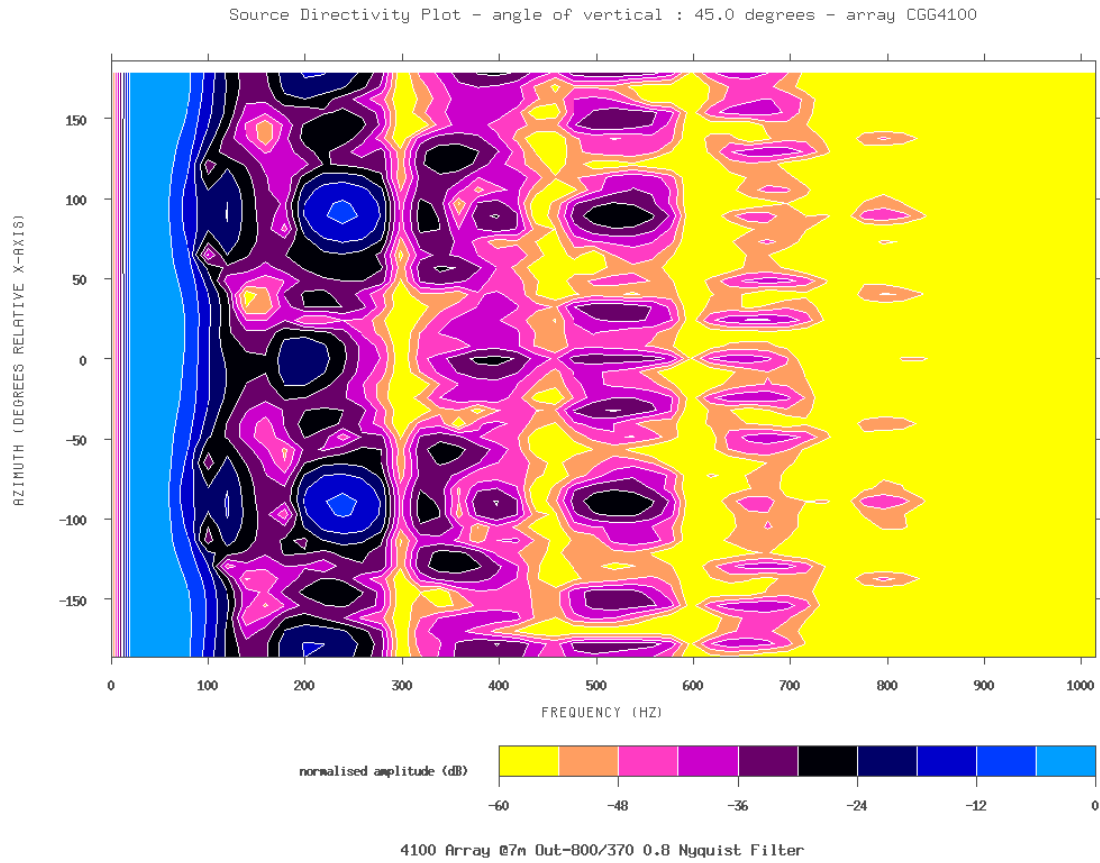
Figure 2-41 - Directivity_angle_of_vertical-45_deg_0-1000Hz

Source Directivity Plot - angle of vertical : 90.0 degrees - array CGG4100

normalised amplitude (dB)

-60   -48   -36   -24   -12   0

4100 Array @7m Out-800/370 0.8 Nyquist Filter
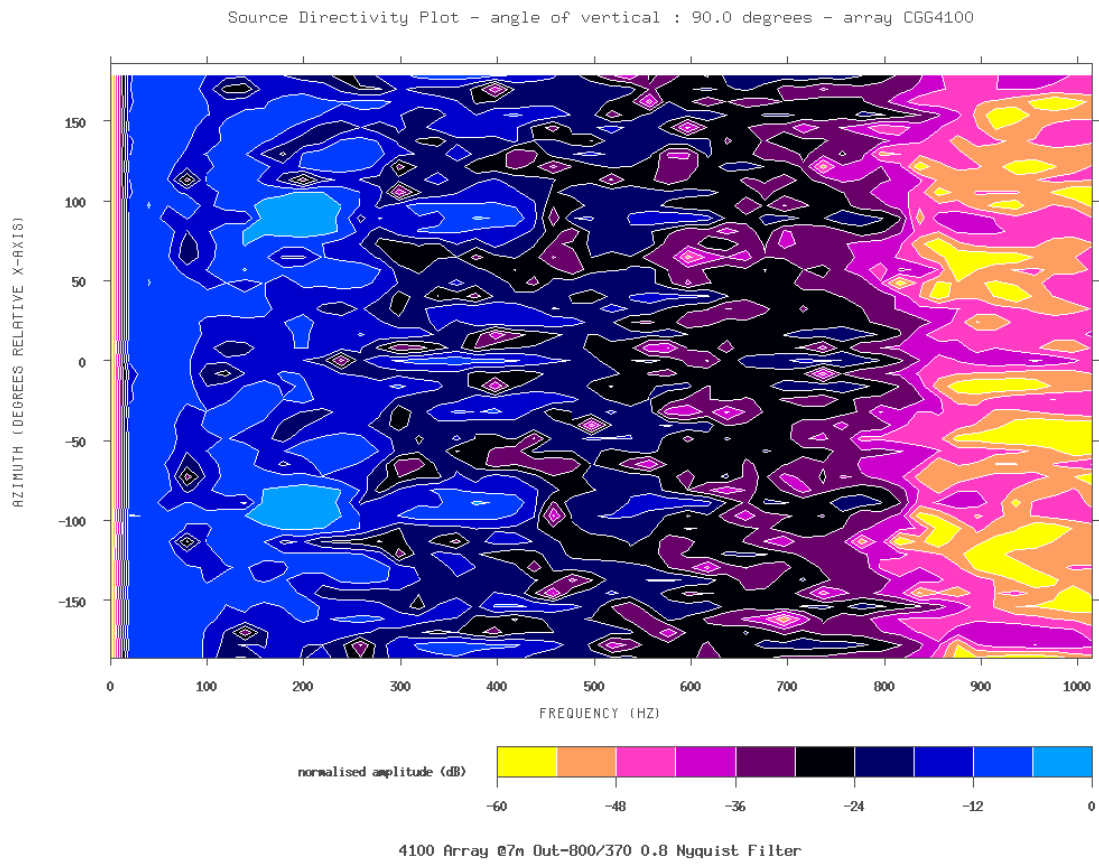
Figure 2-42 - Directivity-angle_of_vertical-90deg_0-1000Hz

Source Directivity Plot - frequency : 30.0 Hz. - array CGG4100

AZIMUTH (DEGREES RELATIVE X-AXIS)

normalised amplitude (dB)

-60   -48   -36   -24   -12   0

4100 Array Modelled with 800Hz/375dB 0.8 Nyquist Filter
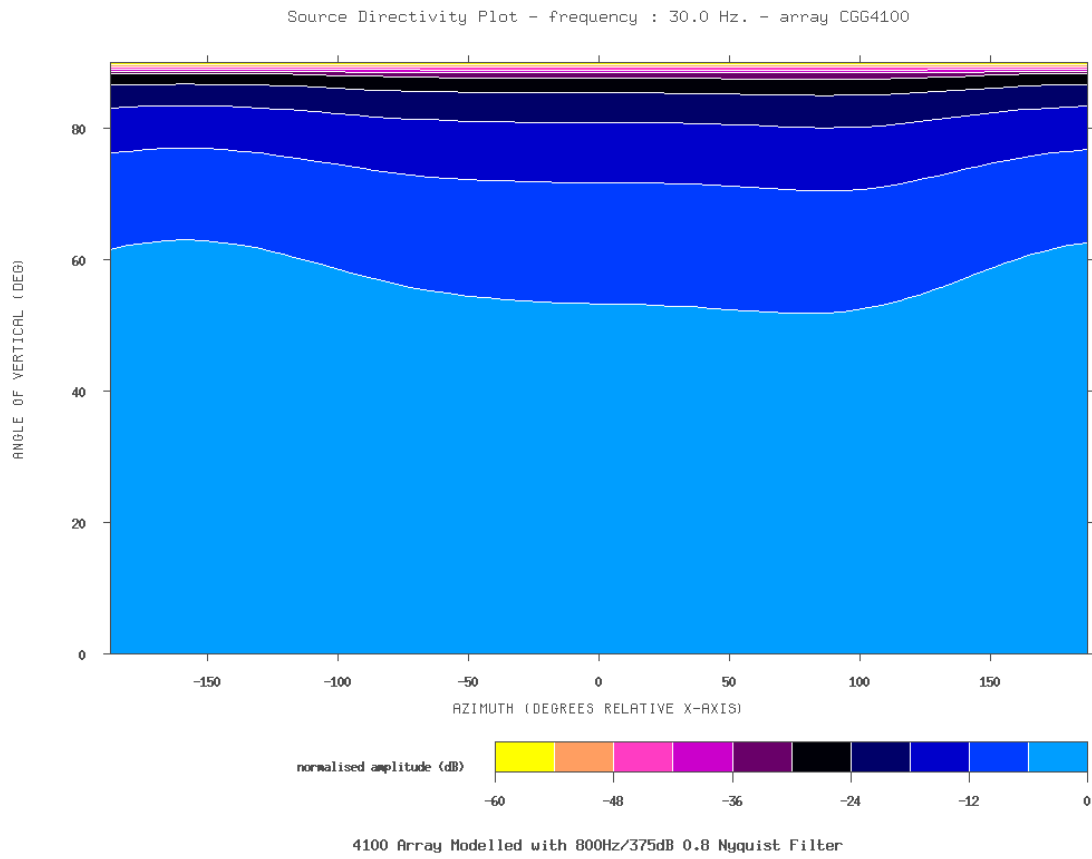
Figure 2-43 - Directivity-frequency_30HZ_-0-1000Hz
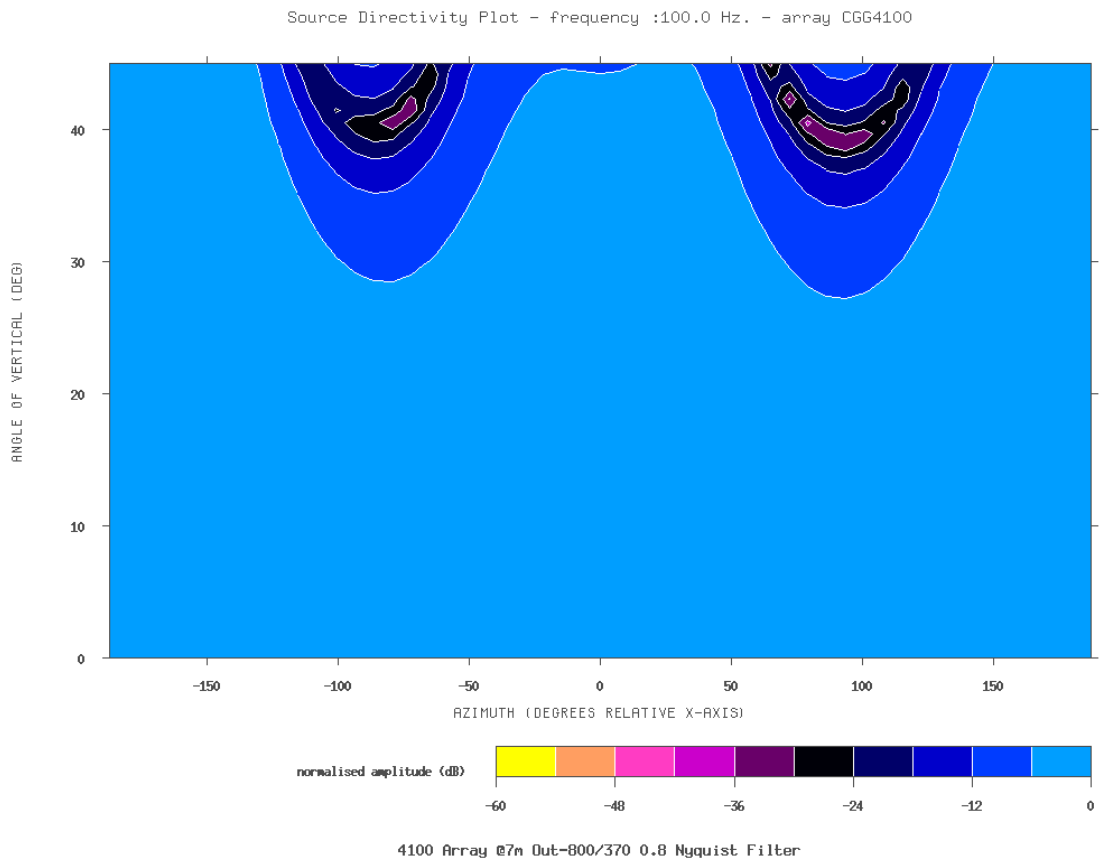
Figure 2-44 - Directivity-frequency_100HZ_-0-1000Hz

Source Directivity Plot - frequency :200.0 Hz. - array CGG4100

normalised amplitude (dB)

4100 Array @7m Out-800/370 0.8 Nyquist Filter
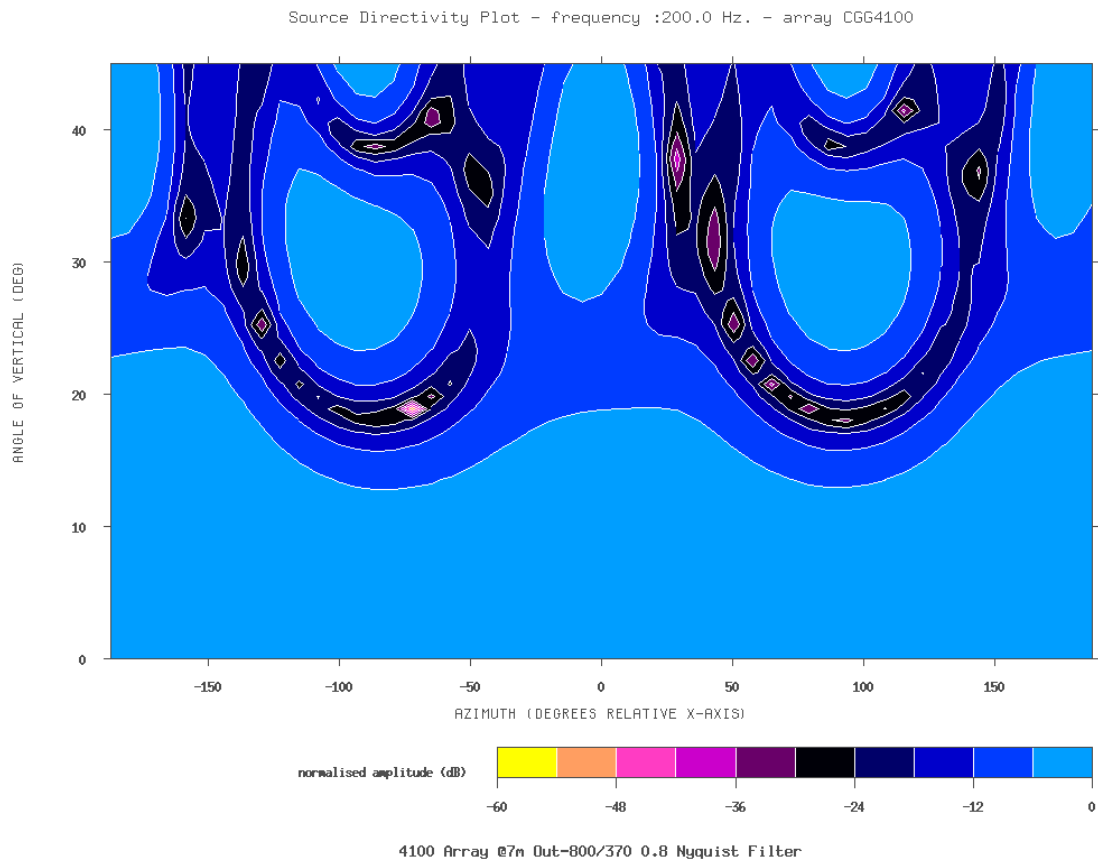
Figure 2-45 - Directivity-frequency_200HZ_-0-1000Hz

Source Directivity Plot - frequency :500.0 Hz. - array CGG4100

4100 Array @7m Out-800/370 0.8 Nyquist Filter
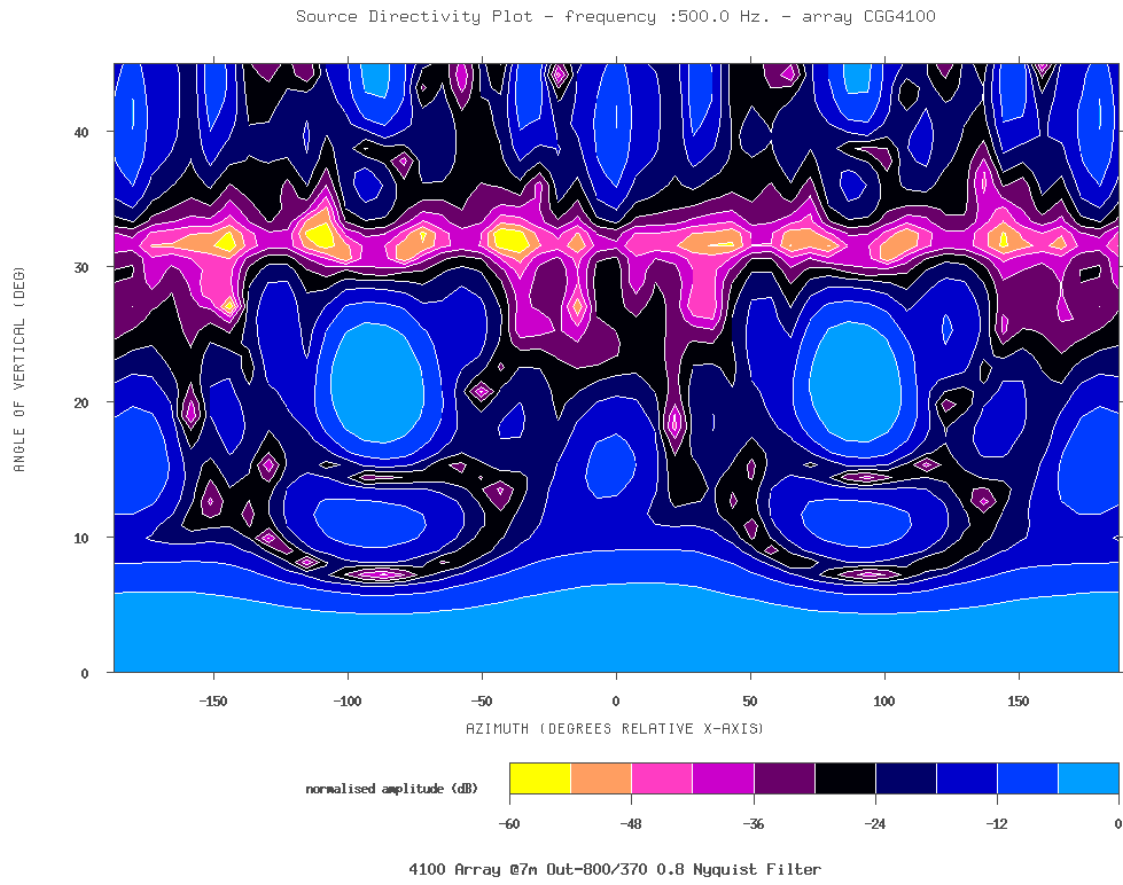
Figure 2-46 - Directivity-frequency_500HZ_-0-1000Hz

Source Directivity Plot - frequency :700.0 Hz. - array CGG4100

4100 Array @7m Out-800/370 0.8 Nyquist Filter
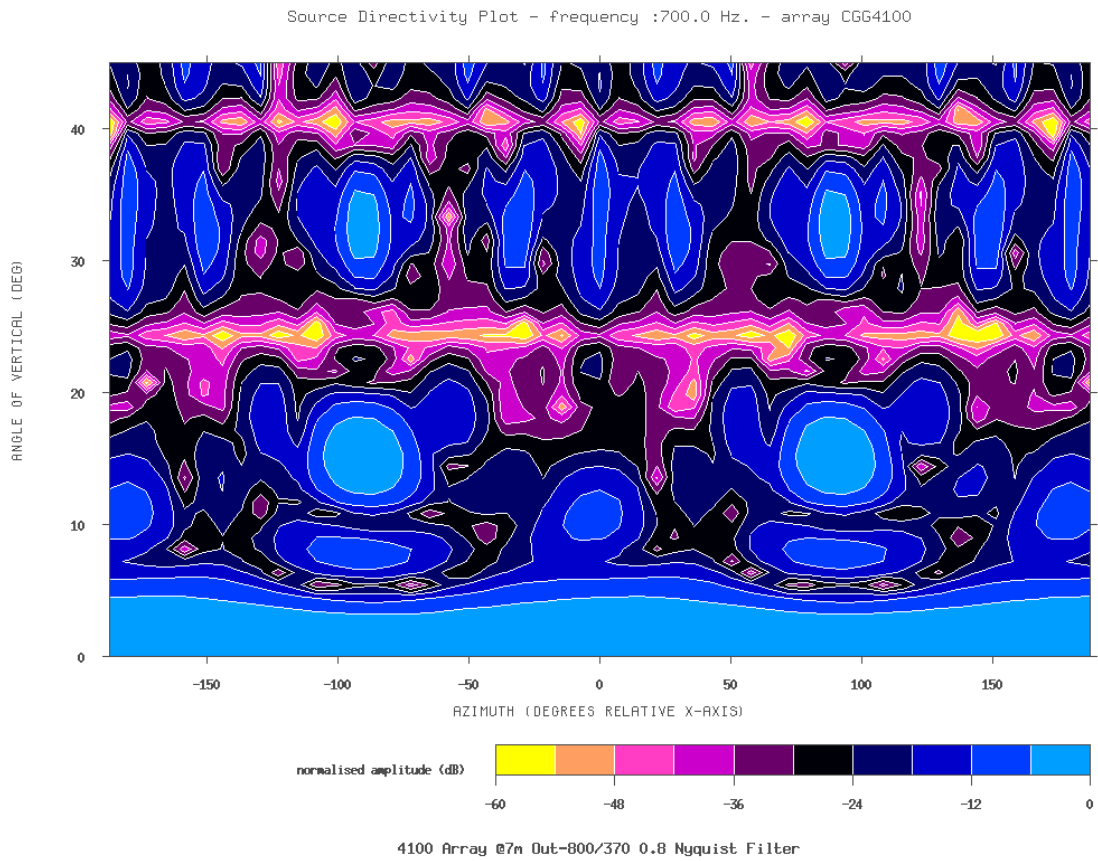
Figure 2-47 - Directivity-frequency_700HZ_-0-1000Hz
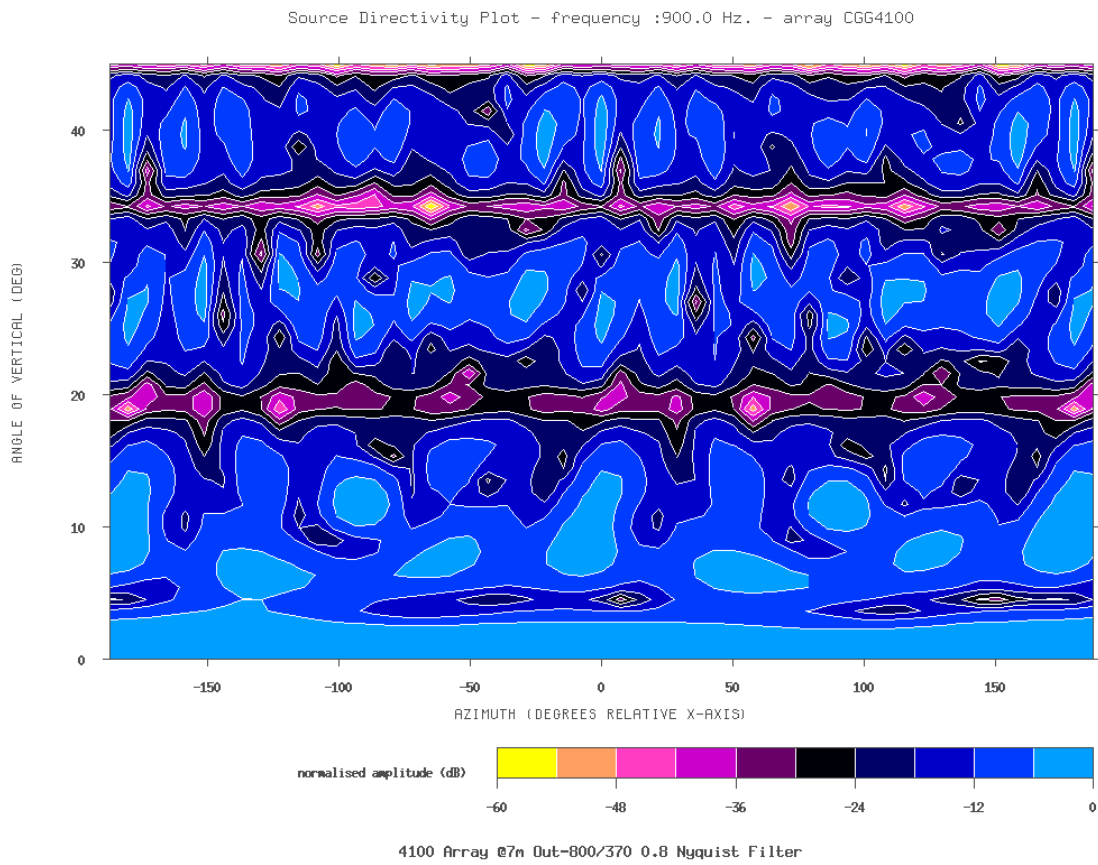
Figure 2-48 - Directivity-frequency_900HZ_-0-1000Hz

Source Directivity Plot - frequency :999.0 Hz. - array CGG4100

4100 Array @7m Out-800/370 0.8 Nyquist Filter
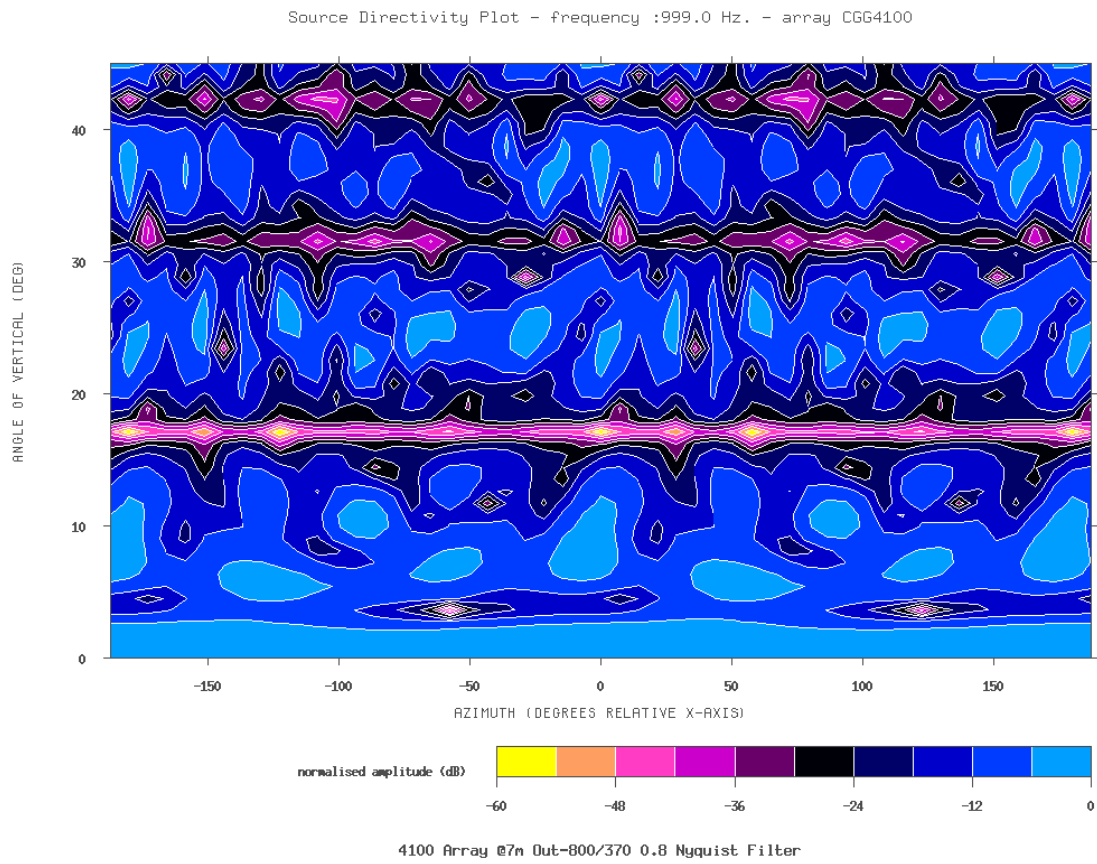
Figure 2-49 - Directivity-frequency_999HZ_-0-1000Hz

Far-field signature of array: CGG4100

Distance: 9000 m   Azimuth: 0 deg   Angle of vertical: 0 deg

Primary : 47.7 barm	Source depth : 7.00 m
Peak-peak : 98.8 barm	Streamer depth : .00 m
P/B ratio : 13.7	Volume : 4100 cu.in.
Period (+/-) : 78.0/ 147.0 msec	Pressure : 2000 psi
	Ghost strength : -1.00
	Sea temperatur : 17.00 C
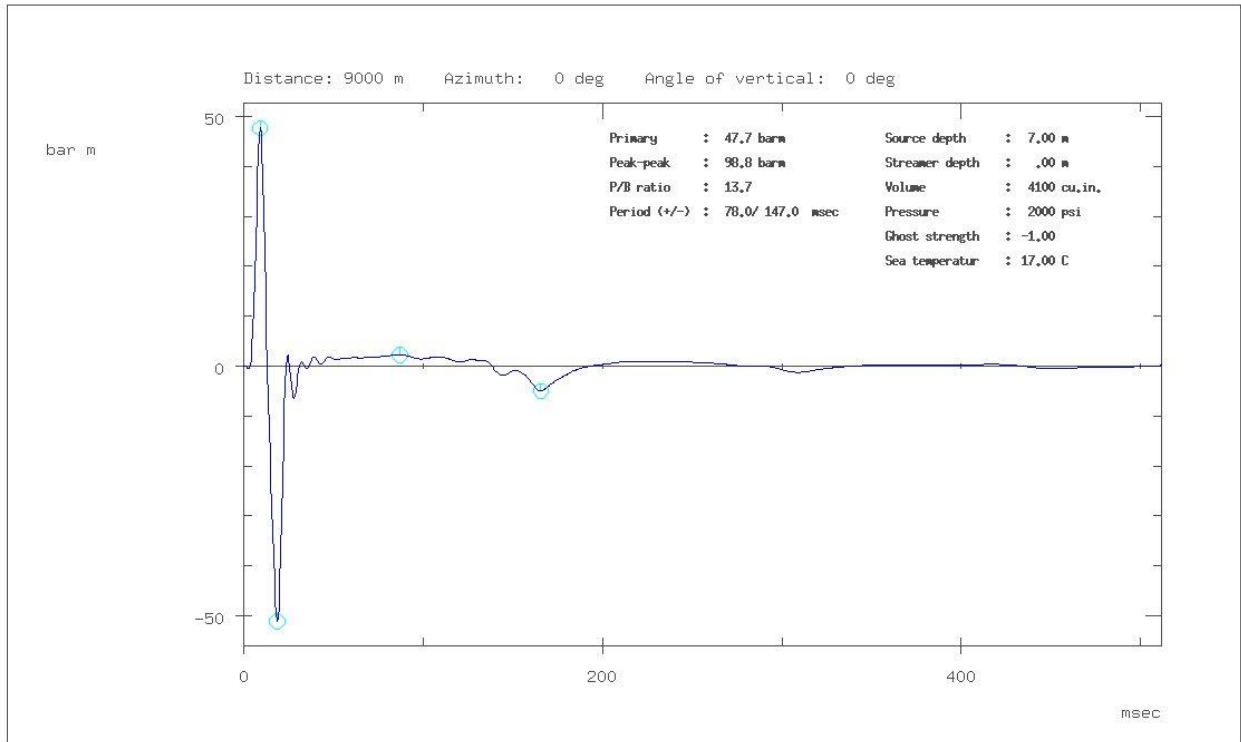
4100 array @7m DFSv Out 128 Filters

Figure 2-50 - CGG4100@7m_DFSV_Out-128-72_Signature_

Amplitude spectrum of far-field signature of array: CGG4100

Figure 2-51 - CGG4100@7m_DFSV_Out-128-72_Relative_Spectrum

Amplitude spectrum of far-field signature of array: CGG4100

Figure 2-52 - CGG4100@7m_DFSV_Out-128-72_Absolute_Spectrum

Far-field signature of array: CGG4100

Distance: 9000 m   Azimuth: 0 deg   Angle of vertical: 0 deg

Primary : 61.2 barm	Source depth : 7.00 m
Peak-peak : 125.4 barm	Streamer depth : .00 m
P/B ratio : 18.4	Volume : 4100 cu.in.
Period (+/-) : 101.0/ 148.0 msec	Pressure : 2000 psi
	Ghost strength : -1.00
	Sea temperatur : 17.00 C

bar m
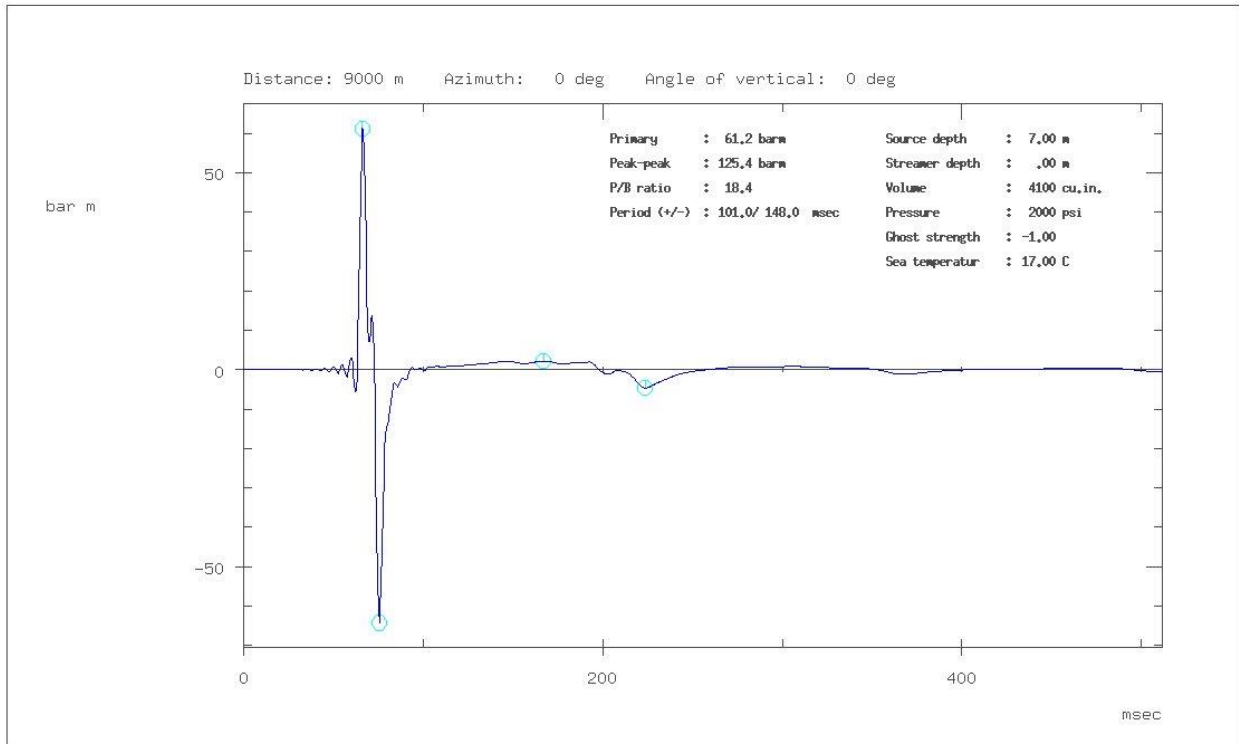
4100 array @ 7M SEAL 3/6-200/270 dB Filter

Figure 2-53 - CGG4100@7m_Seal_3-6_200-270_Signature

Amplitude spectrum of far-field signature of array: CGG4100

Distance: 9000 m   Azimuth: 0 deg   Angle of vertical: 0 deg
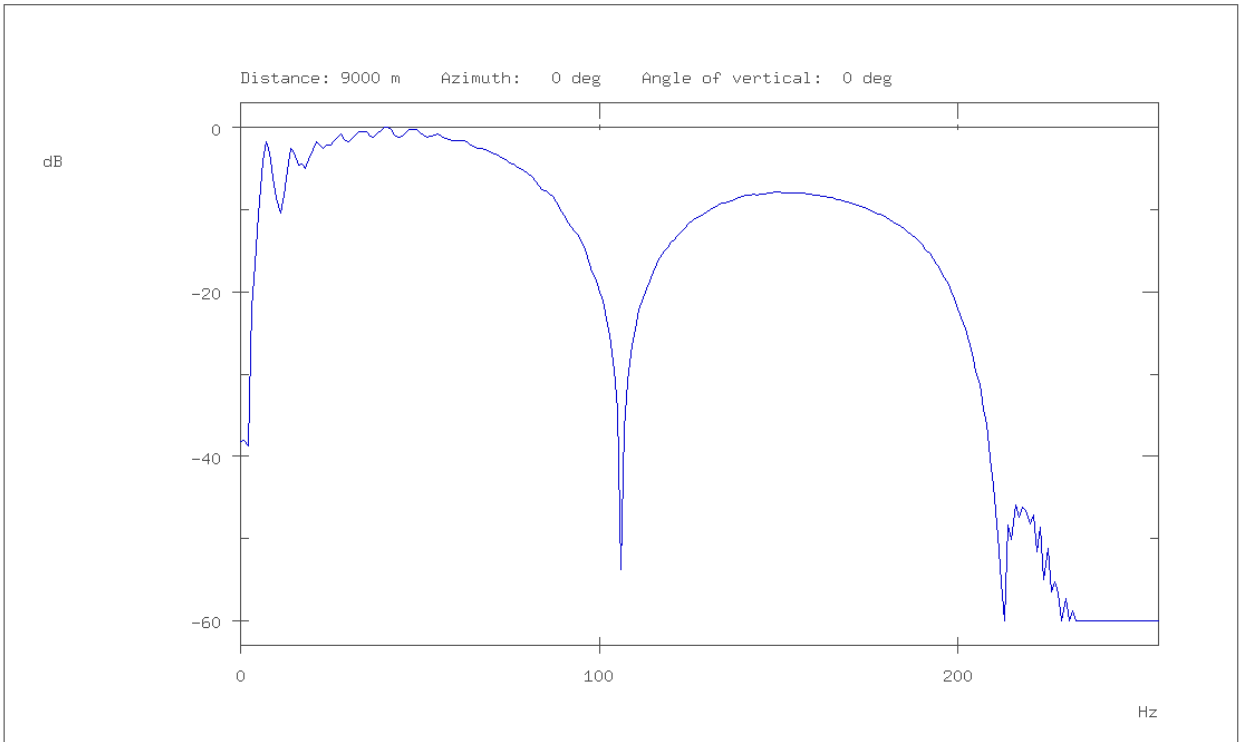
4100 array @ 7M SEAL 3/6-200/270 dB Filter

Figure 2-54 - CGG4100@7m_Seal_3-6_200-270_Relative_Spectrum_

Amplitude spectrum of far-field signature of array: CGG4100

Distance: 9000 m   Azimuth: 0 deg   Angle of vertical: 0 deg

4100 array @ 7M SEAL 3/6-200/270 dB Filter
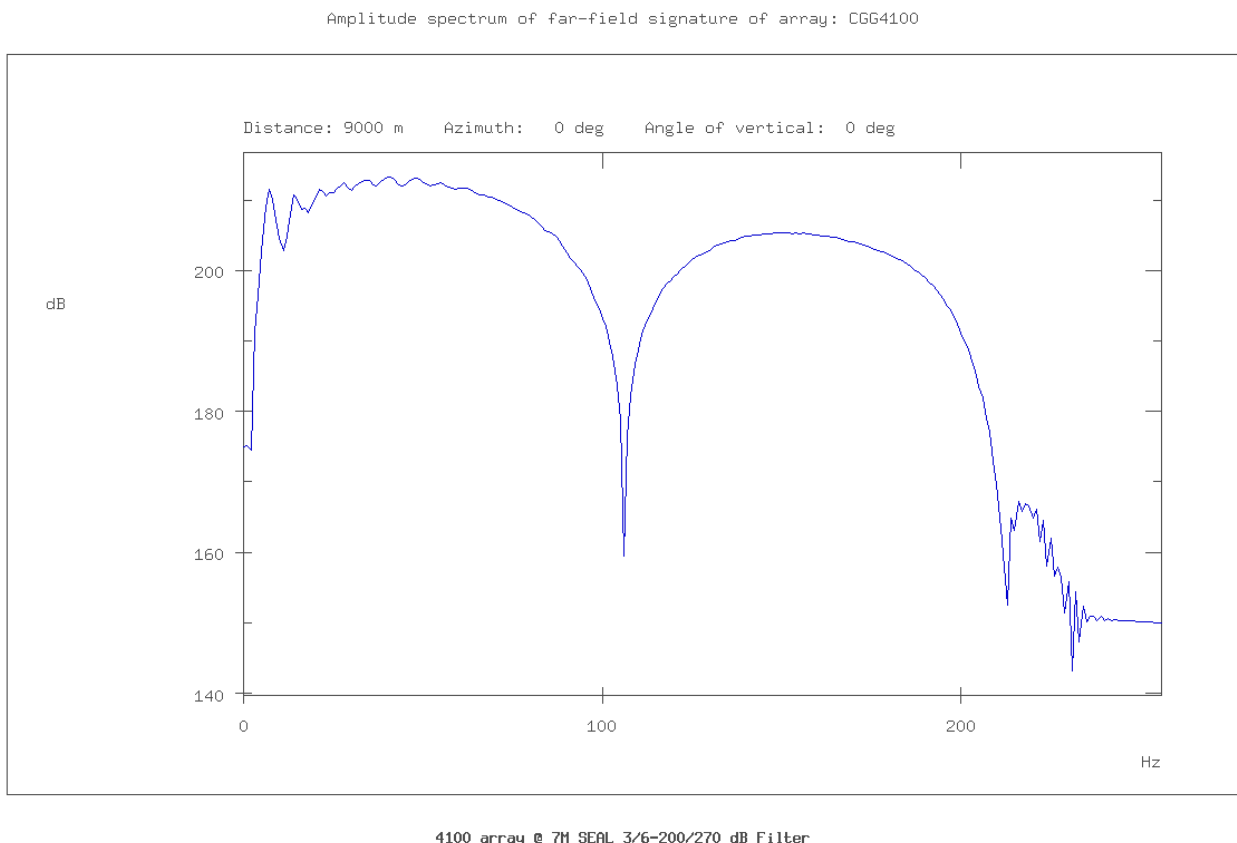
Figure 2-55 - CGG4100@7m_Seal_3-6_200-270_Absolute_Spectrum

2.5.3   Array 3 – 4390 in³

The third array we consider is the 4390in³ array as illustrated in Figure 2-56. The P-P strength is 101 bar-m and PBR is 17.4 (assuming DFS-V instrumentation). Proposed depth of tow is 7m. This source is an improvement over arrays 1 and 2.

Specific details on the source array modelling are as follows:

- Modeled using SERES/Nucleus Software by Greg Glanville (RPS)
- All models sampled at 0.5ms.
- Filters used include:
  - Out-800/375 0.8 Nyquist Minimal Phase filter for 0-1000hz bandwidth displays.
  - Standard DFSV Out-128/72 for source comparisons
  - Sercel Seal Out-200/370 – typical production filter.
- **Note:** The Out-200/370 Seal filter includes the analog 3 Hz 6dB/octave streamer response.

Figure 2-57 - Figure 2-59 display the far field signature, relative and absolute spectra for the Filter Out-800/375 model. Figure 2-60 - Figure 2-62 display directivity plots for azimuths of 0, 45 and 90 degrees respectively. Figure 2-63 - Figure 2-65 display directivity plots for

vertical angles of 0, 45 and 90 degrees respectively. Figure 2-66 - Figure 2-72 display directivity plots at various frequencies between 30-1000Hz.

Figure 2-73 - Figure 2-75 display the far field signature, relative and absolute spectra for the model filtered with standard DFSV Out-128/72. Finally Figure 2-76 - Figure 2-78 display the far field signature, relative and absolute spectra for the model filtered with Sercel Seal Out-200/370.
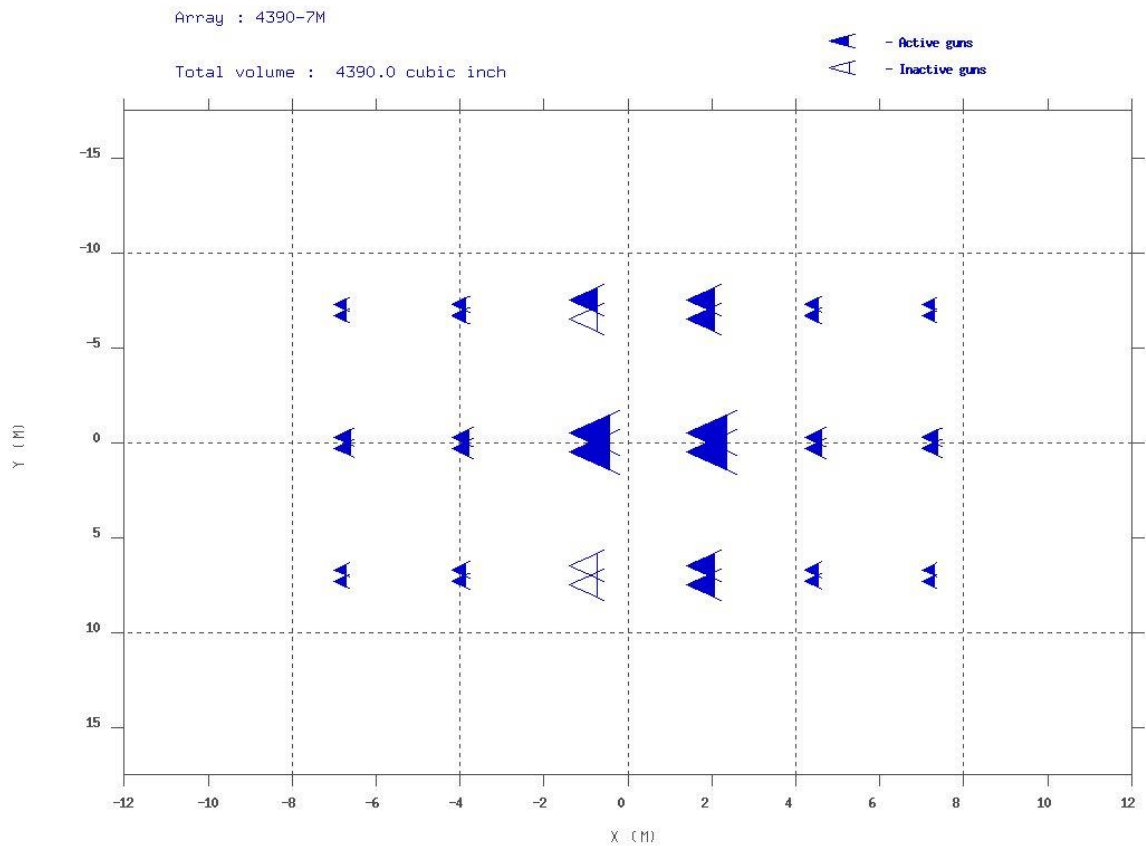
Figure 2-56 - 4390@7m_Array_layout

Far-field signature of array: 4390-7M

Distance: 9000 m   Azimuth: 0 deg   Angle of vertical: 0 deg

Primary : 81.5 barm	Source depth : 7.00 m
Peak-peak : 160.5 barm	Streamer depth : .00 m
P/B ratio : 31.9	Volume : 4390 cu.in.
Period (+/-) : 176.0/ 178.5 msec	Pressure : 2000 psi
	Ghost strength : -1.00
	Sea temperatur : 17.00 C

bar m
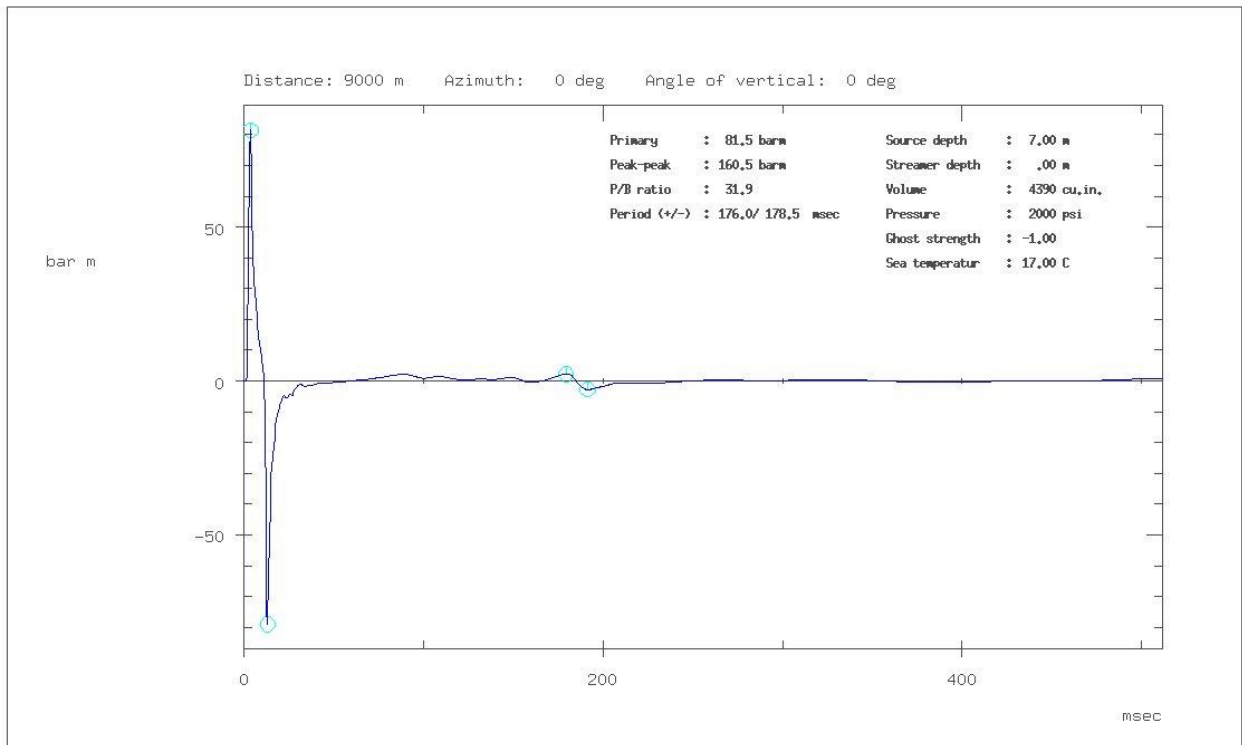
4390@7m Out-800/375 Filter

Figure 2-57 - 4390@7m_Out_800-375_Signature

Amplitude spectrum of far-field signature of array: 4390-7M

Distance: 9000 m   Azimuth: 0 deg   Angle of vertical: 0 deg
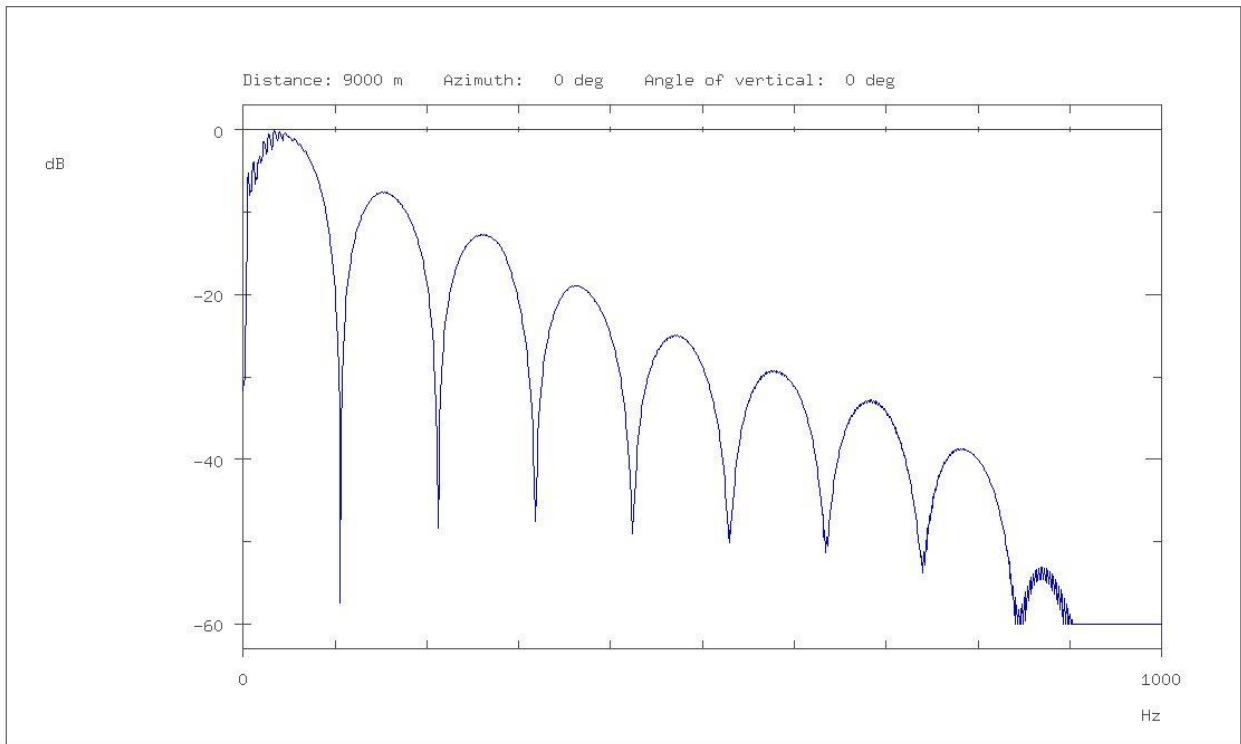
4390@7m Out-800/375 Filter

Figure 2-58 - 4390@7m_Out_800-375_Relative_Spectrum

Amplitude spectrum of far-field signature of array: 4390-7M
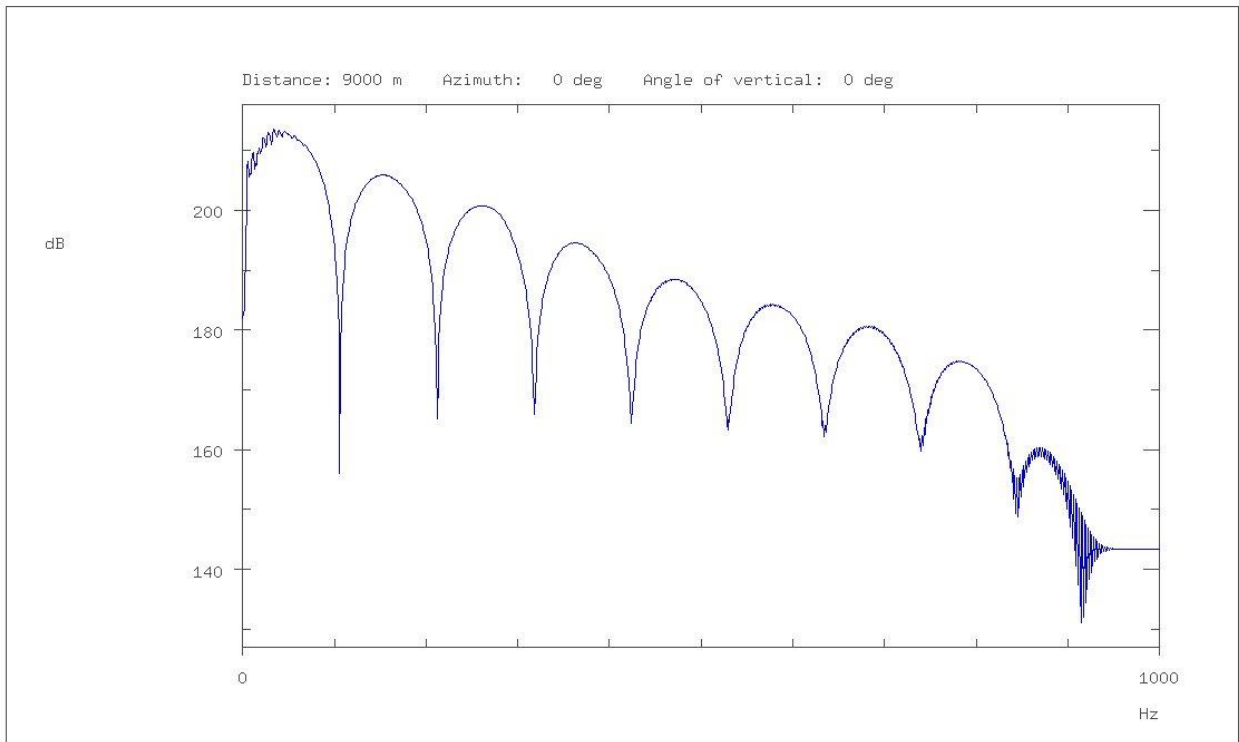
4390@7m Out-800/375 Filter

Figure 2-59 - 4390@7m_Out_800-375_Absolute_Spectrum

Source Directivity Plot – azimuth :   .0 degrees – array 4390-7M

4390@7m Out-800/375 Filter
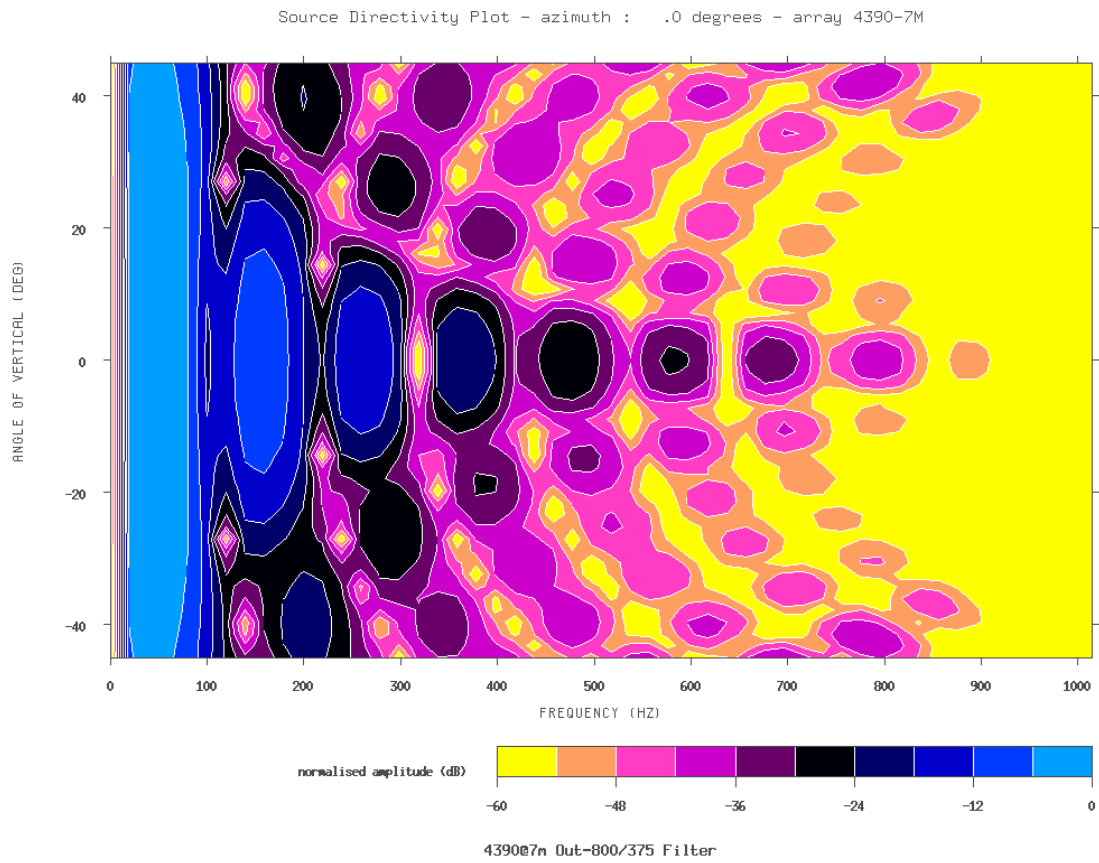
Figure 2-60 - 4390@7m_Out_800-375_directivity_azimuth-0deg_0-1000hz

Source Directivity Plot – azimuth : 45.0 degrees – array 4390-7M

normalised amplitude (dB)

4390@7m Out-800/375 Filter
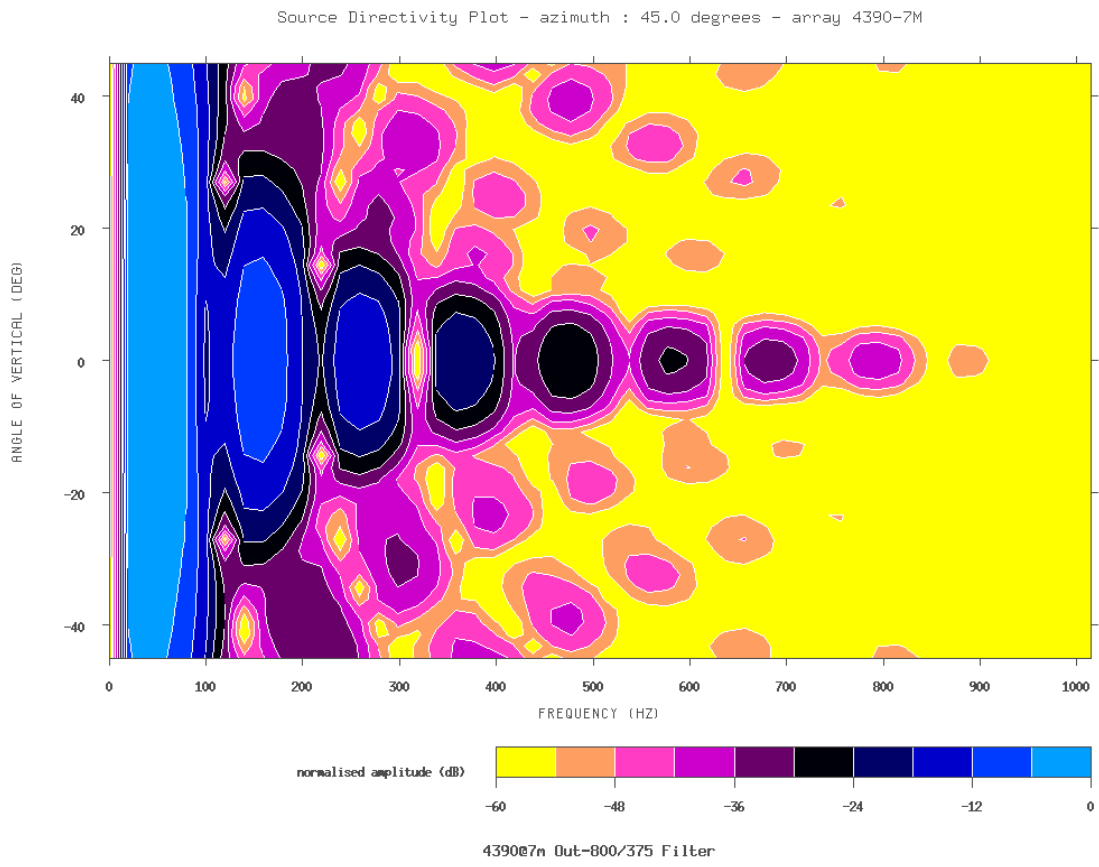
Figure 2-61 - 4390@7m_Out_800-375_directivity_azimuth-45deg_0-1000hz
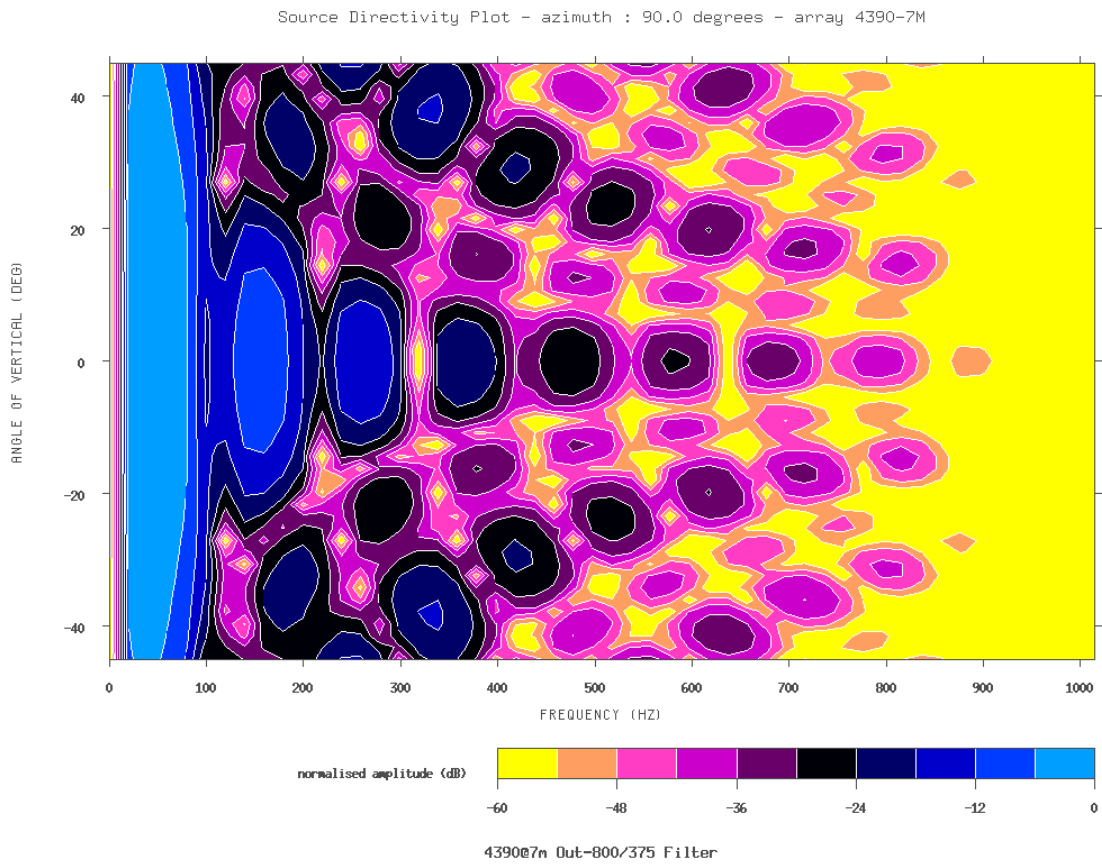
Figure 2-62 - 4390@7m_Out_800-375_directivity_azimuth-90deg_0-1000hz

Source Directivity Plot — angle of vertical :   .0 degrees — array 4390-7M
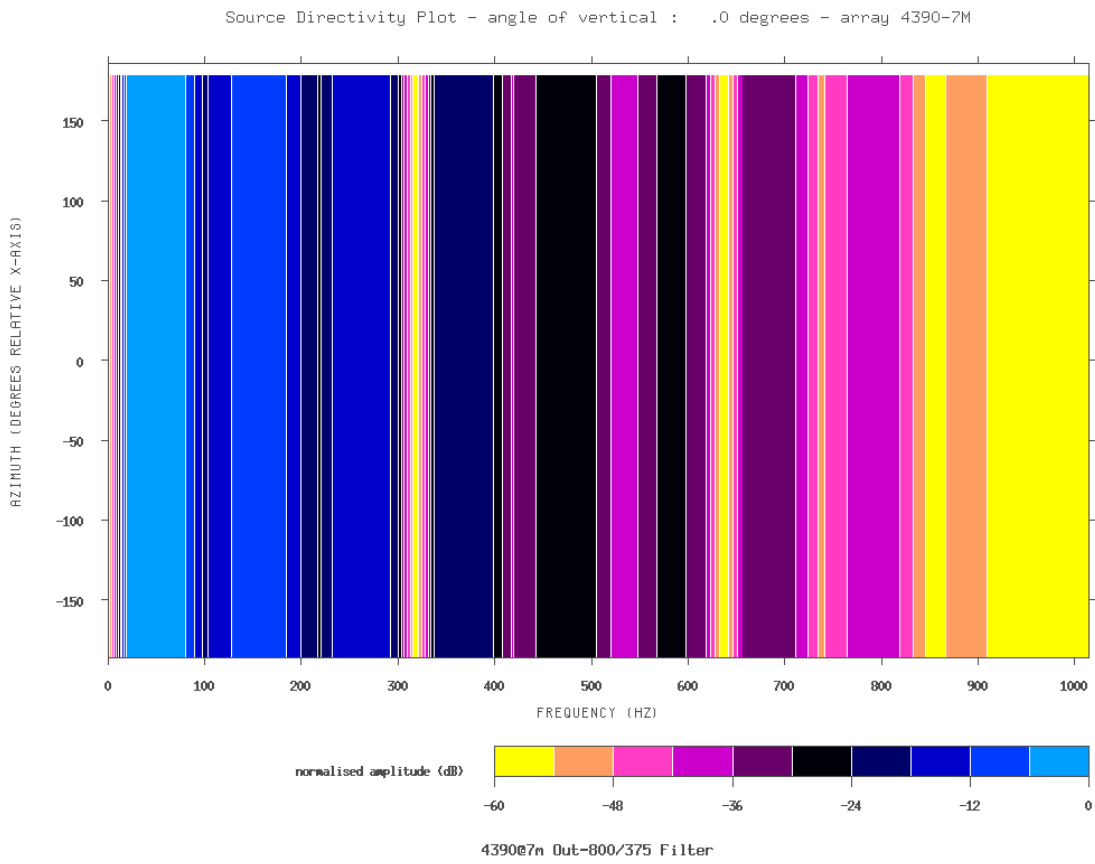
Figure 2-63 - 4390@7m_Out_800-375_directivity_angle_of_vertical-0deg_0-1000hz

Source Directivity Plot - angle of vertical : 45.0 degrees - array 4390-7M
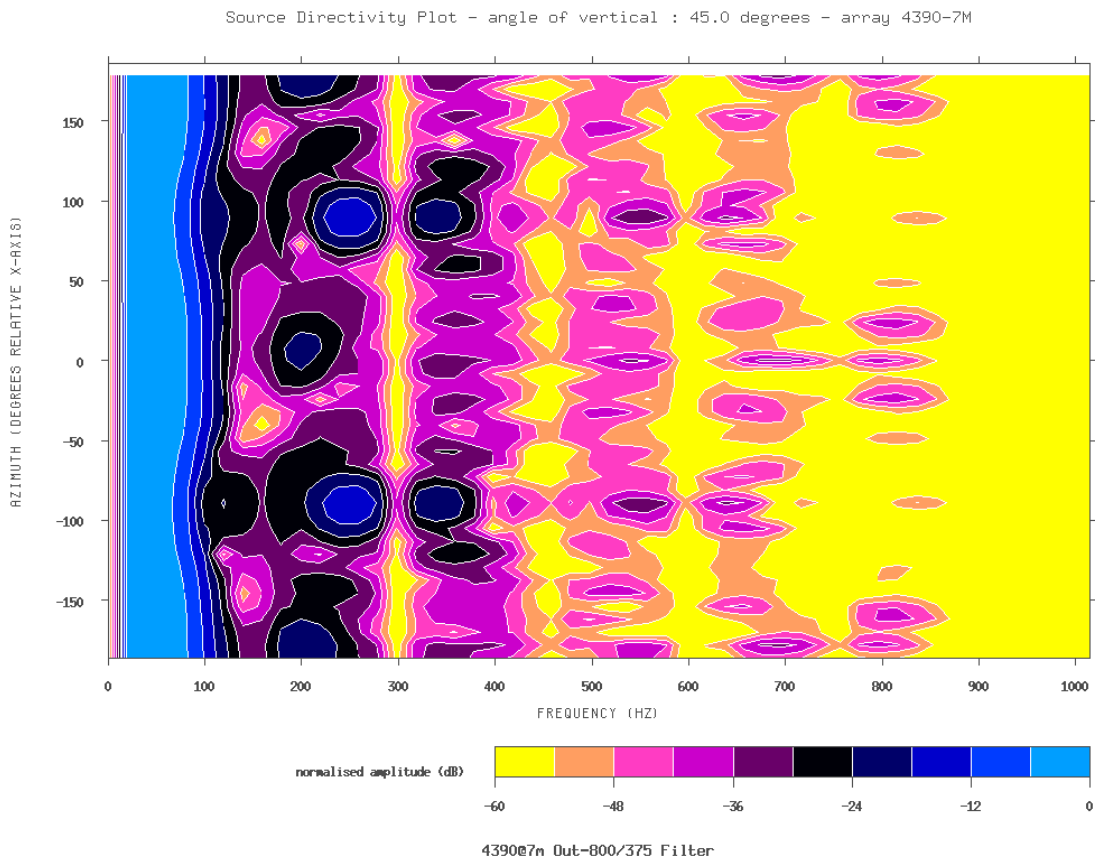
Figure 2-64 - 4390@7m_Out_800-375_directivity_angle_of_vertical-45deg_0-1000hz

Source Directivity Plot – angle of vertical : 90.0 degrees – array 4390-7M
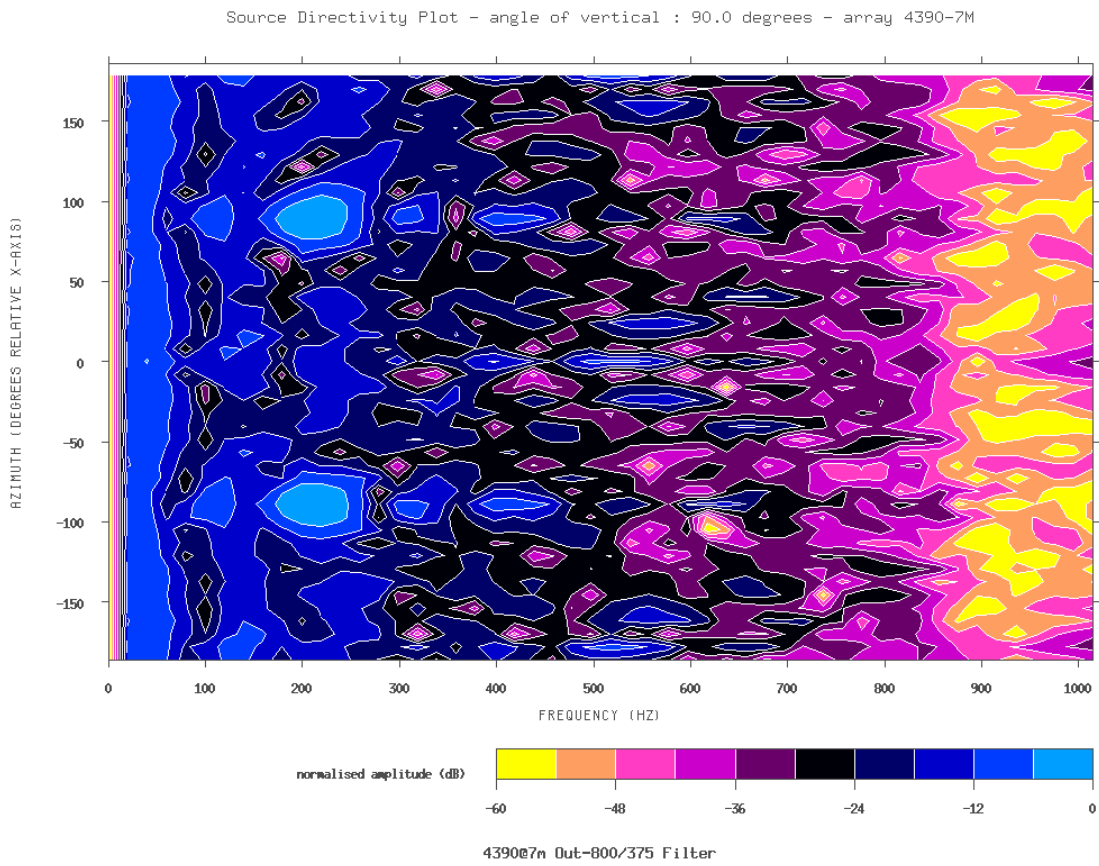
Figure 2-65 - 4390@7m_Out_800-375_directivity_angle_of_vertical-90deg_0-1000hz

Source Directivity Plot — frequency : 30.0 Hz. — array 4390-7M
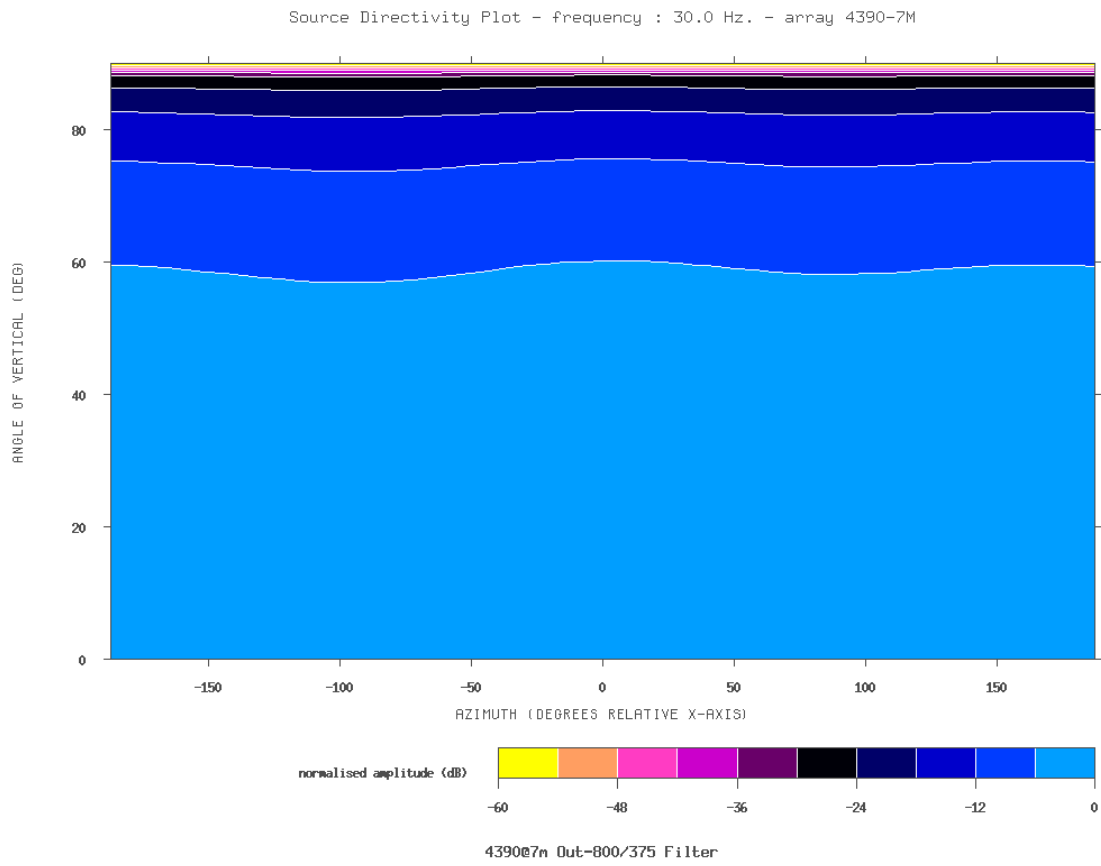
Figure 2-66 - 4390@7m_Out_800-375_directivity_Frequency-30Hz_0-1000hz
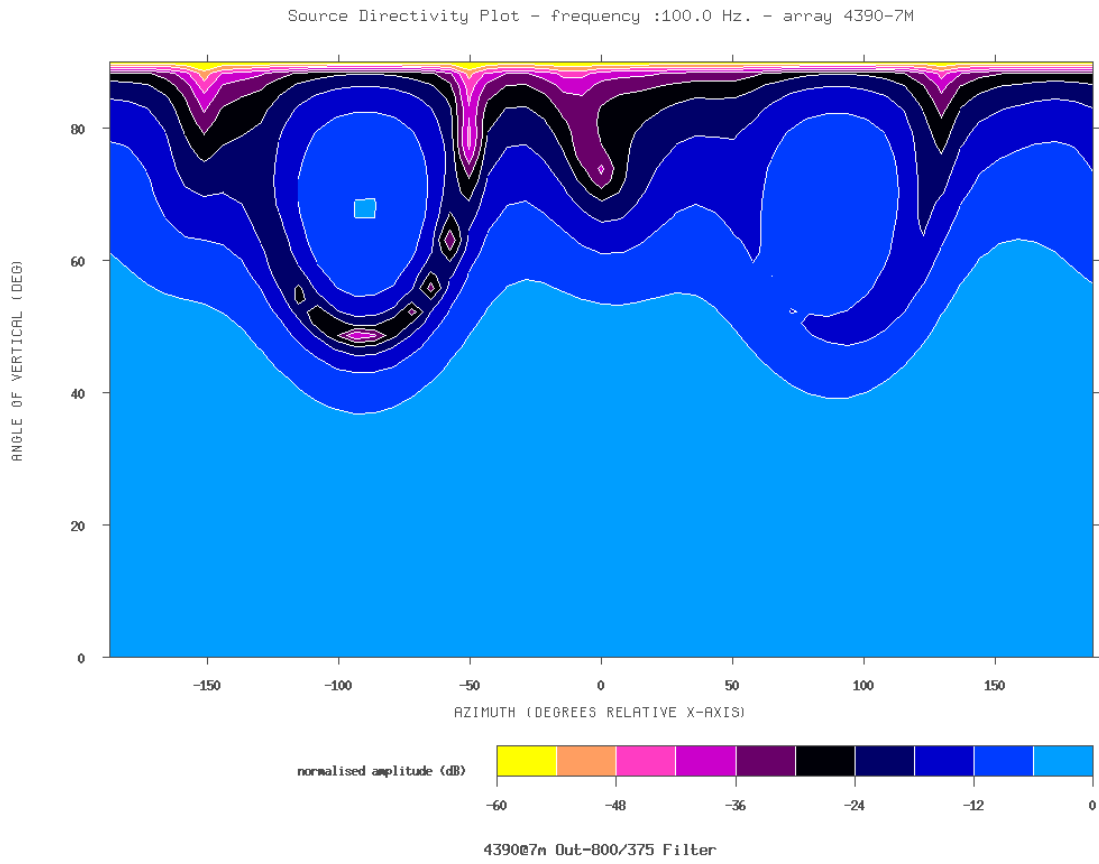
Figure 2-67 - 4390@7m_Out_800-375_directivity_Frequency-100Hz_0-1000hz
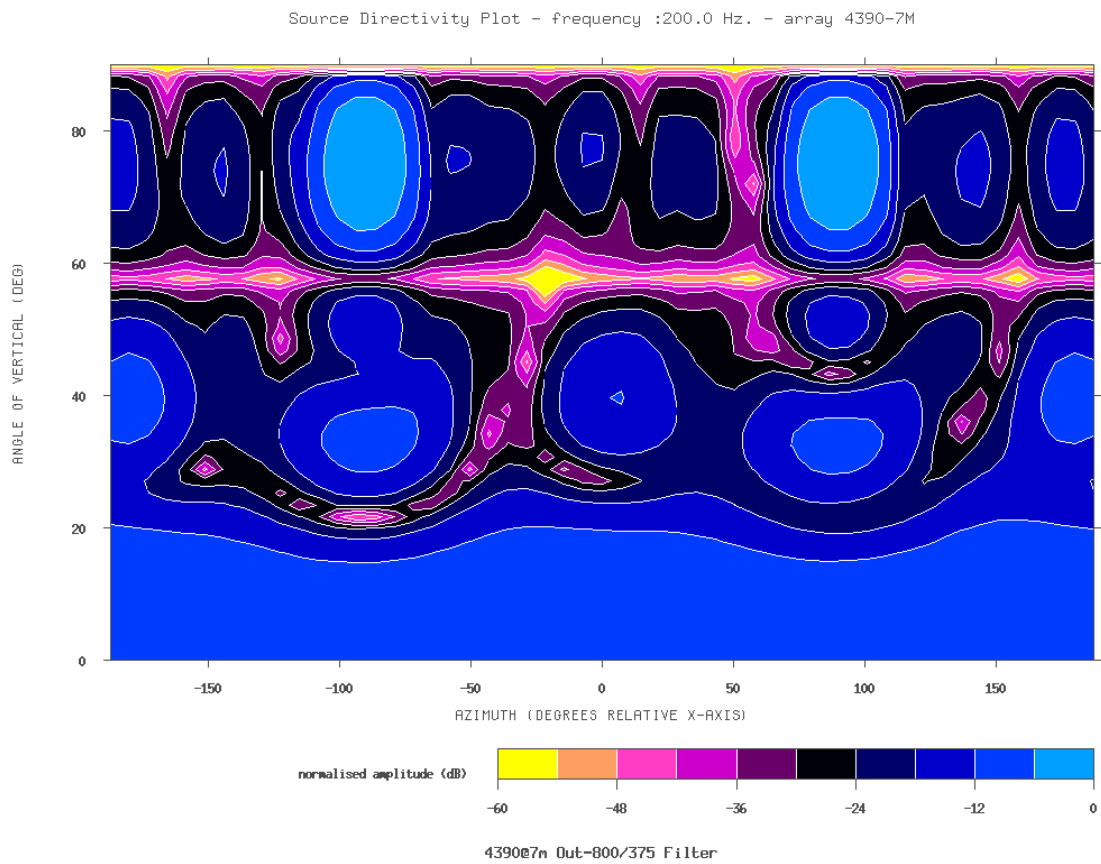
Figure 2-68 - 4390@7m_Out_800-375_directivity_Frequency-200Hz_0-1000hz
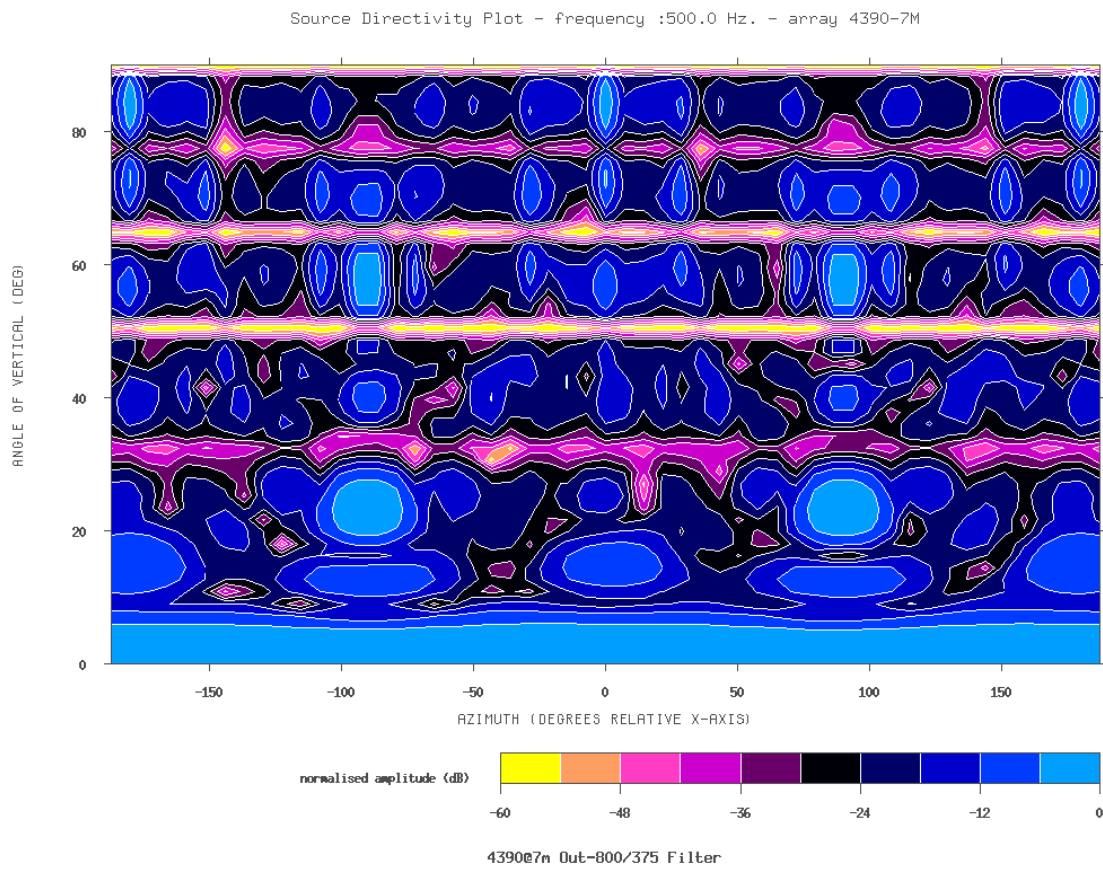
Figure 2-69 - 4390@7m_Out_800-375_directivity_Frequency-500Hz_0-1000hz
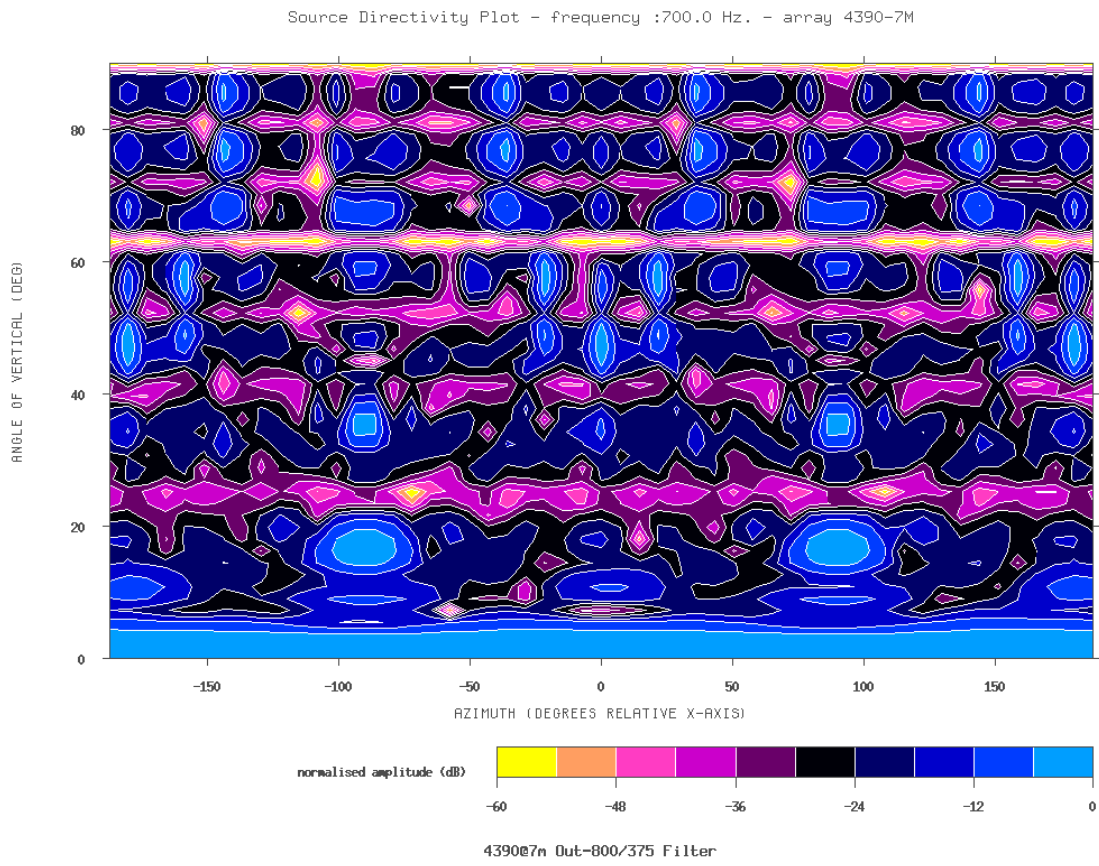
Figure 2-70 - 4390@7m_Out_800-375_directivity_Frequency-700Hz_0-1000hz

Source Directivity Plot - frequency :900.0 Hz. - array 4390-7M
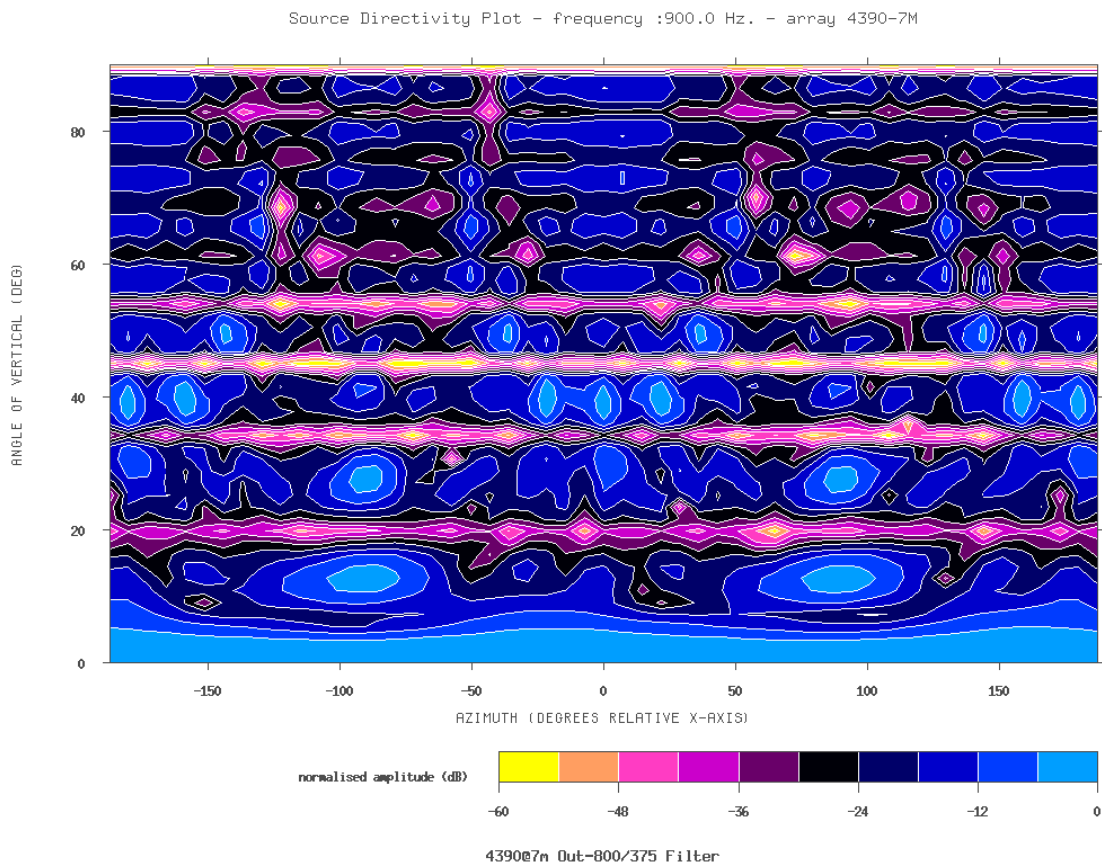
Figure 2-71 - 4390@7m_Out_800-375_directivity_Frequency-900Hz_0-1000hz
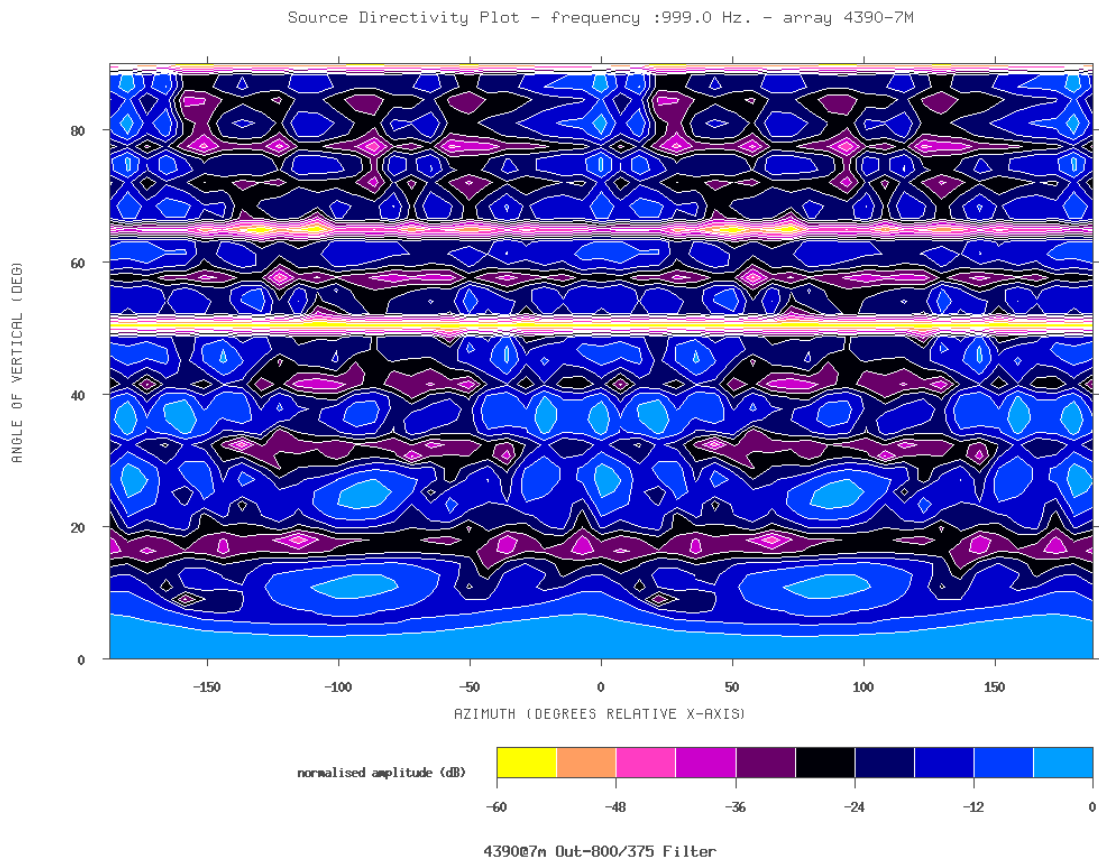
Figure 2-72 - 4390@7m_Out_800-375_directivity_Frequency-999Hz_0-1000hz

Far-field signature of array: 4390-7M

Distance: 9000 m   Azimuth: 0 deg   Angle of vertical: 0 deg

Primary : 49.3 barm	Source depth : 7.00 m
Peak-peak : 101.0 barm	Streamer depth : .00 m
P/B ratio : 17.4	Filter: out - 128.0/72 DFS V
Period (+/-) : 80.5/ 177.0 msec	Volume : 4390 cu.in.
	Pressure : 2000 psi
	Ghost strength : -1.00
	Sea temperatur : 17.00 C

bar m
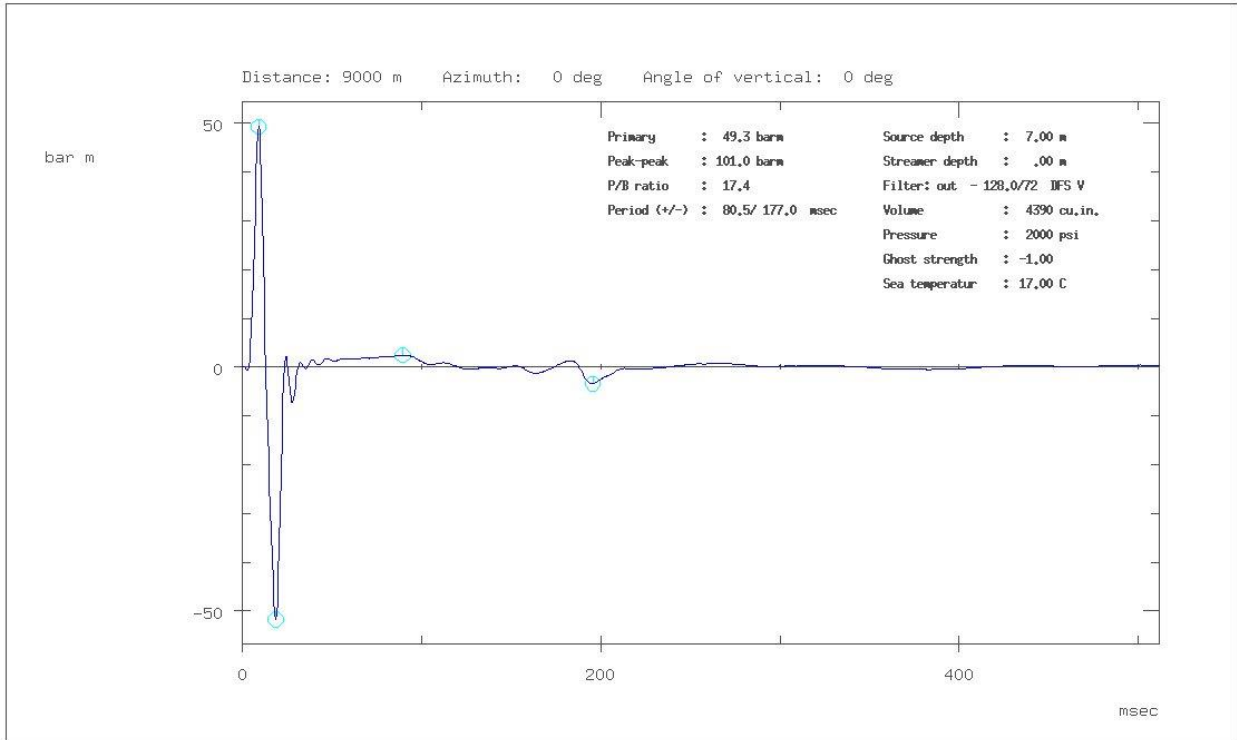
4390 @7m DFSV Out-128/72 Filter

Figure 2-73 - 4390@7m_DFSVI_Out_128-72_Signature

Amplitude spectrum of far-field signature of array: 4390-7M

Distance: 9000 m   Azimuth: 0 deg   Angle of vertical: 0 deg
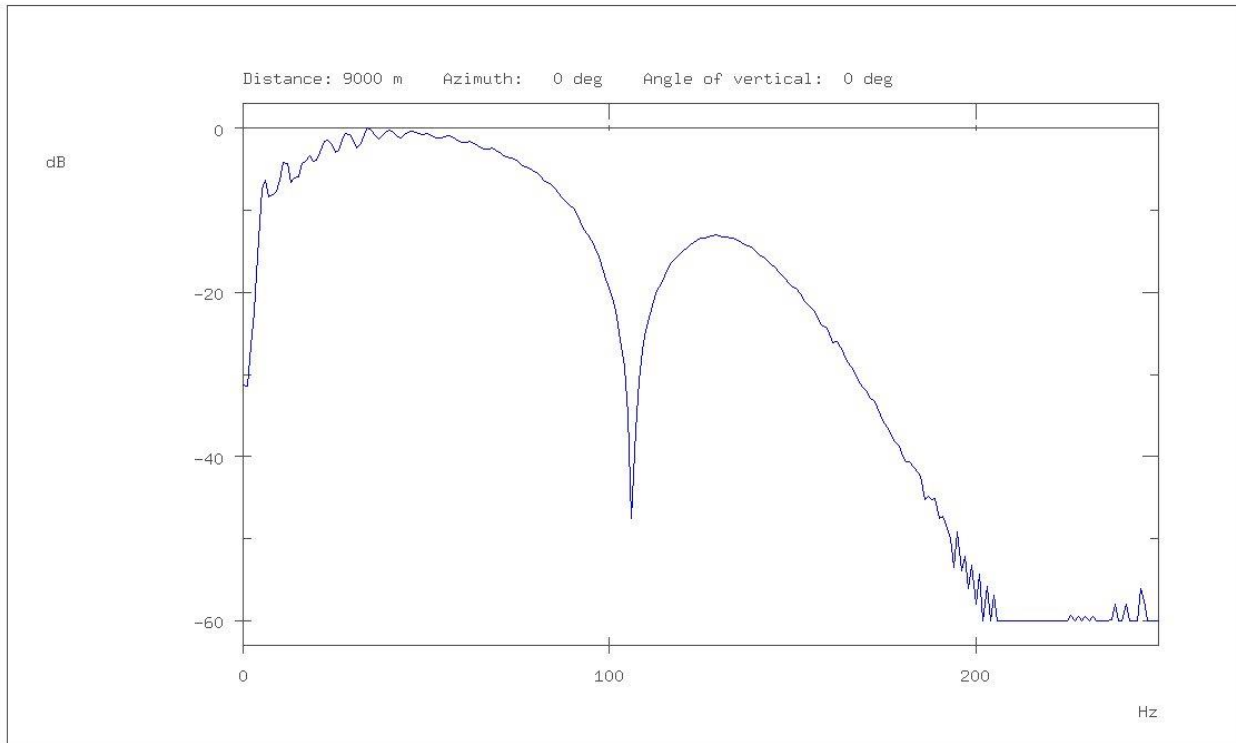
4390 @7m DFSV Out-128/72 Filter

Figure 2-74 - 4390@7m_DFSVI_Out_128-72_Relative_Spectrum

Amplitude spectrum of far-field signature of array: 4390-7M

Distance: 9000 m   Azimuth: 0 deg   Angle of vertical: 0 deg
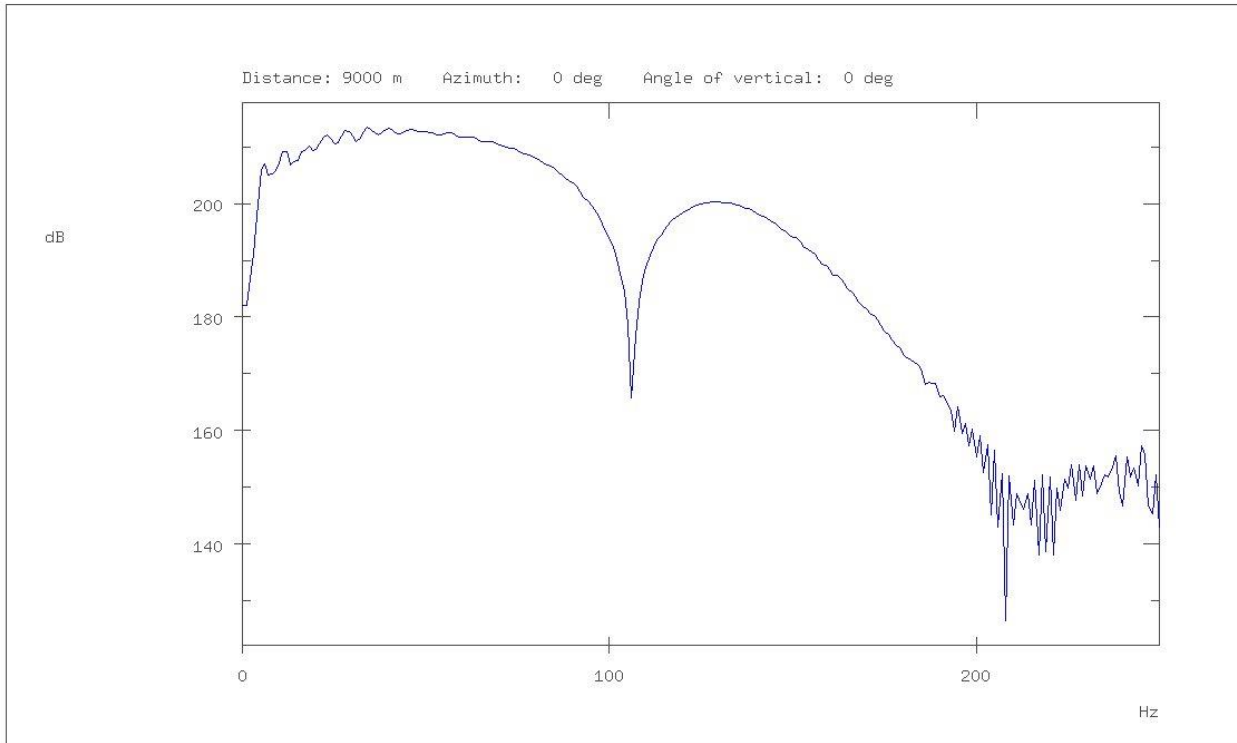
4390 @7m DFSV Out-128/72 Filter

Figure 2-75 - 4390@7m_DFSVI_Out_128-72_Absolutr_Spectrum

Far-field signature of array: 4390-7M
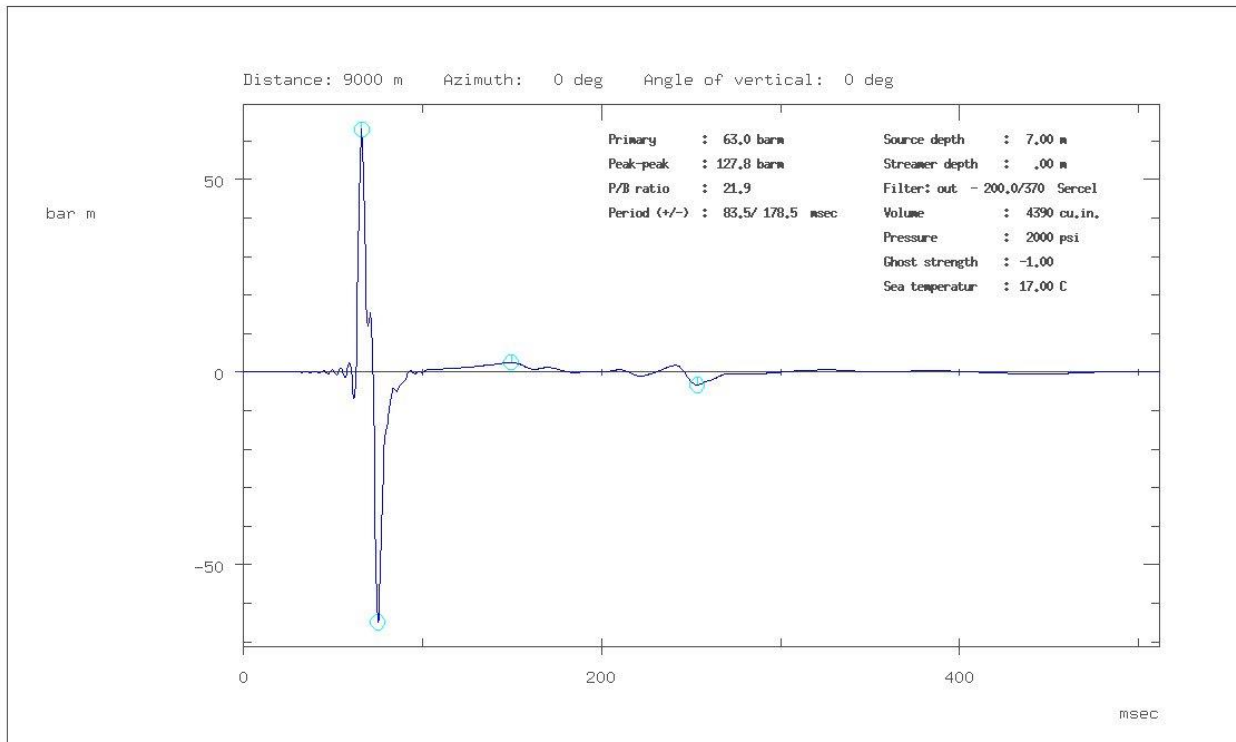
Figure 2-76 - 4390@7m_Seal_Out(3-6)_200-370_Signature

Amplitude spectrum of far-field signature of array: 4390-7M

Distance: 9000 m   Azimuth: 0 deg   Angle of vertical: 0 deg

4390 @7m Seal Out(3/6)-200/370 Filter (production)
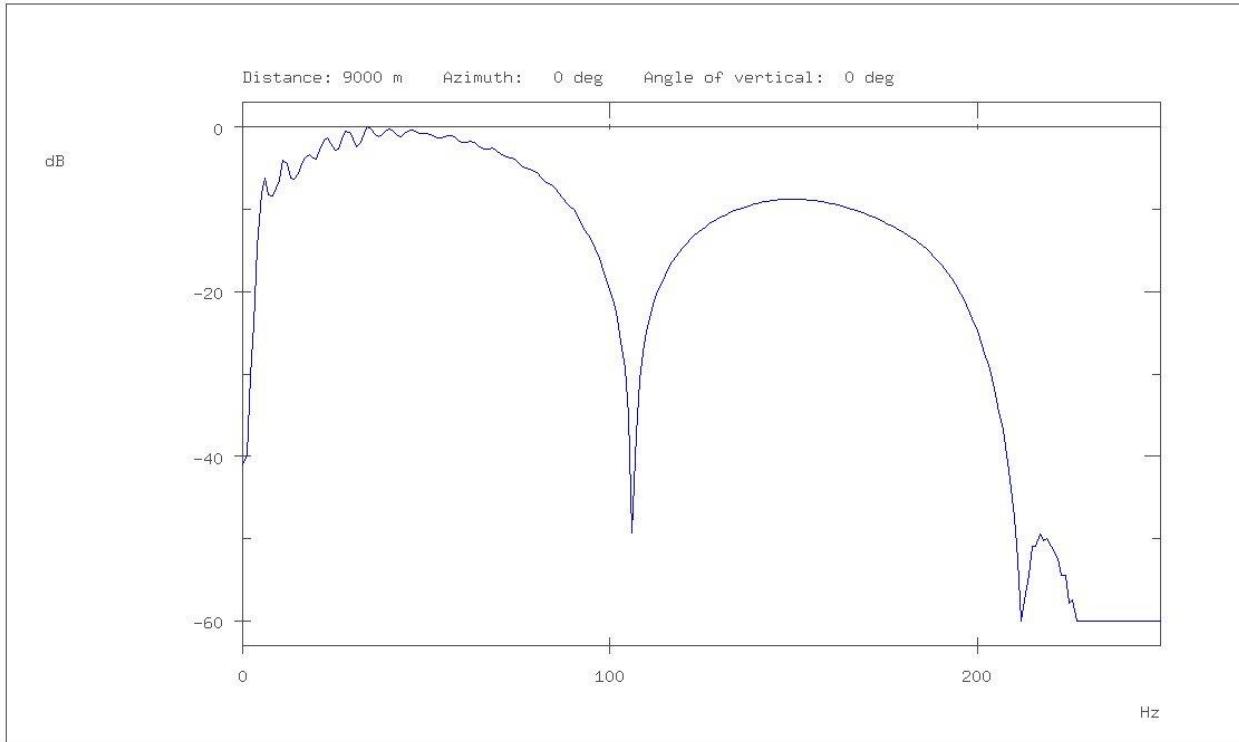
Figure 2-77 - 4390@7m_Seal_Out(3-6)_200-370_Relative_Spectrum_0-250Hz

Amplitude spectrum of far-field signature of array: 4390-7M

4390 @7m Seal Out(3/6)-200/370 Filter (production)
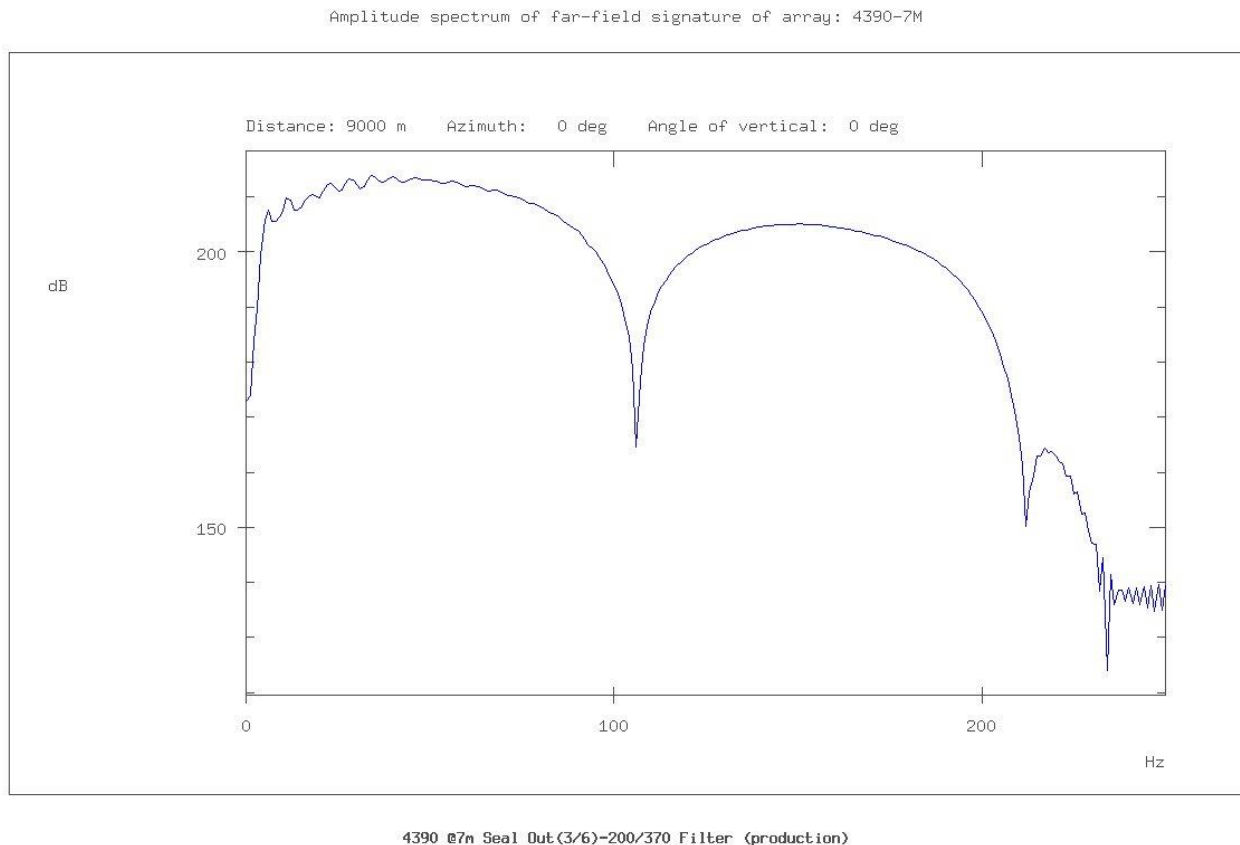
Figure 2-78 - 4390@7m_Seal_Out(3-6)_200-370_Absolute_Spectrum_0-250Hz

2.6   Conclusions

2.6.1   General:

Legacy data from the 1970's was reviewed and the following observations were made:

- Energy source was Vaporchoc. This kind of source is not used anymore due to it's unrealibility, the mixed phase of the source signature and its undesirable source charteristics

- Extracted wavelet demonstrates

  o   Minimal low frequencies due to the acquisition filters and processing.

  o   Multiple notches in the spectra due to the streamer ghost (19m tow depth results in a notch every ~40Hz).

  o   Low PBR compared to modern standards

RPS considers the following aspects of the marine seismic source to be critical in choosing an array:

- Ambient and source generated noise

  o High P-P strength – 100bar-m for modern sources

  o High PBR

- Temporal bandwidth of the wavelet.

  o We want as close to spike as possible. Marine source limited due to absorption at high end and what a seismic source can produce at the low end

  o Modern sources can produce useful frequencies in the range 5-250Hz

  o In the available legacy data the bandwidth was extremely low and this negatively impacts interpretation of the data

2.6.2   RPS recommended marine seismic sources

- RPS suggests the following bolt-gun arrays:

  1. 3640 in^3 @7m

  2. 4100 in^3 @7m

  3. 4390 in^3 @7m

- Array 1 represents the minimum source volume to fulfill the survey objectives as recommended by RPS.

- Array 2 represents the medium volume recommended by RPS.

- RPS considers the high peak to peak amplitude of ~100bar-m to be suitable for both the primary and secondary targets for the seismic survey.

- Array 3 is a higher volume alternative. It is more capable of meeting the objectives for the deeper top Jurassic platform and will have the best chance of maintaining signal to noise, and bandwidth in addition to penetration through any high impedance layers.

- All three source arrays are industry standard arrays and are proven to work well in a wide range of geological environments

3.0   REFERENCES

M. Landrø, L. Amundsen, 2010 "Marine Seismic Sources Part 1", GEOExPro, Vol. 7, No. 1

M. Egan, J Seissiger, A Salama, G El-Kaseeh, 2010 "The influence of spatial sampling on resolution", March 2010 CSEG Recorder

D Gisolf and Eric Vershuur, 2010, "The principles of quantitative acoustical imaging", EAGE Publications BV

Jack Caldwell et al, 2000," A brief overview of seismic air-gun arrays", The Leading Edge, p898

R.M Laws, R. Kragh, E. Morgan, G., 2008, "Are Seismic Sources Too Loud?", 70th EAGE Conference and Exhibition incorporating SPE EUROPEC 2008

G. Baeten, J.W. De Maag, R.-E. Plessix, R. Klaassen, T. Qureshi, M. Kleemeyer, F. T Kroode and Z. Rujie, 2013, "The use of low frequencies in a full-waveform inversion and impedance inversion land seismic case study", EAGE Vol 61, No 4, July 2013 pp. 701 – 711

S Ventosa, S Le Roy, I Huard, A Pica, H Rabeson, P Ricarte, L Duval, 2012, "Adaptive multiple subtraction with wavelet-based complex unary Wiener filters", Geophysics 183: 77. 183-192 Nov.-Dec

B.S Hart, 2013, "Whither Seismic Stratigraphy?", Interpretation A Journal of subsurface characterization, SEG and AAPG, Vol. 1 No. 1.

S. Hegna, G.E Parkes, 2011, "How to Influence the Low Frequency Output of Marine Air-gun Arrays", EAGE Publications

APPENDIX A: ARRAY LISTINGS

A-1 ARRAY 1 - 3640 @ 7M

```
ARRAY NAME          : Pol3640-7m
NUMBER OF ACTIVE GUNS:       33
TOTAL ACTIVE VOLUME :    3640 CU.IN.
NUMBER OF SPARE GUNS :       3
```

GUN #	GUN TYPE	X (m)	Y (m)	Z (m)	VOLUME (cu.in)	PRESSURE (psi)	WSK	DELAY (ms)
1	18	7.00	7.10	7.00	45	2000	1.00	.00
2	18	7.00	6.50	7.00	45	2000	1.00	.00
3	18	4.20	7.10	7.00	70	2000	1.00	.00
4	18	4.20	6.50	7.00	70	2000	1.00	.00
5	13	1.40	7.30	7.00	175	2000	1.00	.00
6	13	1.40	6.30	7.00	175	2000	1.00	.00
7	13	-1.40	7.30	7.00	175	SPARE	1.00	.00
8	13	-1.40	6.30	7.00	175	2000	1.00	.00
9	18	-4.20	7.10	7.00	70	2000	1.00	.00
10	18	-4.20	6.50	7.00	70	2000	1.00	.00
11	18	-7.00	7.10	7.00	45	2000	1.00	.00
12	18	-7.00	6.50	7.00	45	2000	1.00	.00
13	18	7.00	.10	7.00	90	2000	1.00	.00
14	18	7.00	-.50	7.00	90	2000	1.00	.00
15	18	4.20	.10	7.00	110	2000	1.00	.00
16	18	4.20	-.50	7.00	110	2000	1.00	.00
17	13	1.40	.30	7.00	290	2000	1.00	.00
18	13	1.40	-.70	7.00	290	SPARE	1.00	.00
19	13	-1.40	.30	7.00	290	2000	1.00	.00
20	13	-1.40	-.70	7.00	290	2000	1.00	.00
21	18	-4.20	.10	7.00	110	2000	1.00	.00
22	18	-4.20	-.50	7.00	110	2000	1.00	.00
23	18	-7.00	.10	7.00	90	2000	1.00	.00
24	18	-7.00	-.50	7.00	90	2000	1.00	.00
25	18	7.00	-6.90	7.00	45	2000	1.00	.00
26	18	7.00	-7.50	7.00	45	2000	1.00	.00
27	18	4.20	-6.90	7.00	70	2000	1.00	.00
28	18	4.20	-7.50	7.00	70	2000	1.00	.00
29	13	1.40	-6.70	7.00	175	2000	1.00	.00
30	13	1.40	-7.70	7.00	175	2000	1.00	.00
31	13	-1.40	-6.70	7.00	175	SPARE	1.00	.00
32	13	-1.40	-7.70	7.00	175	2000	1.00	.00
33	18	-4.20	-6.90	7.00	70	2000	1.00	.00
34	18	-4.20	-7.50	7.00	70	2000	1.00	.00
35	18	-7.00	-6.90	7.00	45	2000	1.00	.00
36	18	-7.00	-7.50	7.00	45	2000	1.00	.00

```
THE GUN TYPES ARE:
   18: BOLT 1900LLXT
   13: BOLT 1500LL


 "WSK" IS THE RATIO BETWEEN THE PRIMARY
      VOLUME AND TOTAL CHAMBER VOLUME
      IN A BOLT 1500C GUN (TYPE 1)
      WITH WAVESHAPE KIT
```

A-2   ARRAY 2 - 4100 @ 7M

```
ARRAY NAME              : CGG4100
NUMBER OF ACTIVE GUNS:      28
TOTAL ACTIVE VOLUME   :     4100 CU.IN.
NUMBER OF SPARE GUNS :       2
```

GUN #	GUN TYPE	X (m)	Y (m)	Z (m)	VOLUME (cu.in)	PRESSURE (psi)	WSK	DELAY (ms)
1	13	.00	8.50	7.00	250	2000	1.00	.00
2	13	.00	7.50	7.00	250	2000	1.00	.00
3	18	4.00	8.40	7.00	70	2000	1.00	.00
4	18	4.00	7.60	7.00	70	2000	1.00	.00
5	13	8.00	8.50	7.00	300	SPARE	1.00	.00
6	13	8.00	7.50	7.00	300	2000	1.00	.00
7	18	10.00	8.40	7.00	100	2000	1.00	.00
8	18	10.00	7.40	7.00	100	2000	1.00	.00
9	18	12.00	8.00	7.00	100	2000	1.00	.00
10	18	14.00	8.00	7.00	70	2000	1.00	.00
11	13	.00	.50	7.00	300	2000	1.00	.00
12	13	.00	-.50	7.00	300	2000	1.00	.00
13	18	4.00	.40	7.00	40	2000	1.00	.00
14	18	4.00	-.40	7.00	40	2000	1.00	.00
15	18	8.00	.40	7.00	150	2000	1.00	.00
16	18	8.00	-.40	7.00	150	2000	1.00	.00
17	18	10.00	.40	7.00	100	2000	1.00	.00
18	18	10.00	-.40	7.00	100	2000	1.00	.00
19	18	12.00	.00	7.00	100	2000	1.00	.00
20	18	14.00	.00	7.00	150	2000	1.00	.00
21	13	.00	-7.50	7.00	250	2000	1.00	.00
22	13	.00	-8.50	7.00	250	SPARE	1.00	.00
23	18	4.00	-7.60	7.00	70	2000	1.00	.00
24	18	4.00	-8.40	7.00	70	2000	1.00	.00
25	13	8.00	-7.50	7.00	300	2000	1.00	.00
26	13	8.00	-8.50	7.00	300	2000	1.00	.00
27	18	10.00	-7.60	7.00	100	2000	1.00	.00
28	18	10.00	-8.40	7.00	100	2000	1.00	.00
29	18	12.00	-8.00	7.00	100	2000	1.00	.00
30	18	14.00	-8.00	7.00	70	2000	1.00	.00

```
THE GUN TYPES ARE:
   13: BOLT 1500LL
   18: BOLT 1900LLXT


 "WSK" IS THE RATIO BETWEEN THE PRIMARY
 VOLUME AND TOTAL CHAMBER VOLUME
 IN A BOLT 1500C/1500LL GUN (TYPE 1/13)
 WITH WAVESHAPE KIT      ARRAY LISTING
```

A-3   ARRAY 3 - 4390 @ 7M

```
ARRAY NAME          : 4390-7M
NUMBER OF ACTIVE GUNS:      33
TOTAL ACTIVE VOLUME :    4390 CU.IN.
NUMBER OF SPARE GUNS :       3
```

GUN #	GUN TYPE	X (m)	Y (m)	Z (m)	VOLUME (cu.in)	PRESSURE (psi)	WSK	DELAY (ms)
1	18	7.00	7.30	7.00	45	2000	1.00	.00
2	18	7.00	6.70	7.00	45	2000	1.00	.00
3	18	4.20	7.30	7.00	70	2000	1.00	.00
4	18	4.20	6.70	7.00	70	2000	1.00	.00
5	18	1.40	7.50	7.00	230	2000	1.00	.00
6	18	1.40	6.50	7.00	230	2000	1.00	.00
7	18	-1.40	7.50	7.00	230	SPARE	1.00	.00
8	18	-1.40	6.50	7.00	230	SPARE	1.00	.00
9	18	-4.20	7.30	7.00	70	2000	1.00	.00
10	18	-4.20	6.70	7.00	70	2000	1.00	.00
11	18	-7.00	7.30	7.00	45	2000	1.00	.00
12	18	-7.00	6.70	7.00	45	2000	1.00	.00
13	18	7.00	.30	7.00	90	2000	1.00	.00
14	18	7.00	-.30	7.00	90	2000	1.00	.00
15	18	4.20	.30	7.00	110	2000	1.00	.00
16	18	4.20	-.30	7.00	110	2000	1.00	.00
17	13	1.40	.50	7.00	380	2000	1.00	.00
18	13	1.40	-.50	7.00	380	2000	1.00	.00
19	13	-1.40	.50	7.00	380	2000	1.00	.00
20	13	-1.40	-.50	7.00	380	2000	1.00	.00
21	18	-4.20	.30	7.00	110	2000	1.00	.00
22	18	-4.20	-.30	7.00	110	2000	1.00	.00
23	18	-7.00	.30	7.00	90	2000	1.00	.00
24	18	-7.00	-.30	7.00	90	2000	1.00	.00
25	18	7.00	-7.30	7.00	45	2000	1.00	.00
26	18	7.00	-6.70	7.00	45	2000	1.00	.00
27	18	4.20	-7.30	7.00	70	2000	1.00	.00
28	18	4.20	-6.70	7.00	70	2000	1.00	.00
29	18	1.40	-7.50	7.00	230	2000	1.00	.00
30	18	1.40	-6.50	7.00	230	2000	1.00	.00
31	18	-1.40	-7.50	7.00	230	2000	1.00	.00
32	18	-1.40	-6.50	7.00	230	SPARE	1.00	.00
33	18	-4.20	-7.30	7.00	70	2000	1.00	.00
34	18	-4.20	-6.70	7.00	70	2000	1.00	.00
35	18	-7.00	-7.30	7.00	45	2000	1.00	.00
36	18	-7.00	-6.70	7.00	45	2000	1.00	.00

```
THE GUN TYPES ARE:
  13: BOLT 1500LL
  18: BOLT 1900LLXT
```

```
 "WSK" IS THE RATIO BETWEEN THE PRIMARY
      VOLUME AND TOTAL CHAMBER VOLUME
      IN A BOLT 1500C/1500LL GUN (TYPE 1/13)
```

APPENDIX B: MIGRATION APERTURE

This section includes a brief analysis on migration aperture and an approximation of the required survey extent to obtain full fold fully migrated data at target.

Migration Aperture

- Migration aperture or halo for survey design purposes can be described as the half aperture required *inside* of the full-fold boundary in order to obtain fully migrated at that inner boundary, the Interpretation area

- To obtain optimum lateral and vertical resolution it is desirable to use a high dip migration operator to collapse the Fresnel zone and ensure that there is sufficient energy recorded below the horizon of interest such that the migration operator can sum the contributions of any diffraction tails correctly.

- Straight-ray assumptions presume constant velocities whereas curved-ray assumptions account for ray-bending at velocity interfaces leading to smaller aperture estimates. Curved-ray calculations are generally accepted to be more representative of the real world where compaction tends to drive the increase of velocity with depth in at least some sections of the subsurface.

Three Zone Acquisition Model

Acquisition: Fold Taper **Processing:** Migration apron **Interpretation Area**

single-fold boundary   full-fold boundary
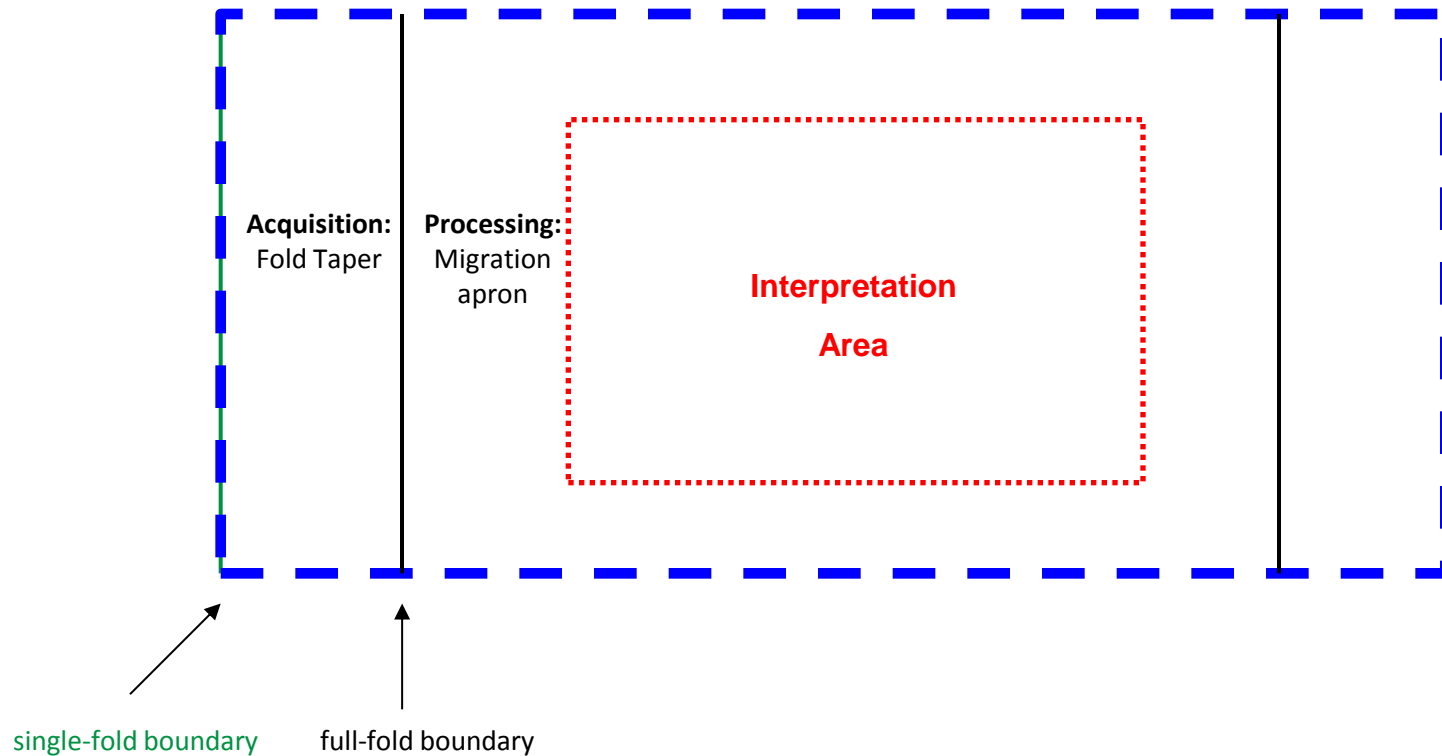
Comparison of migration impulse responses for different algorithms
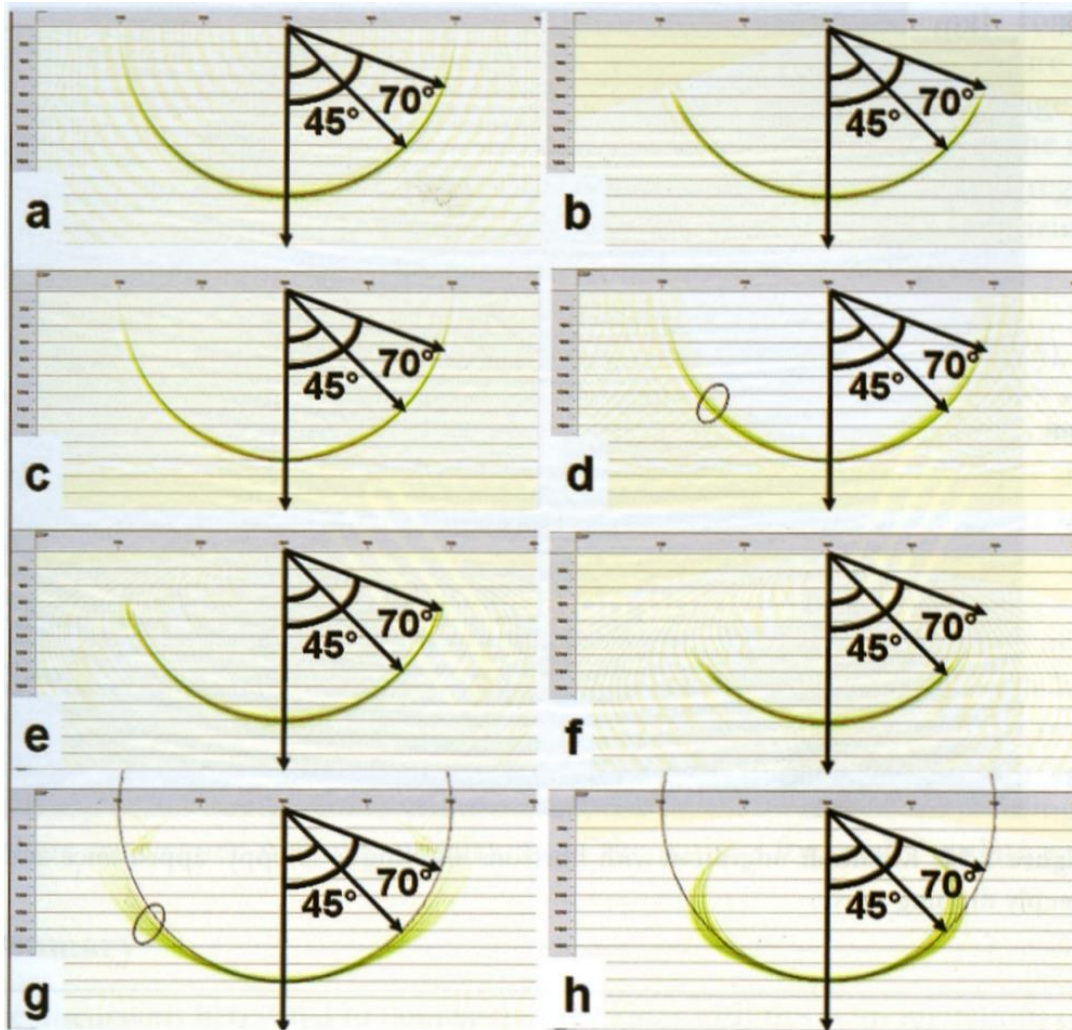
For optimum imaging we can argue that we should have an aperture equal to the dip accuracy of the migration algorithm, which can generally be said to be around 60 degrees for most modern applications

Comparison of migration impulse responses for different algorithms:
A) Phase shift,
B) Kirchhoff with explicit dip limit of 70-degrees ,
C) High Order FD RTM
D) Low order FD RTM
E) 70-degree explicit FD result
F) 50-degree explicit FD result
G) 80-degree explicit FD result
H) 15-degree explicit result

(Jones 2010)

Straight-ray migration distance

A   B

This diagram represents a constant velocity model in depth with the surface at 'A-B' and a dip 'u-v' of angle α. A seismic source and receiver at 'A' would reflect at the dip 'u-v' at C and be plotted vertically down on the 'plumb' coloured line. The migration distance is the lateral movement required to position the reflector in its true position above C.

Depth = d

v

α

migration distance

α

C

u
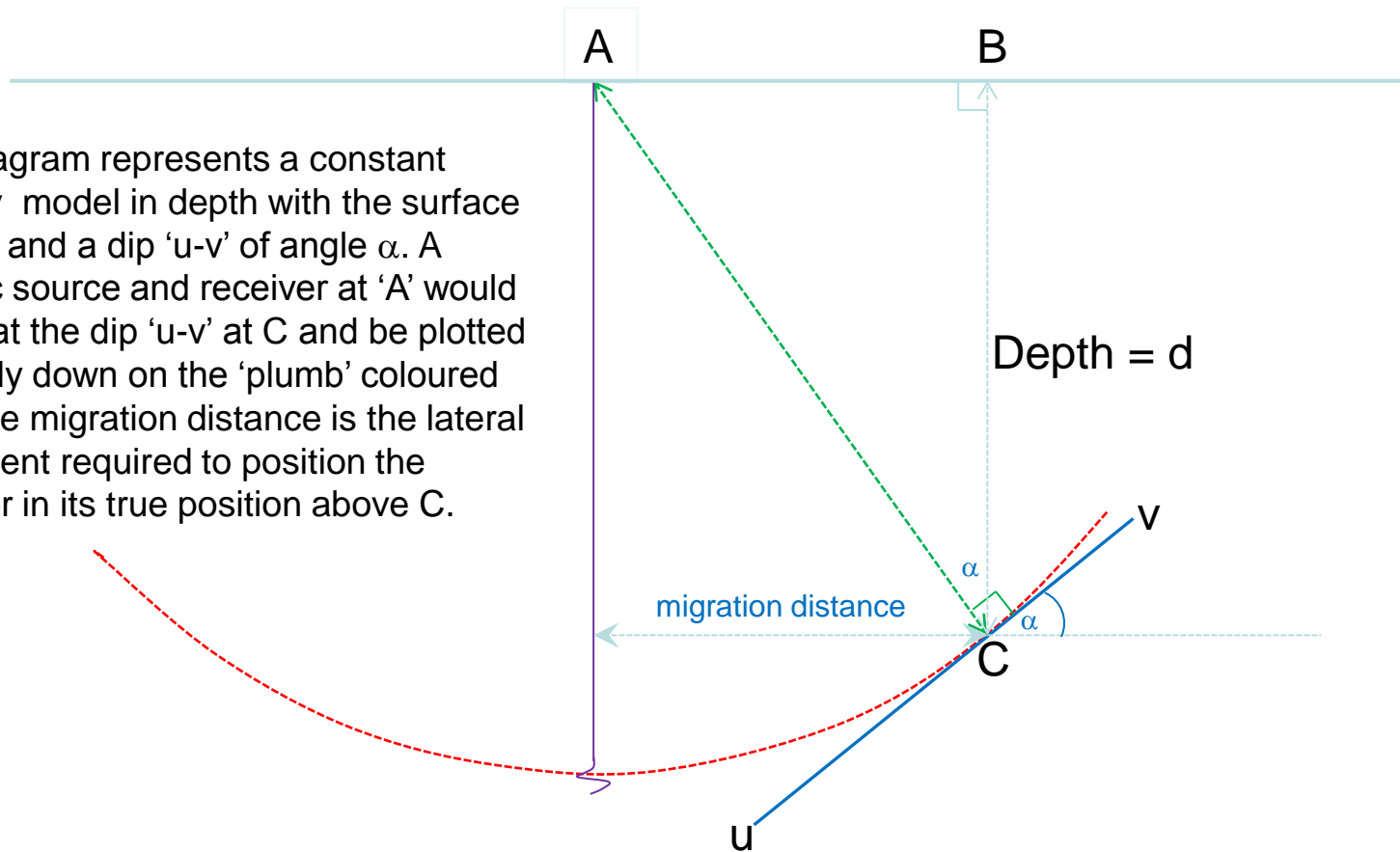
Curved-ray migration distance

This diagram represents a depth-variant velocity version of the previous slide. We can use Resnick for estimating the migration aperture here by re-formulating the straight ray using $\mathrm{Sin}(\alpha)$ and replacing $\mathrm{Sin}(\alpha)$ with $(V/V_i).\mathrm{Sin}(\alpha)$.

$$Tan = \frac{Sin}{Cos} = \frac{Sin}{\sqrt{1 - Sin^2}}$$

$$d.Tan(\alpha) = \frac{d.Sin(\alpha)}{\sqrt{1 - Sin^2(\alpha)}}$$

Substituting V/Vi we have

$$d.Tan(\alpha) = d.\frac{V}{Vi}\frac{Sin(\alpha)}{\sqrt{1 - \left(\left(\frac{V}{Vi}Sin(\alpha)\right)^2\right)}}$$

$$AB = d.\frac{V}{Vi}\frac{Sin(\alpha)}{\sqrt{1 - \left(\left(\frac{V}{Vi}Sin(\alpha)\right)^2\right)}}$$

A A' B

Depth = d

v

migration distance

α

α

C

u
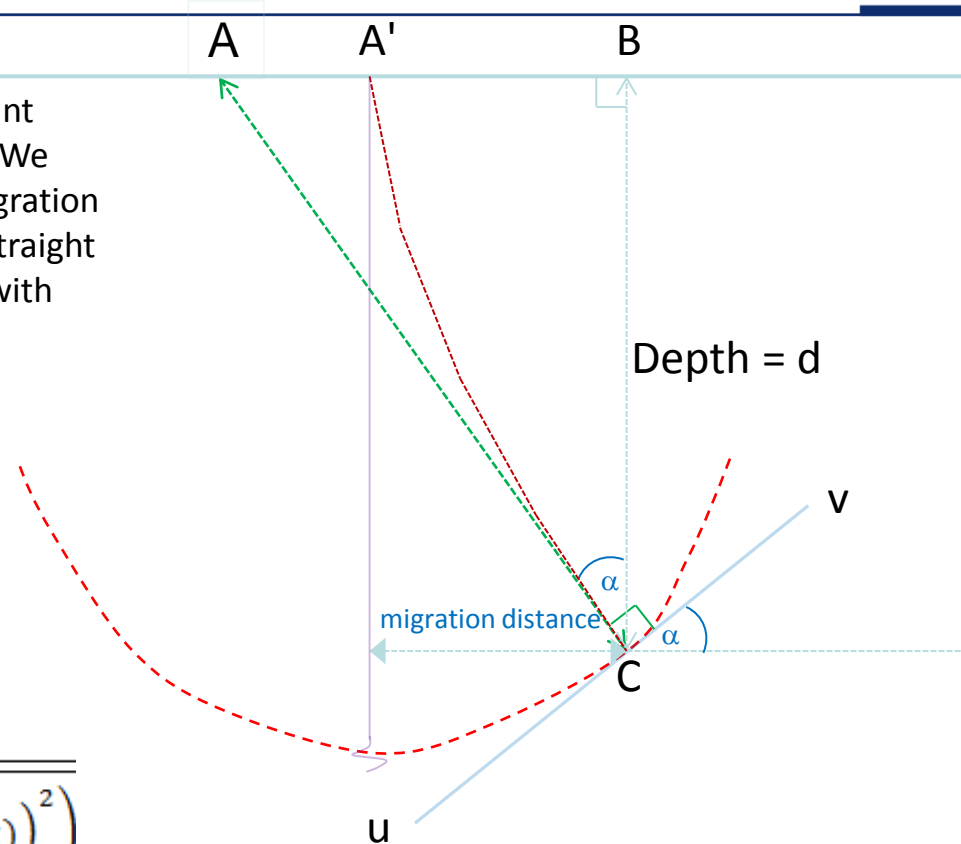
Migration aperture and resolution

FMAX = 60 Hz
Aperture = 30 deg

FMAX = 120 Hz
Aperture = 30 deg

FMAX = 60 Hz
Aperture = 90 deg

840 ft

840 ft

840 ft
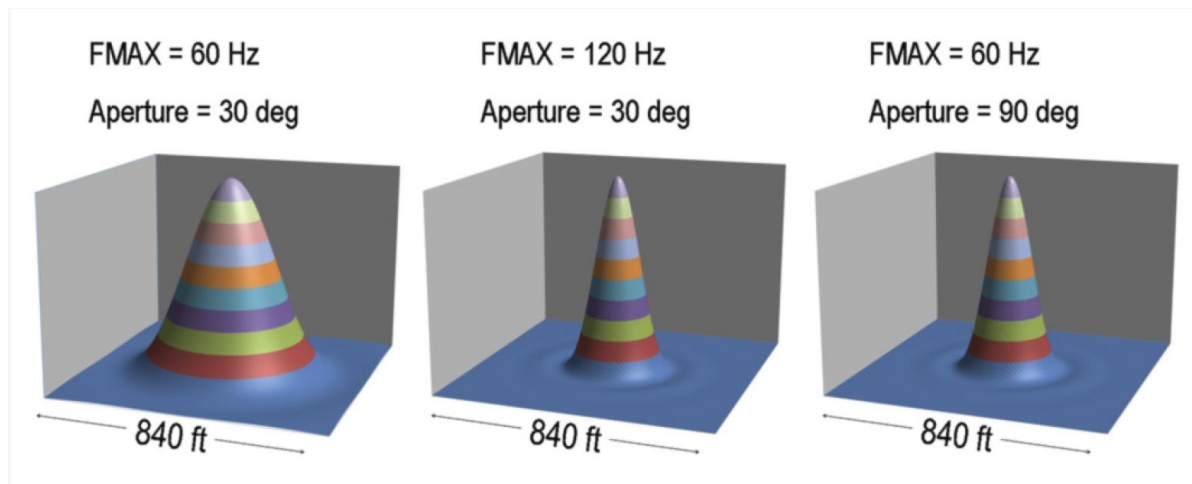
Taken from Egan et al 2010. Sample spatial wavelets after PSTM. These demonstrate the dependence of lateral resolution on temporal frequency and migration aperture.

F1 NW - Straight-ray migration distance
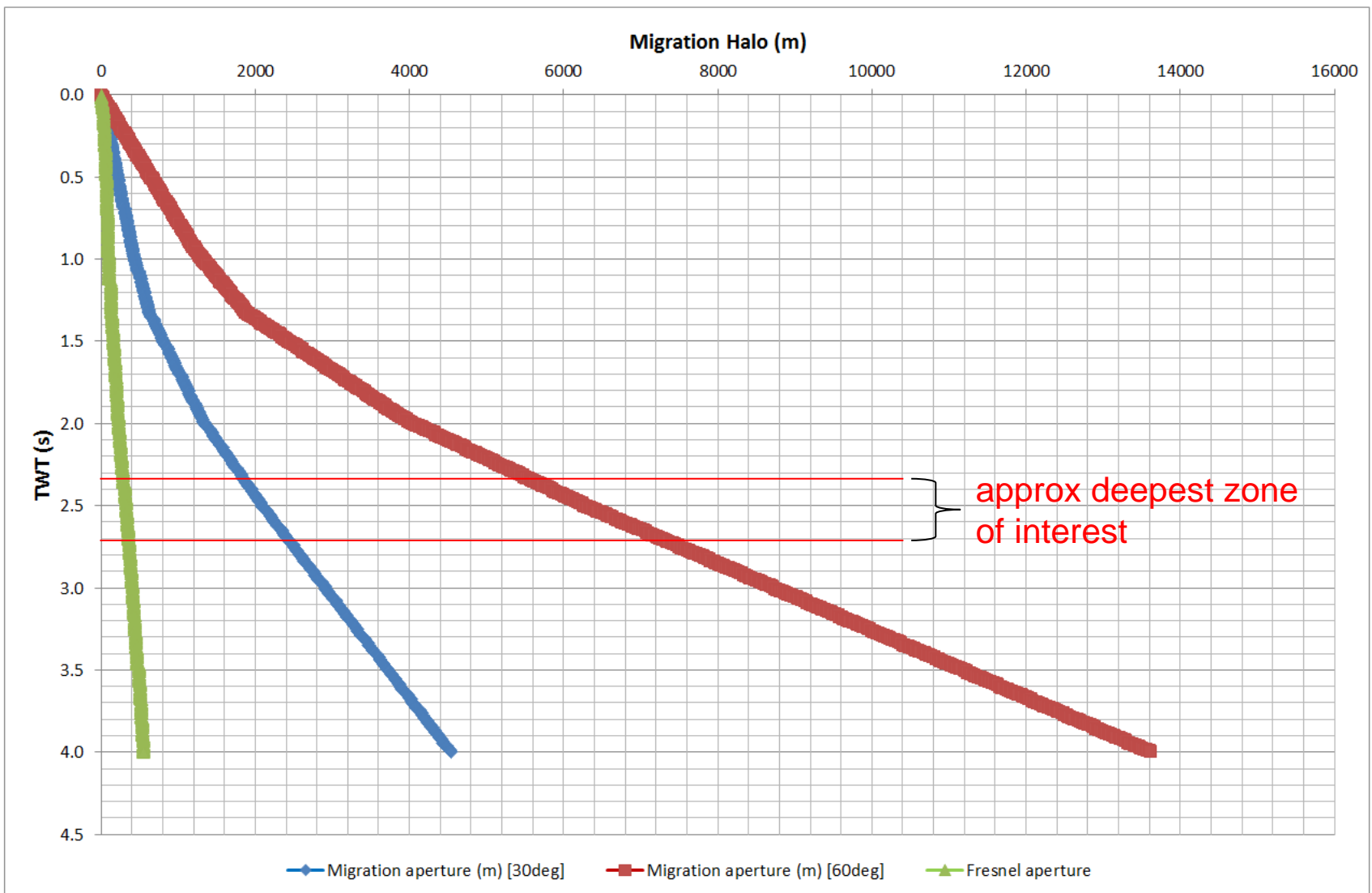
F1 - Straight-ray migration distance
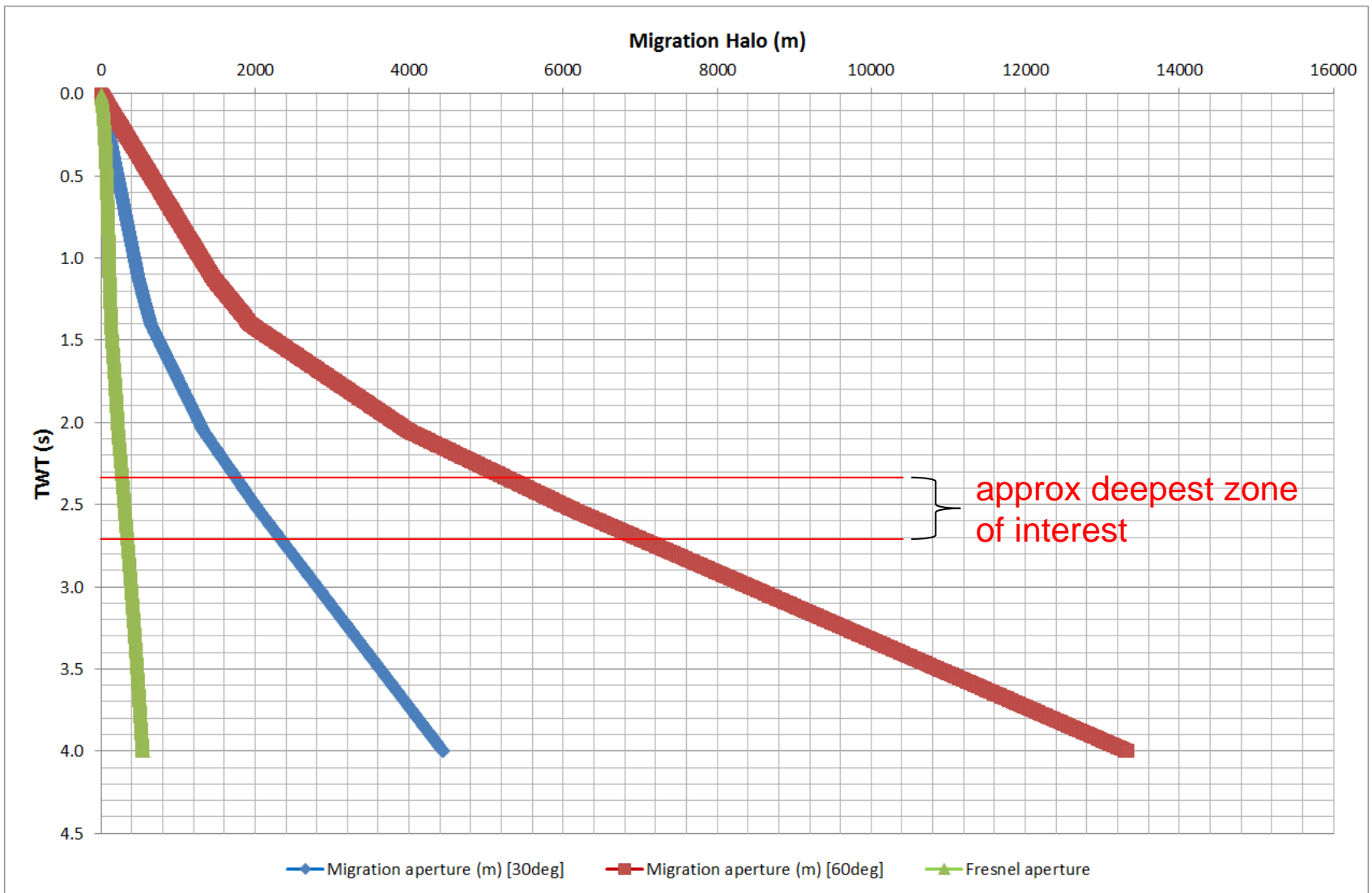
F1 NW - Curved-ray migration distance

approx deepest zone of interest
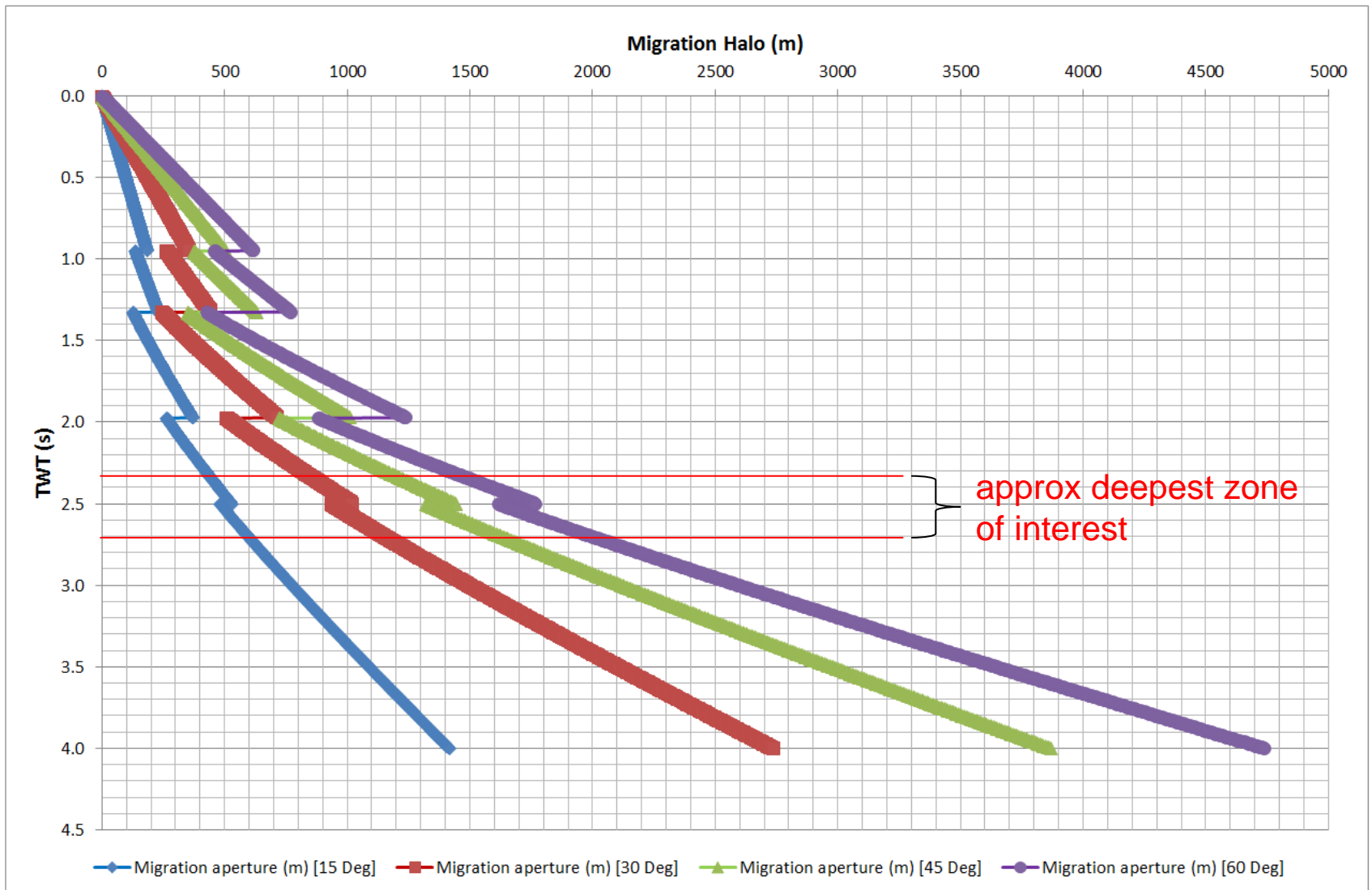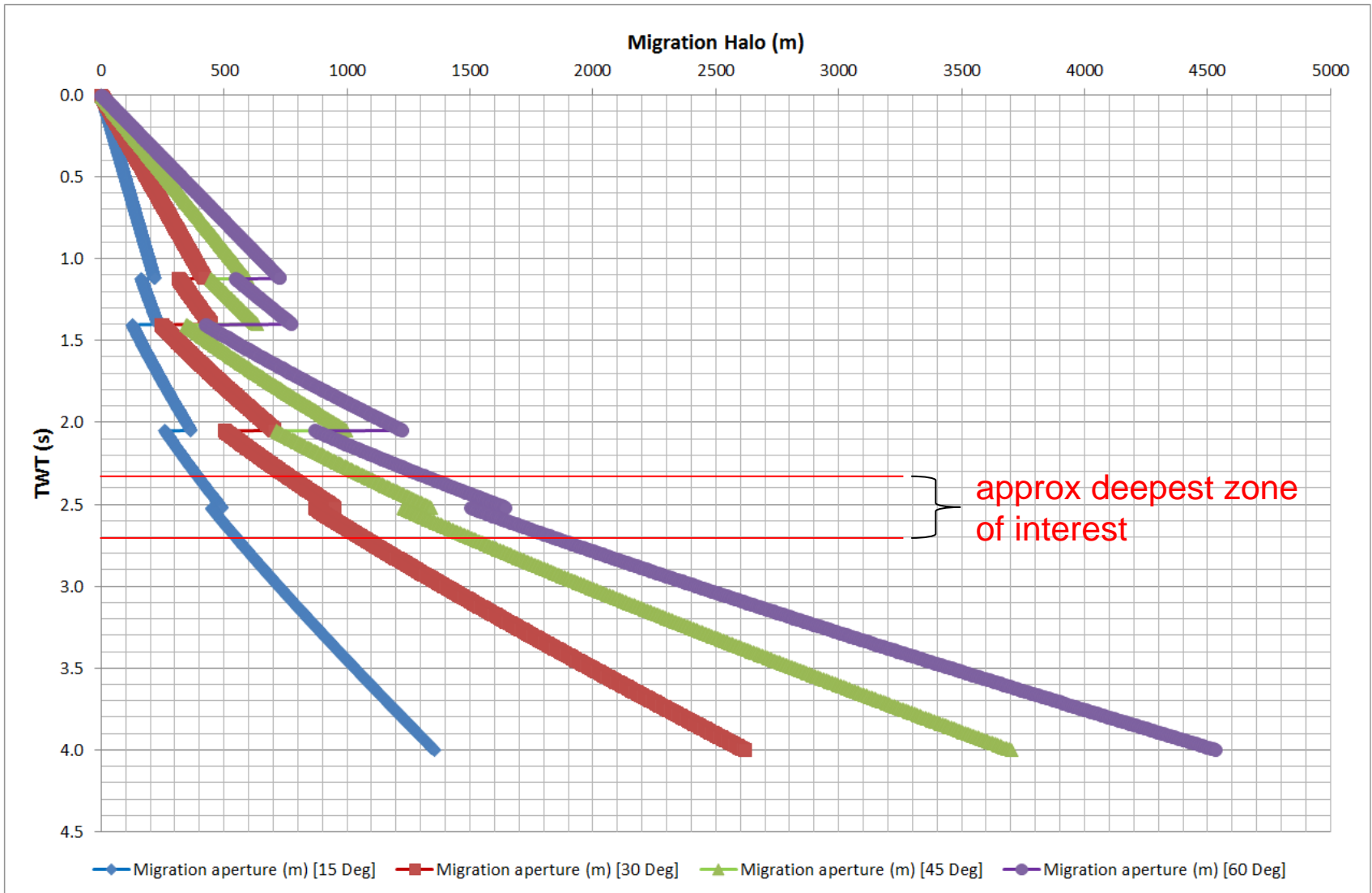
Conclusions

- Migration aperture calculations can make a large difference to predicted costs, particularly for smaller survey areas. There are sound arguments for both smaller and larger migration apertures. For the former we can argue that in practise the migration halo can be reduced by using the full-fold taper-on as part of the migration aperture. An argument for larger migration apertures is that the migration aperture increases with offset to at least half the offset concerned.

- For increased resolution a 60 degree aperture is typically recommended because only by fully summing all the amplitude back to its source can we obtain the theoretically best resolution. In the real world a whole host of factors, including SNR and sampling considerations, work to limit the obtainable resolution. In practice the migration aperture chosen in processing will be determined by testing because of factors such as SNR and sampling.

- Based on the above we can ascertain a theoretical curved-ray migration aperture somewhere between 1.5 km and ~2km which covers a 60° aperture. Note that as mentioned already in practise the migration halo can be reduced by using the full-fold taper-on as part of the migration aperture.

RPS

Seismic Source Array Sound Modelling
d84F.R-EL
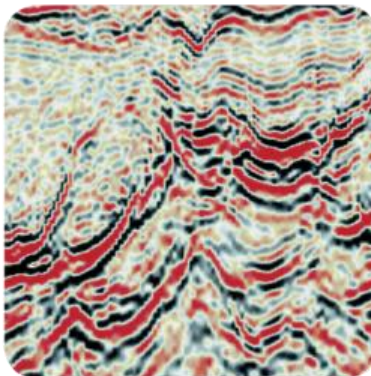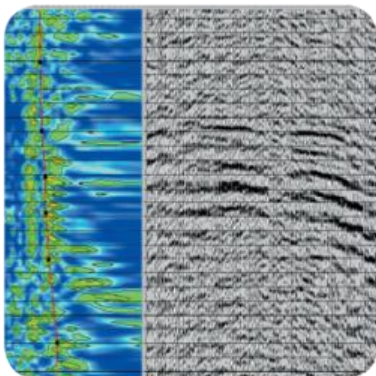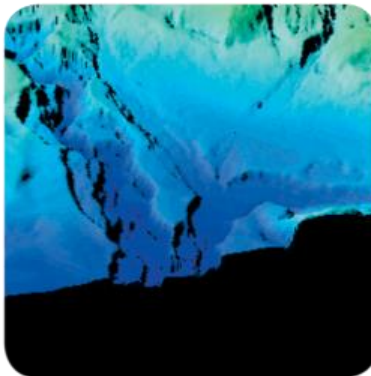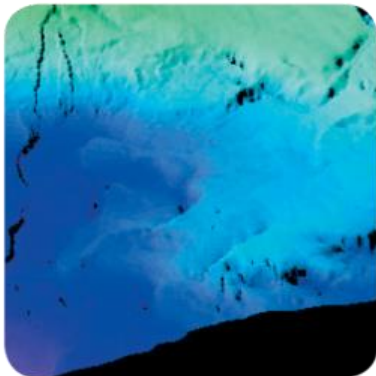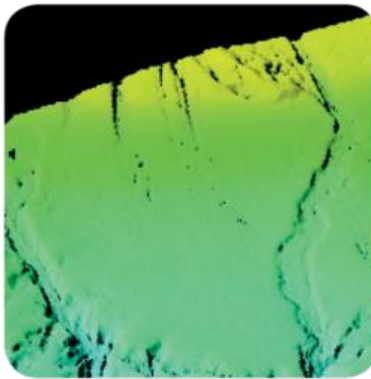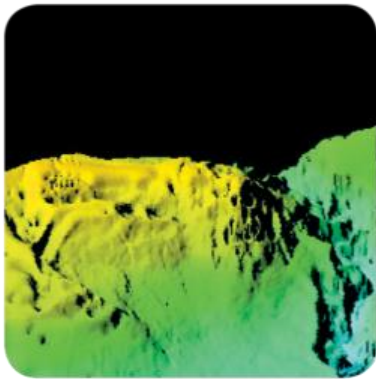
Seismic Source Array Sound Modelling
d84F.R-EL

Prepared for:
Petroceltic

Prepared by:
RPS Energy

6th September 2017

Project Title	Seismic Source Array Sound Modelling - d84F.R-EL		
Project Number	ECD1589	Date of Issue:	6th September 2017
	Author:	Project Manager	Peer Review
Name	Simon Stephenson		Phil Evans / Chris Helly

Document Description	Date	Issued By	Checked By	Accepted by Client	Comments
Version Draft	1st August 2017	Simon Stephenson	Chris Helly		
Version Final					
File Location:	RPS Goldvale House 27-41 Church Street West, Woking, Surrey, GU21 6DH, United Kingdom **T** +44 (0)1483 746500 **F** +44 (0)1483 746505 **E** rpswo@rpsgroup.com **W** www.rpsgroup.com				

Table of Contents

List of Tables

List of Figures

1.0   INTRODUCTION

Petroceltic proposes to undertake a 3D seismic survey in the Southern Ionian Sea. The survey area is located approximately 15 nautical miles offshore of Leuca, Italy. Water depths within the survey area range from approximately 200 to 900 m. The location of the survey areas is illustrated in Figure 1.1.
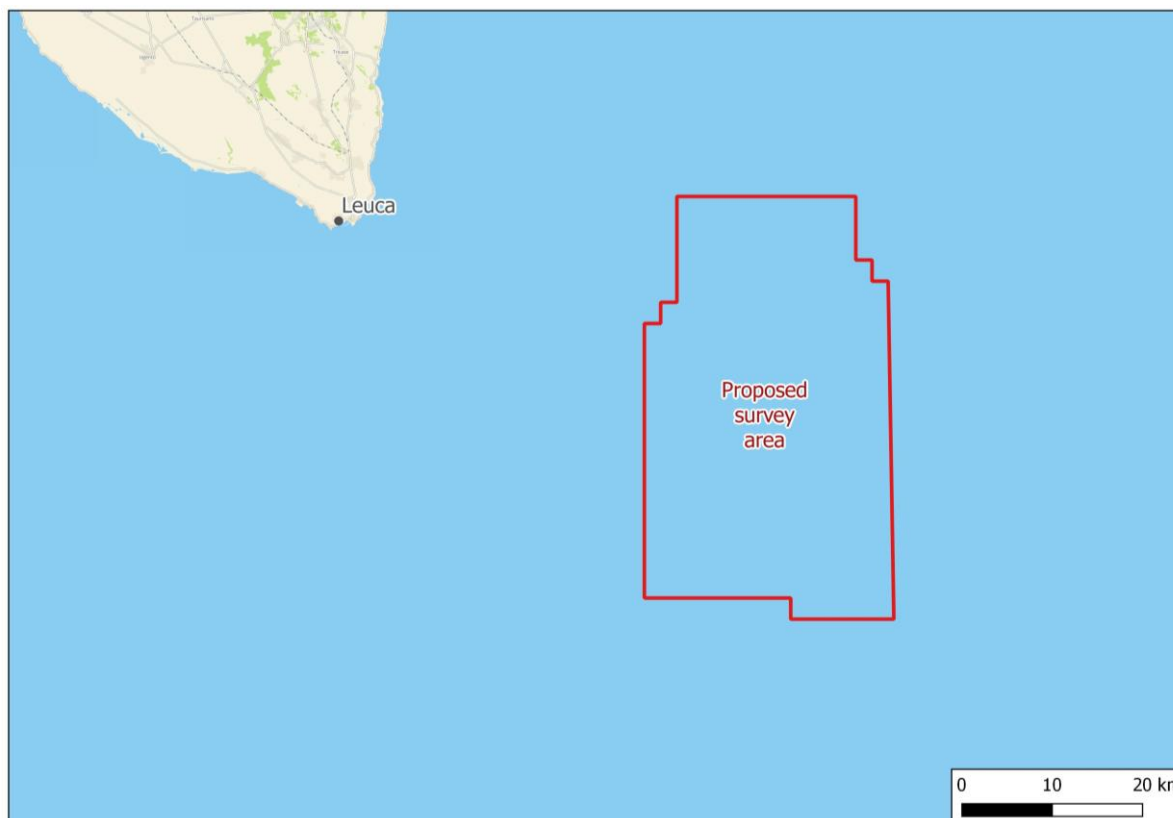
Figure 1.1   Location of survey area

The Phase 1 source array modelling and selection study identified three source arrays that would be best suited to the requirements of the seismic survey. Based on the outcome of the Phase 1 study, it is proposed to utilise one of three potential source arrays as follows:

- 3,640 cu in source array;

- 4,100 cu in source array; or

- 4,390 cu in source array.

Sound is readily transmitted underwater and there is potential for sound emissions from the survey to affect marine mammals and turtles. At long ranges, the introduction of additional sound could potentially cause short-term behavioural changes, for example to the ability of cetaceans to communicate and to determine the presence of predators, food, underwater features and obstructions. At close ranges and with high sound source levels, permanent or temporary hearing damage may occur, while at very close range, gross physical trauma is possible. This report provides an overview of the potential effects due to underwater sound from the survey on the surrounding marine environment.

The primary purpose of this underwater sound study is to predict the likely range of distances for the onset of potential injury (i.e. permanent threshold shifts in hearing) and behavioural effects for the proposed source arrays.

2.0   ACOUSTIC CONCEPTS AND TERMINOLOGY

Sound travels through the water as vibrations of the fluid particles in a series of pressure waves. The waves comprise a series of alternating compressions (positive pressure variations) and rarefactions (negative pressure fluctuations). Because sound consists of variations in pressure, the unit for measuring sound is usually referenced to a unit of pressure, the Pascal (Pa). The unit usually used to describe sound is the decibel (dB) and, in the case of underwater sound, the reference unit is taken as 1 µPa, whereas airborne sound is usually referenced to a pressure of 20 µPa. To convert from a sound pressure level referenced to 20 µPa to one referenced to 1 µPa, a factor of 20 log (20/1) i.e. 26 dB has to be added to the former quantity. Thus 60 dB re 20 µPa is the same as 86 dB re 1 µPa, although differences in sound speed and densities mean that the difference in sound intensity is much more than this from air to water. All underwater sound pressure levels in this report are described in dB re 1 µPa. In water the strength of a sound source is usually described by its sound pressure level in dB re 1 µPa, referenced back to a representative distance of 1 m from an assumed (infinitesimally small) point source. This allows calculation of sound levels in the far-field. For large distributed sources, the actual sound pressure level in the near-field will be lower than predicted.

There are several descriptors used to characterise a sound wave. The difference between the lowest pressure variation (rarefaction) and the highest pressure variation (compression) is the peak to peak (or pk-pk) sound pressure level. The difference between the highest variation (either positive or negative) and the mean pressure is called the peak pressure level. Lastly, the root mean square (rms) sound pressure level is used as a description of the average amplitude of the variations in pressure over a specific time window. These descriptions are shown graphically in Figure 2.1.

The rms sound pressure level (SPL) is defined as follows:

$$SPL_{rms} = 10 log_{10} \left(\frac{1}{T} \int_0^T \left(\frac{p^2}{p_{ref}^2} \right) dt \right)$$

The magnitude of the rms sound pressure level for an impulsive sound (such as that from a seismic source array) will depend upon the integration time, T, used for the calculation (Madsen 2005). It has become customary to utilise the T90 time period for calculating and reporting rms sound pressure levels. This is the interval over which the cumulative energy curve rises from 5% to 95% of the total energy and therefore contains 90% of the sound energy.
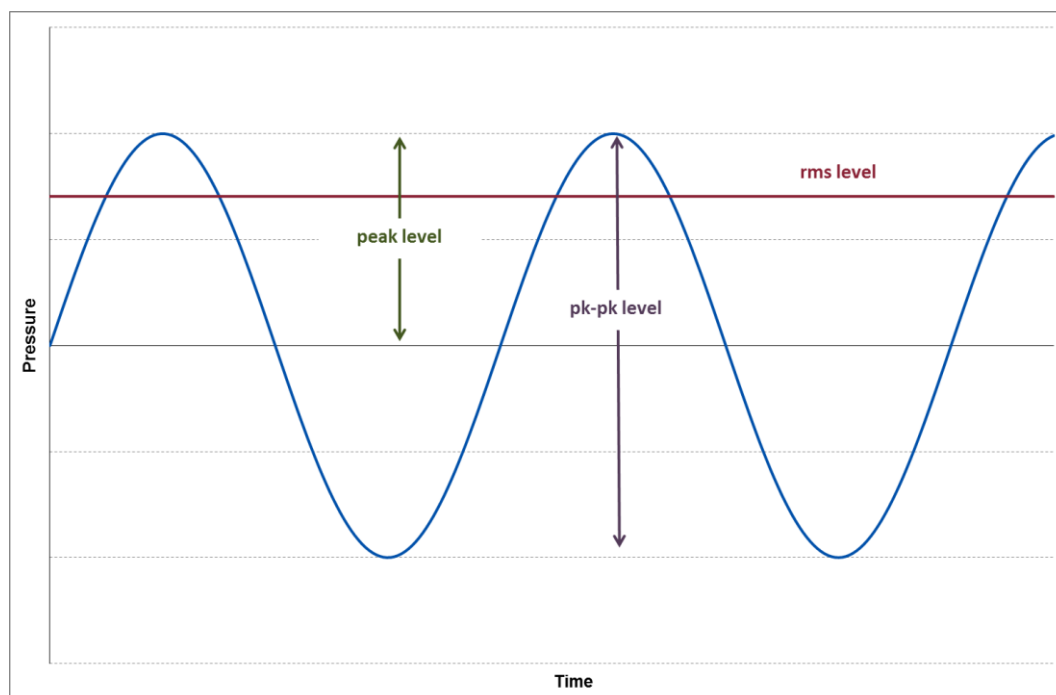
Figure 2.1   **Graphical representation of acoustic wave descriptors**

Another useful measure of sound used in underwater acoustics is the Sound Exposure Level, or SEL. This descriptor is used as a measure of the total sound energy of an event or a number of events (e.g. over the course of a day) and is normalised to one second. This allows the total acoustic energy contained in events lasting a different amount of time to be compared on a like for like basis[1]. The SEL is defined as follows:

$$SEL = 10 log_{10} \left(\int_0^T \left(\frac{p^2(t)}{p_{ref}^2 \, t_{ref}} \right) dt \right)$$

The frequency, or pitch, of the sound is the rate at which these oscillations occur and is measured in cycles per second, or Hertz (Hz). When sound is measured in a way which approximates to how a human would perceive it using an A-weighting filter on a sound level meter, the resulting level is described in values of dBA. However, the hearing faculty of marine mammals is not the same as humans, with marine mammals hearing over a wider range of frequencies and with a different sensitivity. It is therefore important to understand how an animal's hearing varies over the entire frequency range in order to assess the effects of sound on marine mammals. Consequently, use can be made of frequency weighting scales to determine the level of the sound in comparison with the auditory response of the animal concerned. A comparison between the typical hearing response curves for fish, humans and marine mammals is shown in Figure 2.2. (It is worth noting that hearing thresholds are sometimes shown as audiograms with sound level on the y axis rather than sensitivity, resulting in the graph shape being the inverse of the graph shown.)

---

[1] Historically, use was primarily made of rms and peak sound pressure level metrics for assessing the potential effects of sound on marine life. However, the SEL is increasingly being used as it allows exposure duration and the effect of exposure to multiple events to be taken into account.
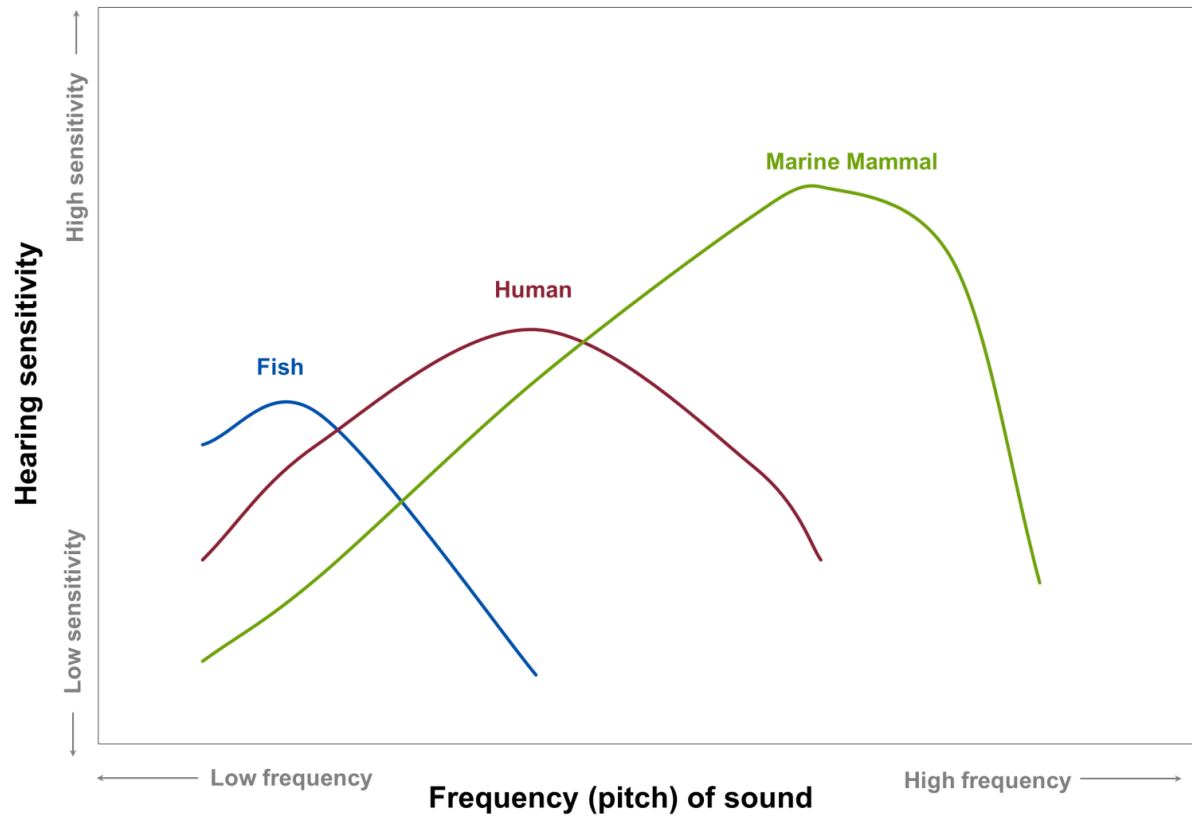
Figure 2.2   **Comparison between hearing thresholds of different animals**

3.0   ACOUSTIC ASSESSMENT CRITERIA

3.1   Introduction

Underwater sound has the potential to affect marine life in different ways depending on its absolute level and characteristics. Richardson *et al.* (1995) defined four zones of sound influence which vary with distance from the source and level. These are:

- **The zone of audibility:** this is the area within which the animal is able to detect the sound. Audibility itself does not implicitly mean that the sound will have an effect on the marine mammal.

- **The zone of masking:** this is defined as the area within which sound can interfere with detection of other sounds such as communication or echolocation clicks. This zone is very hard to estimate due to a paucity of data relating to how marine mammals detect sound in relation to masking levels (for example, humans are able to hear tones well below the numeric value of the overall sound level).

- **The zone of responsiveness:** this is defined as the area within which the animal responds either behaviourally or physiologically. The zone of responsiveness is usually smaller than the zone of audibility because, as stated previously, audibility does not necessarily evoke a reaction.

- **The zone of injury / hearing loss:** this is the area where the sound level is high enough to cause tissue damage in the ear. This can be classified as either temporary threshold shift (TTS) or permanent threshold shift (PTS). At even closer ranges, and for very high intensity sound sources (e.g. underwater explosions), physical trauma or even death are possible.

For this study, it is the zones of injury and disturbance (i.e. responsiveness) that are of concern (there is insufficient scientific evidence to properly evaluate masking). In order to determine the potential spatial range of injury and disturbance, a review has been undertaken of available evidence, including international guidance and scientific literature. The following sections summarise the relevant thresholds for onset of effects and describe the evidence base used to derive them.

3.2   Injury (Physiological Damage) to Mammals

Sound propagation models can be constructed to allow the received sound level at different distances from the source to be calculated. To determine the consequence of these received levels on any marine mammals which might experience such sound emissions, it is necessary to relate the levels to known or estimated impact thresholds. The injury criteria proposed by NOAA (2016) are based on a combination of linear (i.e. un-weighted) peak pressure levels and mammal hearing weighted sound exposure levels (SEL). The hearing weighting function is designed to represent the bandwidth for each group within which acoustic exposures can have auditory effects. The categories include:

- **low-frequency (LF) cetaceans** (i.e. marine mammal species such as baleen whales with an estimated functional hearing range between 7 Hz and 35 kHz);

- **mid-frequency (MF) cetaceans** (i.e. marine mammal species such as dolphins, toothed whales, beaked whales and bottlenose whales with an estimated functional hearing range between 150 Hz and 160 kHz);

- **high-frequency (HF) cetaceans** (i.e. marine mammal species such as true porpoises, Kogia, river dolphins and cephalorhynchid with an estimated functional hearing range between 275 Hz and 160 kHz);

- **phocid pinnipeds** (PW) (i.e. true seals with an estimated functional hearing range between 50 Hz and 86 kHz); and

- **otariid pinnipeds** (OW) (i.e. sea lions and fur seals with an estimated functional hearing range between 60 Hz and 39 kHz).

These weightings have therefore been used in this study and are shown in Figure 3.1.
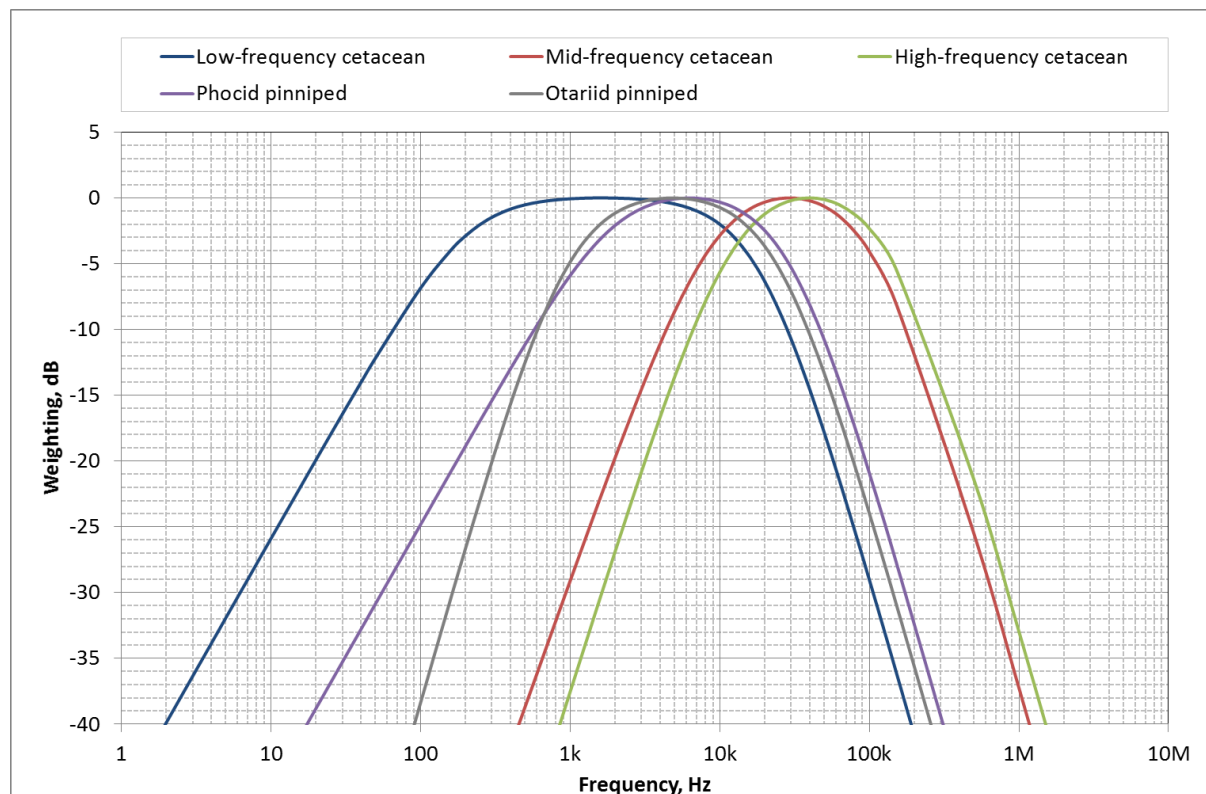
Figure 3.1   Hearing weighting functions for pinnipeds and cetaceans (NOAA, 2015)

The injury criteria proposed in NOAA (2016) are for two different types of sound as follows:

- **Impulsive sounds** which are typically transient, brief (less than 1 second), broadband, and consist of high peak sound pressure with rapid rise time and rapid decay (ANSI 1986; NIOSH 1998; ANSI 2005); this category includes sound sources such as seismic surveys, impact piling and underwater explosions; and

- **Non-impulsive sounds** which can be broadband, narrowband or tonal, brief or prolonged, continuous or intermittent and typically do not have a high peak sound pressure with rapid rise/decay time that impulsive sounds do (ANSI 1995; NIOSH 1998). This category includes sound sources such as continuous running machinery, sonar and vessels.

The criteria for impulsive sound have been adopted for this study given the nature of the sound source used during seismic surveys, where the sound source is activated at regular intervals as an array toing seismic vessel traverses along a pre-determined data acquisition sail-line. Since sound from the vessel is of significantly lower magnitude than sound emitted by the airguns, and since the two sources would not act additively to result in increased sound emissions compared to the airguns themselves, sound emissions from the vessel are not considered in the modelling.

The relevant criteria proposed by NOAA (2016) are as summarised in Table 3.1.

Table 3.1   Summary of PTS onset acoustic thresholds (NOAA 2016)

Hearing Group	Parameter	Impulsive	Non-impulsive
Low-frequency (LF) cetaceans	Peak, unweighted	219	-
	SEL, LF weighted	183	199
Mid-frequency (MF) cetaceans	Peak, unweighted	230	-
	SEL, MF weighted	185	198
High-frequency (HF) cetaceans	Peak, unweighted	202	-
	SEL, HF weighted	155	173
Phocid pinnipeds (PW)	Peak, unweighted	218	-
	SEL, PW weighted	185	201
Otariid pinnipeds (OW)	Peak, unweighted	232	-
	SEL, OW weighted	203	219

3.3   Disturbance to Mammals

Beyond the area in which injury may occur, the effect on marine mammal behaviour is the most important measure of impact. Significant disturbance may occur when there is a risk of a significant group of animals incurring sustained or chronic disruption of behaviour or when a significant group of animals are displaced from an area, with subsequent redistribution being significantly different from that occurring due to natural variation.

To consider the possibility of disturbance resulting from the proposed seismic operations, it is necessary to consider both the likelihood that the sound could cause disturbance and the likelihood that the sensitive receptors (marine mammals) will be exposed to that sound. Southall *et al.* (2007) recommended that the only currently feasible way to assess whether a specific sound could cause disturbance is to compare the circumstances of the situation with empirical studies. The more severe the response on the scale, the lower the amount of time that the animals will tolerate it before there could be significant negative effects on life functions.

Southall *et al.* (2007) present a summary of observed behavioural responses during various seismic surveys. However, although these datasets contain much relevant data for low-frequency cetaceans, there is no strong data for mid-frequency or high-frequency cetaceans. Low-frequency cetaceans other than bow-head whales were typically observed to respond significantly at a received level of 140 to 160 dB re 1 µPa (rms). Behavioural changes at these levels during multiple pulses of the source may have included visible startle response, extended cessation or modification of vocal behaviour, brief cessation of reproductive behaviour or brief / minor separation of females and dependent offspring.

The data that are available for mid-frequency cetaceans indicate that some significant response was observed at a sound pressure level of 120 - 130 dB re 1µPa (rms), however the majority of cetaceans in this category did not display behaviours of this severity until exposed to a level of 170 to 180 dB re 1µPa (rms). Furthermore, other mid-frequency cetaceans within the same study were observed to have no behavioural response even when exposed to a level of 170 – 180 dB re 1µPa (rms).

According to Southall *et al.* (2007), there is a general paucity of data relating to the effects of sound on pinnipeds in particular. One study using ringed, bearded and spotted seals (Harris *et al.*, 2001) found the onset of a significant response at a received sound pressure level of 160 to 170 dB re 1 µPa (rms), although larger numbers of animals showed no response at

sound levels of up to 180 dB re 1 µPa (rms). It is only at much higher sound pressure levels in the range of 190 to 200 dB re 1 µPa (rms) that significant numbers of seals were found to exhibit a significant response. For non-pulsed sound, one study elicited a significant response on a single harbour seal at a received level of 100 to 110 dB re 1 µPa (rms), although other studies found no response or non-significant reactions occurred at much higher received levels of up to 140 dB re 1 µPa (rms). No data are available for higher sound levels and the low number of animals observed in the various studies means that it is difficult to make any firm conclusions from these studies.

Southall *et al.* (2007) also notes that, due to the uncertainty over whether high-frequency cetaceans may perceive certain sounds and due to paucity of data, it was not possible to present any data on responses of high frequency-cetaceans. However, Lucke *et al.* (2008) showed a single harbour porpoise consistently showed aversive behavioural reactions at received sound pressure levels above 174 dB re 1 µPa (peak-peak) or a SEL of 145 dB re 1 µPa[2]s, equivalent to an estimated[2] rms sound pressure level of 166 dB re 1 µPa.

The High Energy Seismic Survey workshop on the effects of seismic sound on marine mammals (HESS, 1997) concluded that mild behavioural disturbance would most likely occur at sound levels greater than 140 dB re 1 µPa (rms). This workshop drew on several studies but recognised that there was some degree of variability in reactions between different studies and mammal groups. This value is similar to the lowest threshold for disturbance of low-frequency cetaceans noted in Southall *et al.* (2007). It is, however, considered unlikely that a threshold for the onset of mild disturbance effects could be defined as significant disturbance.

Clearly, there is much intra-category and perhaps intra-species variability in behavioural response. Therefore, this assessment adopts a conservative approach and uses the US National Marine Fisheries Service (NMFS 2005) Level B harassment threshold of 160 dB re 1 µPa (rms) for impulsive sound. Level B Harassment is defined as having the potential to disturb a marine mammal or marine mammal stock in the wild by causing disruption of behavioural patterns, including, but not limited to, migration, breathing, nursing, breeding, feeding, or sheltering but which does not have the potential to injure a marine mammal or marine mammal stock in the wild. This is similar to the JNCC (2010 in prep) description of non-trivial disturbance and has therefore been used as the basis for onset of behavioural change in this assessment.

It is important to understand that exposure to sound levels in excess of the behavioural change threshold stated above does not necessarily imply that the sound will result in significant disturbance. As noted previously, it is also necessary to assess the likelihood that the sensitive receptors will be exposed to that sound and whether the numbers exposed are likely to be significant at the population level.

3.4 Marine Mammal Criteria Summary

The criteria used in this assessment are summarised in Table 3.2.

---

[2] Based on an analysis of the time history graph in Lucke et al. (2007) the T90 period is approximately 8 ms, resulting in a correction of 21 dB applied to the SEL to derive the rms T90 sound pressure level. However, the T90 was not directly reported in the paper.

Table 3.2   Proposed criteria for marine mammals

Effect	Criteria		
Behavioural change	Exceedance of criteria in NMFS (2005) for impulsive sound: rms sound pressure level greater than 160 dB re 1 µPa		
Physiological damage	Exceedance of NOAA (2016) criteria for PTS due to impulsive sound:		
	Low-frequency (LF) cetaceans	peak pressure level	219 dB re 1 µPa
		SEL	183 dB re 1 µPa^{2}s
	Mid-frequency (MF) cetaceans	peak pressure level	230 dB re 1 µPa
		SEL	185 dB re 1 µPa^{2}s
	High-frequency (HF) cetaceans	peak pressure level	202 dB re 1 µPa
		SEL	155 dB re 1 µPa^{2}s
	Phocid pinnipeds (PW)	peak pressure level	218 dB re 1 µPa
		SEL	185 dB re 1 µPa^{2}s
	Otariid pinnipeds (OW)	peak pressure level	232 dB re 1 µPa
		SEL	203 dB re 1 µPa^{2}s

3.5   Injury and Disturbance to Sea Turtles

The most relevant criteria for injury are considered to be those contained in the recent Sound Exposure Guidelines for Fishes and Sea Turtles (Popper *et al.*, 2014). The guidelines set out criteria for injury due to different sources of sound. Those relevant to this project are considered to be those for injury due to seismic sound[3]. The criteria include a range of indices including SEL, rms and peak sound pressure levels. Where insufficient data exist to determine a quantitative guideline value, the risk is categorised in relative terms as "high", "moderate" or "low" at three distances from the source: "near" (i.e. in the tens of metres), "intermediate" (i.e. in the hundreds of metres) or "far" (i.e. in the thousands of metres). It should be noted that these qualitative criteria cannot differentiate between exposures to different sound levels and therefore all sources of sound, no matter how noisy, would theoretically elicit the same assessment result. However, because the qualitative risks are generally qualified as "low", with the exception of a moderate risk at "near" range (i.e. within tens of metres) for some types of animal and impairment effects, this is not considered to be a significant issue with respect to determining the potential effect of sound on fish and turtles.

The injury criteria used in this acoustic assessment are given in Table 3.3.

Table 3.3   Criteria for injury to sea turtles due to seismic airguns (Popper *et al.*, 2014)

Type of animal	Parameter	Mortality and potential mortal injury	Impairment	
			Recoverable injury	TTS
Sea turtles	SEL, dB re 1 µPa^{2}s	210	(*Near*) High (*Intermediate*) Low (*Far*) Low	(*Near*) High (*Intermediate*) Low
	Peak, dB re 1 µPa	>207		

---

[3] Guideline exposure criteria for explosions, piling, continuous sound and low and mid-frequency naval sonar are also presented though are not applicable to this Project.

				(*Far*) Low

The most recent criteria for disturbance are considered to be those contained in Popper et al. (2014) which set out criteria for disturbance due to different sources of sound. As with the injury criteria, the risk of behavioural effects is categorised in relative terms as "high", "moderate" or "low" at three distances from the source: "near" (i.e. in the tens of metres), "intermediate" (i.e. in the hundreds of metres) or "far" (i.e. in the thousands of metres), as shown in Table 3.4.

Table 3.4   ASA criteria for onset of behavioural effects in sea turtles (Popper *et al.*, 2014)

Type of animal	Relative risk of behavioural effects
Sea turtles	(*Near*) High
	(*Intermediate*) Moderate
	(*Far*) Low

It is important to note that the Popper *et al.* (2014) criteria for disturbance due to sound are qualitative rather than quantitative. Consequently, a source of sound of a particular type would result in the same predicted impact, no matter the level of sound produced or the propagation characteristics.

4.0   ASSESSMENT METHODOLOGY

4.1   Source Term Derivation for Seismic Source Array

Source sound levels are usually described in dB re 1 µPa at 1m (as if measured at 1 m from the source). In practice, it is not usually possible to measure at 1 m from an active seismic source that is physically distributed over an area of typically tens of square metres, but this method allows different source levels to be compared and reported on a like-for-like basis. Far-field source modelling is typically based on the following basic assumptions:

- at some far distance from the source (typically vertically downwards) the energy from the source elements add constructively; and

- the source level is derived by back projecting a far field calculation to 1 m.

After completing Phase 1 of this study, the proposed arrays were output from the Nucleus software model as source data. Data were provided for three potential arrays that could be used and this study has examined the potential impact of all three. A key assumption is that the source data accurately reflects the source level of the array in practice, as encountered in the far field of the source.

 The airgun array signatures are shown in Figure 4.1.

3,640 cu in

Primary	: 76.5 barm	Source depth	: 7.00 m
Peak-peak	: 151.7 barm	Streamer depth	: .00 m
P/B ratio	: 24.5	Volume	: 3640 cu.in.
Period (+/-)	: 109.0/ 154.5 msec	Pressure	: 2000 psi
		Ghost strength	: -1.00
		Sea temperatur	: 17.00 C

4,100 cu in

Primary	: 77.8 barm	Source depth	: 7.00 m
Peak-peak	: 153.5 barm	Streamer depth	: .00 m
P/B ratio	: 21.2	Volume	: 4100 cu.in.
Period (+/-)	: 127.0/ 149.0 msec	Pressure	: 2000 psi
		Ghost strength	: -1.00
		Sea temperatur	: 17.00 C

4,390 cu in

Primary	: 81.5 barm	Source depth	: 7.00 m
Peak-peak	: 160.5 barm	Streamer depth	: .00 m
P/B ratio	: 31.9	Volume	: 4390 cu.in.
Period (+/-)	: 176.0/ 178.5 msec	Pressure	: 2000 psi
		Ghost strength	: -1.00
		Sea temperatur	: 17.00 C

Figure 4.1   Airgun array source time signatures

The supplied source data also includes information of the source frequency characteristics (Figure 4.2) but for a limited frequency range of up to 1 kHz, and filtering above 1 kHz has been applied to the Nucleus model. Although the highest sound pressure levels (in terms of

un-weighted levels) are generated in this bandwidth, significant energy is also generated by seismic source arrays at much higher frequencies which are within the hearing sensitivities of marine mammals.
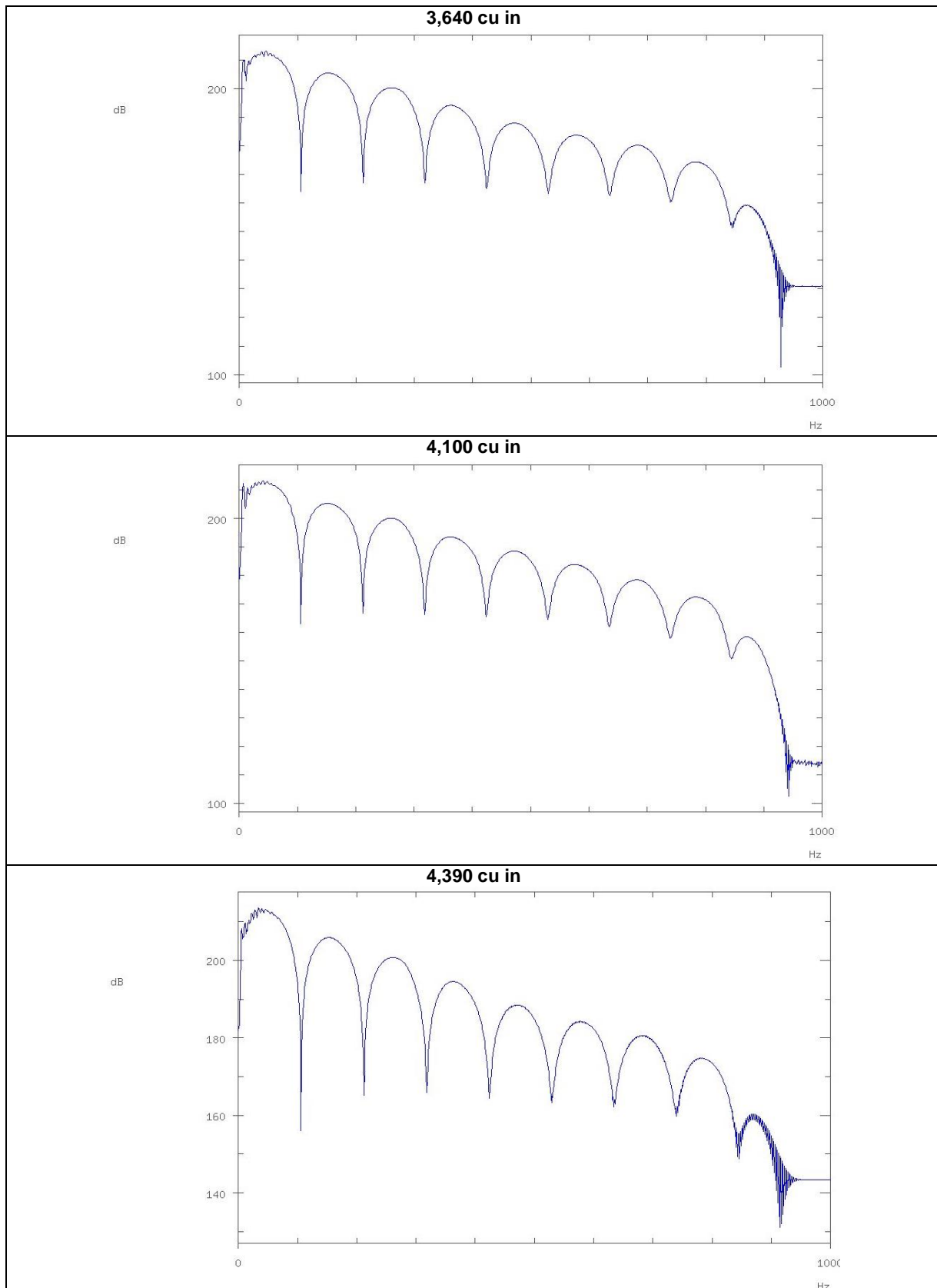
Figure 4.2   Source frequency characteristics (1 kHz low-pass filtered)

For this study, the source sound levels have been based on a combination of those provided by the Nucleus model, supplemented by measured sound data from other studies over a much wider bandwidth (Breitzke et al., 2008; Tolstoy et al., 2009; Richardson et al., 1995) in order to produce low- and mid-frequency data. The low- and mid-frequency data have been extrapolated to derive the third-octave frequency spectra at higher frequencies (>1 kHz) based on the gradient of the power spectral density[4] and third-octave band plots.

The SEL represents the total energy of an event or number of events normalised to a standardised one second interval. This allows a comparison of the total energy of different sounds lasting for different time periods. As a pressure pulse from a source array propagates towards the receiver, the duration of the pulse increases. Thus the relationship between the peak sound pressure level and the SEL changes with distance. The peak level from the Nucleus software model was converted to an SEL based on the gun signature time history graph and compared to measured data from Patterson *et al.* (2007). The peak sound pressure level and SEL input values are shown in Table 4.1. The single pulse SEL values have been combined for each pulse as part of the various cumulative SEL modelling scenarios.

Table 4.1   Source array input sound levels for acoustic modelling

Array	Peak SPL, dB re 1 µPa re 1 m	SEL, dB re 1 µPa^{2}s re 1 m	rms$_{T90}$ SPL, dB re 1 µPa re 1 m	T90, ms
3,640 cu in	257.7	233.3	252.0	13.5
4,100 cu in	257.8	233.6	252.1	14.0
4,390 cu in	258.2	233.7	252.6	13.0

It is important to note that the rms sound pressure level will depend upon the integration window used or, in other words, the measurement time for the rms. Using a longer duration measurement would result in a lower rms sound pressure level than using a shorter one. Therefore, the rms sound pressure source level has been calculated by scanning the Nucleus time history plot in order to re-calculate the rms sound pressure level using the relevant T90 time period (i.e. the interval which contains 90% of the sound energy). This integration procedure gives a more relevant and consistent value for comparison between various studies and is the suggested metric in Southall *et al.* (2007).

An additional phenomenon occurs where the seismic waveform elongates with distance from the source due to a combination of dispersion and multiple reflections. Measurements presented by Breitzke *et al.* (2008) indicate elongation of the T90 window up to approximately 800 ms at 1 km. This temporal "smearing" reduces the rms amplitude with distance (because the rms window is longer) and has been included within the disturbance modelling scenarios. Since the ear of most marine mammals integrates low frequency sound over a window of around 200 ms (Madsen *et al.,* 2006), this duration was used as a maximum integration time for the received rms sound pressure level.

The source levels stated above are likely to be overestimated in the near-field as the modelled back projection to 1 m does not consider the interaction between the source elements. This in turn overestimates near-field received levels, which are then compared to animal thresholds. In reality, near-field source sound levels will be lower than that predicted by this vertical far-field calculation.

Another important factor affecting the received sound pressure level from seismic source arrays is the source directivity characteristics. Source arrays are designed so that the majority of acoustic energy is directed downwards towards the ocean bottom. Therefore, the amount

---

[4] The power spectral density (PSD) is the power carried by the wave, per unit frequency of the signal.

of energy emitted horizontally will be significantly less than directed downwards. The directivity plots are shown in Figure 4.3.
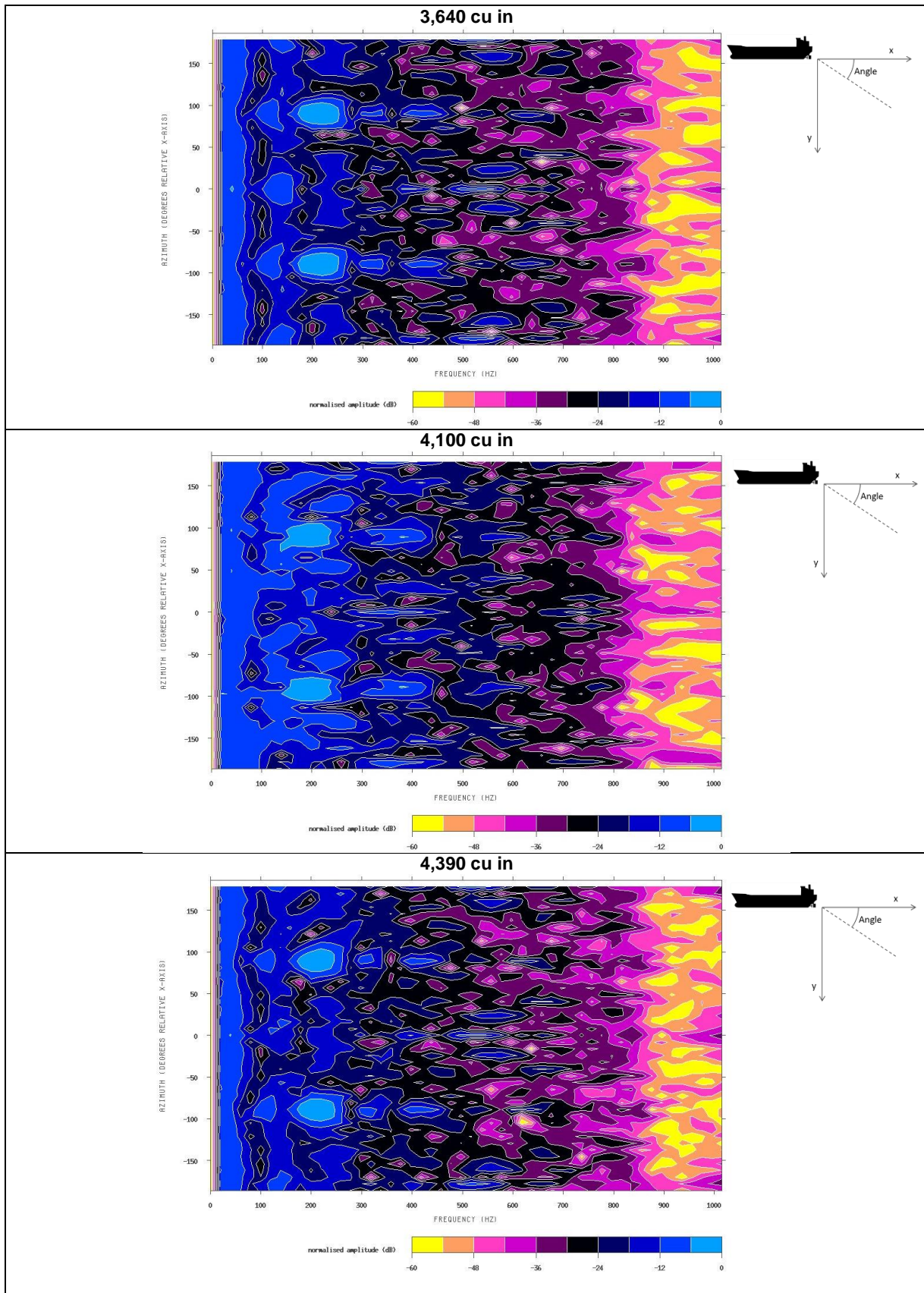
Figure 4.3   Directivity plots for source arrays (90 degrees vertical)

An example SPL plot showing this directivity effect directly under the source array is shown in Figure 4.4 (the plot shows a "typical" array as opposed to the specific array used in the acoustic modelling for this study). From the figure, it can clearly be seen that an animal swimming in deeper water would be subject to higher sound exposure levels than one in shallow water at the same aerial distance from the source array.
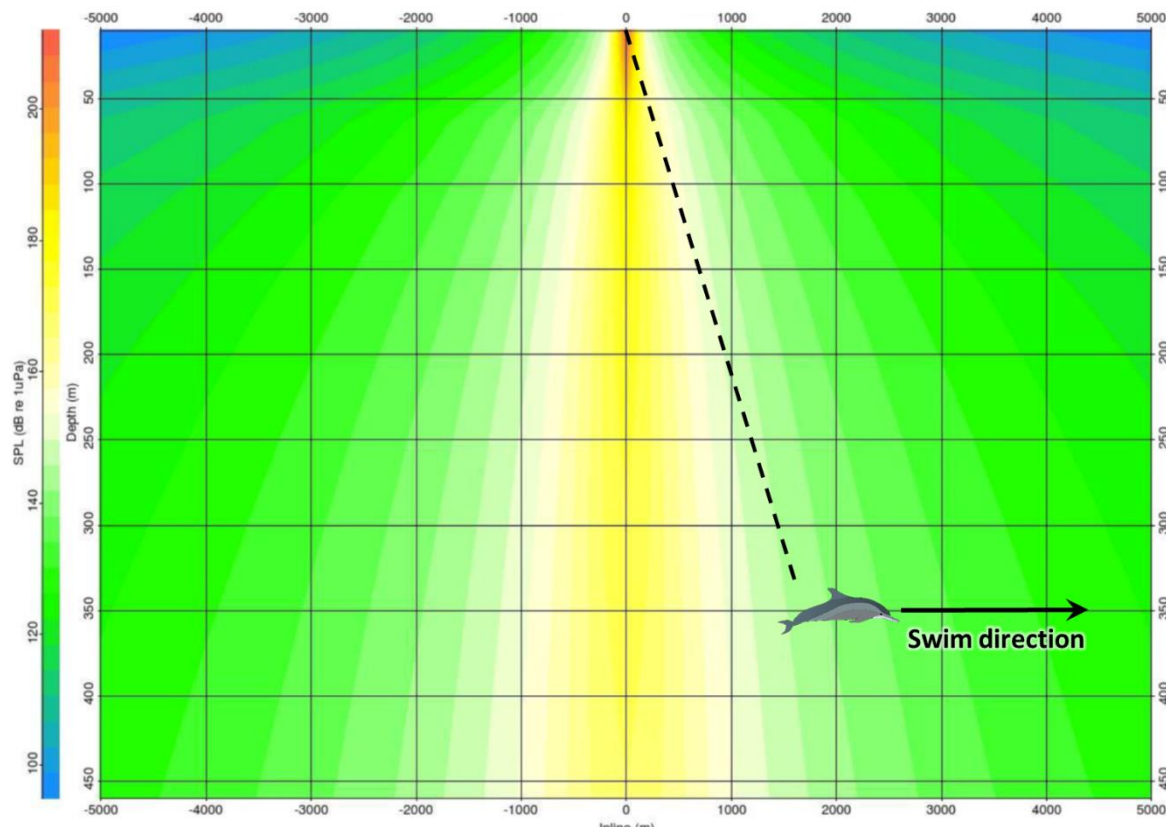
Figure 4.4   Example inline SPL showing array directivity

Directivity is a frequency dependent effect and is more pronounced at higher frequencies than at lower frequencies. Directivity corrections have been applied to the source sound level data based on supplied directivity characteristics for the proposed array. Directivity factors were derived based on source take-off angle for an animal on the bottom of the ocean, assuming that the receiver is to the side of the array (as opposed to in front of or behind the array). This results in a greater correction (reduction in level) due to directivity at distances further from the source than for receivers close to the source.

At distances closer to the source (i.e. less than the water depth), no directivity correction is made because the animal could be directly underneath the array. This scenario is shown illustratively in Figure 4.5. It should be noted that these figures and examples are illustrative and simplified scenarios in order to demonstrate the principal of take-off angles (and that the directivity patterns shown are typical array illustrations and not specific to this project).
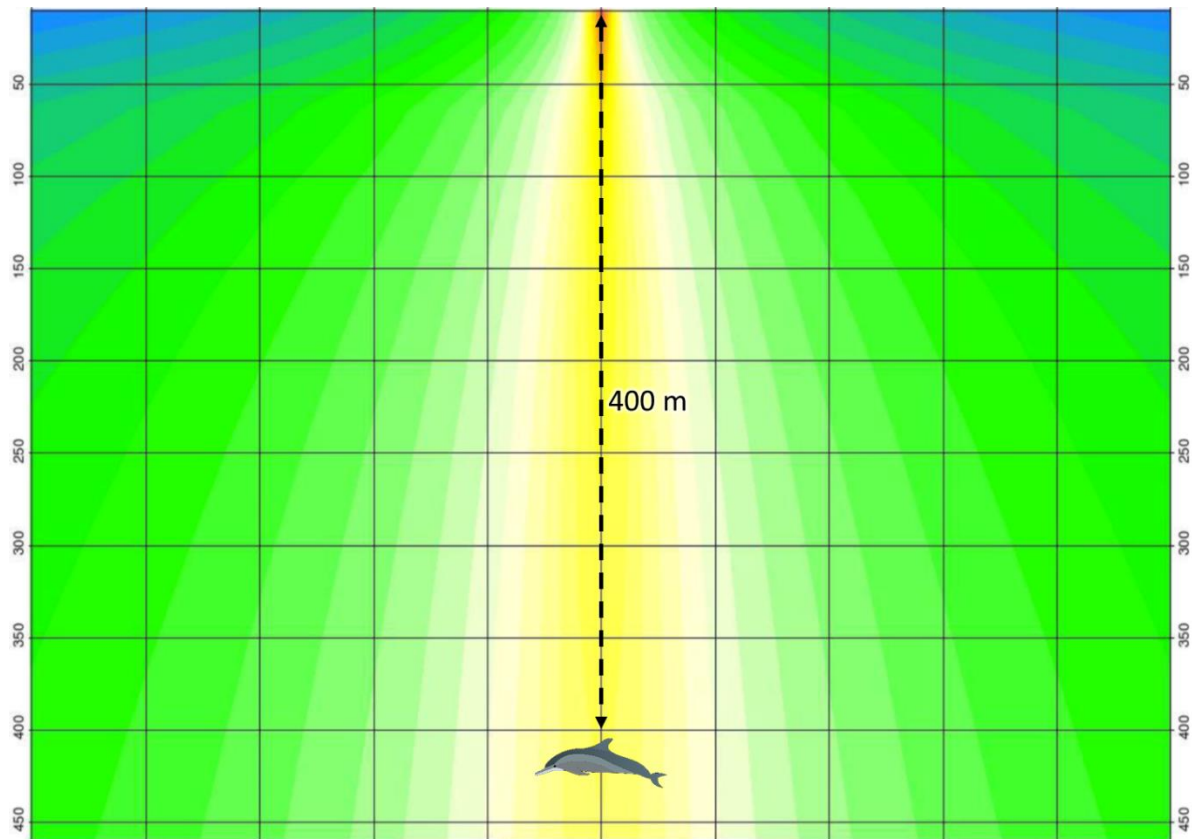
Figure 4.5   Example showing injury range less than water depth

As the injury range increases, the take-off angle between the source array and animal becomes larger. Hence, when the injury range is large in comparison to the water depth, the effects of the source array's directivity will have a much greater bearing on the received sound level. Once the injury range becomes larger than the water column depth then the array directivity effects will become increasingly important. Figure 4.6 shows an example where the injury range is slightly greater than the water column depth.
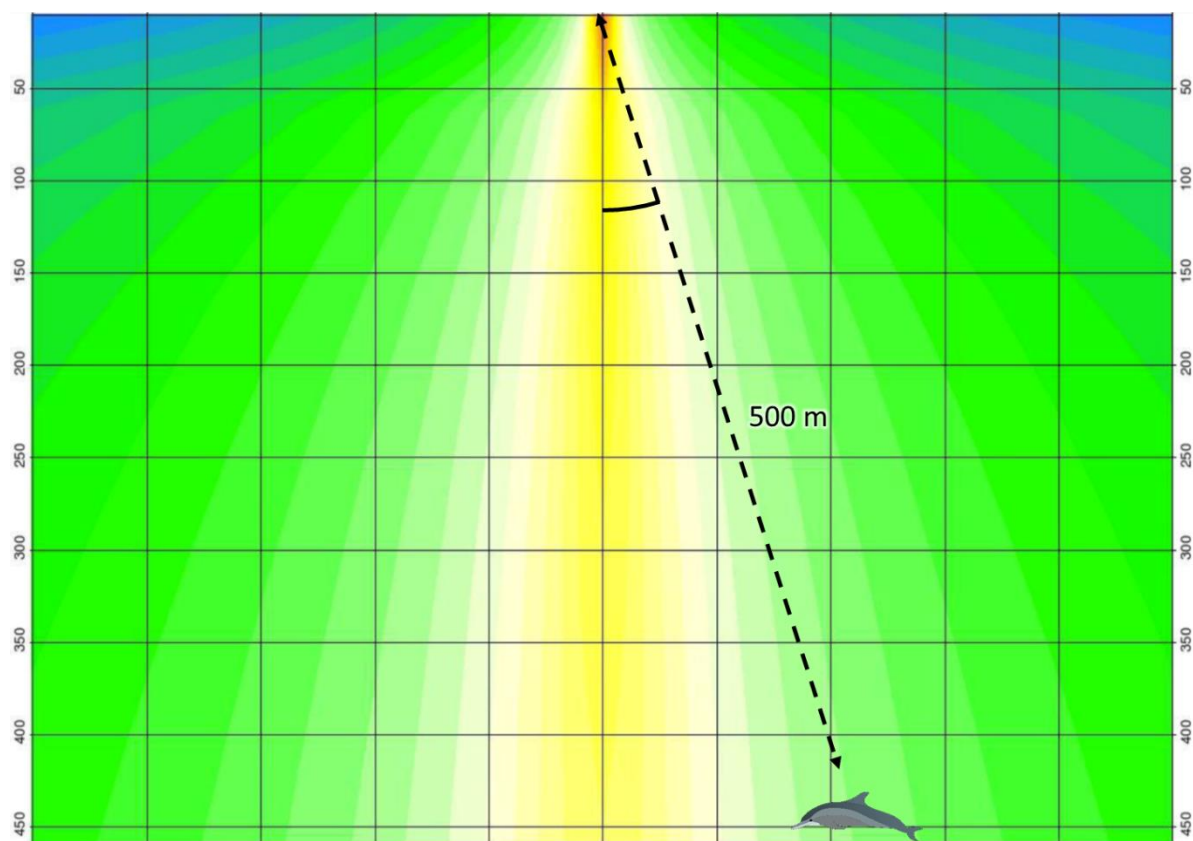
Figure 4.6   Example showing injury range slightly greater than water depth

For injury ranges which are much greater than the water column depth, the effects of directivity will be much more significant. This is shown illustratively in Figure 4.7.
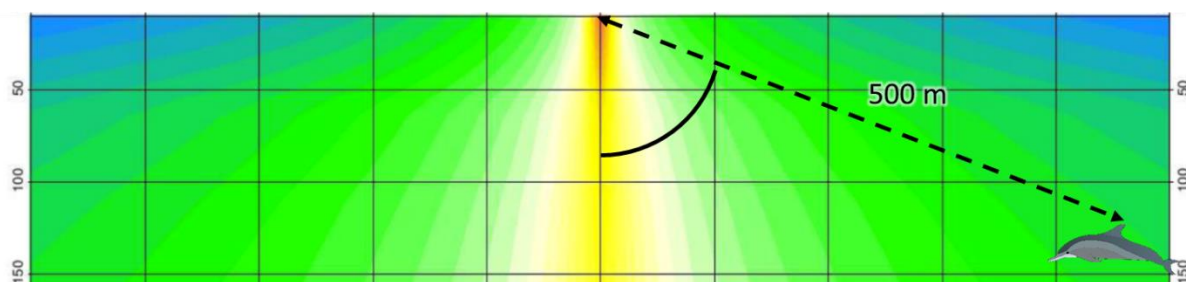
Figure 4.7   Example showing injury range much larger than water depth

4.2   Propagation Model

Increasing the distance from the sound source usually results in the level of sound reducing, due, primarily, to the spreading of the sound energy with distance, analogous to the way in which the ripples in a pond spread after a stone has been thrown in, in combination with attenuation due to absorption of sound energy by molecules in the water. This latter mechanism is more important for higher frequency sound than for lower frequencies.

The way that the sound spreads (geometrical divergence) will depend upon several factors such as water column depth, pressure, temperature gradients, salinity as well as water surface and bottom (i.e. seabed) conditions. Thus, even for a given locality, there are temporal variations to the way that sound will propagate. However, in simple terms, the sound energy

may spread out in a spherical pattern (close to the source) or a cylindrical pattern (much further from the source), although other factors mean that decay in sound energy may be somewhere between these two simplistic cases.

In acoustically shallow waters[5] in particular, the propagation mechanism is coloured by multiple interactions with the seabed and the water surface (Lurton 2002; Etter 2013; Urick 1983; Brekhovskikh and Lysanov 2014; Kinsler et al. 1999). Whereas in deeper waters, the sound will propagate further without encountering the surface or bottom of the sea, in shallower waters the sound may be reflected from either or both boundaries (potentially more than once).

At the sea surface, the majority of sound is reflected back in to the water due to the difference in acoustic impedance (i.e. sound speed and density) between air and water. However, scattering of sound at the surface of the sea can be an important factor with respect to the propagation of sound. In an ideal case (i.e. for a perfectly smooth sea surface), the majority of sound wave energy will be reflected back into the sea. However, for rough seas, much of the sound energy is scattered (e.g. Eckart 1953; Fortuin 1970; Marsh, Schulkin, and Kneale 1961; Urick and Hoover 1956). Scattering can also occur due to bubbles near the surface such as those generated by wind or fish or due to suspended solids in the water such as particulates and marine life. Scattering is more pronounced for higher frequencies than for low frequencies and is dependent on the sea state (i.e. wave height). However, the various factors affecting this mechanism are complex.

Because surface scattering results in differences in reflected sound, its effect will be more important at longer ranges from the source sound and in acoustically shallow water (i.e. where there are multiple reflections between the source and receiver). The degree of scattering will depend upon the sea state/wind speed, water depth, frequency of the sound, temperature gradient, grazing angle and range from source. It should be noted that variations in propagation due to scattering will vary temporally within an area primarily due to different sea-states / wind speeds at different times. However, over shorter ranges (e.g. several hundred meters or less), the sound will experience fewer reflections and so the effect of scattering should not be significant.

When sound waves encounter the bottom, the amount of sound reflected will depend on the geoacoustic properties of the bottom (e.g. grain size, porosity, density, sound speed, absorption coefficient and roughness) as well as the grazing angle and frequency of the sound (Cole 1965; Hamilton 1970; Mackenzie 1960; McKinney and Anderson 1964; Etter 2013; Lurton 2002; Urick 1983). Thus, bottoms comprising primarily of mud or other acoustically soft sediment will reflect less sound than acoustically harder bottoms such as rock or sand. This will also depend on the profile of the bottom (e.g. the depth of the sediment layer and how the geoacoustic properties vary with depth below the sea floor). The effect is less pronounced at low frequencies (a few kHz and below). A scattering effect (similar to that which occurs at the surface) also occurs at the bottom (Essen 1994; Greaves and Stephen 2003; McKinney and Anderson 1964; Kuo 1992), particularly on rough substrates (e.g. pebbles).

Another phenomenon is the waveguide effect, which means that shallow water columns do not allow the propagation of low frequency sound (Urick 1983; Etter 2013). The cut-off frequency of the lowest mode in a channel can be calculated based on the water depth and

---

[5] Acoustically, shallow water conditions exist whenever the propagation is characterised by multiple reflections with both the sea surface and bottom (Etter 2013). Consequently, the depth at which water can be classified as acoustically deep or shallow depends upon numerous factors including the sound speed gradient, water depth, frequency of the sound and distance between the source and receiver.

knowledge of the sediment geoacoustic properties. Any sound below this frequency will not propagate far due to energy losses through multiple reflections.

Another important factor is the sound speed gradient. Changes in temperature and pressure with depth mean that the speed of sound varies throughout the water column. This can lead to significant variations in sound propagation and can also lead to sound channels, particularly for high frequency sound. Sound can propagate in a duct-like manner within these channels, effectively focussing the sound, and conversely they can also lead to shadow zones. The frequency at which this occurs depends on the characteristics of the sound channel but, for example, a 25 m thick layer would not act as a duct for frequencies below 1.5 kHz. The temperature gradient can vary throughout the year and thus there will be potential variation in sound propagation depending on the season.

Sound energy is also absorbed due to interactions at the molecular level converting the acoustic energy into heat. This is another frequency dependent effect with higher frequencies experiencing much higher losses than lower frequencies.

There are several methods available for modelling the propagation of sound between a source and receiver ranging from very simple models which simply assume spreading according to a 10 log (r) or 20 log (r) relationship (as discussed above) to full acoustic models (e.g. ray tracing, normal mode, parabolic equation, wavenumber integration and energy flux models). In addition, semi-empirical models are available which lie somewhere in between these two extremes in terms of complexity.

In choosing which propagation model to employ, it is important to ensure that it is fit for purpose and produces results with a suitable degree of accuracy for the application in question, taking into account the context (as detailed in Monitoring Guidance for Underwater Noise in European Seas Part III, NPL Guidance and Farcas *et al.*, 2016). Thus, in some situations (e.g. low risk due to underwater sound, range dependent bathymetry is not an issue, non-impulsive sound) a simple (N log R) model will be sufficient, particularly where other uncertainties outweigh the uncertainties due to modelling. On the other hand, some situations (e.g. very high source levels, impulsive sound, complex source and propagation path characteristics, highly sensitive receivers and low uncertainties in assessment criteria) warrant a more complex modelling methodology.

The first step in choosing a propagation model is therefore to examine these various factors, such as set out below:

- balancing of errors / uncertainties;

- range dependant bathymetry;

- frequency dependence; and

- source characteristics.

For impulsive sound, such as that produced by a seismic survey source array, the sound propagation is rather more complex than can be modelled using a simple N log (R) relationship.

For example, the rms sound pressure level of an impulsive sound wave will depend upon the integration window used or, in other words, the measurement time for the rms. Using a longer duration measurement would result in a lower rms sound pressure level than using a shorter one. An additional phenomenon occurs where the seismic waveform elongates with distance from the source due to a combination of dispersion and multiple reflections. This temporal "smearing" can significantly affect the peak pressure level and reduces the rms amplitude with distance (because the rms window is longer). Furthermore, source levels stated in the Nucleus (or NUCLEUS) reports are likely to be overestimated in the near-field as the modelled

back projection to 1 m does not consider the interaction between the source elements. This in turn overestimates near-field received levels, which are then compared to animal thresholds. In reality, near-field source sound levels will be lower than that predicted by this vertical far-field calculation. Another important factor affecting the received sound pressure level from seismic source arrays is the source directivity characteristics. Source arrays are designed so that the majority of acoustic energy is directed downwards towards the ocean bottom. Therefore, the amount of energy emitted horizontally will be significantly less than directed downwards. This is a frequency dependent effect and is more pronounced at higher frequencies than at lower frequencies.

It is a common miscomprehension that seismic sound does not contain high frequency energy above a few hundred Hz. Seismic source arrays contain significant (unwanted) high frequency energy although this is often not shown in Nucleus or Nucleus reports due to the source filtering applied. This is because it is the low frequency energy content of the signature that is of interest for geophysical analysis and the source array modelling software is therefore written using a sample rate to reflect this lower frequency range of interest.

In the past, acoustic propagation modelling has often been based solely on a parabolic equation methodology based on the assumption that seismic sound energy is primarily low frequency in content. According to Wang *et al.* (2014) parabolic equation models are useful for frequencies up to approximately 1 kHz. However, as described above, the seismic source will contain a significant amount of energy above this frequency. Inspection of the NOAA hearing weighting curves shown in Figure 3.1 shows that the majority of energy contributing to the hearing weighted SELs is above this frequency for the majority of hearing groups (excluding low-frequency cetaceans). Indeed, the suitable frequency range for parabolic equation models would not cover *any* of the sound energy within the high and mid frequency cetacean weighting curves. Consequently, the use of parabolic equation modelling would fail to assess the energy content most applicable to the majority of marine mammals. For this reason, it is concluded that parabolic equation modelling is not the most suitable method for assessing the effects of the seismic source signature on marine mammals.

Sound propagation modelling for this assessment was therefore based on an established, peer reviewed, range dependent sound propagation model which utilises the semi-empirical model developed by Rogers (1981). The model provides a robust balance between complexity and technical rigour over a wide range of frequencies, has been validated by numerous field studies and has been benchmarked against a range of other models. The following inputs are required for the model:

- third-octave band source sound level data;

- range (distance from source to receiver);

- water column depth (input as bathymetry data grid);

- sediment type;

- sediment and water sound speed profiles and densities;

- sediment attenuation coefficient; and

- source directivity characteristics.

The propagation loss is calculated using the formula:

$$TL = 15 log_{10} R + 5 \log_{10}(H\beta) + \frac{\beta R \theta_L^2}{4H} - 7.18 + \alpha_w R$$

Where R is the range, H the water depth, β the bottom loss, θ_L the limiting angle and α_w the absorption coefficient of sea water (α_w is a frequency dependant term which is calculated based on Ainslie and McColm, 1998).

The limiting angle, θ_L is the larger of θ_g and θ_c where θ_g is the maximum grazing angle for a skip distance and θ_c is the effective plane wave angle corresponding to the lowest propagating mode.

$$\theta_g = \sqrt{\frac{2Hg}{c_w}} \qquad \theta_c = \frac{c_w}{2fH}$$

Where g is the sound speed gradient in water and f is the frequency.

The bottom loss β is approximated as:

$$\beta \approx \frac{0.477(\rho_s/\rho_w)(c_w/c_s)K_s}{[1-(c_w/c_s)^2]^{3/2}}$$

Where ρ_s is the density of sediment, ρ_w the density of water, c_s the sound speed in the sediment, c_w the sound speed in water and K_s is the sediment attenuation coefficient.

The propagation model also takes into account the depth dependent cut-off frequency for propagation of sound (i.e. the frequency below which sound does not propagate):

$$f_{cut-off} = \frac{c_w}{4h\sqrt{1-\frac{c_w^2}{c_s^2}}}$$

Where c_s and c_w are the sound propagation speeds in the substrate and water.

The water column depth in the area of interest ranges between ~200 m closer to the coast to ~900 m further offshore. The propagation and sound exposure calculations were conducted over a range of water column depths in order to determine the likely range for injury and disturbance. It should be noted that the effect of directivity has a strong bearing on the calculated zones for injury and disturbance because a marine mammal could be directly underneath an array for greater distances in deep water compared to shallow water.

It should be borne in mind that sound levels (and associated range of effects) will vary depending on actual conditions at the time (day-to-day and season-to-season) and that the model predicts a typical worst case scenario. Taking into account factors such as animal behaviour and habituation, any injury and disturbance ranges should be viewed as indicative and probabilistic ranges to assist in understanding potential impacts on marine life rather than lines either side of which an impact definitely will or will not occur. (This is a similar approach to that adopted for airborne sound where a typical worst case is taken, though it is known that day to day levels may vary to those calculated by 5 - 10 dB depending on wind direction etc.).

The sound absorption coefficient in a sediment is proportional to frequency of the sound.

Bottom conditions for a large proportion of the survey area are bathyal mud, based on EMODnet data. The following geoacoustic parameters for the bottom have been utilised in the acoustic model based on Jensen (1994):

- Sediment sound speed c_s = 1,700 m/s

- Density of sediment ρ_s = 1,500 kg/m^3

- sediment attenuation coefficient K_s = 1 dB/m/kHz

The sound speed gradient is based on data supplied for the temperature and salinity of the Ionian, as shown in Figure 4.8 (temperature) and Figure 4.9 (salinity).
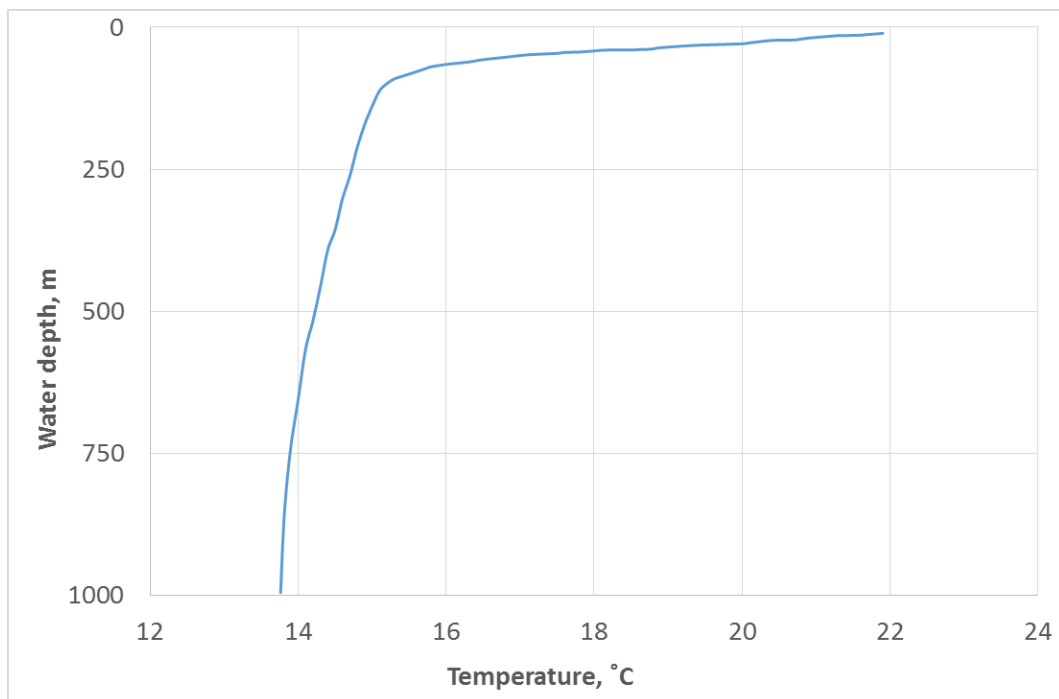
Figure 4.8   **Temperature vs depth profile – Southern Ionian**
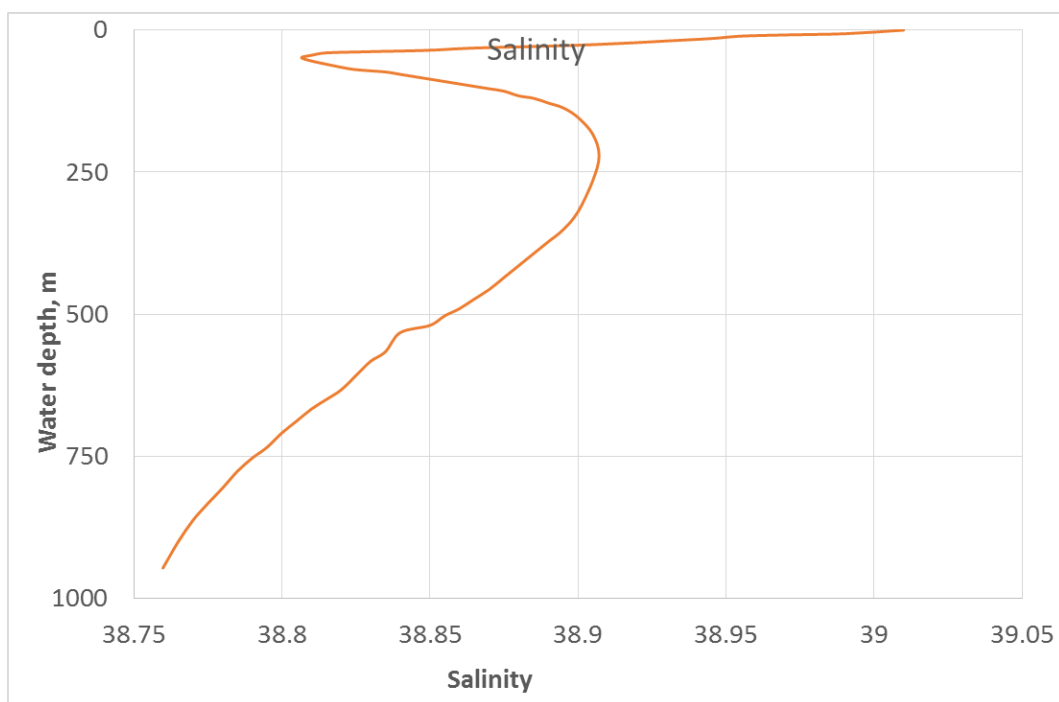
Figure 4.9   **Salinity vs depth profile – Southern Ionian**

The bathymetry data used for the acoustic modelling is shown in Figure 4.10.
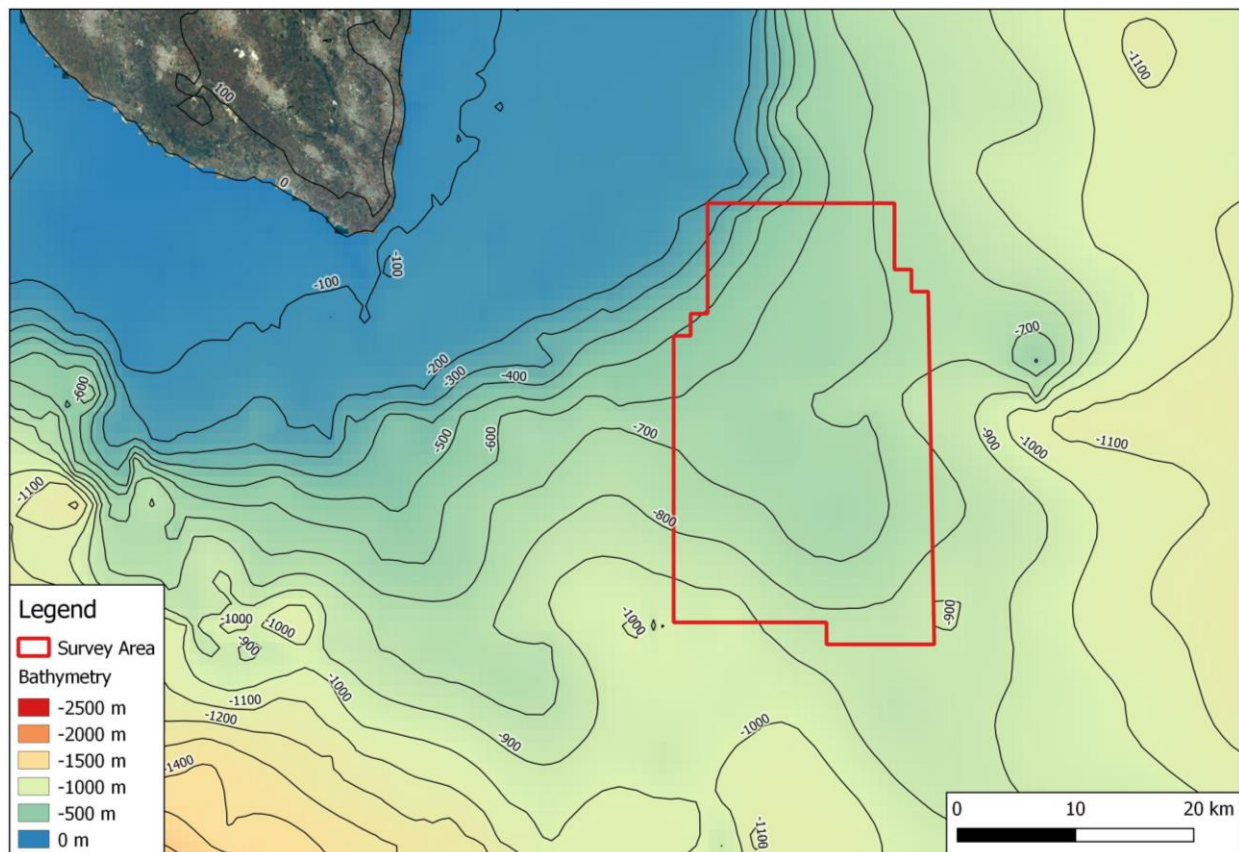
Figure 4.10   Southern Ionian bathymetry used in acoustic model

4.3   Exposure Calculations

As well as calculating the un-weighted rms and peak sound pressure levels at various distances from the source, it is also necessary to calculate the SEL for a mammal using the relevant hearing weightings described above taking into account the number of pulses to which it is exposed. For operation of the source array, the SEL sound data for a single pulse was utilised, along with the maximum number of pulses expected to be received by marine mammals in order to calculate cumulative exposure.

Exposure modelling was based on the assumption of a mammal swimming at a constant speed in a perpendicular direction away from a moving vessel (see Figure 4.11):
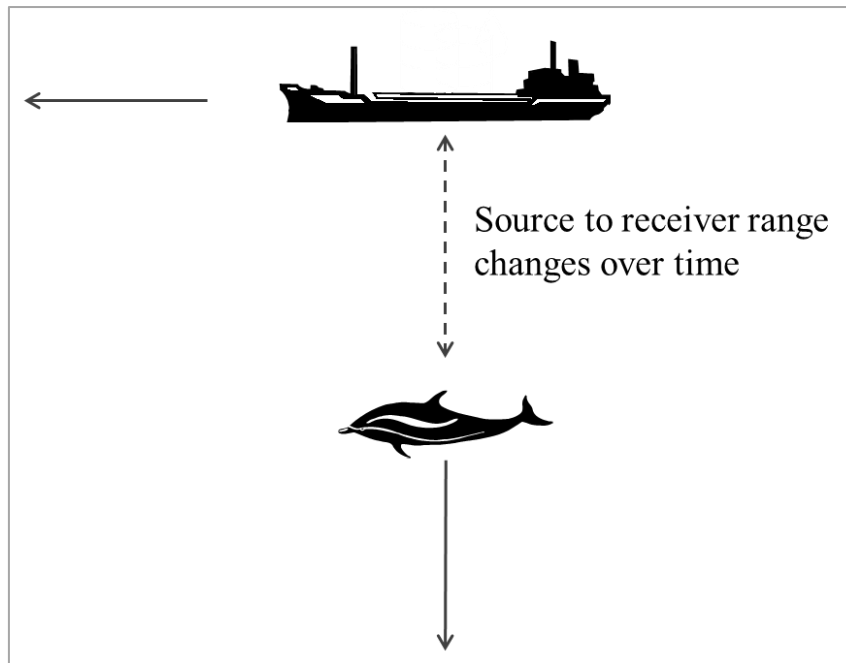
Figure 4.11   Sound exposure modelling

The above case was modelled for a range of start distances (initial or closest passing distance between the animal and vessel) in order to calculate cumulative exposure for a range of scenarios. In each case, the pulses to which the mammal is exposed in closest proximity to the vessel dominate the sound exposure. This is due to the logarithmic nature of sound energy summation.

In order to carry out the swimming mammal calculation, it has been assumed that a mammal will swim away from the sound source at an average speed of 1.5 ms^{-1}. The calculation considers each pulse to be established separately; resulting in a series of discrete SEL values of decreasing magnitude (see Figure 4.12).
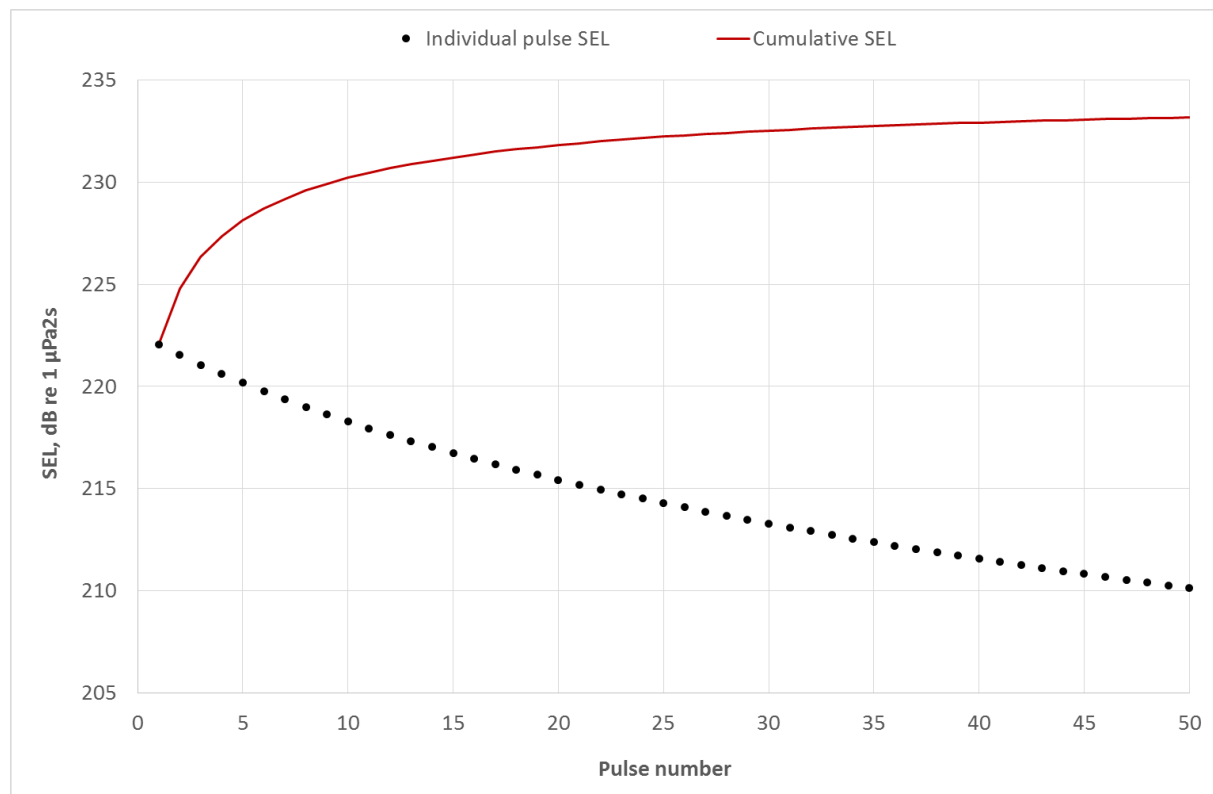
Figure 4.12   Example of discrete pulse SEL and cumulative SEL

As a mammal swims away from the source array, the sound level will progressively reduce; the cumulative SEL is worked out by logarithmically adding the SEL to which the mammal is exposed as it travels away from the source. This calculation was used to estimate the approximate minimum start distance for a marine mammal in order for it to be exposed to sufficient sound energy to result in the onset of potential injury. It should be noted that the sound exposure calculations are based on the simplistic assumption that the animal will continue to swim away at a fairly constant relative speed. The real world situation is more complex and the animal is likely to move in a more complex manner. Swim speeds of marine mammals have been shown to be up to 5 ms^{-1} (e.g. cruising minke whale 3.25 ms^{-1} (Cooper *et al.,* 2008) and harbour porpoise up to 4.3 ms^{-1} (Otani *et al.,* 2000)). The more conservative swim speed of 1.5 ms^{-1} used in this assessment allows some headroom to account for the potential that the marine mammal might not swim directly away from the source, could change direction or does not maintain a fast swim speed over a prolonged period.

It should be noted that the sound exposure calculations are based on the simplistic assumption that the seismic source is active continuously over the entire survey period, being activated at the same interval. The real world situation is more complex. It is understood that, typically, a vessel would traverse each sail-line in turn, each taking 2.3 hours on average, with a 195 minute line-change between sail-lines when the source is not active. The SEL calculations presented in this study do not take any breaks in activity into account. Furthermore, the multiple pulse sound criteria described in the NOAA guidelines assume that the animal does not recover hearing between each pulse or series of pulses. It is likely that both the intervals between pulses and the breaks in operations for line changes could allow some recovery from temporary hearing threshold shifts for animals exposed to the sound and, therefore, the assessment of sound exposure level is considered to be conservative. This over-estimate is, however, considered to be small because, as stated previously, the majority of sound energy to which an animal is exposed occurs when it is at the closest distance to the source, with

subsequent exposure at greater ranges making an insignificant contribution to the overall exposure.

The SEL calculations described above have also been conducted to estimate the benefit of soft start operations. In this case, the individual pulse SELs are reduced in magnitude for a period of time before reverting back to the full source array values. For this assessment, it has been assumed that the each pulse SEL will be attenuated by 10 dB for a period of 20 minutes during the soft start procedures. The sound modelling makes the assumption that the mammal does not re-approach the source array in the same day. As it is likely that there will be a soft-start associated with each line change, any mammals re-approaching the array will have the opportunity to swim away before commencement of full energy seismic activity.

In reality, the sound level due to a soft-start will increase over time as the soft-start is implemented (i.e. as more source elements are added). In a typical scenario, the sound pressure will be nominally 20 to 30 dB lower for the starting case of a single gun and increase in an approximately logarithmic manner until the maximum energy is reached. Consequently, the sound level to which an animal is exposed reduces (as they swim away from the source) as the energy at source slowly rises. It is considered that the assumption of a constant sound reduction over the soft start period provides a sufficiently robust and pessimistic estimate of an animal's exposure because the majority of the cumulative sound exposure level results from initial tens of pulses.
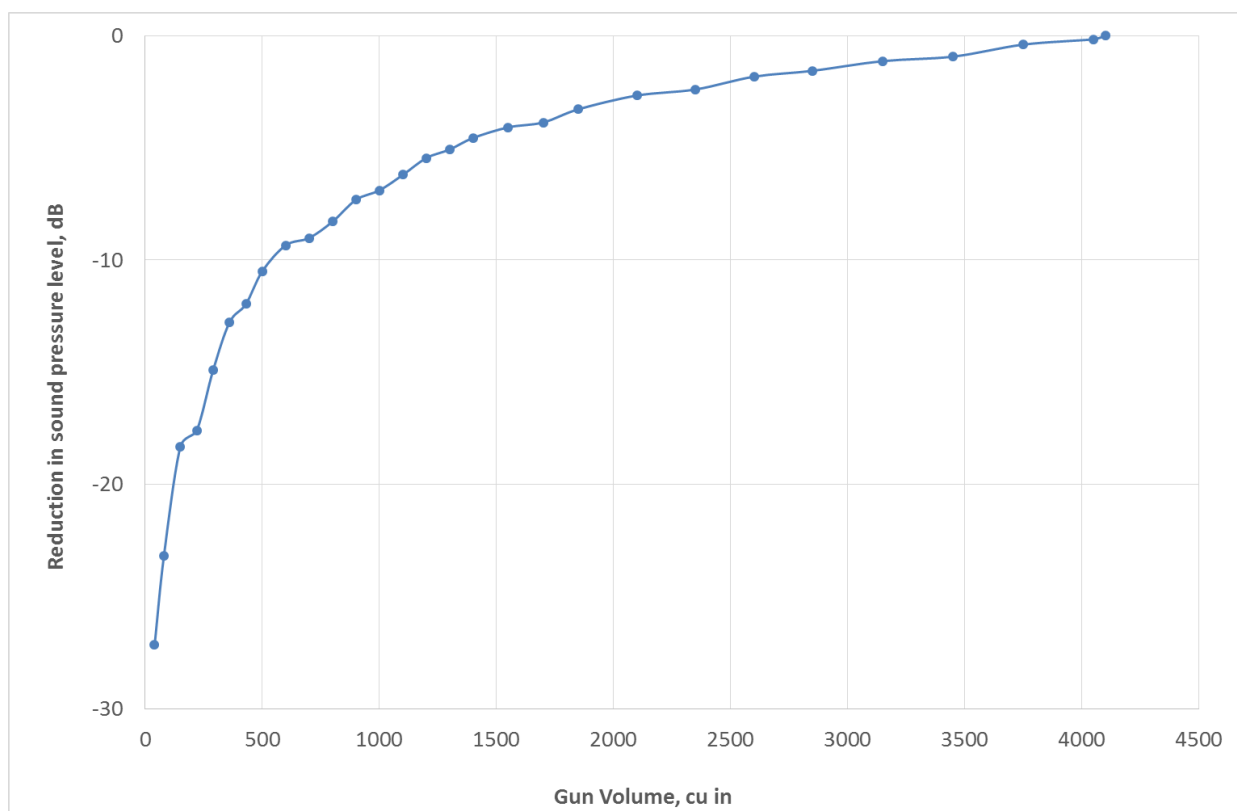
Figure 4.13   Gun volume vs reduction in sound pressure level (example)

Sound emissions due to the survey vessel are considered negligible when compared with the source array, so have not been included for purposes of the sound exposure calculation.

5.0   SOUND MODELLING RESULTS

5.1   Injury of Marine Mammals

Based on the results of the propagation and exposure modelling for peak pressure, the expected injury zones with and without mitigation in place are shown in Figure 5.1 for all three source arrays. It should be noted that the calculated sound pressure level in the near-field will be overestimated, as discussed in Section 4.0.

It should be noted that the reduction in injury zones for peak pressure with mitigation refers to the injury zone during soft start operations. Once the soft start has finished, potential injury zones will be the same as those as presented without mitigation. However, because marine mammals are expected to swim away from operations upon start of the soft start procedures, it is expected that marine mammals will be outside the range of the peak injury zone by the time soft start finishes.

■ 3640 cu in	■ 4100 cu in	■ 4390 cu in	**No Mitigation**	**20 minutes soft start**

Low frequency cetacean: 65 m / 72 m / 76 m
Low frequency cetacean + mitigation: 16 m / 21 m / 23 m
Mid frequency cetacean: 15 m / 19 m / 20 m
Mid frequency cetacean + mitigation: Not exceeded
High frequency cetacean: 501 m / 506 m / 601 m
High frequency cetacean + mitigation: 150 m / 166 m / 175 m
Phocid pinniped: 72 m / 81 m / 86 m
Phocid pinniped + mitigation: 19 m / 24 m / 26 m
Otariid pinniped: 12 m / 14 m / 15 m
Otariid pinniped + mitigation: Not exceeded

Figure 5.1   Peak pressure injury zones with and without mitigation

The results of the modelling for cumulative SEL of moving mammals for each of the three source arrays is summarised in Figure 5.2.
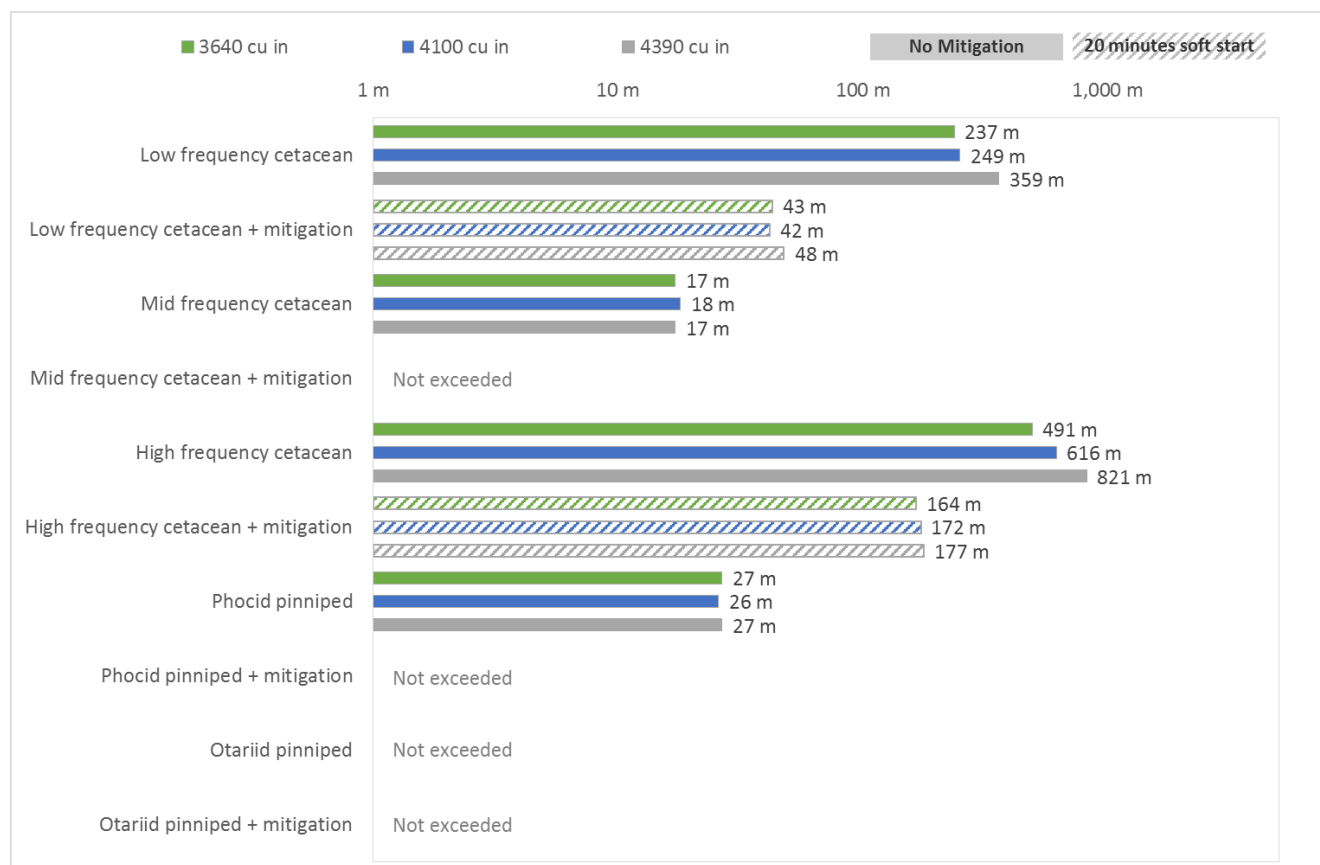
Figure 5.2   Cumulative SELs for moving animal, with and without mitigation

These same data are presented in Table 5.1 at the end of this section. The distances presented in the table and figures reflect the start point of the mammal relative to the source when the source first starts up. The mammal would then move away from the source, so the distance between the mammal and the source would increase over time.

The potential ranges presented for injury and disturbance are not a hard and fast 'line' where an impact will occur on one side and not on the other. Potential impact is more probabilistic than that; dose dependency in PTS onset, individual variations and uncertainties regarding behavioural response and swim speed/direction all mean that in reality it is much more complex than drawing a contour around a location. These ranges are designed to provide an understandable way in which a wider audience can understand the potential spatial extent of the impact.

The calculations are based on an individual mammal being exposed to sound resulting from continuous source activation which, as noted in previously, could be a simplification.

The benefit of soft start operations is greater at shorter ranges from the source than if the mammal starts further away from the source. This is because at short distances the sound level is higher and falls away at a faster rate, so an animal swimming at a constant speed will see a larger relative reduction in sound if it starts closer to the source. Care should be taken in interpreting any results within tens of meters of the source due to near-field effects potentially overestimating exposure.

5.2 Assessment of Ranges for Potential Behavioural Change for Marine Mammals

The relationship between rms sound pressure level and range from the 3,640 cu in source array is shown in Figure 5.3, plotted with the behavioural change criterion of 160 dB re 1 µPa (rms_{T90}).   The graph shows that the radius for potential behavioural change for marine mammals is up to 1.7 km from the source array. It should be noted that the rms values plotted in the graph use the estimated T90 time window at various distances from the source, up to a maximum value of 200 ms.
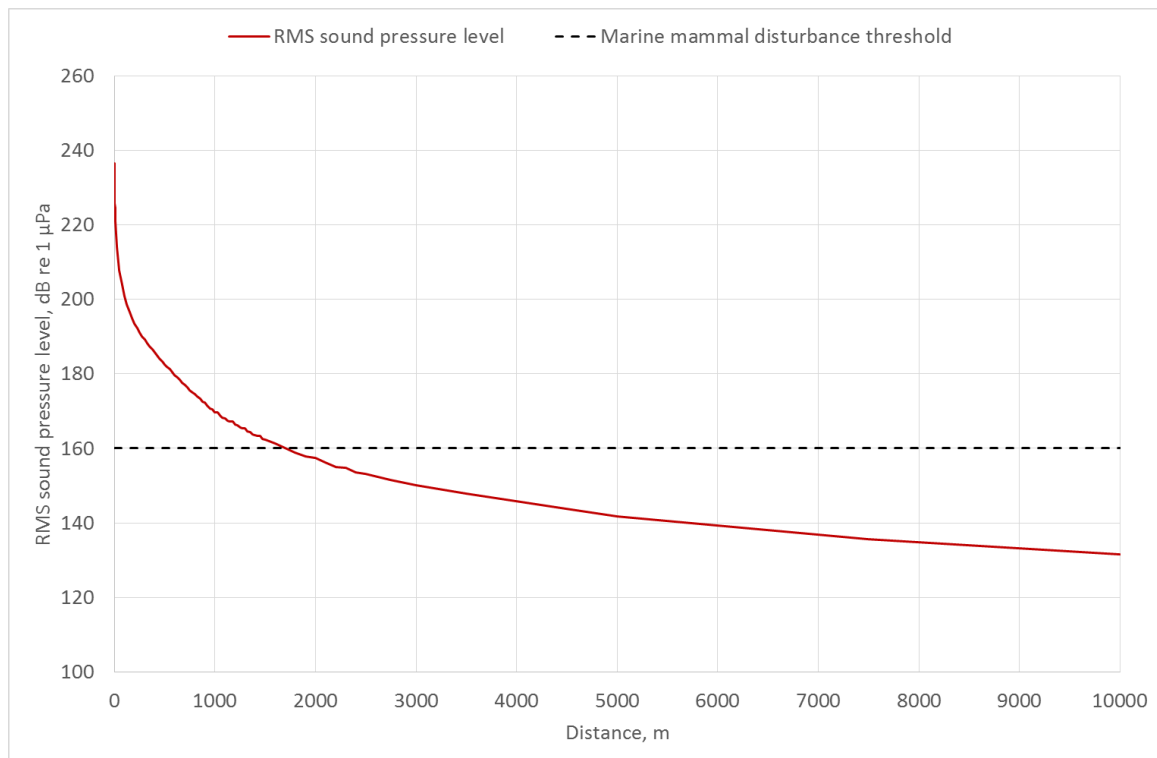
Figure 5.3 **RMS_{T90} sound pressure level against distance for behavioural change – 3,640 cu in**

The relationship between rms sound pressure level and range from the source array is shown in Figure 5.4 for the 4,100 cu in source array. The graph shows that the radius for potential behavioural change for marine mammals is up to 3.9 km from the source array.
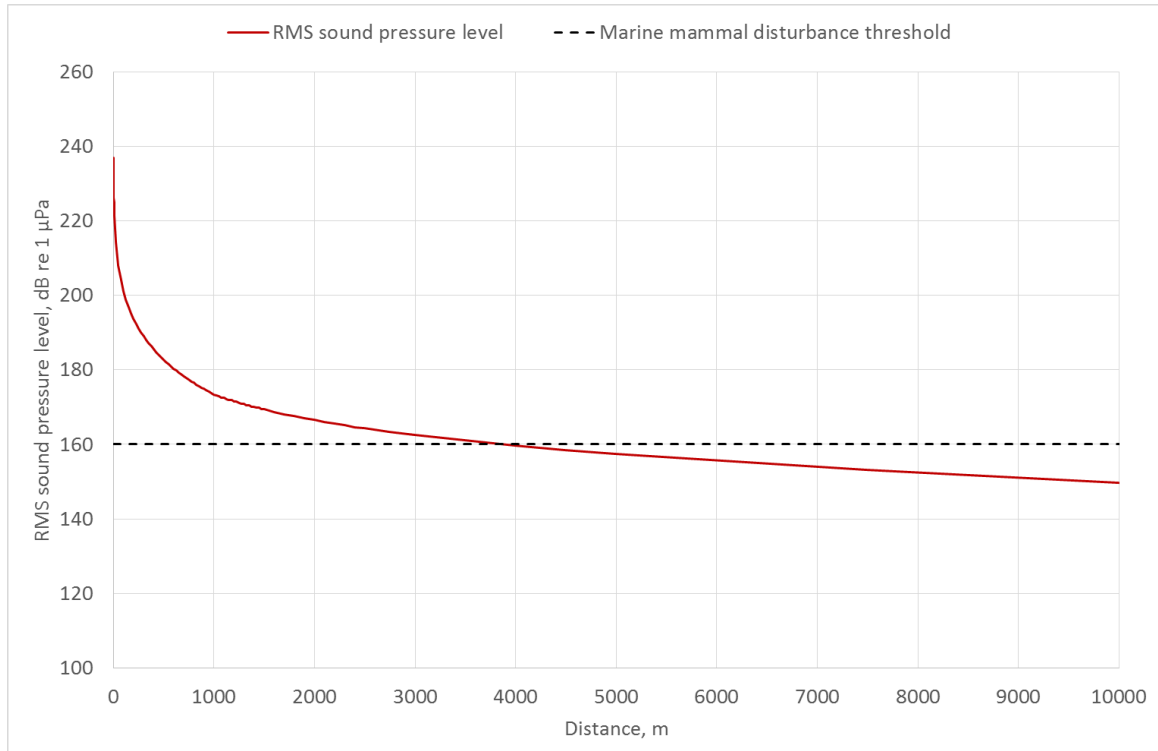
Figure 5.4 **RMST90 sound pressure level against distance for behavioural change – 4,100 cu in**

The relationship between rms sound pressure level and range from the source array is shown in Figure 5.5 for the 4,390 cu in source array. The graph shows that the radius for potential behavioural change for marine mammals is up to 5.8 km from the source array.
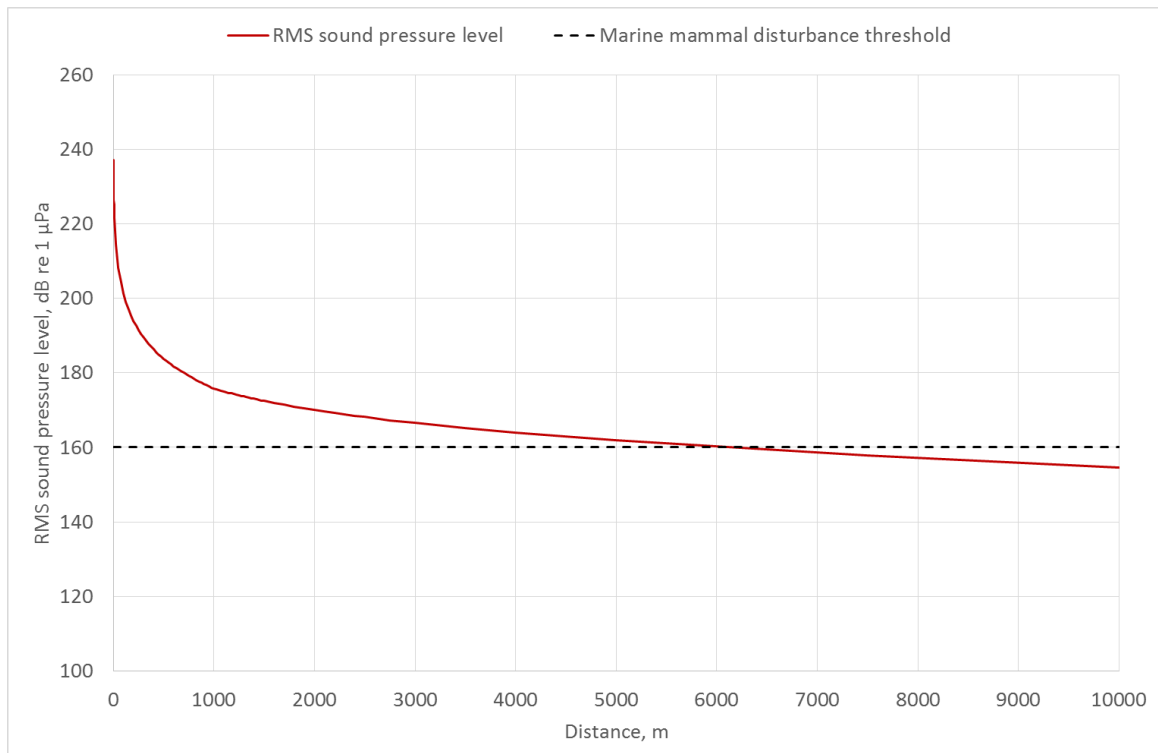
Figure 5.5 **RMST90 sound pressure level against distance for behavioural change – 4,390 cu in**

It should be noted that the differences between the rms behavioural change ranges are much larger for each array size than the difference between injury ranges. This is primarily because at these larger ranges (i.e. much greater ranges than the water depth) the frequency dependent directivity of the array has a significant bearing on the resultant sound pressure level.

Figure 5.6 shows the plotted rms T90 sound pressure level contours for the largest (4,390 cu in) seismic source operating in the middle of the seismic survey area.
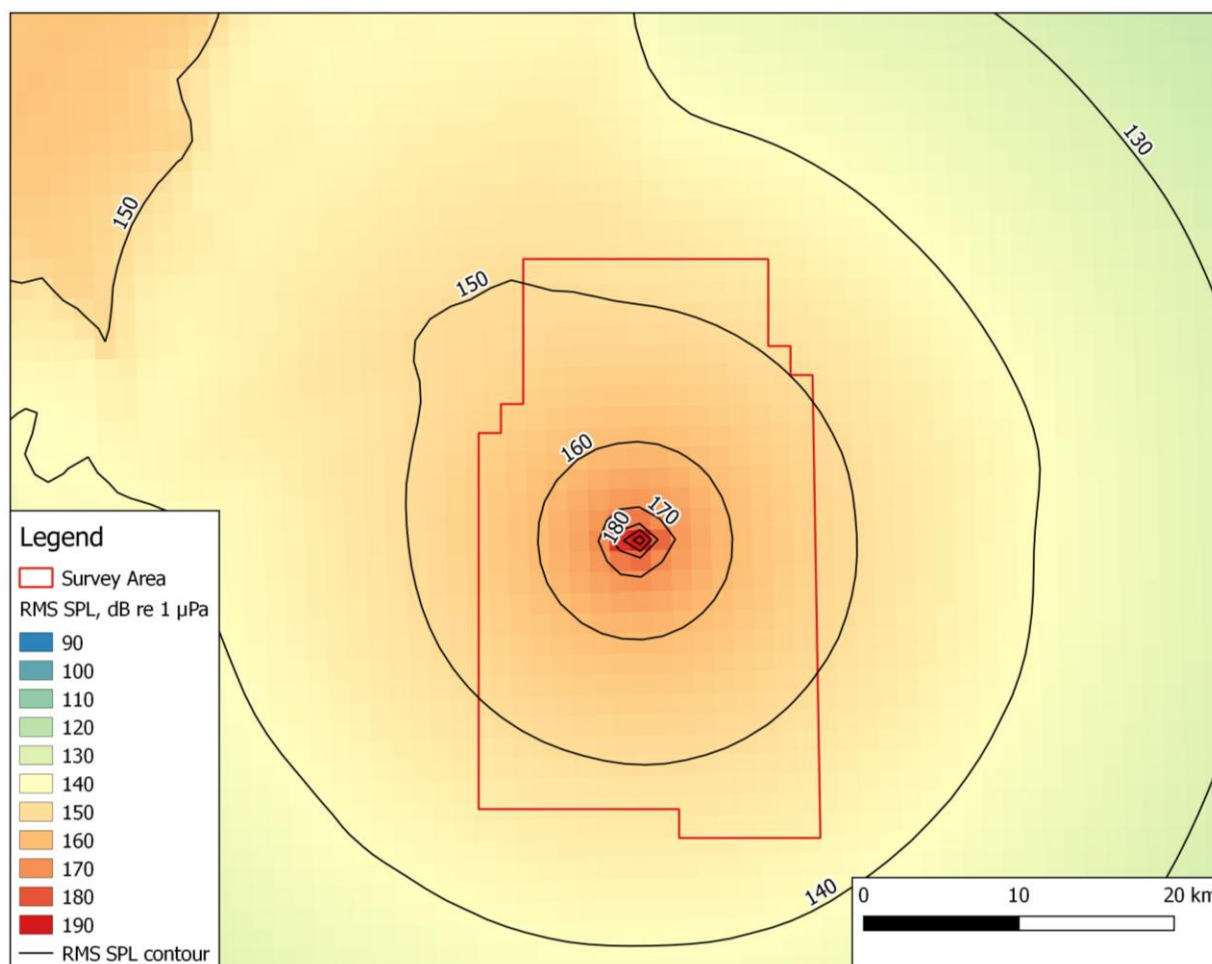
Figure 5.6   **RMS$_{T90}$ sound pressure level contour, dB re 1 µPa (rms) – 4390 cu in array**

5.3   Marine Mammals - Injury and Behavioural Change Zone Summary

The radius of the potential injury and disturbance zones for the different modelled situations are summarised in Table 5.1, based on a comparison of the calculated sound level at various ranges against the criteria.

Table 5.1   Summary of potential injury and disturbance zones for marine mammals

Scenario	Source array	Radius of Effect, m				
		LF Cetacean	MF Cetacean	HF Cetacean	Phocid Pinniped	Otariid Pinniped
Peak pressure (SPL) physiological damage	3640 cu in	65	15	501	72	12
	4100 cu in	72	19	506	81	14
	4390 cu in	76	20	601	86	15
Peak pressure (SPL) physiological damage + soft start	3640 cu in	16	N/E	150	19	N/E
	4100 cu in	21	N/E	166	24	N/E
	4390 cu in	23	N/E	175	26	N/E
SEL of mammal swimming away from moving vessel	3640 cu in	237	17	491	27	N/E
	4100 cu in	249	18	616	26	N/E
	4390 cu in	359	17	821	27	N/E
SEL of mammal swimming away from moving vessel + soft start	3640 cu in	43	N/E	164	N/E	N/E
	4100 cu in	42	N/E	172	N/E	N/E
	4390 cu in	48	N/E	177	N/E	N/E
NMFS 2005 Level A harassment 180 dB re 1 µPa (rms$_{T90}$)	3640 cu in	600				
	4100 cu in	650				
	4390 cu in	725				
RMS behavioural change 160 dB re 1 µPa (rms$_{T90}$)	3640 cu in	1,700				
	4100 cu in	3,900				
	4390 cu in	5,800				

Assuming that marine mammals will swim away from the source array upon hearing start-up and with soft start procedures in place, the SEL injury zones for a swimming animal reduce to less than approximately 180 m for high frequency cetaceans for the largest of the proposed source arrays. It is important to note that injury ranges are based on the worst case take-off angle between the animal and the source array. In other words, for an injury range which is less than the water depth, the assumption is that a marine mammal could be directly underneath the source array, meaning that the effects of directivity are minimal. In reality, it is more likely that the animal would be some distance away horizontally from the source array, in which case directivity effects would mean that their sound exposure would be significantly lower than predicted in this worst case modelling scenario. The scenario of a marine mammal being directly under the array during start-up is considered highly unlikely, even if it is theoretically possible. It can therefore be concluded that the ranges presented for injury and disturbance and very precautionary and overly pessimistic.

It is unlikely that any high-frequency cetaceans will be present in the survey area. For low-frequency cetaceans, the injury range will be approximately 50 m or less and the injury range thresholds are unlikely to be exceeded for mid-frequency cetaceans.

5.4   Sea Turtles

The spatial extent of the range of effects on sea turtles is summarised in Table 5.2 assuming a moderate swim speed of 0.5 m/s.

Table 5.2 Summary of potential injury and disturbance zones for fish and sea turtles

Type of animal	Parameter	Source array	Range of effect, m		
			Mortality and potential mortal injury	Recoverable injury	TTS
Sea turtles	210 SEL, dB re 1 µPa²s	3640 cu in	11	(*Near*) High (*Intermediate*) Low (*Far*) Low	(*Near*) High (*Intermediate*) Low (*Far*) Low
		4100 cu in	12		
		4390 cu in	12		
	207 Peak, dB re 1 µPa	3640 cu in	289		
		4100 cu in	292		
		4390 cu in	322		
Predicted range of behavioural effect	(*Near*) High (*Intermediate*) Moderate (*Far*) Low				

For sea turtles, there is a high level of risk of behavioural effects within tens of meters of the seismic source, a moderate risk within hundreds of meters and a low risk within thousands of meters.

6.0   MITIGATION

Without any mitigation measures in place, seismic survey activities have been identified as having the potential to cause injury to high frequency cetaceans at a range of up to 821 m from the source array. However, high frequency cetaceans are unlikely to be present in the survey area and the injury radius is only 20 m for mid-frequency cetaceans and 76 m for low frequency cetaceans. Disturbance to marine mammals could occur at distances of up to 1.7 km from the smallest of the proposed source arrays, up to 3.9 km from the mid-sized array and up to 5.8 km from the largest array but this is based on the assumption of an animal being at the maximum possible depth in areas with deep bathymetry which, as discussed previously, is a very unlikely scenario. It is more likely that animals would be in the upper half of the water column and for the largest array, the disturbance zone would reduce from 5.8 km to 4.2 km in this scenario.   Given the potential for injury (and disturbance) from the survey, it is recommended that further mitigation measures should be adopted. These include:

- **Marine Mammal Observers**

- Provision of qualified and experienced Marine Mammal Observer (MMO) to be present for the duration of the survey to undertake cetacean visual monitoring during all daylight hours.

- **Passive Acoustic Monitoring (PAM) – if starting at night**

- PAM comprises of a short hydrophone array station, a deck cable and data processing system which processes and stores selected data. The PAM system could be used for night-time and low visibility shooting to detect any cetaceans within close proximity to the survey.

- **Pre-shooting search**

- The MMO (or PAM operative) would begin observations 60 minutes before the commencement of the first use of the seismic source and the survey would be delayed if any cetaceans are detected within 1 km of the airgun array before work commences; and

- if cetaceans are observed or detected within 1 km during this first observation, then the start of the seismic sources would be delayed until cetaceans have moved away (not sighted for at least 20 minutes).

- **Airguns Soft Start**

- To ensure that marine mammals are given the opportunity to move away from the airguns as they commence firing, energy should be slowly increased to the maximum level over a period of 20 minutes, in a process called 'soft-start'.

Taking the effect of soft start into account, the potential injury ranges reduce further. It is therefore concluded that the injury ranges for all marine mammals are well within the 1 km MMO observation zone. This effectively reduces the risk of injury to marine mammals to negligible levels.

7.0   CONCLUSIONS

Based on the propagation and sound exposure modelling carried out for this assessment, it is concluded that:

- There is potential for disturbance to marine mammals within up to 5.8 km of the source array for the largest of the proposed arrays, although this assumes that the animal is at the bottom of the water column and is considered to be an unlikely scenario.

- Some sea turtles could be injured at ranges of up to 322 m from the source array.

- Assuming a swimming animal, it is likely that potential injury zones for high frequency cetaceans could be up to 821 m before mitigation measures are applied. With soft start procedures in place, the potential injury zone will reduce to less than 177 m.

- For low-frequency cetaceans, the injury range will be 359 m or less before mitigation measures are applied, reducing to 48 m with mitigation measures in place.

- For mid frequency cetaceans the potential injury zone will be up to 20 m before mitigation measures are applied. With mitigation in place, the injury thresholds are unlikely to be exceeded.

- These injury zones can effectively be monitored using MMOs during daylight or PAM at night.

- It is therefore concluded that it is unlikely that marine mammals will be injured as a result of the survey.

8.0   REFERENCES

Ainslie, Michael A., and James G. McColm. 1998. "A Simplified Formula for Viscous and Chemical Absorption in Sea Water." The Journal of the Acoustical Society of America 103 (3): 1671–72.

Breitzke, Monika, Olaf Boebel, Saad El Naggar, Wilfried Jokat, and Berthold Werner. 2008. "Broad-Band Calibration of Marine Seismic Sources Used by R/V Polarstern for Academic Research in Polar Regions." Geophysical Journal International 174 (2): 505–24.

Brekhovskikh, Leonid Maksimovich, and I͡Uriĭ Lysanov. 2014. Fundamentals of Ocean Acoustics.

Cole, B. F. 1965. "Marine Sediment Attenuation and Ocean-Bottom-Reflected Sound." The Journal of the Acoustical Society of America 38 (2): 291–97.

Cooper, Lisa Noelle, Nils Sedano, Stig Johansson, Bryan May, Joey D. Brown, Casey M. Holliday, Brian W. Kot, and Frank E. Fish. 2008. "Hydrodynamic Performance of the Minke Whale (Balaenoptera Acutorostrata) Flipper." Journal of Experimental Biology 211 (12): 1859–67.

Eckart, Carl. 1953. "The Scattering of Sound from the Sea Surface." The Journal of the Acoustical Society of America 25 (3): 566–70.

Essen, H.-H. 1994. "Scattering from a Rough Sedimental Seafloor Containing Shear and Layering." The Journal of the Acoustical Society of America 95 (3): 1299–1310.

Etter, Paul C. 2013. Underwater Acoustic Modeling and Simulation. CRC Press.

Farcas, Adrian, Paul M. Thompson, and Nathan D. Merchant. 2016. "Underwater Noise Modelling for Environmental Impact Assessment." Environmental Impact Assessment Review 57: 114–22.

Fortuin, Leonard. 1970. "Survey of Literature on Reflection and Scattering of Sound Waves at the Sea Surface." The Journal of the Acoustical Society of America 47 (5B): 1209–28.

Greaves, Robert J., and Ralph A. Stephen. 2003. "The Influence of Large-Scale Seafloor Slope and Average Bottom Sound Speed on Low-Grazing-Angle Monostatic Acoustic Scattering." The Journal of the Acoustical Society of America 113 (5): 2548–61.

Hamilton, Edwin L. 1970. "Reflection Coefficients and Bottom Losses at Normal Incidence Computed from Pacific Sediment Properties." Geophysics 35 (6): 995–1004.

Harris, Ross E., Gary W. Miller, and W. John Richardson. 2001. "Seal Responses to Airgun Sounds during Summer Seismic Surveys in the Alaskan Beaufort Sea." Marine Mammal Science 17 (4): 795–812.

Hastings, M. C. 2002. "Clarification of the Meaning of Sound Pressure Levels & the Known Effects of Sound on Fish."

HESS 1997. "Summary of Recommendations Made by the Expert Panel at the HESS Workshop on the Effects of Seismic Sound on Marine Mammals.". In . Pepperdine University, Malibu, California.

Jensen, Finn Bruun. 1994. Computational Ocean Acoustics. Springer.

JNCC Guidelines for Minimising the Risk of Injury and Disturbance to Marine Mammals from Seismic Surveys." 2010 in prep. JNCC.

JNCC, Natural England, and Countryside Council for Wales. 2010. "The Protection of Marine European Protected Species from Injury and Disturbance: Guidance for the Marine Area in England and Wales and the UK Offshore Marine Area."

Kastelein, Ronald A., Jessica Schop, Robin Gransier, and Lean Hoek. 2014. "Frequency of Greatest Temporary Hearing Threshold Shift in Harbor Porpoises (Phocoena Phocoena) Depends on the Noise Level." The Journal of the Acoustical Society of America 136 (3): 1410–18.

Kastelein, Ronald A., Robin Gransier, Lean Hoek, and Juul Olthuis. 2012. "Temporary Threshold Shifts and Recovery in a Harbor Porpoise (Phocoena Phocoena) after Octave-Band Noise at 4 kHz." The Journal of the Acoustical Society of America 132 (5): 3525–37.

Kinsler, Lawrence E., Austin R. Frey, Alan B. Coppens, and James V. Sanders. 1999. "Fundamentals of Acoustics." Fundamentals of Acoustics, 4th Edition, by Lawrence E. Kinsler, Austin R. Frey, Alan B. Coppens, James V. Sanders, Pp. 560. ISBN 0-471-84789-5. Wiley-VCH, December 1999. 1. http://adsabs.harvard.edu/abs/1999fuac.book.....K.

Kuo, Edward YT. 1992. "Acoustic Wave Scattering from Two Solid Boundaries at the Ocean Bottom: Reflection Loss." Oceanic Engineering, IEEE Journal of 17 (1): 159–70.

Lucke, Klaus, Paul A. Lepper, Marie-Anne Blanchet, and Ursula Siebert. 2008. "Testing the Acoustic Tolerance of Harbour Porpoise Hearing for Impulsive Sounds." Bioacoustics 17 (1-3): 329–31.

Lurton, Xavier. 2002. An Introduction to Underwater Acoustics: Principles and Applications. Springer Science & Business Media.

Mackenzie, K. V. 1960. "Reflection of Sound from Coastal Bottoms." The Journal of the Acoustical Society of America 32 (2): 221–31.

Madsen, P. T. 2005. "Marine Mammals and Noise: Problems with Root Mean Square Sound Pressure Levels for Transients." The Journal of the Acoustical Society of America 117: 3952.

Madsen, Peter Teglberg, M. Johnson, P. J. O. Miller, N. Aguilar Soto, J. Lynch, and P. L. Tyack. 2006. "Quantitative Measures of Air-Gun Pulses Recorded on Sperm Whales (Physeter Macrocephalus) Using Acoustic Tags during Controlled Exposure Experiments." The Journal of the Acoustical Society of America 120 (4): 2366–79.

Marsh, H. Wyser, and M. Schulkin. 1962. "Shallow-Water Transmission." The Journal of the Acoustical Society of America 34: 863.

Marsh, H. Wysor, M. Schulkin, and S. G. Kneale. 1961. "Scattering of Underwater Sound by the Sea Surface." The Journal of the Acoustical Society of America 33 (3): 334–40.

McKinney, C. Mo, and C. D. Anderson. 1964. "Measurements of Backscattering of Sound from the Ocean Bottom." The Journal of The Acoustical Society of America 36 (1): 158–63.

Nedwell, J. R., A. W. H. Turnpenny, J. Lovell, S. J. Parvin, R. Workman, J. A. L. Spinks, and D. Howell. 2007. "A Validation of the dBht as a Measure of the Behavioural and Auditory Effects of Underwater Noise." Report Reference: 534R1231.

NMFS. 2005. "Scoping Report for NMFS EIS for the National Acoustic Guidelines on Marine Mammals." National Marine Fisheries Service.

NOAA. 2016. "Technical Guidance for Assessing the Effects of Anthropogenic Sound on Marine Mammal Hearing: Underwater Acoustic Thresholds for Onset of Permanent and Temporary Threshold Shifts." National Marine Fisheries Service (NOAA).

Otani, Seiji, Yasuhiko Naito, Akiko Kato, and Akito Kawamura. 2000. "DIVING BEHAVIOR AND SWIMMING SPEED OF A FREE-RANGING HARBOR PORPOISE, PHOCOENA PHOCOENA." Marine Mammal Science 16 (4): 811–14.

Patterson, H., Susanna B. Blackwell, B. Haley, A. Hunter, M. Janowski, R. Rodriques, D. Ireland, and D.W. Funk. 2007. "Marine Mammal Monitoring and Mitigation During Open Water Seismic Exploration by Shell Offshore Inc, in the Chuchi Beaufort Seas, July - September 2006: 90-Day Report." LGL Draft Rep. P891-1. LGL Alaska Research Associates Inc.

Popper, Arthur N., Anthony D. Hawkins, Richard R. Fay, David A. Mann, Soraya Bartol, Thomas J. Carlson, Sheryl Coombs, et al. 2014. ASA S3/SC1.4 TR-2014 Sound Exposure Guidelines for Fishes and Sea Turtles: A Technical Report Prepared by ANSI-Accredited Standards Committee S3/SC1 and Registered with ANSI. Springer.

Richardson, William John, Denis H. Thomson, Charles R. Greene, Jr., and Charles I. Malme. 1995. Marine Mammals and Noise. Academic Press.

Rogers, P. H. 1981. "Onboard Prediction of Propagation Loss in Shallow Water." DTIC Document..

Southall, Brandon L., Ann E. Bowles, William T. Ellison, James J. Finneran, Roger L. Gentry, Charles R. Greene Jr, David Kastak, et al. 2007. "Marine Mammal Noise-Exposure Criteria: Initial Scientific Recommendations." Aquatic Mammals 33 (4): 411–521.

Tolstoy, M., J. Diebold, L. Doermann, S. Nooner, S. C. Webb, D. R. Bohnenstiehl, T. J. Crone, and R. C. Holmes. 2009. "Broadband Calibration of the R/V Marcus G. Langseth Four-String Seismic Sources." Geochemistry, Geophysics, Geosystems 10 (8).

Urick, Robert J. 1983. Principles of Underwater Sound. McGraw-Hill.

Urick, Robert J., and Robert M. Hoover. 1956. "Backscattering of Sound from the Sea Surface: Its Measurement, Causes, and Application to the Prediction of Reverberation Levels." The Journal of the Acoustical Society of America 28 (6): 1038–42.

Wang, Lian, Kevin D. Heaney, Tanja Pangerc, Pete Theobald, Stephen Robinson, and Michael A. Ainslie. 2014. "Review of Underwater Acoustic Propagation Models." AIR (RES) 086. NPL.

WSDOT. 2011. "Biological Assessment Preparation for Transport Projects - Advanced Training Manual." Washington State Department of Transport.